A Membrane Separation Process for Biodiesel Purification

By

Jehad Saleh

A thesis submitted to the Faculty of Graduate and Postdoctoral Studies in partial fulfillment of the requirements for the degree of

Doctor of Philosophy in Environmental Engineering

Ottawa Carleton Institute of Environmental Engineering (OCIENE)

Department of Chemical and Biological Engineering

University of Ottawa

Statements of Contribution of Collaborators

I hereby declare that this thesis was accomplished under the supervision of Professors Marc A. Dubé and André Y. Tremblay of the Department of Chemical and Biological Engineering at the University of Ottawa. The material in this thesis is the outcome of four years of research efforts by the author and his two supervisors. I personally wrote the thesis and my supervisors made editorial corrections. I assembled the membrane separation set up with the help of the technical support staff of the Department of Chemical and Biological Engineering under the supervision and training received from Professors I performed the biodiesel production experiments, membrane separation experiments, sample characterizations, data modeling and analysis. Papers published as a result of the thesis were co-authored by J. Saleh, A. Y. Tremblay and M. A. Dubé.

Signature: Date:

Jehad Saleh

Abstract

In the production of biodiesel via the transesterification of vegetable oils, purification to international standards is challenging. A key measure of biodiesel quality is the level of free glycerol in the biodiesel. In order to remove glycerol from fatty acid methyl ester (FAME or biodiesel), a membrane separation setup was tested. The main objective of this thesis was to develop a membrane process for the separation of free glycerol dispersed in FAME after completion of the transesterification reaction and to investigate the effect of different factors on glycerol removal. These factors included membrane pore size, pressure, temperature, and methanol, soap and water content.

First, a study of the effect of different materials present in the transesterification reaction, such as water, soap, and methanol, on the final free glycerol separation was performed using a modified polyacrylonitrile (PAN) membrane, with 100 kD (ultrafiltration) molecular weight cut off for all runs at 25°C. Results showed low concentrations of water had a considerable effect in removing glycerol from the FAME. The mechanism of separation of free glycerol from FAME was due to the removal of an ultrafine dispersed glycerol-rich phase present in the untreated (or raw) FAME. The size of the droplets and the free glycerol separation both increased with increasing water content of the FAME.

Next, three types of polymeric membranes in the ultrafiltration range with different molecular weight cut off, were tested at three fixed operating pressures and three operating temperatures (0, 5 and 25^{o}C) to remove the free glycerol from a biodiesel reactor effluent. The ASTM standard for free glycerol concentration was met for the experiments performed at 25°C. The results of this study indicate that glycerol could be separated from raw FAME to meet ASTM and EN standards at methanol feed concentrations of up to 3 mass%. The process was demonstrated to rely on the formation of a dynamic polar layer on the membrane surface.

Ceramic membranes of different pore sizes (0.05 μm (ultrafiltration (UF) range) and 0.2 μm (microfiltration (MF) range)) were used to treat raw FAME directly using the membrane separation set up at temperatures of 0, 5 and 25°C. The results were encouraging for the 0.05 μm pore size membrane at the highest temperature (25°C). The

effect of temperature on glycerol removal was evident from its relation with the concentration factor (CF). Higher temperatures promoted the achievement of the appropriate CF value sooner for faster separation. Membrane pore size was also found to affect separation performance.

A subsequent study revealed the effect of different variables on the size of the glycerol droplets using dynamic light scattering (DLS). A key parameter in the use of membrane separation technology is the size of the glycerol droplets and the influence of other components such as water, methanol and soaps on that droplet size. The effect of water, methanol, soap and glycerol on the size of suspended glycerol droplets in FAME was studied using a 3-level Box-Behnken experimental design technique. Standard statistical analysis techniques revealed the significant effect of water and glycerol on increasing droplet size while methanol and soap served to reduce the droplet size.

Finally, a study on the effect of trans-membrane pressure (TMP) at different water concentrations in the FAME phase on glycerol removal using UF (0.03 μm pore size, polyethersulfone (PES)) and MF (0.1 and 0.22 μm pore sizes, PES) membranes at 25, 40 and 60°C was performed. Results showed that running at 25°C for the two membrane types produced the best results for glycerol removal and exceeded the ASTM and EN standards. An enhancement of glycerol removal was found by adding small amounts of water up to the maximum solubility limit in biodiesel. An increase in temperature resulted in an increase in the solubility of water in the FAME and less effective glycerol removal. Application of cake filtration theory and a gel layer model showed that the gel layer on the membrane surface is not compressible and the specific cake resistance and gel layer concentration decrease with increasing temperature. An approximate value for the limiting (steady-state) flux was reported and it was found that the highest fluxes were obtained at the lowest initial water concentrations at fixed temperatures.

In conclusion, dispersed glycerol can be successfully removed from raw FAME (untreated FAME) using a membrane separation system to meet the ASTM biodiesel fuel standards. The addition of water close to the solubility limit to the FAME mixture enables the formation of larger glycerol droplets and makes the separation of these droplets straightforward.

Résumé

Dans la production du biodiésel via la transestérification d'huiles végétales, la purification aux normes internationales est difficile. Une mesure clé de qualité du biodiésel est le niveau de glycérol libre dans le biodiésel. Pour enlever le glycérol des esters methyliques d'acides gras (la EMAG ou biodiésel), une technologie de séparation à membrane a été évaluée. L'objectif principal de cette thèse était de développer un processus de séparation par membrane du glycérol libre dispersé dans la EMAG après l'achèvement de la réaction de transestérification et enquêter sur l'effet de différents facteurs sur la séparation du glycérol. Ces facteurs étaient , le type de membrane, la dimension des pores de membrane, la pression transmembranaire, la température et les concentrations de méthanol, savon et d'eau. D'abord, une étude sur l'effet de différentes substances présentes lors de la réaction de transestérification, tels que l'eau, le savon et le méthanol, sur la séparation du glycérol libre du EMAG a été exécutée en utilisant une membrane de polyacrylonitrile (PAN) modifiée, ayant un seuil de coupure de 100 kD (ultrafiltration ou UF). Les résultats ont montrés que de petites quantités d'eau avaient un effet bénéfique sur la séparation du glycérol. Le mécanisme de séparation du glycérol libre des EMAG était l'enlèvement d'une phase riche en glycérol dispersée dans le EMAG. La grandeur des particules et la séparation du glycérol libre des EMAG ont tous les deux augmenté avec l'augmentation du contenu en eau dans l'EMAG.

Ensuite, trois types de membranes polymères dans la gamme UF avec différents seuils de coupure, ont été évalués à trois pressions fixes et à trois températures (0, 5 et 25^{o}C) pour enlever le glycérol libre d'un effluent d'EMAG d'un réacteur. La norme ASTM pour la concentration du glycérol libre a été rencontrée pour les expériences exécutées à 25°C. Les résultats de cette étude indiquent que le glycérol pourrait être séparé des EMAG pour rencontrer les normes ASTM et EN jusqu'à une concentration massique de méthanol de 3%.

Les membranes céramiques de différentes grandeur de pores (0.05 μm (la gamme UF) et 0.2 μm (la gamme de microfiltration ou MF)) ont été utilisées pour traiter les EMAG brute en utilisant directement une membrane aux températures de 0, 5 et 25°C. Les résultats étaient encourageants pour les membranes à diamètre de pore de 0.05 μm à

la plus haute température (25°C). L'effet de température sur l'enlèvement du glycérol était évident de sa relation avec le facteur de concentration (CF.). La grandeur des pores de membrane a été aussi trouvée à affecter la performance de séparation.

Une étude ultérieure a révélée l'effet de différentes variables sur la grandeur des particules de glycérol en utilisant la diffusion dynamique de la lumière (DDL). Un paramètre clé dans l'utilisation de technologie de séparation membranaire est la grandeur des particules de glycérol et de l'influence d'autres composantes comme l'eau, le méthanol et les savons sur cette grandeur de particule. L'effet d'eau, méthanol, savon et glycérol sur la grandeur de particules de glycérol suspendues dans l'EMAG a été étudié en utilisant un choix de conditions expérimentales de type Box-Behnken à 3 niveaux. Les techniques d'analyses statistiques standards ont révélés l'effet significatif de l'eau et du glycérol sur la grandeur de particules pendant que le méthanol et le savon diminuaient la grandeur des particules.

Finalement, une étude sur l'effet de la pression trans-membranaire (PTM) lorsque différentes concentrations d'eau sont ajoutées au EMAG sur l'enlèvement du glycérol en utilisant les membranes UF (diamètre de pores = 0.03 µm, polyethersulfone (PES)) et MF (diamètre de pores = 0.1 et 0.22 µm, PES) à 25, 40 et 60°C a été exécuté. Les résultats ont montrés qu'à 25°C, pour les deux gammes de membranes, on a trouvé les meilleurs résultats pour l'enlèvement du glycérol et on a excédé les normes ASTM et EN en ajoutant de petites quantités d'eau jusqu'à la limite de solubilité de l'eau dans le EMAG. A une température plus élevée, la solubilité de l'eau dans l'EMAG a diminué la séparation du glycerol. L'application de la théorie de filtration et d'un modèle de couche de gel ont démontrés que la couche de gel sur la surface de la membrane n'est pas compressible et que la résistance spécifique du gâteau coïncide avec la diminution de concentration de la couche de gel et avec une augmentation de la température. Une valeur approximative pour le flux limitant a été déterminée et on a constaté, qu'a à une température donnée, que le flux augmentais avec une réduction de la quantité d'eau ajoutée aux EMAG.

En conclusion, le glycérol dispersé peut être enlevé avec succès de l'EMAG brute pour rencontrer les normes ASTM du biodiésel en utilisant un système de séparation par membrane. L'addition d'eau près de sa limite de solubilité dans les EMAG permet la

formation de plus grandes particules de glycérol et rend la séparation de ces particules plus facile.

Acknowledgements

This thesis would not have been possible if it were not for many people.

First and foremost, I would like to express my most sincere gratitude to my supervisors Dr. Marc A. Dubé and Dr. André Y. Tremblay, for accepting me in their research group and for their patience and guidance over these years. Both of you gave me invaluable guidance, continued encouragement, and constructive advice throughout the course of this study; the perfect combination of your supervisions brought me out of the darkness of the unknown biodiesel world. I grew up and went through the challenges thanks to this unparalleled enlightenment.

I am grateful to all the professors and the office staff of the Department of Chemical and Biological Engineering at the University of Ottawa, for their cooperation and generous help. I am also grateful to the technical support staff in the department, Gérard Nina, Franco Ziroldo and Louis Tremblay for always being there when I needed help.

To my colleagues and all the members in the Ottawa Biodiesel Research Group (Peigang Cao, Fadi Ataya, Michele Hastie, Raghda Hasswa), I wish to express my sincere appreciation for creating a friendly, inspirational, supportive environment, which helped me complete this research process, and for their useful discussions and comments, our cooperation and friendship are precious to me.

In these acknowledgements I must, of course, express my love and respect to my mother and my sisters for their encouragement and support. To my wife: without you, your prayers, your patience and your strong support to finish this no matter what happened, I would never grown into the person I am today. To my kids: Qusai, Mahmood, Leena, Suhib, Ayham and Omar, for their love and pride in me to be their father.

For the financial support during this project, I am grateful to the University of Ottawa International Research Initiative and to the National Science and Engineering Research Council of Canada.

Table of Contents

List of Figures

List of Tables

Nomenclature

This nomenclature lists some of the most frequently used abbreviations in this thesis. It is not meant to be exhaustive. Other symbols used in formulas, tables, and figures are explained in the text as they appear.

List of abbreviations

AOCS	– American oil chemists' society
ASTM	– American Society for Testing and Materials
CF	– Concentration factor
COD	– Total chemical oxygen demand, mg/L;
DG	– Diglyceride
DLS	– Dynamic light scattering
ED	– Electro-dialysis
EN	– European standard
FAAE	– Fatty acid alkyl ester
FAME	– Fatty acid methyl ester
FFA	– Free fatty acid
FID	– Flame ionization detector
FTIR	– Fourier transform infrared
GC	– Gas chromatography
GS	– Gas separation
kD	– kiloDalton
KF	– Karl Fisher
MF	– Microfiltration
MG	– Monoglyceride
MSS	– Mineral suspended solids, mg/L;
MSTFA	– N-methyl-N-(trimethylsilyl) trifluoracetamide
MWCO	– Molecular weight cut-off
NF	– Nanofiltration

PES – Polyethersulfone

ppm – Parts per million

PAN – Polyacrylonitrile

PVDF – Polyvinylidene fluoride

PV – Pervaporation

RO – Reverse osmosis

SEM – Scanning electron microscope

TG – Triglyceride

TMP – Trans-membrane pressure

TSS – Total suspended solids, mg/L

UF – Ultrafiltration

VSS – Volatile suspended solids, mg/L

RMSE – Root mean squared error

Symbols

D_{shear} – Shear diffusion of a droplet, (m^2/s)

a_p – Radius of the droplet, (m)

d – Droplet diameter (m)

C_D – Coefficient of drag = f (Re)

t – Time, (s)

V – Cumulative filtrate volume, (m^3)

C – Concentration of solute, (kg/m^3)

ΔP – Applied TMP, (Pa)

A – Filtrate medium area, (m^2)

R_m – Membrane resistance, (m^{-1})

R_s – Cake resistance, (m^{-1})

J – Flux, (m/s)

C_f – Feed concentration, (kg/m^3)

C_p – Concentration in the permeate, (kg/m^3)

C_{gel} – Concentration near the membrane surface, (kg/m^3)

Greek letters

$\dot{\gamma}$ – Shear rate, s^{-1}

ρ_p – Density of the droplets (glycerol) (g/cm^3) = 1.261

ρ_{BD} – Density of fluid (biodiesel) (g/cm^3) = 0.875

g – Gravitational acceleration constant (9.81 m/s^2)

υ – Settling velocity of the droplet (m/s)

μ_{BD} – Viscosity of the biodiesel (dynamic viscosity) = $3.5*10^{-2}$ g/cm·s

α – Specific resistance of the cake, m/kg

Chapter 1 Introduction

Chapter 1 - Introduction

Biodiesel is a renewable, biodegradable and environmentally safe fuel for use in diesel engines that can be produced from vegetable oils, animal fats and/or used cooking oils (a.k.a., triglycerides) via alcohol transesterification using, for example, methanol. It is comprised of fatty acid methyl esters (FAME). It can be used in its neat form or as a blend with conventional diesel fuel. The similarities between biodiesel and diesel fuel reveal that biodiesel is a successful alternative source of energy in diesel engines (Demirbas, 2003).

The purity of biodiesel is an important issue, and affects the cost of the final product. In order to produce high quality biodiesel, a series of purification processes are usually needed. These can include: gravitational settling, centrifugation, water washing, adsorption and distillation (Karaosmanoglu et al., 1996). It is necessary to remove the impurities in the ester phase (FAME phase) because they will strongly affect the properties of the biodiesel fuel produced. Some problems with conventional purification steps are the production of significant amounts of waste (e.g., wastewater) or toxic materials (e.g., residual methanol and catalyst). Karaosmanoglu et al. (1996) noted that for conventional production processes, for each litre of biodiesel, 10 L of waste water are produced.

Glycerol is a by-product of the transesterification of triglycerides to FAME. There is typically a phase-separated glycerol layer in the transesterification output stream but a significant amount of glycerol also appears as droplets dispersed in the FAME phase. Many standard specifications have been created to specify the quality of biodiesel. For example the North American (ASTM D6751) and European (EN14214) standards allow 0.02 mass% free glycerol in the biodiesel product (Mao et al., 2004; Ghadge et al., 2005). A high free glycerol content in biodiesel can result in its eventual separation from the biodiesel during storage (e.g., in the fuel tank of an automobile), forming gum-like deposits around injector tips and valve heads, thereby causing problems in the fuel system (Van Gerpen et al., 1996).

Conventional biodiesel purification steps are usually energy intensive and many have a negative impact on the environment. Thus, alternatives are actively being sought for

these purification steps. One promising solution involves the use of membrane separation technology. At present, membrane separation technologies are new to biodiesel purification processes. However, recent work has shown the efficacy of using membrane technology in the production of biodiesel (Dubé et al., 2007; Cao et al., 2007). The membrane materials, the effects of operating parameters and the possibility of using membrane separation processes in biodiesel purification have not been studied to a great extent. Membrane separation technology has been used for many applications in fields outside of biodiesel production and purification. There is great potential that membrane technology can provide solutions for many environmental problems by recovering valuable products as well as treating effluents and minimizing their harm to the atmosphere.

1.1 Thesis Objectives

Membranes, in general, separate different sized particles by using a chosen membrane pore size. The main objective of this project was to develop a membrane process for the separation of free glycerol dispersed in the FAME phase after completion of the transesterification reaction. Glycerol has a limited solubility in biodiesel of 0.144 mass% which exceeds the permitted level dictated by international standards (0.02 mass %) (Van Gerpen et al., 1996). The permeate product from the membrane separation system should meet the standards for free glycerol in biodiesel, and therefore the specific objectives of the project were:

1) To determine the effect of ultrafiltration and microfiltration membranes (ceramic and polymeric) on the separation of glycerol from FAME.
2) To investigate the effect of methanol on the removal of glycerol from FAME.
3) To study the effect of water, methanol, soap and glycerol on the glycerol droplet size in FAME.
4) To study the effect of temperature on glycerol separation from FAME.
5) To study the effect of trans-membrane pressure (TMP) and the effect of membrane pore size on the separation of glycerol from FAME.
6) To study the effect of different initial water concentration in FAME on the performance of glycerol removal.

7) To optimize the operating conditions of the membrane separation system.

1.2 Organization of Thesis and Significance of the Contributions

This thesis consists of eight chapters. Chapter 2 (Theoretical Background) presents a literature review of biodiesel production and purification. The chapter also includes an overview of various glycerol removal techniques, a general overview on membrane separation technology and the principle of operation for the separation system used in this compatibility of thesis research. Chapters 3 to 7 consist of a series of manuscripts submitted to refereed scientific journals for publication. Due to this structure, the repetition of some common ideas (e.g., experimental procedures) was inevitable in these chapters. Chapter 8 contains a general discussion which relates Chapters 3 to 7 and offers several conclusions and the recommendations for future work. References and appendices (as appropriate) for each chapter are provided throughout the thesis. Several appendices are also provided. Further details on Chapters 3 to 7 are presented below:

CHAPTER 3 - ***Glycerol removal from biodiesel using membrane separation technology; published in Fuel, 2010, 89: 2260-2266.***

The effect of different materials present in the transesterification reaction, such as water, soap, and methanol, on the final glycerol/FAME separation performance was studied using a modified polyacrylonitrile (PAN) membrane, with a 100 kD molecular weight cut off. Results showed that low concentrations of water had a considerable effect in removing glycerol from the FAME even at approx 0.08 mass %. This will increase the size of the distributed glycerol phase in the untreated FAME leading to its separation by the ultrafiltration membrane.

CHAPTER 4 - ***Effect of methanol and temperature in glycerol removal from biodiesel using membrane separation technology; to be submitted.***

The effect of methanol and temperature on the separation of glycerol from FAME after the first gravity separation step and without water washing was studied. Three types of polymeric membranes in the ultrafiltration range, (100 kD (Ultrafilic™ membrane), 30 kD (PVDF), and 5 kD (PES)) were tested at three fixed operating pressures (172.4 kPa

for the Ultrafilic type, 344.7 kPa for the PVDF and 551.6 kPa for the PES) and three operating temperatures (0, 5 and 25^{o}C) for each membrane type. This paper illustrated that the separation of glycerol was attributed to the formation of a hydrophilic glycerol rich layer on the surface of the membrane, as well as methanol is also retained by the membrane along with glycerol.

CHAPTER 5 – ***Separation of glycerol from FAME using a ceramic membrane; submitted to Fuel Processing Technology.***

This chapter presents results for the effect of using membrane separation to remove free glycerol from FAME using ceramic membranes in the ultrafiltration (0.05 μm) and microfiltration (0.2 μm) ranges at various operating pressures at three different operating temperatures: 0, 5 and 25°C. All runs separated glycerol from the crude FAME. International standards for glycerol content in biodiesel were met after 3 h when utilizing the ultrafiltration membrane setup at 25°C with a concentration factor greater than 1.6.

CHAPTER 6 - ***Effect of soap, methanol and water on glycerol droplet size in biodiesel purification*****;** ***published in Energy & Fuel , 2010, 24: 6179-6186.***

The effect of the various components in the transesterification product stream, i.e., methanol, soap, water and glycerol, on the size of the dispersed glycerol-rich droplets in the FAME was studied. A regression model was calculated to identify which factors had the most significant effect on droplet size and hence, the ability of the membrane separation system to separate glycerol from FAME. The statistical analysis revealed the significant effect of water and glycerol on increasing the droplet size while methanol and soap served to reduce the droplet size. Experimental results using a polyacrylonitrile (PAN) membrane at a temperature of 25°C, showed that addition of small amounts of water was found to improve the removal of glycerol from FAME and a glycerol content as low as 0.013 mass%, well below the standard of 0.020 mass%.

CHAPTER 7 - ***Effects of water concentration, trans-membrane pressure (TMP) and temperature on free glycerol removal from biodiesel using membrane separation technology; to be submitted.***

The effect of trans-membrane pressure (TMP) when different concentrations of water are added to the FAME phase on glycerol removal using ultrafiltration (UF 0.03 μm, polyethersulfone (PES)) and microfiltration (MF 0.1 and 0.22 μm, PES) at 25, 40 and 60°C was studied. Results showed that running at 25°C for the two ranges of membranes produced the best results for glycerol removal and exceeded the ASTM and EN standards. An enhancement of glycerol removal was found by adding small amounts of water up to the maximum solubility limit in FAME. An increase in temperature resulted in an increase in the solubility of water in the FAME and less effective glycerol removal. Application of cake filtration theory and a gel layer model showed that the gel layer on the membrane surface is not compressible and the specific cake resistance and gel layer concentration decrease with increasing temperature. An approximate value for the limiting (steady-state) flux was reported and it was found that the highest fluxes were obtained at the lowest initial water concentrations at fixed temperatures.

1.3 References

[1] Cao, P., Tremblay, A.Y., Dubé, M.A., Morse, K., Effect of membrane pore size on the performance of a membrane reactor for biodiesel production, *Ind. Eng. Chem. Res*., 46: 52-58, **2007**.

[2] Demirbas, A., Biodiesel fuels from vegetable oils via catalytic and non-catalytic supercritical alcohol transesterifications and other methods: a survey, *Energ. Convers. Manage*., 44: 2093–2109, **2003**.

[3] Dubé, M.A., Tremblay, A.Y., Liu, J., Biodiesel production using a membrane reactor, *Biores. Tech*., 93: 639-647, **2007**.

[4] Ghadge, S.0.V., Raheman, H., Biodiesel production from mahua (Madhuca indica) oil having high free fatty acids, *Biomass. Bioenerg*., 28: 601–605, **2005**.

[5] Karaosmanoglu, F., Cıgızoglu, K.B., Melek, T., Ertekin, S., Investigation of the refining step of biodiesel production, *Energy Fuels*., 10: 890-895, **1996**.

[6] Mao, V., Konar, S.K., and Boocock, D.G.B., The Pseudo-single-phase, base-catalyzed transmethylation of soybean oil, *J. Am. Oil Chem. Soc*., 81: 803-808, **2004**.

[7] Van Gerpen, J., Hammond, E.G., Johnson, L.A., Marley, S.J., Yu, L., Lee, I., Monyem, A., determining the influence of contaminants on biodiesel properties, Final report prepared for: The Iowa Soybean Promotion Board, July 31, **1996**.

Chapter 2 Theoretical Background

Chapter 2 – Theoretical Background

2.1 Definition of Biodiesel

Biodiesel is a renewable, biodegradable and environmentally safe fuel for use in diesel engines that can be produced from vegetable oils, animal fats and/or used cooking oils via alcohol transesterification. It is comprised of fatty acid alkyl esters (FAAE). It can be used in its neat form or as a blend with conventional diesel fuel. The similarities between biodiesel and diesel fuel show that biodiesel is a successful alternative source of energy in diesel engines (Demirbas, 2003).

2.2 Environmental Advantages

Over one hundred years ago, Rudolf Diesel tested vegetable oil as a fuel for his combustion engine. Between 1930 and 1940, diesel fuel made from vegetable oil was used in emergency situations. Research on vegetable oils was not developed to a great extent because of the low price of crude oil at that time. Recent increases and instabilities in oil prices combined with limited oil resources and environmental issues associated with greenhouse gas (e.g., carbon dioxide) emissions has forced researchers to refocus on vegetable oil and its derivatives as an alternative diesel fuel source. This has the potential to reduce the level of pollutants and carcinogens in our environment (Pryde, 1983; Shay et al., 1993; Ma et al., 1999; Fukuda et al., 2001).

Besides the attractive features of biodiesel listed above, the advantage of using neat biodiesel or blending with petroleum diesel is that it is a plant- and not petroleum-derived fuel which can be domestically produced. In a study performed by the University of Idaho, biodiesel placed in water where microorganisms propagate biodegraded by 95% in 28 days. During the same time period, petroleum diesel fuel degraded by only 40% (Zhang et al., 1998). Compared to petroleum diesel, biodiesel combustion emissions, such as carbon monoxide, particulates, unburned hydrocarbons, SOx emissions and soot are much lower. A slight increase in NOx emissions, however, can be positively influenced by delaying the injection timing in engines (Varese et al., 1996).

A life cycle analysis carried out by Sheehan et al. (1998) using pure biodiesel (B100) in urban buses, showed a substantial reduction in the life cycle emissions of total

particulate matter (32%), CO (35%), and SOx (8%), relative to petroleum diesel. Figure 2.1 shows a net energy balance for various fuels. It is noted that the net energy yield for biodiesel is more than three times that of petroleum diesel fuel on a life cycle basis.

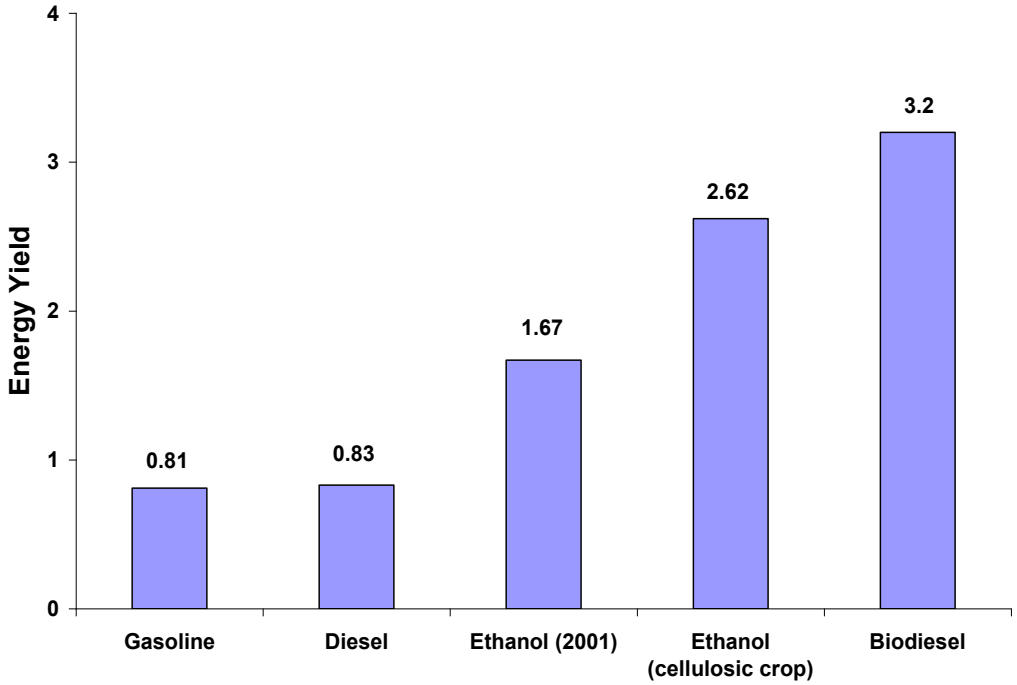

Figure 2.1: Net energy balance for various fuels

USDA / DOE Study, "Lifecycle inventory of biodiesel and petroleum diesel for use in an urban bus". May 1998.

Ethanol (2001) USDA study, "The **2001** Net Energy balance of corn – ethanol."

A small percentage of biodiesel can be used as an additive in low-sulphur formulations of diesel to increase lubricity. Blends containing as low as 1% biodiesel can provide up to 30% more lubricity than petroleum diesel (Knothe et al., 1997). Biodiesel is miscible with petroleum-based fuel in any ratio. As a result, most modern direct-injection diesel engines can be operated without any modification when fuelled with biodiesel-diesel blends or pure biodiesel. Blends of biodiesel and petroleum diesel, such as B20 (a blend of 20% biodiesel and 80% petroleum diesel), provide fuel economy and power output with several health and environmental advantages (Sheehan et al., 1998).

2.3 Economic Feasibility

The price of vegetable oil is a big problem in expanding the use of biodiesel despite its many environmental and socio-economic advantages. As Bender (1999) mentioned in his economic feasibility review for community-scale farmer cooperatives for biodiesel, a review of 12 economic feasibility studies showed that the projected costs for biodiesel from oilseed or animal fats had a range of US$0.30 to 0.69/L, including meal and glycerol credits. Rough projections of the cost of biodiesel from vegetable oil and waste grease are, respectively, US$0.54 to 0.62/L and US$0.34 to 0.42/L.

At the same time, the average US price for pre-tax petro-diesel was priced at US$0.18/L and US$0.20 to 0.24/L in some European countries. Therefore, the high cost of biodiesel has been a major obstacle for commercializing biodiesel produced from neat vegetable oils as compared to the cheaper petroleum based diesel fuel.

2.4 Physical and Chemical Properties of Biodiesel and Diesel

The physical and chemical properties of biodiesel and diesel fuels are shown in Table 2.1 (Fukuda et al., 2001). The volumetric heating value is the heat released when a known quantity of fuel is burned under specific conditions. The cetane number expresses the ignition quality of the fuel and the flash point expresses the tendency of the fuel to form a flammable mixture with air.

The data in Table 2.2 show that biodiesel has a higher cetane number that can reduce the ignition delay of the air-fuel mixture resulting in a smoother running engine producing less noise. The higher flash point of biodiesel indicates that its storage and transportation are much safer than that of petroleum diesel. The viscosity of biodiesel is slightly higher than that of diesel fuel but is within an acceptable range. The properties of biodiesel at low temperatures, such as the higher cloud point and freezing point, are poorer than those of petroleum diesel.

Table 2.1: Physical and chemical properties of vegetable oil sources and petroleum diesel (Fukuda et al., 2001)

Vegetable oil methyl ester	**Kinematic viscosity (mm^2/s)**	**Cetane number**	**Volumetric heating value (MJ/L)**	**Cloud point (°C)**	**Flash point (°C)**	**Density (g/cm^3)**
Peanut	4.9 (37.8°C)	54	33.6	5	176	0.883
Soybean	4.5 (37.8°C)	45	33.5	1	178	0.885
Babassu	3.6 (37.8°C)	63	31.8	4	127	0.879
Palm	5.7 (37.8°C)	62	33.5	13	164	0.880
Sunflower	4.6 (37.8°C)	49	33.5	1	183	0.860
Tallow	----	----	----	12	96	----
Rapeseed	4.2 (40°C)	51 – 59.7	32.8	----	----	0.882 (15°C)
Used rapeseed	9.48 (30°C)	53	36.7	----	192	0.895
Used corn oil	6.23 (30°C)	63.9	42.3	----	166	0.884
Diesel fuel	**1.2 – 3.5 (40°C)**	**51**	**35.5**	**----**	**----**	**0.83 – 0.84**

The chemical composition of the fatty acid alkyl esters (FAAE or biodiesel) shows a considerable amount of oxygen (10 – 11%) and a reduced amount of carbon (77%), while the hydrogen content is similar to that of petroleum diesel. Biodiesel also contains negligible amounts of sulphur and phosphorus and no aromatic compounds. These chemical characteristics lead to a favourable emission profile, i.e., a decrease of CO, polycyclic aromatic hydrocarbon (PAH) and particulates in exhaust gas, compared

with fossil petroleum diesel. Therefore, biodiesel derived from vegetable oils and animal fats is rated as a strong candidate as an environmentally friendly alternative to diesel fuels in many countries (Korbitz, 1999; Van Gerpen, 2005).

2.5 Specifications of Biodiesel

To limit and reduce hazards and mechanical failure and promote engine life, standard specifications have been created that define the quality of biodiesel. The first biodiesel fuel standard was established in Austria in 1991 for rapeseed oil methyl esters as diesel fuel, followed eventually by the North American (ASTM D6751) and European (EN14214) standards (Mao et al., 2004; Ghadge et al., 2005). The Canadian General Standards Board (CGSB) recognizes ASTM D6751 as the Canadian biodiesel standard. Table 2.2 gives general quality parameters for biodiesel. Density and cetane number are dependent on the choice of vegetable oil. Impurities, such as free and total glycerol (total glycerol is the sum of free glycerol and glycerol bound as mono-, di-, and triglycerides), water (moisture), free fatty acid (by limiting the acid number), and residual alcohol (by limiting the flash point), need to be limited in biodiesel because their presence can lead to fuel degradation during storage and to significant operational problems such as engine deposits. The viscosity also reflects the content of unreacted triglycerides.

Table 2.2: General parameters of the quality of biodiesel (Meher et al., 2006)

Parameters	**Austria (ON)**	**Czech republic (CSN)**	**France (Journal Official)**	**Germany (DIN)**	**Europe (EN 14214)**	**North America (ASTM D6751)**
Density at 15°C (gm/cm^3)	0.85 – 0.89	0.87 – 0.89	0.87 – 0.89	0.876 – 0.89	0.86 – 0.9	-
Viscosity at 40°C (cSt)	3.5–5.0	3.5–5.0	3.5–5.0	3.5–5.0	3.5-5.0	1.9–6.0
Flash Point (°C)	100	110	100	110	>101	130
CFPP* (°C)	0 / -5	- 5	-	- 10 / -20	-	-
Pour Point (°C)	-	-	-10	-	0 / -5	-
Cetane Number	≥ 49	≥ 48	≥ 49	≥ 49	≥ 51	≥ 47
Acid Number (mg KOH/g)	≤0.8	≤0.5	≤0.5	≤0.5	≤0.5	≤0.8
Carbon residue (%)	0.05	0.05	-	0.05	<0.03	0.05
Methanol/ Ethanol (% mass)	≤0.2	-	≤ 0.1	≤ 0.3	≤ 0.2	-
Ester (content) (% mass)	-	-	≥ 96.5	-	≥ 96.5	-
Monoglyceride (% mass)	-	-	≤ 0.8	≤ 0.8	<0.8	-
Diglyceride (% mass)	-	-	≤ 0.2	≤ 0.4	<0.2	-
Triglyceride (% mass)	-	-	≤ 0.2	≤ 0.4	<0.4	-
Free glycerol (% mass)	≤ 0.02	≤ 0.02	≤ 0.02	≤ 0.02	≤ 0.02	≤ 0.02
Total glycerol (% mass)	≤ 0.24	≤ 0.24	≤ 0.25	≤ 0.25	< 0.25	≤ 0.24
Iodine Number	≤ 120	-	≤ 115	≤ 115	120	-

CFPP* --- cold-filter plugging point.

2.6 Biodiesel Production by Transesterification

There are four primary ways of using vegetable oils to make biodiesel: direct use and blending, micro emulsion, thermal cracking (pyrolysis) and transesterification. The most commonly used method is transesterification, which is the reaction of vegetable oil with an alcohol to form esters and glycerol. The reaction is shown in Figure 2.2.

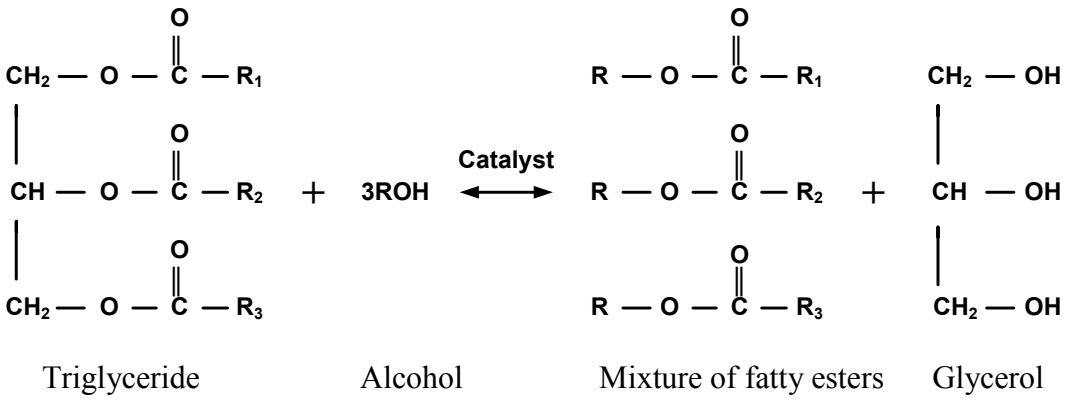

Figure 2.2: Transesterification reaction

R_1, R_2, and R_3 are hydrocarbon chains called fatty acids. For common vegetable oils and animal fats, they are usually fatty acids of 16-18 carbons with 0-3 double bonds, which are mostly stearic, palmitic, oleic, linoleic and linolenic. These types are:

Palmitic: R = - $(CH_2)14 – CH_3$, 16 carbons, with no double bonds (16:0)

Stearic: R = - $(CH_2)16 – CH_3$, 18 carbons, 0 double bonds (18:0)

Oleic: R = - $(CH_2)7$ CH=CH $(CH_2)7CH_3$, 18 carbons, 1 double bond (18:1)

Linoleic: R = - $(CH_2)7$ CH=CH-CH_2-CH=CH $(CH_2)4CH_3$, 18 carbons, 2 double bonds (18:2)

Linolenic: R = - $(CH_2)7$ CH=CH-CH_2-CH=CH-CH_2-CH=CH-CH_2-CH_3, 18 carbons, 3 double bonds (18:3).

Different types of alcohols can be used in the transesterification reaction such as methanol, ethanol, propanol, and butanol. Methanol and ethanol are used most frequently,

especially methanol because of its low cost and ease of recovery compared to other alcohols. As shown in Figure 2.2, the transesterification is an equilibrium reaction. To force the reaction towards completion, a molar ratio of alcohol to triglyceride in excess of stoichiometry (3:1) is needed. In practice, a ratio between 6:1 to 12:1 is used to drive the reaction to a maximum ester yield. The products of the transesterification of triglyceride with methanol are FAME and glycerol, but due to the reversibility of the reaction and the excess methanol used, unreacted oil, unreacted methanol, and traces of water and residual catalyst are often found in the product stream. The transesterification reaction can be promoted by a variety of catalytic methods, the most popular being sodium or potassium methoxide.

Transesterification consists of a number of consecutive, reversible reactions as shown in Figure 2.3 (Freedman et al., 1986; Schwab et al., 1987). A mole of ester is liberated at each step. The reactions are reversible, although the equilibrium lies towards the production of fatty acid esters and glycerol. The reaction mechanism for alkali-catalyzed transesterification was formulated as three steps (Eckey, 1956). The first step is an attack on the carbonyl carbon atom of the triglyceride molecule by the anion of the alcohol (methoxide ion) to form a tetrahedral intermediate. In the second step, the tetrahedral intermediate reacts with an alcohol (methanol) to regenerate the anion of the alcohol (methoxide ion). In the last step, rearrangement of the tetrahedral intermediate results in the formation of a fatty acid ester and a diglyceride. The triglyceride is converted to diglyceride, monoglyceride and finally, glycerol. Figure 2.4 shows the mechanism of alkali-catalyzed transesterification of triglycerides with alcohol.

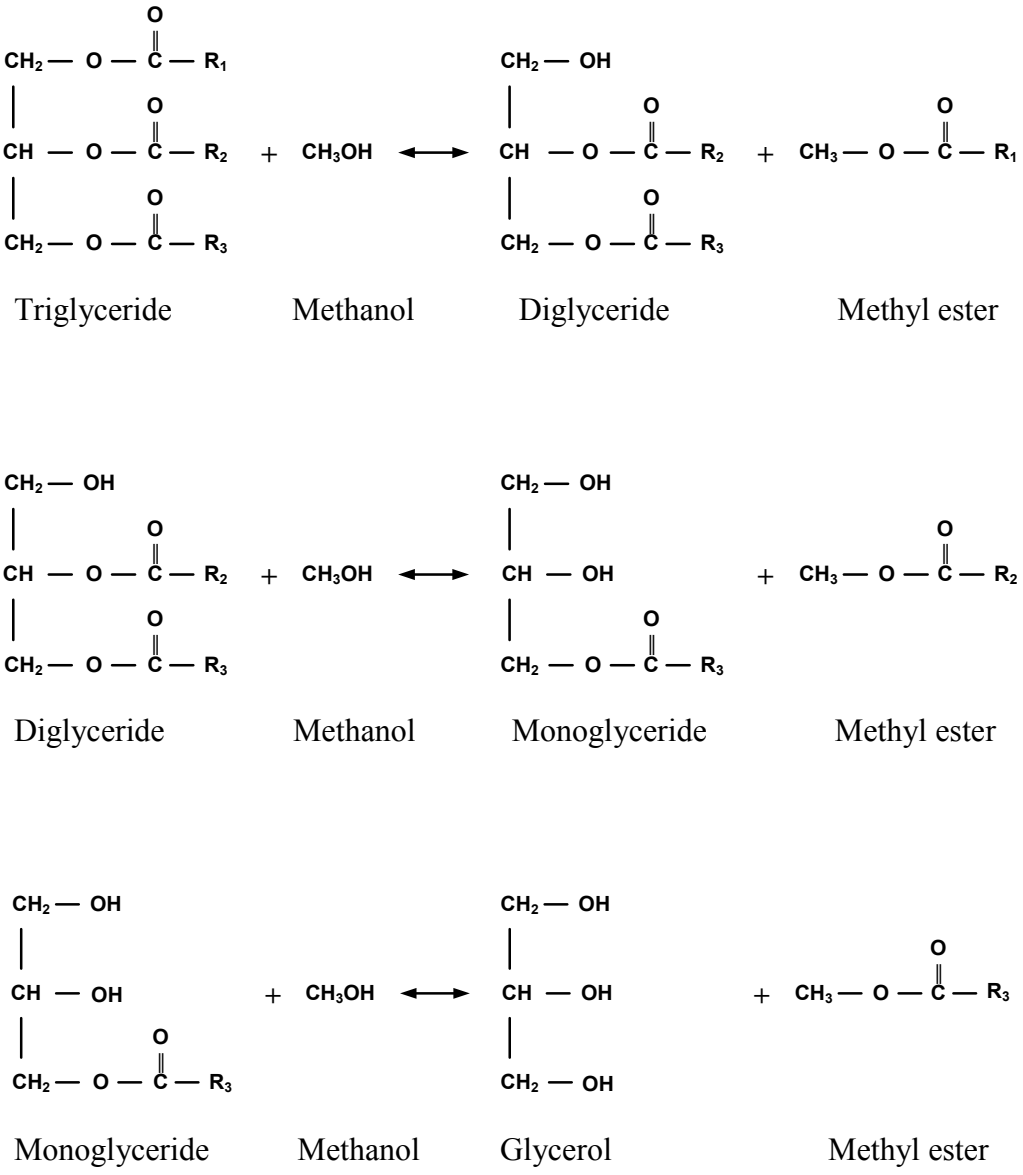

Figure 2.3: General equation for transesterification of triglycerides

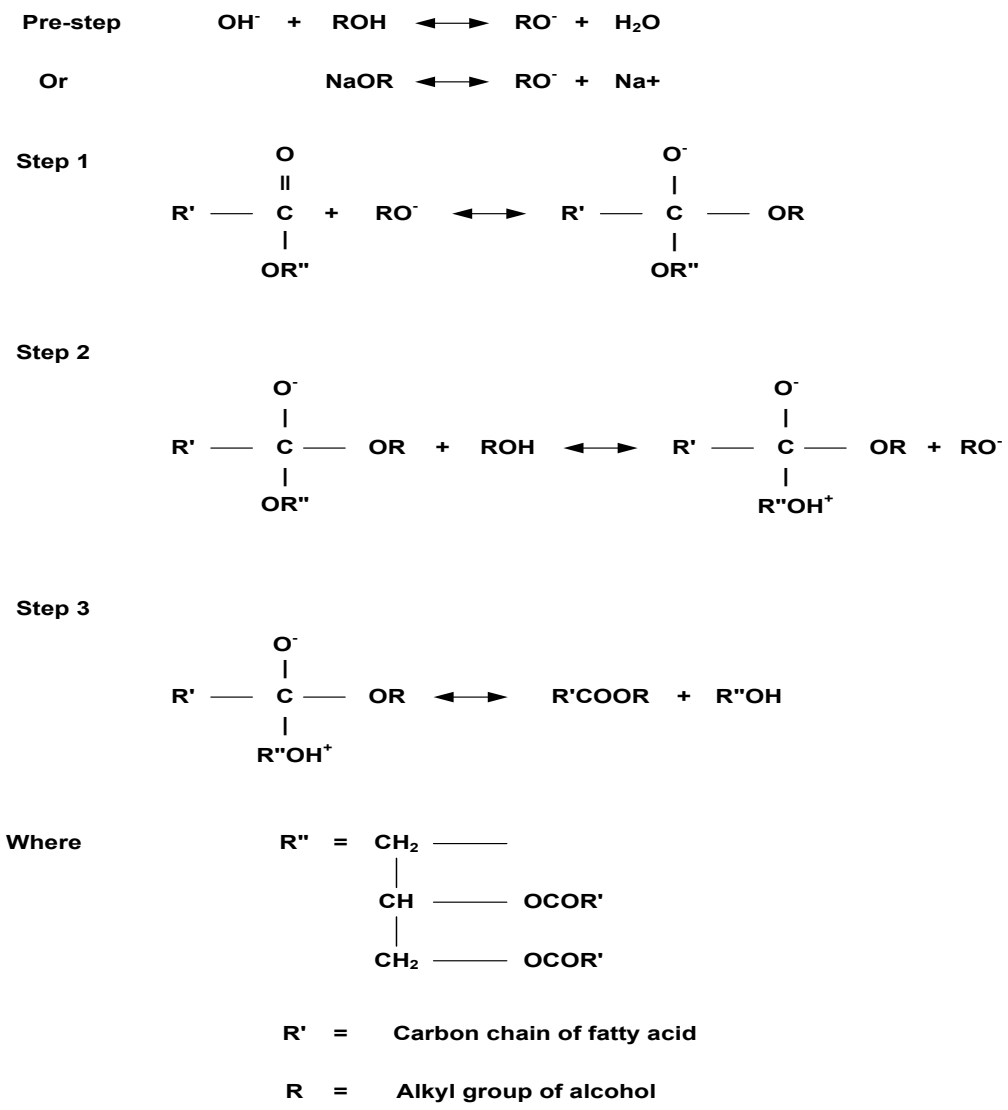

Figure 2.4: The mechanism of alkali-catalyzed transesterification of triglycerides with alcohol (Eckey, 1956).

The presence of free fatty acid (FFA) and water in the alkali-catalyzed transesterification process can reduce biodiesel yield, and impede downstream separation and purification. Thus, one would preferably employ oils and fats with low FFA and water contents and all other materials (e.g., methanol) should be substantially anhydrous. In the case for high (FFA) in the oil feedstock, a reaction with the alkaline catalyst will result in a saponification reaction as shown in Figure 2.5. This soap affects the separation

of glycerol during the water wash step. In the presence of water, hydrolysis of the triglycerides to diglycerides to form FFA is highly likely as shown in Figure 2.6. This reaction results in the consumption of triglycerides and catalyst, and therefore reduces the biodiesel yield. Ma et al. (1999) suggested that the FFA content of the vegetable oils should be as low as possible, below 0.5%.

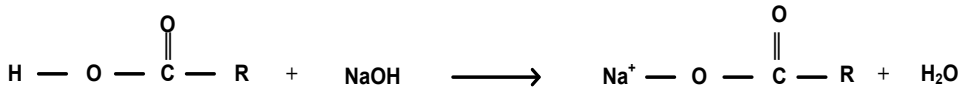

FFA Sodium hydroxide Sodium soap Water

Figure 2.5: FFA effects in the transesterification

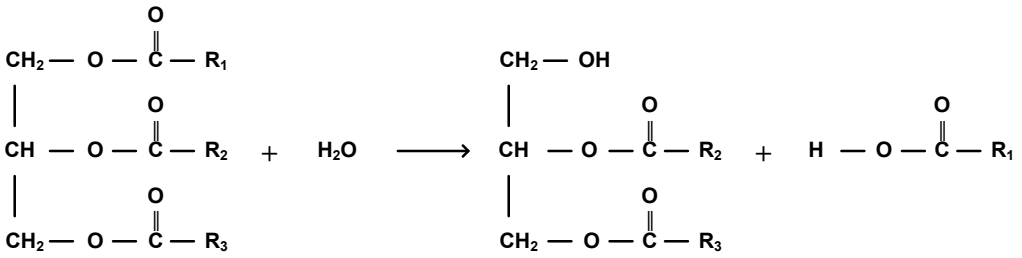

Triglyceride Water Diglyceride FFA

Figure 2.6: Hydrolysis of triglyceride to form FFA

2.7 General Transesterification Process

Most commercial biodiesel producers use a multi-step alkali-catalyzed process for the transesterification process. Figure 2.7 shows a typical process diagram for biodiesel production. Other approaches have been proposed including using acid catalysis and enzymes. The use of acid catalysts has been found to be useful for pre-treating high free

fatty acid feedstocks but the reaction rates for converting triglycerides to methyl esters are very slow (Van Gerpen, 2005). Enzymes have shown good tolerance for the free fatty acid level of the feedstock but the enzymes are expensive and unable to provide the degree of reaction completion required to meet the ASTM fuel specification (Huang et al., 2010; Van Gerpen, 2005).

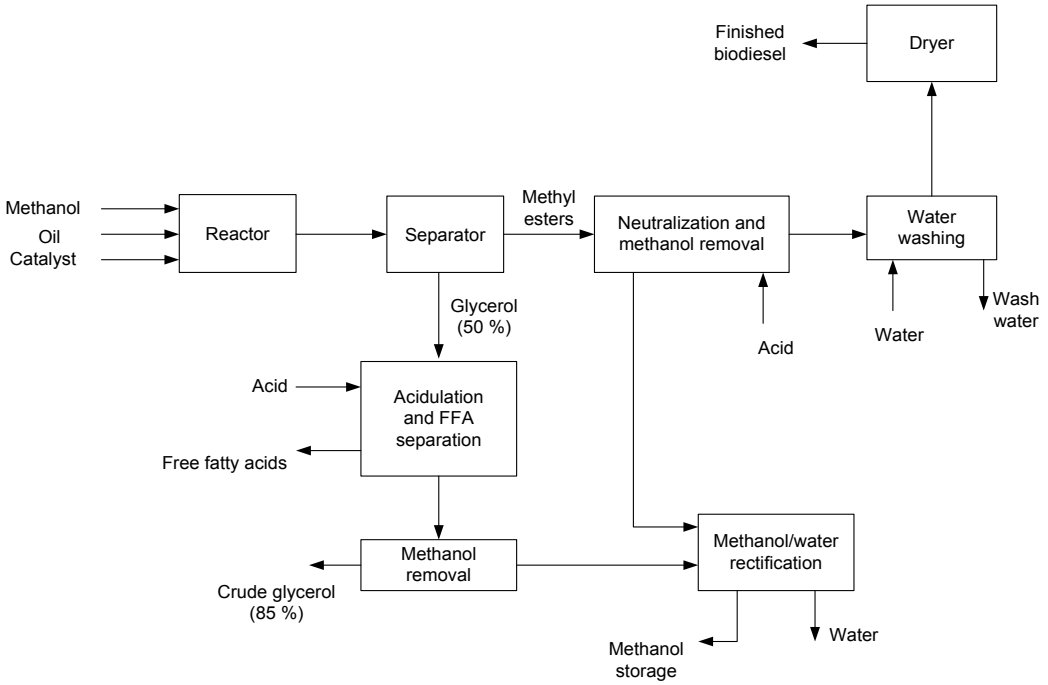

Figure 2.7: General process flow diagram for biodiesel production (Van Gerpen, 2005)

2.8 Alkali -Catalyzed Biodiesel Production

A schematic diagram of the alkaline-catalyzed process for biodiesel production is shown in Figure 2.8. The overall process includes transesterification, separation of the crude ester layer from the glycerol layer, purification of the methyl esters, and recovery of the glycerol as a high-grade co-product. Usually, the process is carried out with an alkaline catalyst dissolved in excess methanol under agitation, controlled temperature and atmospheric pressure. After the more or less complete conversion of oils or fats, the reaction mixture is allowed to cool to room temperature and settle under gravity.

Due to the low solubility of the by-product glycerol in the esters, the heavier glycerol settles down in the bottom layer and the esters are left in the upper layer. Traces of glycerol can remain suspended in the ester phase along with small amounts of tri-, di- and monoglycerides, while the residual catalyst and unreacted alcohol are distributed between the two layers. The lower glycerol layer is removed, while the upper methyl ester layer is washed with water to remove the residual glycerol and base catalyst and any soaps formed during the reaction. Finally, methanol and water present in the ester layer are eliminated by distillation or evaporation under vacuum or atmospheric pressure. Alkaline-catalyzed transesterification can be completed within 1-2 h near the boiling point of the alcohol (60 – 65°C). It can achieve nearly 100% conversion and can be operated under moderate reaction conditions.

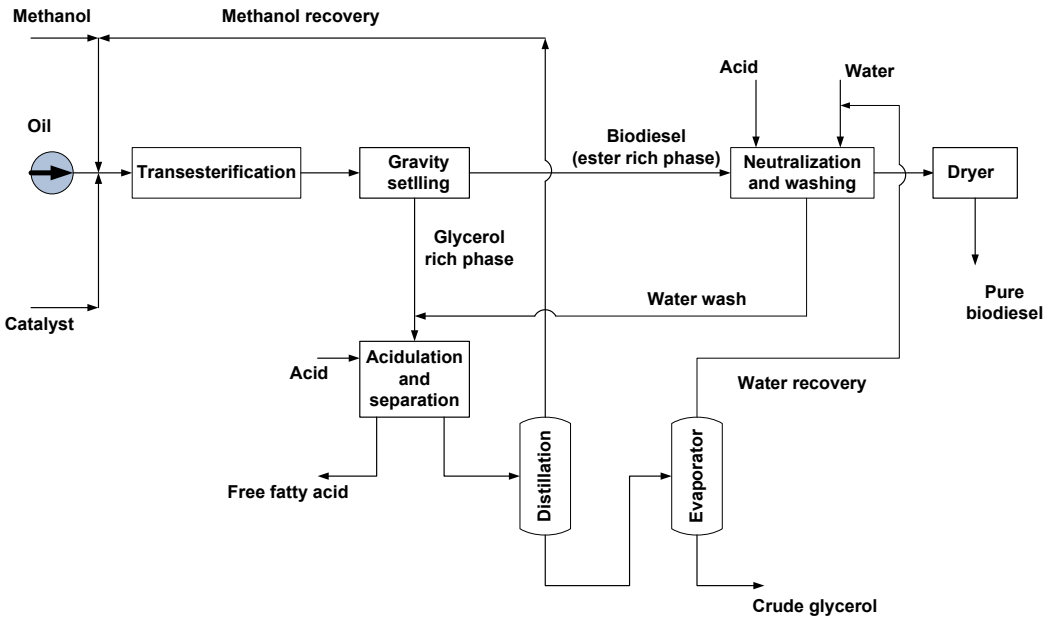

Figure 2.8: Process flow diagram of the alkaline-catalyzed transesterification process

2.9 Biodiesel Purification Steps

The purity of biodiesel is an important issue, and is specified in the biodiesel standards (see Table 2.2) and affects the cost of the final product. In order to produce high quality biodiesel, a series of purification processes are usually needed. These can include: gravitational settling, centrifugation, water washing, adsorption and distillation. It is necessary to remove the impurities in the ester phase (non-polar phase) because they will strongly affect the properties of the biodiesel fuel produced. For instance, the presence of catalyst in biodiesel fuel may damage the injector pump and pose corrosion problems in the engine. The presence of high levels of methanol can accelerate the deterioration of natural rubber seals and gaskets. A high content of glycerol, which is a product from the transesterification reactions, may be present in biodiesel as a result of inappropriate processing, such as insufficient separation of the glycerol phase or insufficient washing by water after separation. As mentioned above, free glycerol can result in its eventual separation from the biodiesel during storage thereby causing problems during engine operation. Monoglycerides can cause turbidity (crystals) in the mixture of esters. This problem is particularly pernicious for the transesterification of animal fats such as beef tallow (Ma et al., 1998). In addition, these impurities can raise the cloud and pour points of the biodiesel.

Methyl ester and unreacted triglycerides are essentially insoluble in water, while soap, methanol and glycerol are soluble. Therefore, adding water to the non-polar phase is usually the first step in purifying it of these impurities. This “water-washing” step allows the soap, the alkaline catalyst residue and small amounts of glycerol, mono- and diglycerides in the product mixture to be removed. Unfortunately, the separation of the non-polar phase from the water layer is usually difficult, and this step produces a large amount of waste water containing methanol; for each litre of biodiesel produced, 10 L of waste water are produced (Karaosmanoglu et al., 1996; Demirbas, 2003). This will increase the size and the cost of the separation equipment. After the washing step, the wash water containing the extracted methanol and the residual catalyst are typically disposed without further treatment, resulting in loss of these materials. This results in both an economic loss and an environmental disposal problem. Also, the process water must be “softened” to eliminate calcium and magnesium salts and treated to remove iron

and copper ions. The wash water will have a fairly high biological oxygen demand (BOD) from the residual fat/oil, ester, and glycerol. Waste waters should meet local municipal waste treatment plant disposal requirements. The existence of saturated fatty acids in the biodiesel can cause sediment formation. The formation of haze in the mixture of these esters will appear if the temperature is decreased. This can cause serious problems if operating an engine in cold weather. With the water washing process, these saturated fatty acid esters cannot be removed.

As mentioned above, in the case of high free fatty acid feedstock, significant soap formation will ensue during the biodiesel production. The presence of soap in large quantities can cause difficulties in separation of the non-polar and polar phases because the sodium soap is a strong surface active agent. Its presence reduces the interfacial tension and prevents coalescence of biodiesel droplets, thus leading to an easy formation of a considerably stable ester-in-water type of emulsification. This emulsified layer will prevent the separation of the non-polar biodiesel phase from the water layer, resulting in a longer separation time and most importantly, losses of esters due to incomplete separation during water washing. Demulsification becomes the main means to solve emulsion problems during water washing and to improve the efficiency of water washing, by using gravity separation, centrifugation, and heating or by the addition of chemical demulsifiers or emulsion breakers (Becher, 2001).

Gravitational settling is based on the significant difference in density between the non-polar biodiesel-rich phase and the polar methanol/glycerol-rich phase. Centrifugation, also used with water washing to accelerate the separation of impurities, works by exposing the mixture to a centrifugal force. The denser phase will be preferentially separated to the outer surface of the centrifuge and because the glycerol is insoluble in biodiesel and soluble in the water phase, almost all of the glycerol is easily removed. A sufficient residence time for the less dense oil to float on top of the water surface is, of course, required. However, this method is less effective for dealing with biodiesel-water emulsions containing very small biodiesel droplets and the time to separate the biodiesel phase completely from the emulsions may take several hours, days, or even may never separate. The disadvantage of the centrifuge is its initial cost, and the need for considerable maintenance.

Vacuum distillation can be used to remove methanol and water from the biodiesel to meet the standards, since the residual methanol level in biodiesel should be very low. The allowable alcohol level is specified in European biodiesel standards (0.2 % mass max), but is not included in the ASTM standard. Tests have shown that as little as 1% methanol in the biodiesel can lower the flashpoint of the biodiesel from 170 to less than 40^{o}C. Distilled biodiesel tends to have a greater problem with free glycerol due to glycerol carry-over during distillation (Van Gerpen et al., 2004).

Many researchers studied the purification steps in different ways, either by using water wash, reducing the time of the reaction (i.e., speeding the reaction), or using certain absorbents in order to reducer the final cost of the biodiesel product. Freedman et al. (1984) reported that the ester layer could be first purified by dissolving in petroleum ether, then by the addition of water, glacial acetic acid or phosphoric acid drop by drop until reaching pH 7. The product was then washed 3 times with water, and dried with anhydrous magnesium sulfate. It was filtered, and the solvent was removed on a rotary evaporator or distilled under atmospheric pressure. A similar washing method was also used by Ikwuagwu (2000).

Nye et al. (1983) reported in his study on the conversion of used frying oil into biodiesel that the top ester layer was washed three times with dilute hydrochloric acid or saturated sodium bicarbonate followed by water (three times) and then dried over anhydrous sodium sulfate.

Dmytryshyn (2004) concluded that water washing was an inefficient method, because the soap emulsions were difficult to remove. A method involved washing the biodiesel with silica gel was used.

Karaosmanoglu et al. (1996) investigated three methods to purify the biodiesel produced from rapeseed oil using alkali-catalyzed transesterification. One was to wash the reaction mixture with hot water, the second was to wash the mixture with petroleum ether and water, and the third was to use sulphuric acid to neutralize the mixture followed by an evaporation to remove the methanol. They concluded that the use of hot water was the best way to purify the products but failed to mention the large amount of waste water produced.

Hayafuji et al. (1999) studied a production method of biodiesel from waste oil. After the product mixtures were separated by a centrifugal separator into two phases, they used solid absorbents selected from a group comprised of activated carbon, activated carbon fibre, activated clay, acid clay, silica gel, activated alumina and molecular sieves, to remove the impurities in the light phase (ester-rich layer). Compared to the process of removing the impurities by warm water washing or by acid neutralization, this purification process is simple and requires no water removal after washing. However, using large amounts of adsorbents leads to another problem of separating the adsorbents from the final products. Moreover, these adsorbents need regeneration, which involves additional expenses.

Bam et al. (1995) provided an economical and environmentally sound process for producing purified alcohol esters of triglycerides from sources such as vegetable oils, fish oil, animal fats and waste oils. Their process relied upon a by-product alcohol, such as glycerol, or recovery alcohol to purify the alcohol ester to a degree that they did not require water washing.

He et al. (2006) studied three traditional methods for biodiesel purification: (i) washing with distilled water; (ii) washing with acid (HCl); and (iii) dissolving and extracting in a solvent (hexane or petroleum ether) and then washing with distilled water. They concluded that biodiesel with a high purity (97.5%) could be obtained by all three methods, but serious emulsification occurred during the refining processes, which led to high product losses. Cetinkaya and Karaosmanoglu (2004) studied the optimum conditions for biodiesel production from restaurant-originated used cooking oil followed by washing with hot water The crude ester phase was washed with hot distilled water, at 50°C, at a ratio of 1:1, two times without stirring and three times with stirring to find the optimum number of washing stages for the chosen reaction conditions by determining the reduction in the total glycerol content. Washing with hot distilled water can be chosen as a purification method. Five to seven consecutive washing steps were sufficient to meet the required EN 14214 and ASTM D 6751 limits.

Saka and Kusdiana (2001) developed a method for transesterification without using catalyst to make the reaction time shorter and the purification procedure for the rich ester phase simpler and avoid water washing. They transesterified the rapeseed oil under

extreme conditions using a batch-type reaction vessel preheated to 350 and 400°C and at a pressure of 45 MPa, and with a molar ratio of 1:42 of the rapeseed oil to methanol. It was consequently demonstrated that, in a preheating temperature of 350°C, 240 s of supercritical treatment of methanol was sufficient to convert the rapeseed oil to methyl esters, and the only component necessary for removal after the reaction was methanol. This process showed an improvement in reaction time as well as simplifying the purification steps but it made the system very complex and costly in terms of both capital and operating costs.

Saka and Kusdiana (2004) investigated the effect of water on the yield of methyl esters in the transesterification of triglycerides and methyl esterification of fatty acids as treated by catalyst-free supercritical methanol. They observed that the separation of methyl esters and glycerol from the reaction mixture became much easier in the presence of water, because it had the capability of dissolving both non-polar and polar solutes since its dielectric constant can be adjusted from a room temperature value of 80 to a value of 5 at its critical point (Holliday et al., 1997).

There are adsorbents on the market that selectively absorb hydrophilic materials such as glycerol and mono- and diglycerides (e.g., Magnesol ($MgSiO_3$) from the Dallas Group). This treatment, followed by an appropriate filter, was useful in removing biodiesel contaminants such as water, soaps, free glycerol and unreacted glycerides. However, this adsorbent cannot be recycled in the process and alternatives for its final disposal are still unclear, particularly in large-scale experiments (Karla et al., 2007).

2.10 Gravitational Settling as a Purification Method

Gravitational settling is often used as the first biodiesel purification step immediately after completion of the reaction. This involves the separation of the polar methanol/glycerol-rich phase from the non-polar biodiesel-rich phase. One can ask what will happen if the gravitational settling time is increased to remove the remaining dispersed glycerol from the biodiesel-rich phase. Additionally, how much of the dispersed glycerol can be removed if we apply centrifugation after gravitational settling? If these steps allow one to achieve the biodiesel purity standards for glycerol content, the water washing step may be avoided and the cost of purification may be reduced. Three

different samples were taken from three different batches of produced biodiesel. These samples were neutralized and heated to vaporize any methanol and were analyzed by dynamic light scattering (DLS) to determine the droplet diameter distribution of the suspended glycerol. We will assume in our gravitational settling calculation that we have only free glycerol, the flow is laminar, and the droplets are spherical in shape. From the results, we calculated the settling velocity of these droplets and the time needed to reach the US (ASTM) and European Standards as follows:

$$\nu = \left(\frac{4g(\rho_p - \rho_{BD})d}{3C_D \rho_{BD}} \right)^{\frac{1}{2}} \qquad (2.1)$$

$$\mathrm{Re} = \frac{\nu \, \mathrm{d} \, \rho_{BD}}{\mu_{\mathrm{BD}}} \qquad (2.2)$$

Where:

ρ_p = Density of the droplets (glycerol) (gm/cm^3) = 1.261

ρ_{BD} = Density of fluid (biodiesel) (gm/cm^3) = 0.875

g = Gravitational acceleration constant (9.81 m/s^2)

d = Droplet diameter (m)

C_D = Coefficient of drag = f (Re)

ν = Settling velocity of the droplet (m/s)

μ_{BD} = Viscosity of the biodiesel (dynamic viscosity) = 3.5 *10^{-2} gm/cm .s

The results of the DLS measurements are shown in Table 2.3 and Figure 2.9 which shows the size distribution (diameter distribution) of the three samples. It is seen that most of the droplets were between two major peaks with different diameters. For our calculations, we took both peaks into consideration, and took the average of each peak for the three samples to get the most representative diameter and the results of the calculations for the settling velocity are shown in Table 2.4.

Table 2.3: Dynamic Light Scattering results

	Diameter Peak 1 (nm)	Diameter Peak 2 (nm)	Wt% glycerol*
Sample 1	83.52	5366	0.18
Sample 2	81.34	5198	0.13
Sample 3	86.26	585.9	0.124
Average	83.70	3716.63	0.144

* ASTM D6751 for free glycerol is 0.02 wt% glycerol

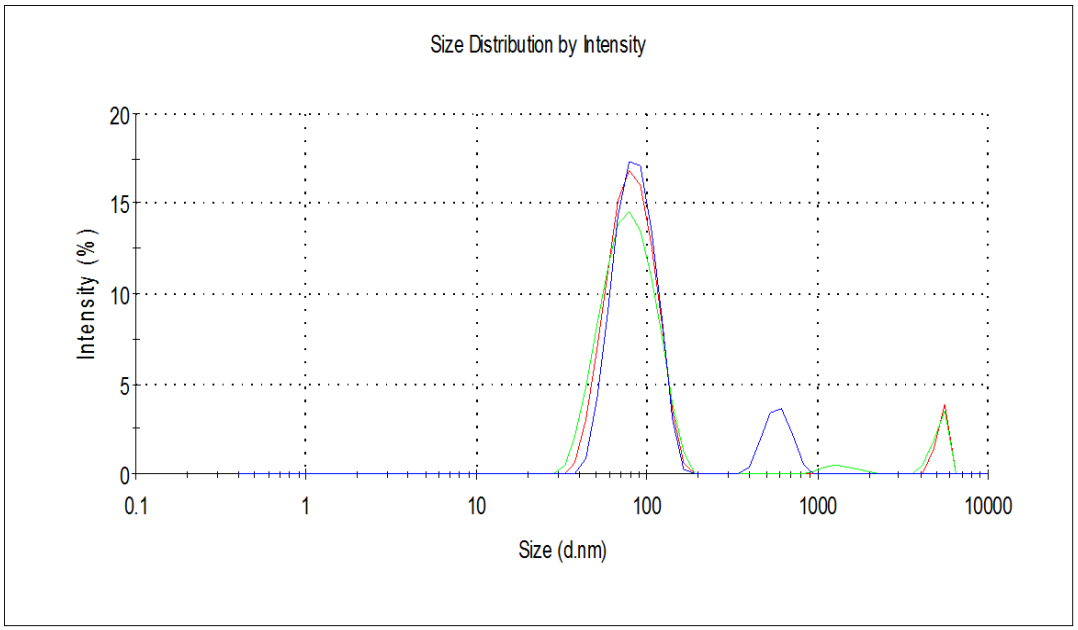

Figure 2.9: Dynamic Light Scattering size distribution of the three samples.

Table 2.4: Calculation results for settling velocity

Droplet diameter (m)	Re	Settling velocity, (m/s)	Mass of the glycerol droplet (kg)
3.7×10^{-06}	7.6×10^{-07}	8.2×10^{-07}	3.3×10^{-14}
8.3×10^{-08}	8.6×10^{-12}	4.1×10^{-10}	3.7×10^{-19}

It is clear that in gravitational settling the only force that affects the droplets is the gravitational force, which is equal to the mass times the gravity. In this case, and for simplicity of explanation the other forces and factors that may affect the settling were ignored such as the drag force, collisions, intermolecular attractions, temperature and viscosity. As an example, if we take the largest likely droplet mass which is 3.3×10^{-14} kg, as shown in Table 2.4, the force exerted on that droplet will be 3.24×10^{-13} N. From Table 2.4, it is clear that the settling velocity needed to precipitate a droplet of glycerol with a mass of 3.3×10^{-14} kg is 8.2×10^{-07} m/s. In other words, if we assume the droplets are of glycerol we would need around fifteen days for the glycerol droplets to settle a distance of one metre, while if we take the smallest likely droplet mass which is 3.7×10^{-19} kg, as shown in Table 2.4, the force exerted on that droplet will be 3.63×10^{-18} N. From Table 2.4, the settling velocity of a glycerol droplet with a mass of 3.7×10^{-19} kg is 4.1×10^{-10} m/s. We would need around ninety years for the glycerol droplets to settle a distance of one metre. For centrifugation in a BTPX 205 high g force disc bowl centrifuge (g-force = 12800 m/s^2) a settling distance will be around 0.45 m in ten days for the smallest droplet mass in Table 2.4. This settling distance is related to a 0.144 wt% glycerol as shown in Table 2.3 and is much higher than the ASTM standard. This would impose unreasonable residence times in a centrifuge and precludes the use of centrifugation (let alone regular gravitational settling) to produce ASTM grade biodiesel.

2.11 Membrane separation technologies

Membrane separation technology has been used for many applications in fields outside of biodiesel production and purification, such as the desalination of sea and brackish water, for treating industrial effluents, and the purification of food and pharmaceutical products (Strathmann, 2001). There is great potential for membrane

technology that can provide solutions for many environmental problems by recovering valuable products as well as treating effluents and minimizing their harm to the atmosphere.

A membrane presents a physical barrier that restricts the transport of various chemical species in a rather specific manner, it can be homogeneous or heterogeneous, symmetric or asymmetric in its structure, and it may be either neutral, or may carry positive or negative charges, or both. Its thickness may vary between less than 100 nm to more than a centimetre (Strathmann, 1981). Common membrane processes include microfiltration (MF), ultrafiltration (UF), reverse osmosis (RO), electro-dialysis (ED), gas separation (GS), nano-filtration (NF), and pervaporation (PV). These are largely differentiated by the size of the molecules being separated and/or the pore size of the membrane.

2.12 Selection of membrane materials

The membrane material and membrane type (e.g., MF, UF and NF) define the membrane separation system. The optimum performance of a membrane often directly correlates with proper membrane material selection. Various membranes can be used to make MF and UF membranes. Most common polymers such as different cellulose derivatives, polysulfone and polyvinylidene fluoride (PVDF) are used to make polymeric membranes. Specific polymers can significantly impact membrane performance, maintenance characteristics, and efficiencies.

Several MF and UF membranes are capable of separating particles in the approximate size range of 0.1 to 10 μm and 1 to 100 nm, respectively (Marion, 2006). They are selected on the basis of: 1- The pore size of the membrane, because it determines to a large extent what substances pass through the membrane and what substances are retained; and 2- the chemical resistance and interaction parameters with particles, because membrane materials determine the chemical resistance and susceptibility to fouling.

Solubility parameters between the solvent and the type of membrane used and resistance to alcohol medium is an important basis for choosing the membrane. After

completion of the reaction, the transesterification product is a multi-component mixture containing mainly FAME, methanol, glycerol, water and salts.

The advantages of ceramic membranes in comparison to polymeric membranes are their enhanced mechanical strength and structural stiffness, corrosion and thermal resistance, stability of operating characteristics, the possibility of multiple regenerations and resistance to bacterial attack (Komolikov et al., 2002). This makes it possible to use ceramic membranes for separation of solutions over a wide pH range (from 0 to 14), at high temperatures and pressures (1 – 10 MPa), and in corrosive media. The material used for ceramic membranes may include oxides of aluminum, titanium and zirconium. Multilayer ceramic membranes made by these materials are used for the separation of oil-in-water emulsions and for treatment of waste effluents. They also could be used in chemical, pharmaceutical and food manufacturing industries (Komolikov et al., 2002).

2.13 Principle of membrane separation

The proposed principle for the membrane separation of glycerol from FAME relies on the creation of large particles during the continuous circulation of a feed mixture based on a "feed and bleed" configuration (Porter, 1990). The continuous phase is non-polar (hydrophobic, in this case, and FAME-rich) and the dispersed phase is polar (hydrophilic, in this case, and methanol/glycerol-rich). The continuous FAME phase contains, as a result of the reaction, dispersed droplets of glycerol, methanol, and traces of mono- and diglyceride, and soap (polar and non-polar structure). The methanol and glycerol have a great affinity to each other and, at the same time, methanol has a slight miscibility with FAME. As a result, if glycerol is present above its solubility limit, it should dephase and form droplets in the continuous FAME phase. In addition to the presence of methanol and glycerol, there are also traces of soap and mono-, and diglyceride in the FAME phase. These materials can act as surfactants (one polar end and one non-polar end), where the polar ends will prefer to associate with the polar glycerol/MeOH droplets and the non-polar ends will stay in the non-polar FAME phase.

2.14 Gas chromatography (GC) analysis

GC analyses are used to determine the amount of a specific contaminant or class of contaminants in methyl esters. The sample mixture is separated mainly by the boiling point and chemical structure. In order to transfer glycerol as well as mono-, di-, and triglyceride into more volatile compounds, their free hydroxyl group are silylated with N-methyl-N-(trimethylsilyl)trifluoroacetamide (MSTFA) prior to analysis. Two internal standards, butanetriol for the determination of free glycerol and tricaprin for the determination of glycerides, are used in the calibration process as well as in the analysis. ASTM method D6584 is to be used for this purpose and states that the calibration plot for each solution standard is to use the response ratio (rsp, y - axis) versus the amount ratio (amt, x - axis), where:

$$rsp = (A_I/A_t) \qquad (2.3)$$

and

$$(amt) = (W_I/W_t) \qquad (2.4)$$

(A_I) = Area of reference substance, and (A_t) = Area of internal standard.
(W_I) = Mass of reference substance, and (W_t) = Mass of internal standard.

The results for the GC calibration for different substances are shown in appendix A. Often, but not always, larger molecules will have longer retention times in the GC (Van Gerpen et al., 2004). A 3800 GC (Varian) with a column from Restek Chromatographic Specialties with a 2 m x 0.53 mm retention gap and a 15 m x 0.32 mm x 0.1 μm film thickness was used. The method used for the GC analysis is based on the test method for determination of free and total glycerol in B-100 (ASTM D6584 and the similar method in EN14105). Calibration for the GC system was achieved by the use of two internal standards (butanetriol and tricaprin) and four reference materials (from Sigma-Aldrich, Canada) glycerol, monoolein (for monoglycerides), diolein (for diglycerides), and triolein (for triglycerides) where Table 2.5 shows these standards. The operating conditions for the oven are 50°C for 1 min, 15°C/min to 180°C, hold 0 min, 7°C/min to 230°C, hold 0 min, 30°C/min to 380°C, hold 8 min. The carrier gas is helium at a constant flow of 3.0 mL/min, the detector is a flame ionization detector (FID) at

400°C, H_2 flow is at 35 mL/min, air is at 350 mL/min, He (make-up) is at 30 mL/min, and cool on-column injection with a sample size of 1 µL is used.

Table 2.5 : GC standards

Standards (CAS #)	**Concentration (µg/mL pyridine)**
Glycerol (56 – 81 – 5)	500
Monoolein (111 – 03 – 5)	5000
Diolein (2465 – 32 – 9)	5000
Triolein (122 – 32 – 7)	5000
Butanetriol (ST # 1), (42890 – 76 – 6)	1000
Tricaprin (ST # 2), (621 – 71 – 6)	8000

The samples collected from the GC analysis are first heated to vaporize any methanol and water. Figure 2.10 shows typical standard reference chromatograms for determining the free and total glycerol in B-100 (ASTM D 6584-00). After finishing the analysis and determining the detected peaks, the mass of each component is calculated based on ASTM D6584-00.

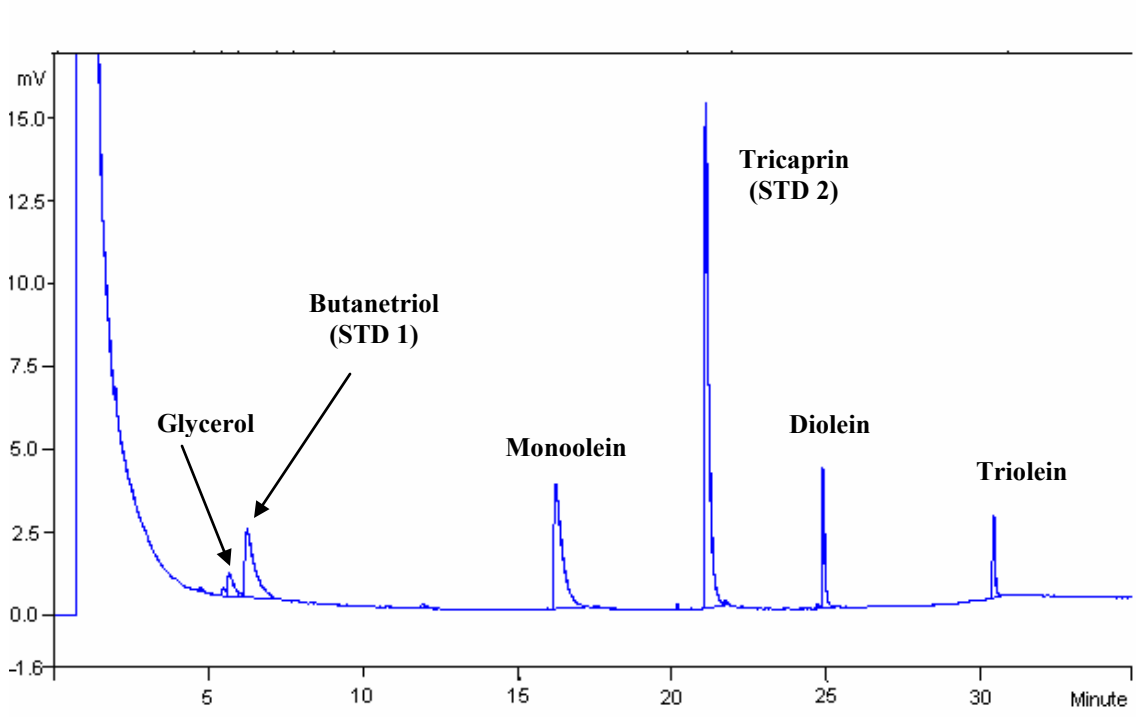

Figure 2.10: GC Chromatograph of mixture of standards.

2.15 Biodiesel and membranes

At present, membrane separation technologies are new to biodiesel purification processes. However, recent work has shown the efficacy of using membrane technology in the production of biodiesel. The group at the University of Ottawa invented a new technology for biodiesel production using membrane reactor (Dubé et al., 2007; Tremblay et al., 2008; Cao et al., 2007; Cao et al., 2008a,b; Cao, et al., 2009).

In parallel to the work described in this thesis, other researchers have employed membrane technology in the purification of FAME. Othman et al. (2010) investigated eight different types of commercial polymeric solvent resistant nanofiltration (SRNF) membranes for separating the methyl esters-rich effluent (biodiesel) from the mixture of the homogeneous catalyst, free glycerol and excess methanol after the transesterification process at various separation pressures and constant temperature. Scanning Electron Microscope (SEM) and Fourier Transform Infrared Spectroscopy (FTIR) were used to examine any changes to all the membranes studied the transesterification product properties was modified by reducing the alkalinity value. The permeation experiment was

conducted for pure polar solvents (water, anhydrous methanol and glycerol) and nonpolar solvents (RBD palm olein and methyl esters) at various ranges of separation pressure (600–3000 kPa) and temperature (28–60^{o}C). At a pH of 12.43 and 40^{o}C, it was found that at the end of the permeation process, the membranes were significantly damaged and the permeability flux for each membrane increased rapidly. The pH of the transesterification products was then modified to 8.68 and the results showed the possibility of separating the methyl esters from methanol and glycerides group.

He et al. (2006) compared the traditional methods for the refining step in biodiesel production with a hollow fiber membrane extraction. Biodiesel with a high purity (97.5%) obtained from: (i) washing with distilled water; (ii) washing with acid (HCl); and (3) dissolving and extracting in a solvent (hexane or petroleum ether) and then washing with distilled water. Serious emulsification occurred during the refining processes. Hollow fiber membranes, polysulfone and polyacrylonitrile, which are hydrophilic and hydrophobic respectively, were used. Membrane extraction effectively avoided emulsification during refining and decreased the refining loss compared with the three traditional refining methods. Polysulfone, decreased the refining loss to 8.1% (by wt), which was the lowest refining loss for all methods; while the highest refining loss was 15.2% by washing with distilled water at 20°C. The refined ester flowing out of the polysulfone hollow fiber was transparent and clear. The purity of the biodiesel, about 99%, obtained by polysulfone membrane extraction and other properties, such as density, kinematic viscosity, water content, and acid value, conformed to standards. Polyacrylonitrile membranes, were not suitable for refining biodiesel due to higher water content, 0.107%, than for the other methods.

Wang et al. (2009) used ceramic membrane separation process for refining biodiesel. Different pore sizes of 0.6, 0.2 and 0.1 μm to remove the residual soap and free glycerol, at the trans-membrane pressure of 0.15 MPa and temperature of 60°C were used. The content of potassium, sodium, calcium and magnesium in the whole permeate was found to be lower than the EN 14538 specifications. The residual free glycerol in the permeate was estimated by water extraction, its value was 0.0108 wt%. They concluded that ceramic membrane with the pore size of 0.1 μm was suitable for this separation process.

Gomes et al. (2010) investigated the efficiency of microfiltration with ceramic membranes in the separation of biodiesel and glycerol. Different pore sizes of 0.2, 0.4, and 0.8μm were used. Feed solution with mass composition of 80% biodiesel, 10% glycerol, and 10% anhydrous ethanol were microfiltered at 60^{o}C and trans-membrane pressures of 1.0, 2.0, and 3.0 bar. Membrane performance was evaluated based on the capacity to retain glycerol and on the permeate flux values. Experimental results showed that trans-membrane pressure has a strong influence on biodiesel microfiltration. The best performance was obtained with the 0.2 μm membrane and 2.0 bar trans-membrane pressure. In these conditions and at the same temperature that was used, the influence of the ethanol concentration on the feed solution separation was evaluated. A higher concentration of ethanol led to a lower retention of glycerol and a lower ethanol concentration gave the best results for glycerol retention.

2.16 Summary

From the literature survey, there were almost no reports on the direct removal of glycerol from untreated biodiesel using a membrane separation system. Certainly, none of the reported uses of such a system resulted in the achievement of ASTM and EN levels for free glycerol in FAME. Nonetheless, it is likely that membrane technology can be successfully used to separate glycerol droplets from FAME while avoiding costly and environmentally deleterious water washing, adsorption or ion exchange methods.

2.17 References

[1] Bam, N., Drown, D.C., Korus, R., Hoffman, D.S., Johnson, T.G. and Washam, J.M., Method for purifying alcohol esters, US patent No 5,424,467, June 13, **1995.**

Becher, P., Emulsions: theory and practice, Washington, D.C. American Chemical Society; Oxford: Oxford University Press., **2001.**

[2] Boocock, D.G.B., Konar, S.K., Mao, V., Lee, C., and Buligan, S., Fast formation of high-purity methyl esters from vegetable oils, *J. Am. Oil Chem. Soc*., 75: 1167-1172, **1998.**

[3] Boocock, D.G.B., Single-phase process for production of fatty acid methyl esters from mixtures of triglycerides and fatty acids, Canadian Patent No. 2,381,394, Feb 22, **2001.**

[4] Canakci, M., and Van Gerpen, J., Biodiesel production from oils and fats with high free fatty Acid, *Trans. ASAE*., 44: 1429–1436, **2001.**

[5] Cao, P., Tremblay, A.Y., Dubé, M.A., Katie, M., Effect of membrane pore size on the performance of a membrane reactor for biodiesel production, *Ind. Eng. Chem. Res*., 46: 52-58, **2007**.

[6] Cao, P., Dubé, M.A., Tremblay, A.Y., High-purity fatty acid methyl ester production from canola, soybean, palm, and yellow grease lipids by means of a membrane reactor, *Biomass. Bioenerg*., 32: 1028-1036, **2008a**.

[7] Cao, P., Dubé, M.A., Tremblay, A.Y., Methanol recycling in the production of biodiesel in a membrane reactor, *Fuel*., 87: 825-833, **2008b**.

[8] Cao, P., Tremblay, A.Y., Dubé, M.A., Kinetics of canola oil transesterification in a membrane reactor, *Ind. Eng. Chem. Res*., 48: 2533-2541, **2009**.

[9] Carraratto, C., Macor, A., Mirandola, A., Stoppato, A., Tonon, S., Biodiesel as alternative fuel: experimental analysis and energetic evaluations, *Energy*., 29: 2195–2211, **2004.**

[10] Cetinkaya, M., and Karaosmanoglu, F., Optimization of base-catalyzed transesterification reaction of used cooking oil, *Energy Fuels*., 18: 1888-1895, **2004.**

[11] Demirbaş, A., Biodiesel fuels from vegetable oils via catalytic and non-catalytic supercritical alcohol transesterifications and other methods: a survey. Energ. Convers. Manage., 44, 2093-2109, **2003.**

[12] Dmytryshyn, S.L., Dalai, A.K., Chaudhari, S.T., Mishra, H.K., and Reaney, M.J., Synthesis and characterization of vegetable oil derived esters: evaluation for their diesel additive properties, *Biores. Technol*., 92: 55-64, **2004.**

[13] Dubé, M.A., Tremblay, A.Y., Liu, J., Biodiesel production using a membrane reactor, *Biores. Technol*., 98: 639–647, **2007.**

[14 Eckey, E.W., Esterification and interesterification, *J. Am. Oil Chem. Soc*., 33: 575 – 579, **1956.**

[15] Freedman, B., Pryde, E.H., Mounts, T.L., Variables affecting the yield of fatty esters from transesterified vegetable oils, *J. Am. Oil Chem. Soc*., 61: 1638-1643, **1984.**

[16] Freedman, B., Butterfield, R.O., Pryde, E.H., Transesterification kinetics of soybean oil, *J. Am. Oil Chem. Soc*., 63: 1375 – 1380, **1986.**

[17] Fukuda, H., Kondo, A., and Noda, H., Review: biodiesel fuel production by Transesterification of Oils, *J. Biosci. Bioeng*., 92: 405-416, **2001.**

[18] Ghadge, S.O.V., Raheman, H., Biodiesel production from mahua (Madhuca indica) oil having high free fatty acids, *Biomass. Bioenerg*., 28: 601-605, **2005.**

[19] Gomes, M.C.S., Pereira, N.C., Davantel de Barros, S.T., Separation of biodiesel and glycerol using ceramic membranes, *J. Membr. Sci*., 352: 271-276, **2010.**

[20] Hayafuji, S., Shimidzu, T., Oh, S., Zaima, H., Method and apparatus for producing diesel fuel from waste edible oil. US patent No 5,972,057, Oct 26, **1999.**

[21] He, H.Y., Guo, X., Zhu, S.L., Comparison of membrane extraction with traditional extraction methods for biodiesel production, *J. Am. Oil. Chem. Soc*., 83: 457-460, **2006.**

[22] Holliday, R.L., King, J.W., List, G.R., Hydrolysis of vegetable oils in sub- and supercritical Water, *Ind. Eng. Chem. Research*., 36: 932-935, **1997.**

[23] Huang, G., Chen, F., Wei, F., Zhang, X., Chen, G., Biodiesel production by microalgal Biotechnology, *Appl. Eng*., 87: 38-46, **2010.**

[24] Ikwuagwu, O.E., Ononogbu, I.C., and Njoku, O.U., Production of biodiesel using rubber [Hevea brasiliensis (Kunth. Muell.)] seed oil, *Ind. Crop. Prod*., 12: 57-62, **2000.**

[25] Karaosmanoglu, F., Cıgızoglu, K.B., Tuter, M., and Ertekin, S., Investigation of the refining step of biodiesel production, *Energy Fuels*., 10: 890-895, **1996.**

[26] Karla, T.K., Maria, A.F., Cesar-Oliveira, Helena, M., Wilhelm and Luiz, P.R., Ethanolysis of refined soybean oil assisted by sodium and potassium hydroxides, *J. Am. Oil Chem. Soc*., 84: 385-392, **2007.**

[27] Knothe, G., Dunn, R.O., and Bagby, M.O., Biodiesel: the use of vegetable oils and their derivatives as alternative diesel fuels, in fuels and chemicals from biomass, edited by Komolikov, Y.I., and Blaginina, L.A., Technology of ceramic micro and ultrafiltration membranes (review), *Refract. Ind. ceram*., 43: 5-6, **2002.**

[28] Korbitz, W., Biodiesel production in Europe and North America. An encouraging prospect, *Renew. Energ*., 16: 1078-1083, **1999.**

[29] Ma, F., Clements, L.D., and Hanna, M.A., The effect of catalyst, free fatty acids, and water on transesterification of beef tallow, *Trans. ASAE*., 41: 1261-1264, **1998.**

[30] Ma, F., and Hanna, M.A., Biodiesel production: a review, *Biores. Technol*., 70: 1-15, **1999.**

[31] Mao, V., Konar, S.K., and Boocock, D.G.B., The pseudo-single-phase, base-catalyzed transmethylation of soybean oil, *J. Am. Oil Chem. Soc*., 81: 803-808, **2004.**

[32] Marion K., The use of solubility parameters to select membrane materials for pervaporation of organic mixtures, The University of Waikato, Hamilton, New Zealand January, **2006.**

[33] Martin, B., Economic feasibility review for community-scale farmer cooperatives for biodiesel, *Biores. Technol*., 70: 81-87, **1999**.

[34] Meher, L.C., Sagar, D.V., and Naik, S.N., Technical aspects of biodiesel production by transesterification — a review, *Renew. Sust. Energ. Rev*., 10: 248-268, **2006.**

[35] Noureddini, H., and Zhu, D., Kinetics of transesterification of soybean oil, *J. Am Oil. Chem. Soc*., 74: 1463-1475, **1997.**

[36] Nye, M.J., Williamson, T.W., Deshpande, S., Schrader, J.H., Snively, W.H., Yurkewich, T.P., French, C.L., Conversion of used frying oil to diesel fuel by transesterification: preliminary tests, *J. Am. Oil Chem. Soc*., 60: 1598-1601, **1983.**

[37] Othman, R., Mohammad, A.W., Ismail, M., Salimon, J., Application of polymeric solvent resistant nanofiltration membranes for biodiesel production, *J. Membr. Sci*., 348: 287–297, **2010.**

[38] Porter, M.C., Handbook of Industrial Membrane Technology, Noyes publications, NJ, **1990**.

[39] Prokop, T., **2002**. Imperial Western Products, 14970 Chandler St., Coachella, CA 91720.

[40] Pryde, E.H., Vegetable oils as fuel alternatives – symposium overview, *J. Am. Oil Chem. Soc*., 61: 1609-1610, **1983.**

[41] Saha , B.C. and Woodword , J., ACS Symposium Series 666, American Chemical Society, Washington, DC, 172–208,**1997.**

[42] Saka, S., and Kusdiana, D., Biodiesel fuel from rapeseed oil as prepared in supercritical methanol, *Fuel*., 80: 225-231, **2001.**

[43] Saka, S., and Kusdiana, D., Effects of water on biodiesel fuel production by supercritical methanol treatment, *Biores. Technol*., 91: 289-295, **2004.**

[44] Schwab, A.W., Bagby, M.O., and Freedman, B., Preparation and properties of diesel fuels from vegetable oils, *Fuel.*, 66: 1372-1378, **1987.**

[45] Shay, E.G., Diesel fuel from vegetable oil: status and opportunities, *Biomass. Bioenerg*., 4:227-242, **1993.**

[46] Sheehan, J., Camobreco, V., Duffield, J., Graboski, M., and Shapouri, H., Life cycle inventory of biodiesel and petroleum diesel for use in an urban bus: Final Report, NREL/SR-580- 24089 UC Category, May **1998.**

[47] Strathmann, H., Membrane separation process, *J. Membr. Sci*., 9: 121-189, **1981.**

[48] Strathmann, H., Membrane Separation Processes: Current relevance and future Opportunities**,** *AIChE Journal*., 47: 1077-1087, **2001.**

[49] Tremblay, A.Y., Cao, P., Dubé, M.A., Biodiesel production using ultralow catalyst Concentrations, *Energy Fuels*., 22: 2748-2755, **2008**.

[50] Van Gerpen, J., Biodiesel processing and production, *Fuel. Process. Technol*., 86: 1097-1107, **2005.**

[51] Van Gerpen, J., Shanks, B., Pruszko, R., Clements, D., Knothe, G., Biodiesel production technology, August 2002–January 2004., July **2004** • NREL/SR-510-36240.

[52] Varese, R., and Varese, M., Methyl ester biodiesel: Opportunity or necessity? *INFORM*., 7: 816-824, **1996.**

[53] Wang, Y., Xingguo, Y., Liu, Y., Ou, S., Yan, Y.,Tang, S., Refining of biodiesel by ceramic membrane separation, *Fuel. Process. Technol*., 90: 422–427, **2009**

[54] Zhang, X., Peterson, C., Reece, D., D. Reece, Möller, G., Haws, R., Biodegradability of biodiesel in the aquatic environment, *Transactions of ASAE.,* 41: 1423–1430, **1998**.

[55]* USDA / DOE Study, "Lifecycle inventory of biodiesel and petroleum diesel for use in an urban bus". May 1998. Ethanol (2001) USDA study, "The **2001** Net Energy balance of corn – ethanol."

Chapter 3

Glycerol Removal from Biodiesel using Membrane Separation Technology

Fuel, 2010, 89: 2260-2266.

Chapter 3 - Glycerol removal from biodiesel using membrane separation technology

Abstract

Membrane separation technology was used to remove free glycerol from biodiesel in order to meet the ASTM D6751 and EN 14214 standards. Fatty acid methyl esters (FAME) produced from canola oil and methanol were purified using ultrafiltration. The effect of different materials present in the transesterification reaction, such as water, soap, and methanol, on the final free glycerol separation was studied. A modified polyacrylonitrile (PAN) membrane, with 100 kD molecular weight cut off was used in all runs. Tests were performed at 25°C and 552 kPa operating pressure. The free glycerol content in the feed, retentate and permeate of the membrane system was analyzed using gas chromatography according to ASTM D6584. Results showed low concentrations of water had a considerable effect in removing glycerol from the FAME even at approx 0.08 mass %. This is four orders of magnitude less than the amount of water required in a conventional biodiesel purification process using water washing. It is suggested that the mechanism of separation of free glycerol from FAME was due to the removal of an ultrafine dispersed glycerol-rich phase present in the untreated FAME. This was confirmed by the presence of particulates in the untreated FAME. The size of the droplets and the free glycerol separation both increased with increasing water content of the FAME. The trends of separation and droplet size vs water content in the FAME phase were very similar and exhibited a sudden increase at 0.08 mass % water in the untreated FAME. This supports the conclusion that water increased the size of the distributed glycerol phase in the untreated FAME leading to its separation by the ultrafiltration membrane. The technology for the removal of free glycerol from biodiesel was found to use 2.0 grams of water per L of treated FAME (0.225 mass% water) vs the current 10 L of water per L of treated FAME.

Keywords: biodiesel, glycerol, separation, fatty acid methyl ester (FAME), ultrafiltration, microfiltration.

3.1 Introduction

Biodiesel has been defined by the American Society for Testing and Materials (ASTM) as mono alkyl esters of long chain fatty acids derived from renewable lipid feedstocks, such as vegetable oils or animal fats, for use in compression ignition (diesel) engines. Biodiesel is an alternative source of energy in diesel engines in its neat form or as a blend with conventional diesel fuel [1,2]. It is non-toxic, clean burning, renewable, biodegradable and environmentally safe compared to its petroleum counterpart, were the biodiesel combustion emissions, such as carbon monoxide, particulates, unburned hydrocarbons, SOx emissions and soot are much lower [3]. The reaction scheme is shown in Figure 3.1.

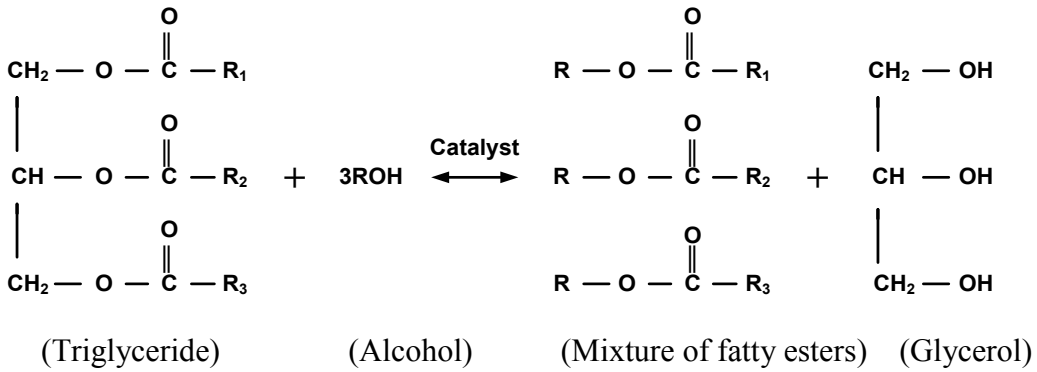

Figure 3.1: Transesterification reaction scheme.

Biodiesel is commercially produced most frequently via alkali-catalyzed (e.g., sodium hydroxide (NaOH), potassium hydroxide (KOH), and sodium methoxide ($NaOCH_3$)) transesterification with methanol, to form esters and glycerol, which results in a relatively short reaction time. The reversible nature of the transesterification means that the reaction can never reach 100% completion. The schematic diagram of the conventional alkaline-catalyzed process for biodiesel production with water distillation is shown in Figure 3.2. The overall process includes the transesterification reaction, separation of the crude ester layer from the glycerol layer, purification of the ester-rich (biodiesel) phase, and recovery of glycerol from the glycerol-rich phase as a by-product [4].

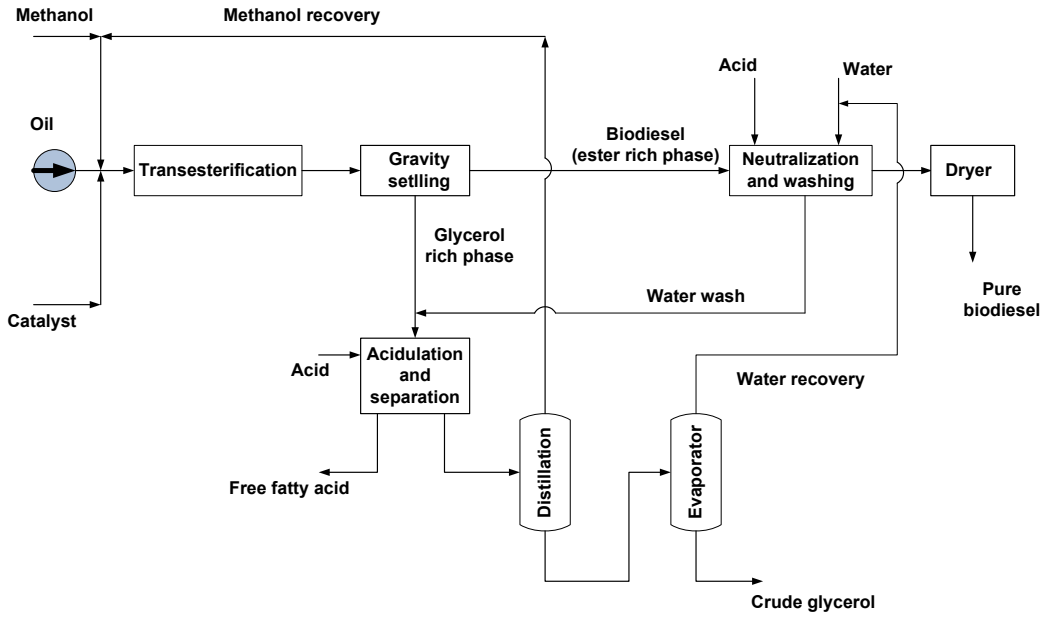

Figure 3.2: Process flow diagram of conventional alkaline-catalyzed transesterification process.

After reaction, the mixture is allowed to cool to room temperature and settle, where the glycerol layer settles to the bottom and the ester-rich phase (FAME) forms the upper layer. The purity of the final FAME product is an important issue and is clearly specified in standards such as ASTM D6751 in North America and EN14214 in Europe [5, 6]. The goal is to limit the presence of impurities that may affect engine performance in both the short and longer terms. Thus, a great deal of cost and effort are put towards the purification of the FAME phase.

The unprocessed ester-rich FAME layer will contain impurities such as glycerol (referred to as "free" glycerol), unreacted methanol, residual catalyst, bound glycerol (i.e., unreacted tri-glyceride (TG), diglyceride (DG) and monoglyceride (MG), and perhaps small amounts of soap and water. As mentioned, it is necessary to remove these impurities because they will strongly affect engine performance. For example, high free glycerol content can result in separation during storage, forming gum-like deposits

around injector tips and valve heads, therefore causing problems in the fuel system. The ASTM D6751 and EN14214 standards limit the free glycerol to ≤0.02 mass% [7].

3.2 Issues with current purification methods

Adding water to the FAME phase allows the soap, the alkaline catalyst residue and small amounts of glycerol, DG and MG in the product mixture to be removed. Unfortunately, the separation of the ester phase from the water phase is usually difficult, and this step produces a large amount of waste water containing methanol; for each litre of biodiesel, ~10 L of waste water are produced [8, 9]. This increases the size and the cost of the separation equipment. After the washing step, the wash water containing the extracted methanol and the residual catalyst will be evaporated to recover the methanol and water. In some instances, the wastewater is treated and disposed of without further treatment, resulting in loss of product and reactants. This is done at great capital and operating costs that impact the environmental benefits of using biodiesel.

In the case of high free fatty acid feedstocks, significant soap formation will ensue during biodiesel production. The presence of soap in large quantities can cause difficulties in separation of the ester phase (non-polar) from water (polar phase) because the sodium soap formed is a strong surface active agent. Its presence reduces the interfacial tension and prevents coalescence of FAME droplets, leading to the formation of an oil-in-water emulsion (i.e., ester-in-water). This emulsified layer will prevent the separation of the non-polar FAME phase from the water layer, resulting in a longer separation time and most importantly, losses of esters due to incomplete separation during water washing. Thus, there is a need to add certain compounds followed by other physical separations, such as gravity separation, centrifugation, and heating, in order to break this emulsion and improve the efficiency of water washing [10].

Gravitational settling is based on the difference in density between the non-polar FAME-rich phase and the polar methanol/glycerol-rich phase. Centrifugation settling is also used with water washing to accelerate the separation of impurities. The denser phase will be preferentially separated to the outer surface of the centrifuge and because the glycerol is insoluble in FAME and soluble in the water phase, almost all of the glycerol is easily removed. A sufficient residence time for the less dense oil to float on top of the

water surface is, of course, required. However, this method is less effective for dealing with FAME-water emulsions containing very small FAME droplets and the time to separate the FAME phase completely from the emulsions may take several hours, days, or even may never separate. The disadvantage of the centrifuge is its initial cost, and the need for considerable maintenance [11].

Vacuum distillation can be used to remove methanol and water from the FAME to meet the standards, since the residual methanol level in FAME should be very low. The allowable alcohol level is specified in European biodiesel standards (0.2 mass% maximum). Tests have shown that as little as 1% methanol in the biodiesel can lower the flashpoint of the biodiesel from 170 to less than 40^{o}C. The use of vacuum distillation to fully evaporate FAME and leave DG, TG impurities behind does not overcome the glycerol purity issue, as glycerol gets carried over during the distillation process.

3.3 Objectives and approaches

At present, membrane separation technologies are new to biodiesel purification processes. However, recent work has shown the efficacy of using membrane technology in the production of biodiesel [12, 13]. The compatibility of membrane materials, the effects of operating parameters and the possibility of using membrane separation processes in biodiesel purification have not been studied to a great extent. Membrane separation technology has been used for many applications in fields outside of biodiesel production and purification. There is great potential that membrane technology can provide solutions for many environmental problems by recovering valuable products as well as treating effluents and minimizing their harm to the atmosphere. The most widely used are membrane microfiltration (MF) and ultrafiltration (UF) pressure-driven processes capable of separating particles in the approximate size range of 0.1 to 10 μm and 1 to 100 nm, respectively. MF is a pressure-driven membrane process for the separation of fine particles, micro-organisms and emulsion droplets [14]. The membranes used have a microporous structure which separates fine particles in the size range of 0.1 to 10 μm. UF is a separation process using membranes with pore sizes in the range of 1 to 100 nm. Typically, UF will remove high molecular weight substances, colloidal

materials, and organic and inorganic molecules. UF processes have several applications such as the rejection of viruses, bacteria, and wastewater reuse and sewage reuse [15].

This study focused on the ability of membrane processes to remove free glycerol droplets from FAME, without using a water wash step, as well as, studying the effect of different materials that are normally present as a result of the transesterification reaction, such as water, soap, and methanol on the final separation performance.

3.4 Experimental section

3.4.1 Production of biodiesel

A reactor with a capacity of 6 L was used to produce FAME using a batch process. A 6:1 molar ratio of methanol to oil and 1 mass% NaOH based on oil was used. The operating temperature was 60°C and the reaction time was 1h. The required amount of NaOH (reagent grade, ACP Chemicals Inc.; Montreal, QC, Canada) was dissolved in the required amount of methanol (99.85% purity, Commercial Alcohols Inc.; Brampton, ON, Canada), and then put in the reactor system with canola oil (refined/bleached/deodorized from Loblaws, ON, Canada). A heat exchanger was used to heat the mixture to 60°C. A circulating pump was used to improve mixing. The finished product from the reaction was transferred to a flask and allowed to settle for 8 to 12 h, where the bottom glycerol-rich layer was removed. The non-polar, FAME-rich phase was then neutralized with sulphuric acid to a pH of 7. Over 12 runs were performed to generate sufficient quantities of FAME for the purification experiments. The FAME produced for all runs from different batches was stored in separate containers in order to prepare different FAME mixtures. The initial feed solutions were characterized before each membrane purification experiment and are reported as “original sample”.

At this point, the FAME-rich phase contained, for the most part, FAME, methanol, glycerol and water. It should be noted that: A) FAME and methanol are totally miscible, B) methanol, glycerol and water are totally miscible, C) glycerol and water have very limited solubility in FAME.

The FAME phase was then evaporated under reduced pressure in a rotary evaporator (vacuum-treated FAME) at 90°C under vacuum (0.94 bar vacuum) for 30 min to ensure that neither methanol nor water was present in the FAME phase. During the

vacuum-treatment step, aggregates began to form and precipitate; these aggregates were removed from the FAME solution by settling. The amount of precipitate was estimated at 1 volume% of the entire amount of FAME produced. The resulting FAME was filtered using Whatman (Maidstone, England) number 50 filter paper.

To determine the nature of the precipitate, two samples of FAME were analyzed for soap content using the modified version of AOCS method Cc 17 – 79 [16]. One was tested as is, and to the second was added 1 mass% of the precipitate and 1 mass% of distilled water followed by mixing using a stirrer for 20 min. The first sample, containing only vacuum-treated FAME gave a soap content reading of ~400 ppm, while the second sample showed a soap content reading of ~3000 ppm. The first sample was considered to be our baseline sample and was referred to as "raw" FAME only. The amount of water in this FAME was determined by Karl Fisher coulometric analysis using a Titroline KF trace analyser (Schott Instruments, Germany) and found to be 250 ppm. Various amounts of water were added to this "raw" FAME. The reported additions of 0.06, 0.1 and 0.2 wt% water represent total amounts of 0.085, 0.125, 0.225 wt% water respectively. Distilled and de-ionized water was used in preparing the samples. Methanol was purchased from Fisher Scientific, with a purity of 99.99%. Eight sample mixtures of varying composition were prepared using the "raw" FAME, and varying amounts of methanol, water and soap (from the aggregate materials). Table 3.1 shows the composition of the prepared FAME mixtures from different batches of FAME.

Table 3.1: Mixtures prepared for testing in the membrane system.

Mixtures #	Type of mixtures (Water, methanol and soap in mass%)
1	FAME only
2	FAME + 0.06% water
3	FAME + 0.1% water
4	FAME + 0.2% water
5	FAME + 1% soap
6	FAME + 1% methanol
7	FAME + 1% methanol + 1% soap + 0.06% water
8	FAME + 1% soap + 0.06% water

3.4.2 Membrane separation of glycerol from FAME phase

A membrane separation system (see Figure 3.3) was used as a "feed and bleed" [17] system equipped with a feed pump and circulating pump. The separation of glycerol from the crude FAME phase was performed over two identical Sepa™ (GE Osmonics) cells containing polymeric membranes with a total filtration surface area of 0.0276 m^2 (2 x [14.5 cm x 9.5 cm]). A modified hydrophilic polyacrylonitrile (PAN) membrane (Ultrafilic™, Sterlitech Corporation, USA) with a molecular weight cut-off of (100 kD) was tested at a temperature of 25°C, and pressure of 552 kPa.

Five litres of the vacuum-treated FAME produced in the batch reactor, were put in the feed tank and pumped to the membrane module. During the run, a circulating pump was used to circulate the feed through the membrane modules. All components were mixed with the FAME using a magnetic stirrer for one hour prior to the run. All runs using membrane separation were performed for 3 hours. A coriolis meter was connected to the circulation pump, which enabled measurement of the mass flow rate of the FAME over the two membrane modules. This reading translated to an average, constant cross-flow velocity in the membrane modules of about 0.6 m/s. The inlet and outlet pressures of the membrane filtration system were achieved by adjusting the related valves. The temperature of the system was controlled to 25°C using a cooling system. The mass flow

rate of the permeate side (g/min) was automatically recorded every minute on a computer by way of a flow meter. Samples of the permeate side (permeate) and rejection side (retentate) were taken at 15 min, 30 min, 1 h, 2 h and 3 h, as well as from the initial mixture for GC analysis. Prior to analysis, all samples were heated to vaporize any methanol. All runs were stopped after 180 minutes.

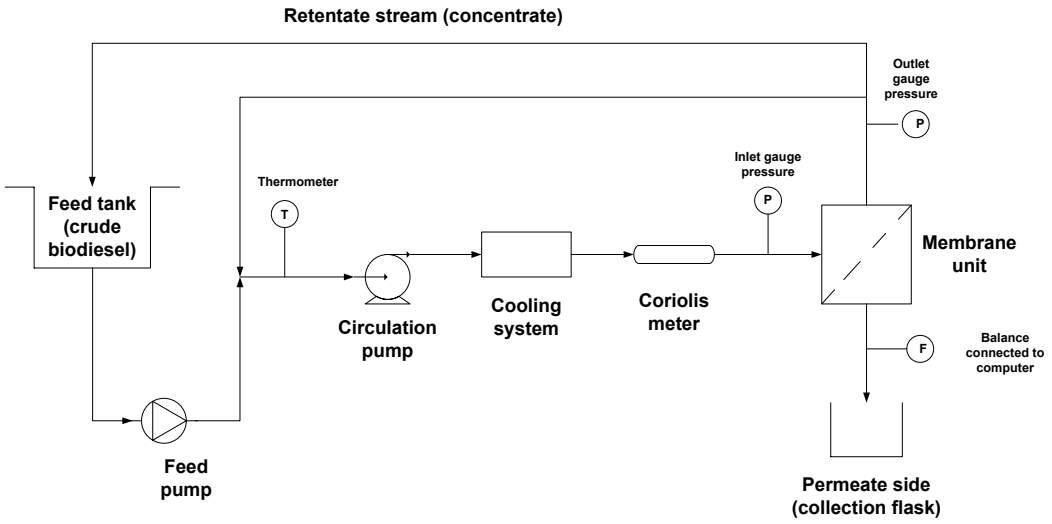

Figure 3.3: Schematic of the membrane separation system.

3.4.3 GC analysis

GC analyses were used to determine the amount of a specific contaminant or class of contaminants in the FAME. In order to transform glycerol as well as MG, DG and TG into more volatile compounds, they were silylated with N-methyl-N-(trimethylsilyl)trifluoroacetamide (MSTFA) prior to analysis. A 3800 GC (Varian) with a column from Restek Chromatographic Specialties with a 2 m x 0.53 mm retention gap and a 15 m x 0.32 mm x 0.1 µm film thickness was used. The method used for the GC analysis is based on the test method for determination of free and total glycerol in B-100 (ASTM D6584 and the similar method in EN14105). Calibration for the GC system was achieved by the use of two internal standards (butanetriol and tricaprin) and four

reference materials (from Sigma-Aldrich, Canada): glycerol, monoolein (for MG), diolein (for DG), and triolein (for TG). The calibrations were performed with three replicate injections at 5 separate concentrations yielding, for the glycerol calibration curve, R^2 = 0.9994. The operating conditions for the oven were 50°C for 1 min, 15°C/min to 180°C, 7°C/min to 230°C, 30°C/min to 380°C, hold 10 min. The carrier gas was helium at a constant flow of 3.0 mL/min, the detector was a flame ionization detector (FID) at 380°C, H_2 flow was at 35 mL/min, air was at 350 mL/min, He (make-up) was at 30 mL/min, and cool on-column injection with a sample size of 1 µL was used.

3.5 Results and discussion

3.5.1 Separation of glycerol in the presence of water

The separation of glycerol from FAME in the presence of water was determined by adding 0.06, 0.1 and 0.2 wt % water (mixtures 2 to 4 in Table 3.1) to vacuum-treated FAME. These mixtures were then treated by the membrane process. The concentrations of glycerol in the original sample, and in the permeate and retentate as a function of time for all runs, are shown in Table 3.2. Each sample was analyzed three times and the averages were reported. The calculated deviations from this average value were +/- 4.5% for all samples. Results for % separation at different times are shown in Table 3.3, where the values of % separation were determined as:

$$\%\text{Separation} = \frac{(\text{Glycerol mass\% in retentate - Glycerol mass\% in permeate})}{\text{Glycerol mass\% in retentate}} \times 100 \quad (3.1)$$

The results for the glycerol content of the permeate are plotted in Figure 3.4 and permeate flux are plotted in Figure 3.5 for cases 1 to 4. The dashed line in Figure 3.4 indicates the ASTM D6751 standard for the level of free glycerol in biodiesel (0.02 mass%). Glycerol was not removed by the membrane for the FAME only case. For the case using FAME + 0.1 and 0.2 mass% water (Figure 3.4 and Table 3.3) excellent separation results were obtained. As seen in Figure 3.5, reasonable steady state fluxes

were obtained over the course of the runs, indicating that the thickness of the filter cake above the membrane had stabilized.

Results of these tests show that the addition of water in small quantities (0.06 mass%), improved the % separation as shown in Table 3.3. The complete miscibility of glycerol and water causes the formation of larger droplets and thus, two immiscible phases were formed: a water and glycerol phase, and a FAME phase. This suggests that the principle of separation for free glycerol from FAME is that of the rejection of a finely dispersed water and glycerol phase by the membrane.

For all 8 runs, the reduction in mass of the retentate both in the feed tank and loop ranged from 18 to 22%. The concentration of glycerol in the retentate stream remained relatively constant over the course of the run (see Table 3.2). For all runs, a small polar phase appeared at the bottom of the feed tank. Glycerol could accumulate in this polar phase. The initial FAME solution was obtained from the dephasing of the polar and non-polar phases produced after transesterification and represents a solution at saturated conditions. The removal of any component from this FAME solution could lead to further phase separation.

A material balance was performed on the glycerol in the retentate over the course of a run (the glycerol loss in the retentate vs. the amount of glycerol leaving in the permeate stream). The amount of glycerol lost in the FAME phase of the retentate could not be fully accounted for by the glycerol in the permeate. This discrepancy was attributed to the extraction of glycerol by the polar phase in the feed tank. This explanation was supported by the fact that only the non-polar phase of the retentate was sampled and that the concentration of glycerol in this stream was relatively constant throughout the run as seen in Table 3.2. The constant glycerol composition indicates that the glycerol in the non polar phase of the retentate remained in equilibrium with the polar phase in the feed tank as the volume of the feed solution was reduced throughout the run.

Table 3.2: Free glycerol mass % in the permeate and retentate streams after membrane separation.

	Time (min)	Free glycerol mass% for Ultrafilic polymeric membrane at 25°C, and 552 kPa							
		FAME Only (1)	FAME + 0.06% water (2)	FAME + 0.1% water (3)	FAME + 0.2% water (4)	FAME + 1% soap (5)	FAME + 1% methanol (6)	FAME + 1% soap + 1% methanol + 0.06% water (7)	FAME + 1% soap + 0.06% water (8)
	Original sample	0.037	0.036	0.032	0.040	0.029	0.039	0.047	0.030
Permeate	**15**	0.027	0.030	0.020	0.013	0.025	0.031	0.041	0.021
	30	0.027	0.029	0.018	0.012	0.029	0.035	0.038	0.020
	60	0.032	0.028	0.017	0.013	0.028	0.033	0.038	0.020
	120	0.032	0.028	0.017	0.014	0.029	0.031	0.041	0.020
	180	0.033	0.027	0.017	0.013	0.030	0.031	0.040	0.018
Retentate	**15**	0.037	0.039	0.033	0.045	0.029	0.037	0.043	0.025
	30	0.037	0.040	0.034	0.037	0.032	0.037	0.042	0.025
	60	0.036	0.040	0.034	0.036	0.032	0.036	0.040	0.026
	120	0.034	0.041	0.032	0.034	0.029	0.034	0.043	0.028
	180	0.034	0.039	0.035	0.035	0.032	0.034	0.041	0.031

Table 3.3: Free Glycerol separation for the test mixtures.

Time (min)	% Separation							
	FAME Only (1)	FAME + 0.06% water (2)	FAME + 0.1% water (3)	FAME + 0.2% water (4)	FAME + 1% soap (5)	FAME + 1% methanol (6)	FAME + 1% soap + 1% methanol + 0.06% water (7)	FAME + 1% soap + 0.06% water (8)
15	27	23	39	71	14	16	5	16
30	27	28	47	67	9	5	9	20
60	11	30	50	64	12	8	5	23
120	6	32	47	59	0	9	5	29
180	3	31	51	63	6	9	2	42

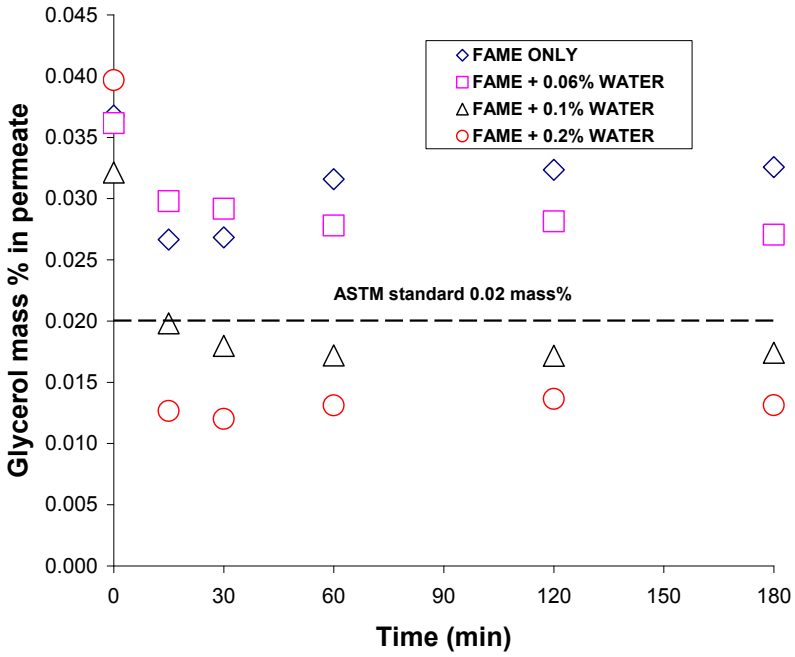

Figure 3.4: Glycerol mass% in permeate vs. time for (FAME only, FAME + 0.06% water, FAME + 0.1% water, and FAME + 0.2% water).

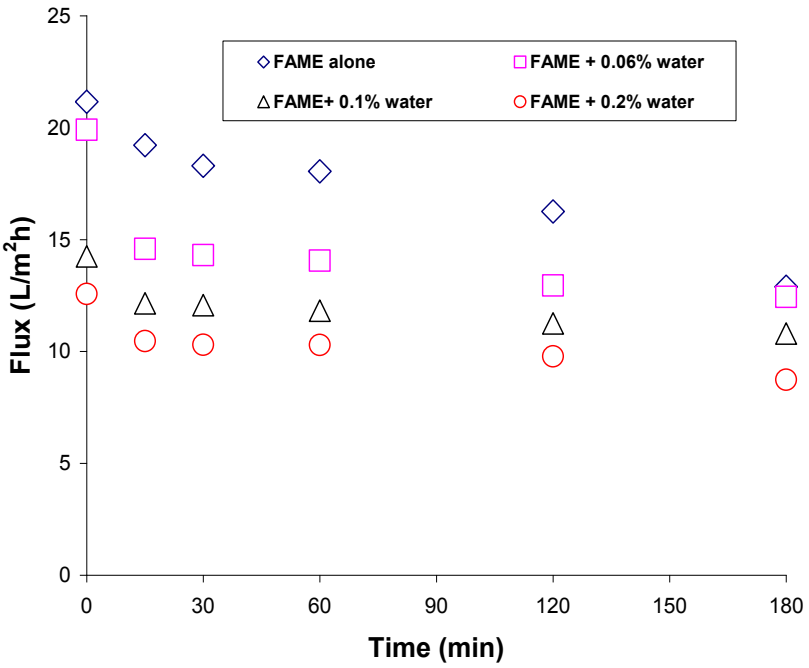

Figure 3.5: Permeate flux vs. time for (FAME only, FAME + 0.06% water, FAME + 0.1% water, and FAME + 0.2% water).

3.5.2 Droplet size of glycerol and water (results of DLS measurements)

The results of this work indicate that adding water to vacuum-treated FAME alone gave excellent results for free glycerol removal that exceeded the ASTM standard. The separation of free glycerol from FAME vs the mass% addition of water to the vacuum-treated FAME was plotted in Figure 3.6 for cases 1 through 4. The results indicate an increase in separation with an increase in water content. The solubility limit of water in glycerol free biodiesel is 0.15 % [18].

In order to verify if the formation of a dispersed phase was responsible for this increase in separation, the droplet size in FAME was determined at various water additions by Dispersive Light Scattering (DLS). Six samples of FAME were prepared as follows: vacuum evaporated FAME was washed with distilled water three times to remove soap, and glycerol, then evaporated from water using a rotary evaporator for 30 min at 90°C, and 0.94 bar vacuum. Then 0.1 mass% of glycerol was added to the FAME

and different amounts of water were added (0.02, 0.04, 0.06, 0.08%). The mixture was well mixed for 45 min and settled for 1 to 2 h before measuring in the DLS system (zetasizer nano series from Malvern Instruments, www.malverninstruments.com).

The average droplet diameter obtained by DLS are included in Figure 3.6. When the addition of water increases above 0.06%, a considerable jump in droplet size is observed. This jump follows the shape of the separation curve. Given the droplet size of 250 nm at the 0.06 mass % level, the membrane should have taken all of the glycerol out of the FAME. The size of the droplets is larger than the 100kD of the Ultrafilic membrane used in this work (50 nm[19]). This indicates that droplet size alone cannot totally affect the separation and that, at low concentrations of water, a certain amount of glycerol is still dissolved in the FAME.

The DLS measurement also indicates that true phase separation occurs between 0.06 and 0.1 mass% as the droplet size increases 10 fold in this range. It is only when the actual phase separation occurs that membrane separation is effective in removing glycerol from FAME.

This further supports the separation mechanism proposed in this work, where free glycerol is best separated from FAME by addition of a small amount of water to induce the formation of a dispersed water phase in the FAME. There should however be a sufficient amount of water to remove the free glycerol dissolved in the FAME phase. The glycerol water phase partitions the free glycerol and can be removed by ultrafiltration. It is interesting to note that the removal of free glycerol from biodiesel used 2.0 grams of water per L of treated FAME (0.225 mass% water) vs the current 10 L of water per L of treated FAME.

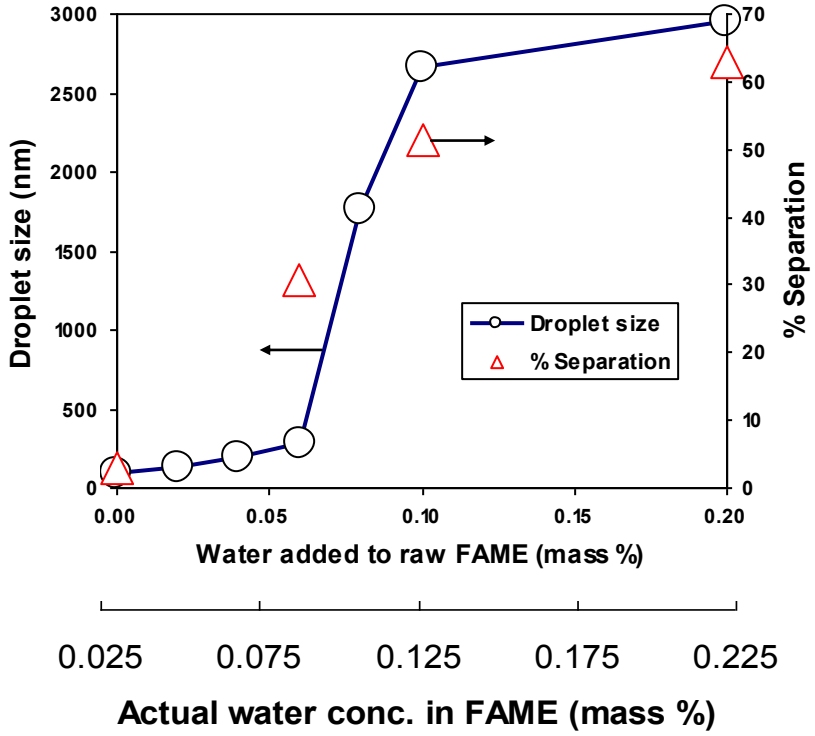

Figure 3.6: Plot of the droplet size and separation versus water added and water content of FAME.

3.5.3 Effect of soap and methanol on the separation of glycerol

This part of the study focused on the ability of the membrane process to remove free glycerol from FAME in the presence of soap and methanol. To evaluate these effects, mixtures (5 to 8) listed in Table 3.1 were treated by the membrane system. All runs were performed for 180 minutes.

The concentration of glycerol in the permeate and retentate as a function of time in the membrane separation system are shown in Table 3.2, while the results for % separation for all runs at different times are shown in Table 3.3. The ASTM standard for

glycerol concentration in FAME was not achieved for the three cases (mixtures, 1, 5 and 6), where no water was present in the FAME phase.

The mass% glycerol in the permeate vs. time for mixtures 1, 7 and 8 are also listed in Table 3.2. As previously mentioned, glycerol was not removed by the membrane for the FAME only case. In case 7, the FAME contained 1% methanol, the separation was low and the ASTM level was not reached. The ASTM level was reached without methanol when 1% soap and 0.06 % of water was added (case 8).

In case 5 using FAME + 1 mass% soap, we observed no separation of glycerol from FAME, and the values for free glycerol mass % were almost the same at all times (Tables 3.2 and 3.3). Adding 1 mass% methanol to the FAME resulted in low separations (see case 6 in Table 3.3). Methanol and glycerol are mutually soluble and FAME and methanol are also mutually soluble. The presence of methanol does not lead to the formation of a separate glycerol-methanol phase at these concentration levels. Overall, the separation of glycerol in case 6 is lower than that in case1. This indicates that methanol does not lead to the formation of a dispersed phase but solubilises glycerol in the FAME. This allows for the passage of glycerol through the membrane as it is dissolved in the FAME mixture.

Mixture 7, (FAME + 1 % soap + 1 % methanol + 0.06 % water) represents typical levels emanating from a conventional transesterification reaction. This mixture did not yield a particularly efficacious separation of glycerol from FAME. This is further supported by the results obtained for mixture 8 (FAME + 1 % soap + 0.06 % water (see Table 3.3, column 8). Table 3.2 shows that the ASTM standard of 0.02 mass% was reached within 30 min of operation.

3.6 Conclusion

FAME can be purified to ASTM and EN free glycerol standards using a membrane separation process. The extent of glycerol separation depends on the concentration of water, methanol, and soap in the FAME phase. Our results indicate that water has a great effect in removing glycerol from the FAME phase, but unlike conventional separation processes, only small quantities of water are needed to form large droplets within the dispersed glycerol in FAME.

The presence of methanol before introducing the crude FAME to the membrane separation system has a negative effect on glycerol separation by the membrane. DLS measurements and the separation results vs water content in the FAME showed the same trends indicating that droplet size enlargement played a considerable role in the separation mechanism. The removal of free glycerol from biodiesel was found to use 2.0 grams of water per L of treated FAME (0.225 mass% water) vs the current 10 L of water per L of treated FAME. This represents significantly lower amounts of water in the downstream purification process and reductions in both capital and operating costs as well as in the environmental impact of the biodiesel production process.

3.7 Acknowledgements

The authors acknowledge the financial support from the Natural Sciences and Engineering Research Council of Canada (NSERC) for financial support.

3.8 References

[1] W. Korbitz, Biodiesel production in Europe and North America. An encouraging prospect, Renewable Energy. 16 (1999) 1078 – 1083.

[2] J. Van Gerpen, Biodiesel processing and production, Fuel Proc. Tech. 86 (2005) 1097-1107.

[3] J. Sheehan, V. Camobreco, J. Duffield, M. Graboski, H. Shapouri, Life Cycle Inventory of Biodiesel and Petroleum Diesel for Use in an Urban Bus: Final Report NREL/SR-580- 24089 UC Category, May 1998.

[4] M.J. Haas, A.J. McAloon, W.C. Yee, T.A. Foglia, A process model to estimate biodiesel production costs, Bioresource Technology. 97 (2006) 671–678.

[5] V. Mao, S.K. Konar, D.G.B. Boocock, The pseudo-single-phase, base-catalyzed transmethylation of soybean oil, J. Am. Oil Chem. Soc. 81 (2004) 803-808.

[6] S.O.V. Ghadge, H. Raheman, Biodiesel production from mahua (Madhuca indica) oil having high free fatty acids, Biomass Bioenergy 28 (2005) 601–605.

[7] L.C. Meher, D.V. Sagar, S.N. Naik, Technical aspects of biodiesel production by transesterification — a review, Renewable Sustainable Energy Rev. 10 (2006) 248–268.

[8] F. Karaosmanoglu, K.B. Cigizoglu, M. Tuter, S. Ertekin, Investigation of the refining

step of biodiesel production, Energy & Fuels 10 (1996) 890-895.

[9] A. Demirbaş, Biodiesel fuels from vegetable oils via catalytic and non-catalytic supercritical alcohol transesterifications and other methods: a survey, Energy Conversion and Management 44 (2003) 2093–2109.

[10] P. Becher, Emulsions: Theory and Practice. American Chemical Society: Oxford University Press, Washington, D.C., 2001.

[11] K. W. Lawrence, C. Shoou-Yuh, H. Yung-Tse, H. S. Muralidhara, P. C. Satya, Centrifugation Clarification and Thickening, Handbook of Environmental Engineering, Humana press., 6 (2007) 101-103.

[12] M.A. Dubé, A.Y. Tremblay, J. Liu, Biodiesel production using a membrane reactor, Biores. Tech. 93 (2007) 639–47.

[13] P. Cao, A.Y. Tremblay, M.A. Dubé, K. Morse, Effect of membrane pore size on the performance of a membrane reactor for biodiesel production, Ind. Eng. Chem. Res. 46 (2007) 52–58.

[14] N.M. Kocherginsky, L. T. Chin, L. F. Wen, Demulsification of water-in-oil emulsions via filtration through a hydrophilic polymer membrane, Journal of Membrane Science. 220 (2003) 117–128

[15] L. Wang, W. Xudong, F. Ken-ichi, Effects of operational conditions on ultrafiltration membrane fouling, Desalination. 229 (2008) 181–191

[16] J. Van Gerpen, B. Shanks, R. Pruszko, Biodiesel Analytical Methods, August 2002–January 2004, July 2004 • NREL/SR-510-36240

[17] M.C. Porter, Handbook of Industrial Membrane Technology, Noyes publications, NJ, 1990.

[18] J. Van Gerpen, E.G. Hammond, L.A. Johnson, S.J. Marley, L. Yu, l. Lee, A. Monyem, Determining the Influence of Contaminants on Biodiesel Properties, Final report prepared for: The Iowa Soybean Promotion Board, Iowa State University, July 31, 1996.

[19] Osmonics "The Filtration Spectrum", https://rs6.eporia.com/company_607//filtrationspectrum.pdf (last visited on Sept 30th, 2009).

Chapter 4

The removal of glycerol and methanol from crude FAME using ultrafiltration

Chapter 4 - The removal of glycerol and methanol from crude FAME using ultrafiltration

Abstract

Ultrafiltration was used to remove glycerol from crude FAME originating from a transesterification reaction, without water washing or other post treatments. Three types of ultrafiltration membranes (5 kD (PES), 30 kD (PVDF), 100 kD Ultrafilic™) were tested at 0, 5 and 25^{o}C.

The results of this study indicate that glycerol can be separated from crude FAME to meet ASTM and EN standards at methanol feed concentrations of up to 3 mass%. The concentration of glycerol in FAME decreased as the concentration run proceeded. This unusual behaviour was attributed to the formation of a hydrophilic glycerol rich layer on the surface of the membrane. The concentration of free glycerol in this layer was determined to be 5.6 mass%. The layer captured the dispersed glycerol rich droplets in the feed. Once the dynamic selective layer was formed, the ASTM and EN standards for free glycerol, 0.02 mass%, were met. The thickness of the layer at the surface of the membrane did not continually increase as steady state fluxes were obtained. The advantage of ultrafiltration is that methanol is also retained by the membrane along with glycerol. The separation of methanol ranged form 79% to 85%. Using the smallest pore size (5 kD PES) membrane, the concentration of methanol in the permeate was reduced to 0.5 mass% down from an initial feed containing 2.4 mass%. This is close to the value of 0.2 mass% methanol specified in ASTM D6751-09 (EN 14110).

Keywords: ultrafiltration, biodiesel, glycerol, separation, fatty acid methyl ester (FAME), methanol

4.1 Introduction

Biodiesel is a non–toxic, biodegradable and renewable fuel that has many environmental benefits. It is a safe fuel and has combustion characteristics similar to that of petro-diesel. Biodiesel is comprised of fatty acid alkyl esters (FAAE) and can be used in its neat form or as a blend with conventional diesel fuel. The similarities between biodiesel and petro-diesel show that biodiesel is a viable alternative source of energy in diesel engines.[1] The replacement of petro-diesel with biodiesel has the potential to reduce the level of pollutants and carcinogens in our environment.[2,3,4] The most commonly used biodiesel production method is transesterification, where an animal fat or vegetable oil is reacted with an alcohol (usually methanol) to form fatty acid methyl esters (FAME) and glycerol.[5]

Many downstream processing treatments are required to produce biodiesel that meets international standards.[6] These post treatments can produce significant amounts of wastewater and consume considerable energy if this wastewater is recycled by evaporation.

In a typical post-transesterification reaction mixture (after removal of the glycerol-rich phase), the FAME phase consists of a non-polar continuous phase and a finely dispersed polar phase. The continuous FAME phase typically contains dispersed droplets of glycerol, methanol, water and traces of monoglyceride (MG), diglyceride (DG), triglyceride (TG), and soap. Methanol, water and glycerol have great affinity for each other and, at the same time, methanol is completely miscible in FAME. As a result, the methanol, water and glycerol will form fine droplets dispersed in the continuous FAME phase.

Water washing is widely used to purify FAME during the production of biodiesel. In this technique, water is contacted with FAME to wash out impurities such as glycerol and salts. This is a simple approach but leads to considerable waste water generation. In conventional production processes, a large amount of waste water is generated which is very energy intensive to treat.[7] This approach can also lead to significant separation problems due to the formation of emulsions in the presence of soaps and surface active compounds in the untreated FAME.

Karaosmanoglu et al.[8] investigated three methods to purify biodiesel produced

from rapeseed oil; one was to wash the reaction mixture with hot water, the second was to wash the mixture with petroleum ether and water, and the third was to use sulphuric acid to neutralize the mixture followed by evaporation to remove the methanol. The best refining process was found to be washing with hot distilled water at 50°C.

He et al.[9] studied three traditional methods for biodiesel purification: (i) washing with distilled water; (ii) washing with acid (HCl); and (iii) dissolving and extracting in a solvent (hexane or petroleum ether) and then washing with distilled water. They concluded that biodiesel of high purity (97.5%) could be obtained by all three methods, but serious emulsification occurred during the refining processes, which led to high product losses.

In a study of biodiesel produced from used restaurant frying oil[10], the crude FAME phase was washed with hot distilled water at 50°C at a ratio of 1:1, two times without stirring and three times with stirring to find the optimum number of washing stages for the chosen reaction conditions by determining the reduction in the total glycerine content. Seven consecutive washing steps were necessary to meet the required EN 14214 and ASTM D6751 limits.

Hayafuji et al.[11] produced biodiesel from waste oil and after separating the product mixtures by a centrifugal separator into two phases; they used solid sorbents such as activated carbon, activated carbon fibre, activated clay, acid clay, silica gel, activated alumina and molecular sieves, to remove the impurities in the FAME phase. Compared to the process of removing the impurities by warm water washing or by acid neutralization, this purification process is simple and requires no water removal after washing. However, using large amounts of sorbents leads to the problem of separating the sorbents from the final products. Moreover, these sorbents need regeneration, which may involve significant additional expense.

Several sorbents are available which are primarily composed of amorphous magnesium silicate (e.g., magnesol).[12] Their application is useful for removing biodiesel contaminants such as water, soaps, free glycerine and unreacted glycerides. However, this type of sorbent cannot be recycled in the process and alternatives for its final disposal are still unclear, particularly on a large-scale.[13] Ion exchange resins are also used to

remove impurities such as retained glycerol and salts.[14,15,16] The resins need to be regenerated which creates methanol loaded with water that must be purified before use.

Most of the above methods operate best when the methanol content of the biodiesel is reduced to a minimum. If glycerol could be removed from the biodiesel prior to methanol recovery it would minimize the reverse reaction from occurring such that additional monoglycerides and diglycerides, above those formed during transesterification, would not be found in the final biodiesel product. All of these methods have limitations related to waste generation and energy consumption. Thus, there is a need for improved purification techniques in biodiesel production.

4.2 The use of membrane separation technologies in biodiesel purification.

At present, membrane separation technologies are new to biodiesel purification processes. However, recent work has shown the efficacy of using membrane technology in the production of biodiesel.[17-21].

Other researchers have employed membrane technology in the purification of FAME. Othman et al.[22] investigated eight different types of commercial polymeric solvent resistant nanofiltration membranes for separating the methyl esters-rich effluent (biodiesel) from the mixture of the homogeneous catalyst, free glycerol and excess methanol after the transesterification process at various separation pressures and constant temperature. Scanning Electron Microscope (SEM) and Fourier Transform Infrared Spectroscopy (FTIR) were used to examine any changes to the membranes studied the transesterification product properties was modified by reducing the alkalinity value. The permeation experiment was conducted for pure polar solvents (water, anhydrous methanol and glycerol) and nonpolar solvents (RBD palm olein and methyl esters) at various ranges of separation pressure (600–3000 kPa) and temperature (28–60^{o}C). At a pH of 12.43 and 40^{o}C, it was found that at the end of the permeation process, the membranes were significantly damaged and the permeability flux for each membrane increased rapidly. The pH of the transesterification products was then modified to 8.68 and the results showed the possibility of separating the methyl esters from methanol and glycerides group.

He et al.[9] compared the traditional methods for the refining step in biodiesel production with a hollow fiber membrane extraction. Biodiesel with a high purity (97.5%) obtained from: (1) washing with distilled water; (2) washing with acid; and (3) extracting using a solvent (4) extraction using water while keeping the phases separated with a membrane. Serious emulsification occurred during the refining processes using the first three methods. Membrane extraction effectively avoided emulsification during refining and decreased the refining loss compared with the three traditional refining methods.

Wang et al.[23] used a ceramic membrane separation process for refining biodiesel. Different pore sizes of 0.6, 0.2 and 0.1 μm were used to remove the residual soap and free glycerol, at the trans-membrane pressure of 0.15 MPa and temperature of 60°C. The content of potassium, sodium, calcium and magnesium in the permeate was found to be lower than the EN 14538 specifications. The residual free glycerol in the permeate was estimated by water extraction, its value was 0.0108 wt.%. They concluded that ceramic membrane with the pore size of 0.1 μm was suitable for this separation process.

Gomes et al.[24] investigated the efficiency of microfiltration with ceramic membranes in the separation of biodiesel and glycerol. Ethanol was used as an alcohol in the transesterification. Different pore sizes of 0.2, 0.4, and 0.8μm were used. Feed solution with mass composition of 80% biodiesel, 10% glycerol, and 10% anhydrous ethanol were microfiltered at 60^{o}C and trans-membrane pressures of 1.0, 2.0, and 3.0 bar. Membrane performance was evaluated based on the capacity to retain glycerol and on the permeate flux values. Experimental results showed that trans-membrane pressure had a strong influence on biodiesel microfiltration. The best performance was obtained with the 0.2 μm membrane and 2.0 bar trans-membrane pressure. In these conditions and at the same temperature that was used, the influence of the ethanol concentration on the feed solution separation was evaluated. A higher concentration of ethanol led to a lower retention of glycerol and a lower ethanol concentration gave the best results for glycerol retention.

4.3 Objectives and approaches

In the present study, ultrafiltration membranes were used to treat unrefined, crude, FAME obtained directly after transesterification. The objective of this study was to develop a process that would eliminate or minimize the use of water and require less energy than the water washing process, while producing fewer wastes than other methods such as the solid sorbent techniques. Membrane separation technologies are well suited for this purpose. They do not involve a phase change and can effectively separate fine dispersions such as oil dispersed in water down to less than 100 ppm oil in water.[25] The requirement for free glycerol in biodiesel is 0.02 mass% (200 ppm). In the case of oil and water, oil is the dispersed phase and water is the continuous phase, whereas in the case of glycerol and FAME, glycerol would be the dispersed phase and FAME the continuous phase.

The objective was to be achieved without washing with large amounts of water or using solid sorbents. To fulfill this objective, we studied the effect of temperature on the glycerol content and percent separation and the effect of methanol on membrane separation performance.

4.4 Experimental section

4.4.1 Production of FAME

Refined canola oil (Loblaws, ON, Canada), methanol (99.85% purity, Commercial Alcohols Inc.; Brampton, ON, Canada), and sodium hydroxide NaOH (reagent grade, ACP Chemicals Inc.; Montreal, QC, Canada) were used to prepare FAME. A batch reactor of 6 L was used for the transesterification reaction. A 6:1 molar ratio of methanol to oil and a catalyst amount of 1 mass% NaOH based on oil was used. The operating temperature was 60°C and the reaction time was 1h. The finished product from the reaction was transferred to a separatory funnel and allowed to settle for 8 to 12 h, where the bottom glycerol-rich layer was removed. The non-polar, FAME-rich phase was then neutralized with sulphuric acid up to a pH of 7. Eleven (11) runs were needed to generate approximately 50 L of FAME for the purification experiments.

4.4.2 Polymeric membrane selection

The separation performance of a membrane is affected by the material forming the membrane and membrane pore size. Various materials can be used to make microfiltration (MF) and ultrafiltration (UF) membranes; the most common are polymers such as cellulose derivatives, polysulfone, polyvinylidene fluoride (PVDF) and polyamides. Specific polymers can impact membrane performance, maintenance characteristics, and efficiencies. Most MF and UF membranes are selected on the basis of: 1) The pore size of the membrane, because it determines to a large extent the substances that are retained by the membrane; 2) the chemical resistance of the material and 3) the interactions between the solutes in the solution and the membrane material. Swelling of the membrane material in the presence of solvents is always a concern when using polymeric membranes to treat solvents such as methanol and FAME.

In general, in the biodiesel production process, one can identify four solvents: FAME, methanol, glycerol and water. Most membranes are used in aqueous applications and glycerol is not expected to create difficulties in the selection of a membrane material. In this application, the resistance to methanol and FAME is the most important basis for choosing the membrane. The following polymeric membranes were studied: polyethersulfone (PES), PVDF and Ultrafilic™ membranes, the latter being made from modified polyacrylonitrile (PAN) that makes it extremely hydrophilic. The membranes had molecular weight cut-offs (MWCO) of 5 kD for the PES membrane, 30 kD for the PVDF, and 100 kD for the Ultrafilic membrane. They were all M-series ultrafiltration membranes purchased from the Sterlitech Corporation (USA).

4.4.3 Membrane separation system

Membrane separation technologies are new to biodiesel processing. Recent work has shown the efficacy of using membrane technology in the production of biodiesel.[17,18] Membrane separation technologies also have recently been applied to biodiesel purification.[26]Wang et al. [23]used ceramic microfiltration membranes to treat the FAME phase from transesterification. The permeate was washed with water and the water was assayed to determine the amount of glycerol left in the permeate. This is not according to ASTM and EN standards. All permeates in this work were tested according to ASTM

D6584 and EN 14105 that are based on gas chromatography (GC) analysis.

A membrane separation system (see Figure 4.1) was designed and constructed to investigate the removal of free glycerol from a biodiesel reactor effluent without using any water wash. The system is based on a feed and bleed configuration as shown in Figure 4.1.[27] A feed cross-flow velocity of 0.6 m/s in two SEPA™ (GE Osmonics) cross-flow cells in series with a filtration surface area of 0.0276 m^2 (2 x [14.5 cm x 9.5 cm]), was used. Identical membranes were used in both cells during a given test.

.

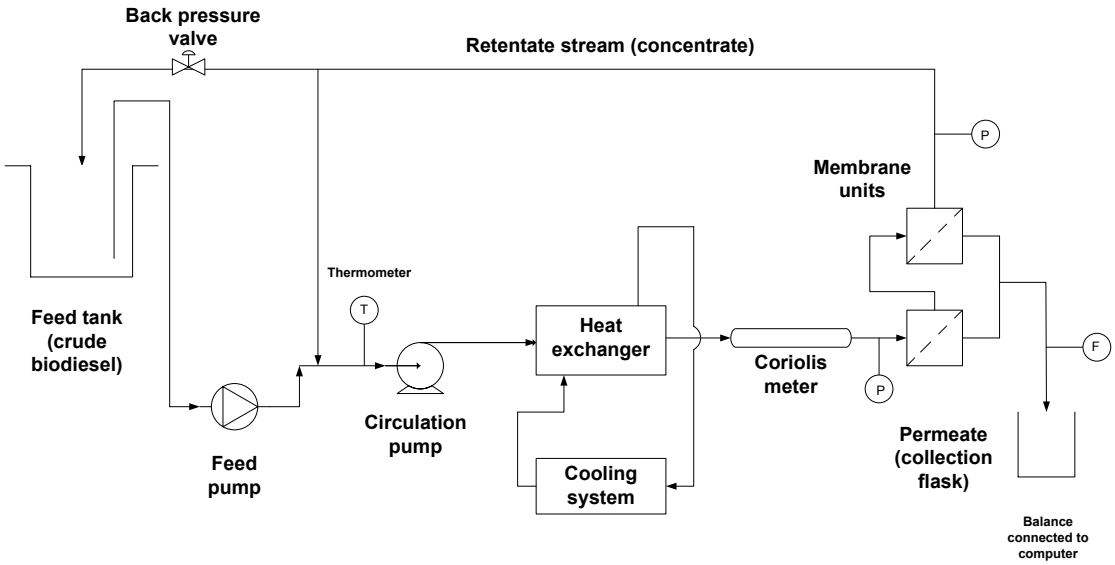

Figure 4.1: Schematic of membrane separation system. (P): pressure gauge, (F): flow meter connected to computer

Five litres (5 L) of crude FAME, produced earlier in the batch reactor, were put in the feed tank and circulated in the cross-flow membrane separation system at the operating conditions shown in Table 4.1. The inlet and outlet pressures of the membrane filtration system and the temperature of the system were controlled. The mass of permeate was automatically recorded on a computer. An initial feed sample was taken from the untreated FAME before all runs. Samples of the permeate side and retentate side of the membrane were taken after 15 min, 30 min, 1 h, 2 h and 3 h. All runs were carried out for a period of three hours. Samples collected from all runs (permeate and retentate),

were first weighed, after which a rotary evaporator was used to vaporize methanol from them under vacuum (0.94 bar vacuum) at 50°C for 30 min. The vaporized samples were reweighed to determine the methanol mass%.

Prior to GC analysis, the FAME was treated in a rotary evaporator at 90°C under vacuum (0.94 bar vacuum) for 30 min. All samples collected were analyzed by GC analysis using ASTM D6584.

Table 4.1: Operating conditions for each membrane type at (0, 5 and 25 °C).

Membrane type	**Conditions**
	Pressure (kPa)
Polymeric PES (5 kD) (Ultrafiltration range)	551.6
Polymeric PVDF (30 kD) (Ultrafiltration range)	344.7
Polymeric Ultrafilic (PAN) (100 kD) (Ultrafiltration range)	172.4

After each run, the membranes were cleaned by soaking in isopropanol for 24 h in order to solubilise any accumulated glycerol and FAME on the membrane surface. The fluid in the membrane pores and on the membrane surface was then gradually replaced by fresh FAME. This was done by soaking in 50:50 isopropanol and FAME for 24 h and soaking in only FAME for 24 h. The membranes were then ready for another run.

4.5 Results and Discussion

4.5.1 Effect of temperature on membrane separation

The concentration of free glycerol in FAME was determined according to ASTM D6584 and EN 14105. All samples were analyzed twice and the averages reported. The calculated deviations are within +/- 5.1% of this average value. This percent error was taken as representative for all other glycerol measurements performed in this work. The

membrane system was found to be effective in separating free glycerol from the untreated FAME. The concentration of free glycerol in the permeate decreased over time for all runs but the decrease was greater for a given membrane at higher temperatures as seen in Figures 4.2 to 4.4.

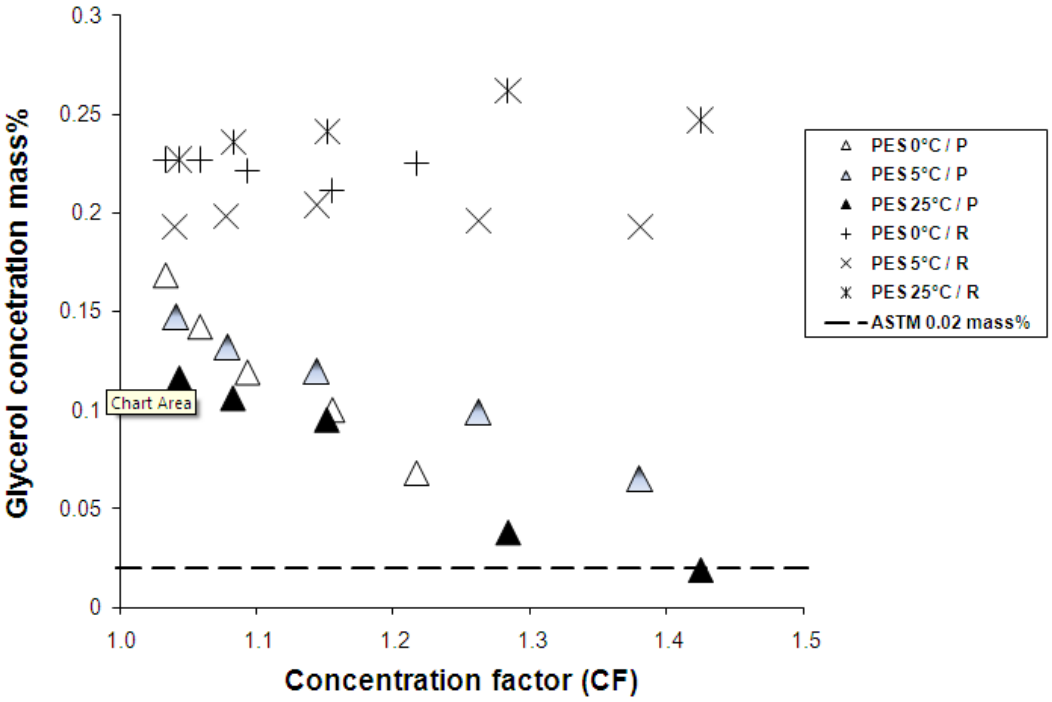

Figure 4.2: Glycerol concentration mass% vs. concentration factor (CF) for 5 kD, PES at different temperatures. (P): permeate, (R): retentate.

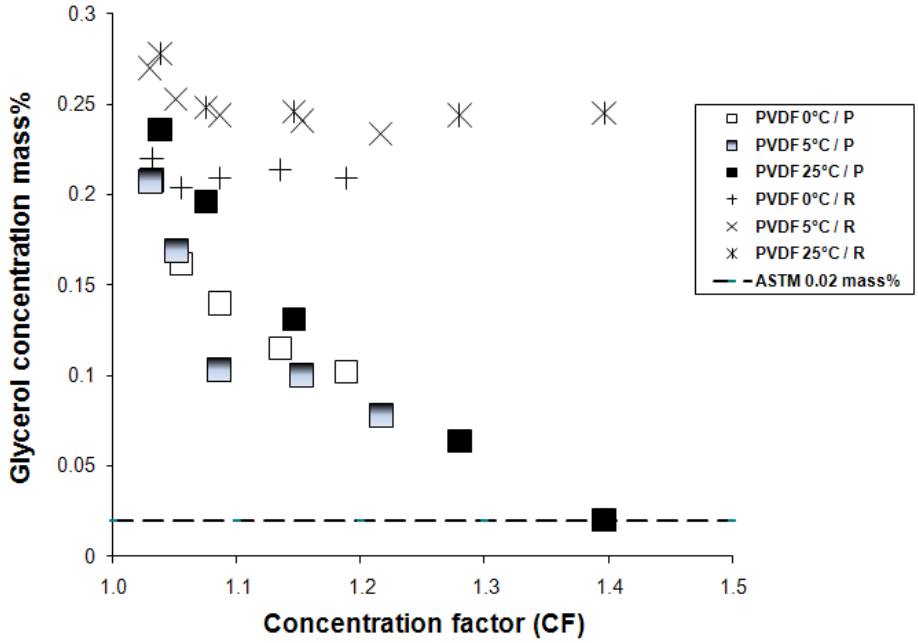

Figure 4.3: Glycerol concentration mass% vs. concentration factor (CF) for 30 kD, PVDF membrane at different temperatures. (P): permeate, (R): retentate.

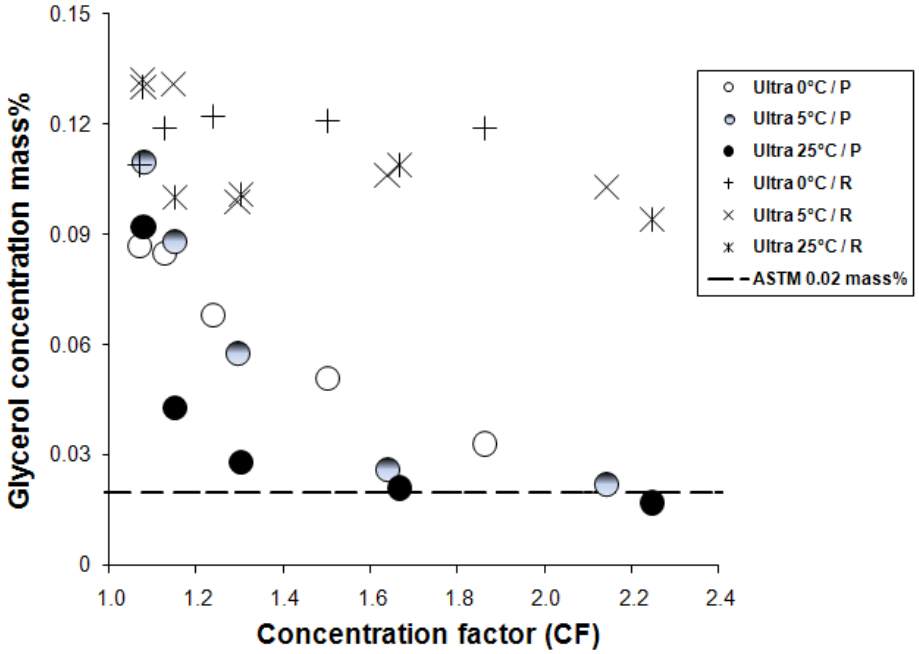

Figure 4.4: Glycerol concentration mass% vs. concentration factor (CF) for 100 kD, ultrafilic membrane at different temperatures.(P): permeate, (R): retentate.

The international standards, which are both set at 0.02 mass% maximum free glycerol content, were eventually met for all runs carried out at 25°C. The three membranes showed a high degree of retention for free glycerol from the crude FAME at the end of the runs (3 h) at 25°C. The free glycerol concentration in these permeates reached 0.019 % for the 5 kD PES, 0.02% for the 30 kD PVDF, and 0.017% for the 100 kD Ultrafilic membrane.

One potential explanation for the time dependent retention of glycerol is the loss of methanol by evaporation from the feed tank. This would decompatibilize glycerol in the FAME phase forming larger droplets that could more easily be separated by the membrane. The feed tank in Figure 4.1 was placed in a fume hood, although it was closed, it was not hermetically sealed, and the evaporation of methanol during the 3-hour run could possibly explain these time-dependent results. However, as seen in Table 4.2 the amount of methanol in the retentate did not substantially drop over the course of the run. It was also noticed that the flux for runs performed at 25°C was consistently higher than that at 0 and 5°C. Values for fluxes at all operating conditions are reported in Appendix B.

Table 4.2: Methanol concentration in the initial feed, retentate and permeate, for the three membranes at different temperatures.

Time (min)	**Methanol mass% at 0°C**			**Methanol mass% at 5°C**			**Methanol mass% at 25°C**		
	PES (5 KD)	**PVDF (30 KD)**	**Ultrafilic (100 KD)**	**PES (5 KD)**	**PVDF (30 KD)**	**Ultrafilic (100 KD)**	**PES (5 KD)**	**PVDF (30 KD)**	**Ultrafilic (100 KD)**
Initial Feed	2.1	3.7	3.8	2.1	3.0	5.6	2.4	4.1	5.2
15 / P	2.0	3.5	3.5	2.0	2.9	5.5	1.9	3.9	4.5
30 / P	1.8	3.1	3.4	1.7	2.6	5.4	1.5	3.1	3.8
60 / P	1.6	2.8	3.3	1.6	2.4	4.2	1.2	2.5	2.8
120 / P	1.5	2.3	2.5	1.4	2.0	2.9	1.0	1.7	2.0
180 / P	1.1	2.2	1.8	1.0	1.3	2.0	0.5	0.6	1.1
15 / R	1.8	3.5	3.1	1.5	2.6	5.0	1.3	3.4	4.6
30 / R	1.8	3.4	3.1	1.5	2.7	5.2	1.4	3.1	2.2
60 / R	1.8	3.5	3.3	1.3	2.7	5.3	1.3	3.3	2.5
120 / R	1.6	3.6	2.9	1.5	2.6	5.2	1.4	3.4	3.1
180 / R	1.6	3.5	3.3	1.4	2.6	5.0	1.3	3.3	3.0

In Figure 4.5, the separation of free glycerol was plotted vs. the concentration factor (CF) during the run. The separation and CF are defined as:

$$\text{Separation } (\%) = \frac{\text{Retentate Concentration (ppm)- Permeate Concentration (ppm)}}{\text{Retentate concentration (ppm)}} \times 100 \quad (4.1)$$

$$\text{CF} = \frac{\text{Initial feed volume}}{\text{Retentate volume at time (t)}} \quad (4.2)$$

As seen in Figure 4.5, the separation of glycerol increased with increasing CF. Figures 4.2 to 4.4 illustrates the composition of glycerol in the permeate and retentate and shows a decline in glycerol concentration with increasing CF and relatively constant retentate values for all membranes types at different temepratures. The ASTM and EN standards were met at CF of 1.4 for the 5 kD PES and 30 kD PVDF membranes and 2.25 for the 100 kD Ultrafilic membrane. This indicated that the smaller pores of the more selective lower molecular weight membranes played a role in retaining the droplets of the cake layer at the surface of the membrane.

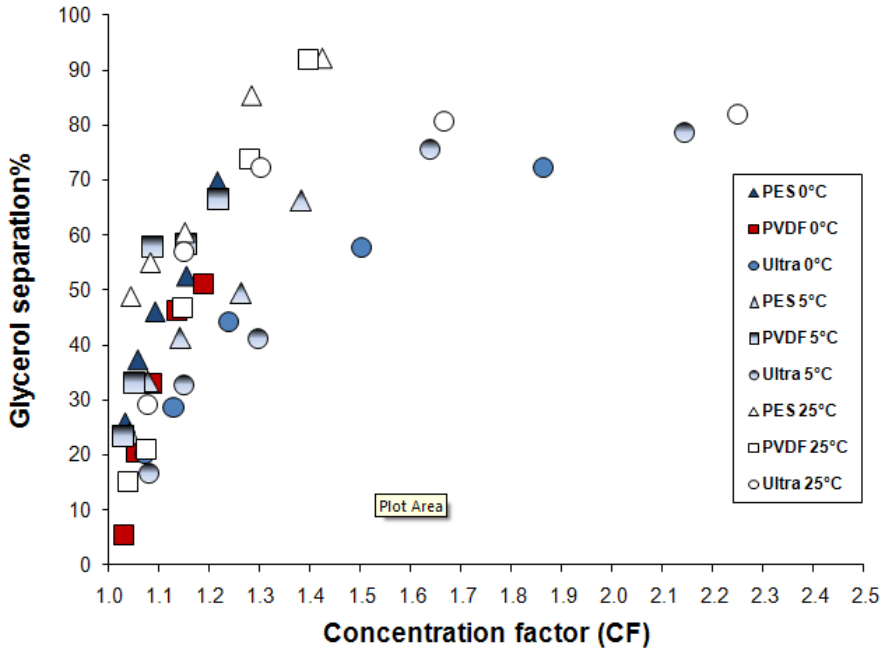

Figure 4.5: Glycerol separation vs. concentration factor (CF) for all membrane runs.

In operating a batch run, the concentration of a substance to be separated in the retentate loop increases as permeate is withdrawn from the loop. When this occurs, the separation of this substance usually decreases as a function of the CF. In the present case, the separation of free glycerine increased with CF which implies that the membrane is more selective as the batch of FAME was concentrated. This suggests that a build-up of a selective layer on the surface of the membrane was occurring. The selective layer was scouring the small glycerol droplets as they attempted to pass through the layer. This enhanced the separation capability of the membrane.

Form Figures 4.2 to 4.4, one can notice that the concentration of glycerol in the retentate stream remained relatively constant over the course of the run. It was also observed that for runs at 25 °C, a small polar phase appeared at the bottom of the feed tank. Glycerol most likely accumulated in this polar phase. The initial feed solution was obtained from the dephasing of the polar and non-polar phases produced after transesterification and represents a solution at saturated conditions. The removal of FAME from this solution would lead to further phase separation.[26] The level of glycerol in the retentate is constant as the FAME in the retentate remains saturated throughout the run.

Under cross-flow operation, when the layer reaches a certain thickness, glycerol will form larger droplets that can be removed from the layer. The layer eventually reached a steady state thickness as illustrated in Figure 4.6, where the flux of the membrane has been plotted vs. time for all 25°C runs. It shows that flux was approached the steady state after one hour in the 3-hour run. This layer was observed on the surface of all membranes prior to cleaning them in isopropanol as described above.

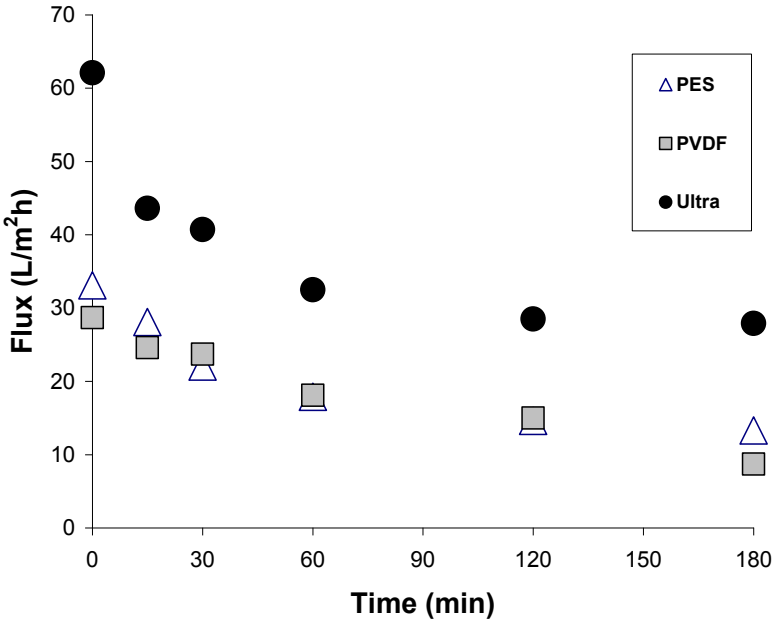

Figure 4.6: Permeate flux vs. time for runs of the three types of membranes performed at 25°C.

To characterize the selective layer at the surface of the membrane; a separate experiment was conducted where 0.24 mass% glycerol, 3.5 mass% methanol, 0.15 mass% water in FAME were permeated through a 100 kD PVDF membrane for 4.5 h at 25°C and 25 psi (173 kPa). One membrane (14.5 x 9.5 cm^2) was used and the CF was 2.2. The membrane was carefully removed from the cell. The surface was scraped and the membrane cut in 1 cm x 1 cm pieces and extracted with 125 mL of methanol for 24 h. The methanol was then evaporated under vacuum. Both samples were then analyzed by GC as in EN 14214 and ASTM D6751. A calibration was performed using standards at five concentrations ranging from 0.3 to 2.5 mass%; the correlation factor for this calibration was R^2=1.000.

The resulting glycerol in the FAME from the membrane extraction was 0.69 mass% while the concentration of the material scraped form the surface of the membrane was 5.6 mass%. This result demonstrates the existence of a dynamically formed, glycerol rich polar layer at the surface of the membrane. The lower concentration of glycerol in

the FAME extracted form the membrane; indicates that the glycerol rich layer at the surface of the membrane did not penetrate through the membrane and was retained at its surface.

4.5.2 Effect of methanol

It has been shown that the presence of methanol in the FAME phase at relatively high concentrations (>5%) has an impact on fuel flash point, lubricity and cetane number, but the effect is reduced at lower concentrations (<1%).[28]

Methanol concentrations were determined for all permeate and retentate samples obtained in the experimental runs described above. The weight of each sample was recorded prior to and after evaporation of the methanol under vacuum at 50°C using a rotary evaporator. Table 4.2 lists the methanol concentrations for the three polymeric membranes and the three operating temperatures.

The methanol concentrations ranged from 1 to 5% for all runs. It is interesting to note that although eventually the permeate concentration reached the ASTM standard, the methanol concentration in the retentate remained relatively constant throughout the run.

The methanol concentrations in the retentate when the ASTM concentration was reached were 1.3, 3.3 and 3.0 mass% for the run of 25 °C. The methanol concentration in the FAME mixture will compatibilize glycerol in the FAME phase, temperature range and pore size of the membrane.

The separation of methanol was determined with an equation similar to equation 4.1 but for methanol and the data in Table 4.2. For the 25°C runs, based on the permeate and initial feed concentrations of methanol at the end of the 3 hour runs, the separation of methanol was 79% for the 5 kD PES, 85 % for the 30 kD PVDF and 79 % for the 100 kD Ultrafilic membranes. These are unexpectedly high separations as methanol and FAME are infinitely soluble and are not expected to be separated by an ultrafiltration membrane. The results demonstrate that both glycerol and methanol are present in a polar phase and retained by the membrane.

The advantage of this separation technique is that methanol is also retained along with glycerol. The energy costs required to remove methanol from biodiesel have been shown to grow exponentially as the recovery of methanol from biodiesel tends to 100%

[29]. The difficulty in removing methanol from FAME by evaporation at ppm levels can be explained by the affinity of methanol for the residual glycerol in FAME. Glycerol has a boiling point of 290°C and will be retrained in FAME at the temperatures and pressures used in evaporating methanol.

Using the smallest pore size 5 kD PES membrane, the concentration of methanol in the permeate was 0.5 mass% down from an initial feed of 2.4 mass%. This is close to the value of 0.2 mass% specified in ASTM D6751-09 (EN 14110).

Ultrafiltration does not involve an increase in temperature and the exposure of the FAME to hot heat exchanger surfaces used in distillation. High temperatures degrade components in biodiesel and in the presence of glycerol leads to the formation of monoglycerides via the inverse of the transesterification reaction.

Based on these results, it can be seen that pore size plays a major role in reaching the desired glycerol separation at a lower CF. The CF also represents the amount of permeate that has passed through the membrane and reflects the accumulation of polar compounds (methanol and glycerol) at the surface of the membrane.

4.5.3 Flux study and membrane performance

The presence of methanol in the untreated FAME was considered to have a beneficial effect on the flux of FAME through the membrane. Methanol has a very low viscosity (0.53 cP) while for canola oil methyl ester it is 6.95 cP (both at 20°C).[30,31] The mass fraction of 5% corresponds to a molar fraction of 32.8% (based on methyl oleate MW = 296.49). The viscosity of a 5% methanol in FAME solution can be estimated based on the contribution of methanol and methyl oleate on a molar basis. This gives a viscosity of 4.5 cP; a reduction of 30% from that of pure FAME. The presence of methanol offers a considerable advantage when permeating FAME through a membrane.

The results in Figure 4.6 indicate that even in the presence of the dynamic selective layer on the membrane, methanol up to a concentration of 3 mass% can be present in the FAME and a reasonable flux of 30 Lmh ($L/m^2/h$) ($8.33x10^{-6}$ $m^3/m^2/s$) can be maintained while producing a permeate that meets ASTM standards.

4.5.4 Proposed separation mechanism

In the early stages of the filtration, polar dispersed droplets gradually accumulate at the surface of the membrane in the form of a cake layer. As the filtration proceeds, a balance sets in and at steady state, the deposition of droplets on the surface of the membrane is balanced by those leaving the layer due to the cross flow of fluid above the membrane. Once the layer is formed, the droplets containing methanol and glycerol in the feed solution can be captured by the layer. In addition to this, the droplets can coalesce at the surface of the membrane and eventually be entrained by the cross-flow of fluid at the surface of the membrane as illustrated in Figure 4.7. The case where solid droplets are ultrafiltered is also illustrated in Figure 4.7; in the absence of coalescence a well defined filter cake forms on the surface of the membrane. This explains the observation that a steady state flux was obtained in this work and that the polar phase did not simply revert at the surface of the membrane. That is, the coalesced droplets have a greater propensity to leave the surface of the membrane than to further coalesce into one homogeneous phase. This sets the dynamic coalescence and replacement of droplets at the surface of the membrane and acts in addition to the case where solid droplets are present in the cake to prevent an increase in the cake thickness and flux decline.

To leave the surface of the membrane, the droplets must diffuse away from it by Brownian or hydrodynamic diffusion. In this case, Brownian diffusion for dispersed phases will be negligible as the droplets' size is expected to be greater than 100 nm. The shear diffusion of a droplet (D_{shear}) in a flow stream was found to be proportional to the radius of the droplet (a_p) squared times the local shear rate in the fluid ($\dot{\gamma}$)[32,33], as follows:

$$D_{shear} \alpha \dot{\gamma} a_p^2 \qquad (4.3)$$

The shear rate at the membrane surface remains constant throughout the run as it is related to the flow rate in the membrane channel. This implies that the ability of a droplet to migrate away from the surface will be linked to the square of its radius (or diameter). If two droplets of equal diameter join to form a new droplet, their combined size will grow by a factor of $2^{1/3}$, while the shear diffusion acting on the new droplet will be $2^{2/3}$ greater than that acting on the original droplets; this is an increase in shear

diffusion of 68%. If more droplets coalesce, then the effect on diffusion will be enhanced. The size of the droplets suspended in the FAME were measured and were found to range between 250 and 2500 nm depending on the water content of the FAME.[26] The aggregation of droplets at the surface of the membrane is not expected to be linear, as a function of glycerol concentration. The crude FAME was obtained from phase separation so the polar droplets suspended in the FAME are at their point of saturation. The presence of a polar surface or the slightest, local, preferential removal of FAME from the solution can lead to dephasing and non-linear droplet size growth. If the increase in size from 250 to 2500 nm were to occur at the surface of the membrane, then the shear diffusion of the droplets at the surface of the membrane would increase by a factor of 100. This is a considerable increase in shear diffusion and would cause the aggregated droplets to easily be transported away from the surface of the membrane.

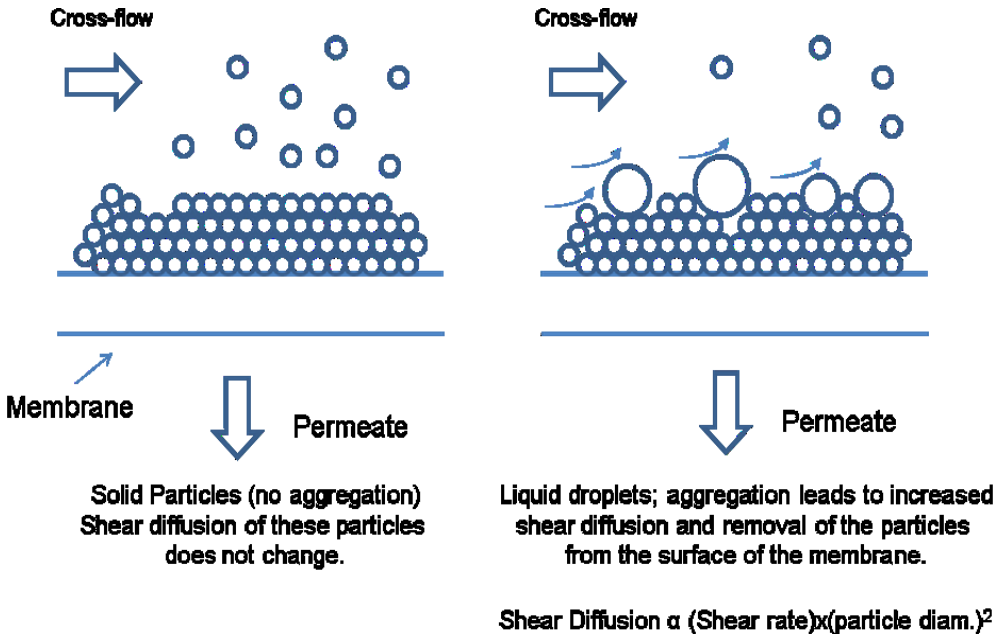

Figure 4.7: Accumulation of droplets at the surface of the membrane in the case of solid droplets and liquid droplets that can coalesce.

The results of this work point to the existence of a dynamic layer of polar droplets at the surface of the membrane, these droplets contain methanol/glycerol and water. Smaller droplets passing through this layer are then dynamically captured and coalesced to form larger droplets that move away from the surface of the membrane due to shear diffusion. This dynamic transport to the surface, coalescence and removal from the surface ensures that phase reversal into a single polar phase does not occur at the surface of the membrane and that the polar phase does not permeate through the membrane.

4.6 Conclusion

Cross flow ultrafiltration has proved to be very useful in separating free glycerol and methanol from crude FAME obtained directly from the transesterification reaction. The technology avoids the use of traditional biodiesel purification methods such as water washing, sorbents and ion exchange.

The process relies on the formation of a dynamic polar layer on the surface of the membrane. Once the layer is formed, the concentration of free glycerol in the permeate reaches ASTM and EN standards. The standards were met at CF of 1.4 for 5 kD PES and 30 kD PVDF and 2.25 for the 100 kD Ultrafilic membrane. Complete phase reversal in the cake present at the membrane surface did not occur. This was due to the aggregation of polar droplets and the substantial increase in shear diffusion of these larger droplets moving them away form the cake. This removed the possibility of phase inversion where only the polar phase would permeate through the membrane.

An added benefit of ultrafiltration was the retention of methanol by the membrane. The limitations in separating methanol form FAME using distillation due to the affinity of methanol for glycerol was not present in this technique. The smallest pore size used in this study reduced the concentration of methanol in FAME to a value close to the ASTM specification for biodiesel.

The nature of the cake remains relatively constant throughout the process as evidenced by the steady state permeation flux described above. The separation of free glycerol can be achieved to meet ASTM standards without the removal of the methanol from the FAME. The resulting permeate is also lower in methanol, requiring less

evaporation downstream and causing less formation of MG and DG by the reversal of the transesterification reaction.

4.7 Acknowledgements

The authors acknowledge the financial support from the Natural Sciences and Engineering Research Council of Canada (NSERC) for financial support.

4.8 References

[1] Fukuda, H.; Kondo, A.; Noda, H. Review: Biodiesel fuel production by transesterification of oils. *J. Biosci. Bioeng*. **2001**, *92*, 405-416.

[2] Pryde, E. H. Vegetable oils as fuel alternatives – symposium overview. *J. Am. Oil Chem. Soc*. **1983**, *61*, 1609-1610.

[3] Shay, E. G. Diesel fuel from vegetable oil: status and opportunities. *Biomass Bioenergy*. **1993**, *4*, 227–242.

[4] Ma, F.; Hanna, M. A. Biodiesel production: a review. *Bioresour. Technol*. **1999**, *70*, 1–15.

[5] Van Gerpen, J. Biodiesel processing and production. *Fuel. Process. Technol*. **2005**, *86*, 1097– 1107.

[6] Berrios, M.; Skelton, R. L. Comparison of purification methods for biodiesel. *J. Chem. Eng*. **2008**, *144*, 459–465.

[7] Tremblay, A. Y.; Cao, P.; Dubé, M. A. Biodiesel production using ultralow catalyst concentrations. *Energy Fuels*. **2008**, *22*, 2748–2755.

[8] Karaosmanoglu, F.; Cıgızoglu, K. B.; Melek, T.; Ertekin, S. Investigation of the refining step of biodiesel production. *Energy Fuels*. **1996**, *10*, 890-895.

[9] He, H. Y.; Guo, X.; Zhu, S. L. Comparison of membrane extraction with traditional extraction methods for biodiesel production. *J. Am. Oil Chem.Soc*. **2006**, *83*, 457–460.

[10] Cetinkaya, M.; Karaosmanoglu, F. Optimization of base-catalyzed transesterification reaction of used cooking oil. *Energy Fuels*.**2004**, *18*, 1888-1895.

[11] Hayafuji, S.; Shimidzu, T.; Zaima, H. Method and apparatus for producing diesel fuel from waste edible oil.**1999**; US patent No 5,972,057.

[12] Bryan, T. Adsorbing it all. Biodiesel magazine. **2005***, 40*.

[13] Kucek, K. T.; César-Oliveira, M. A, F.; Wilhelm, H. M.; Ramos, L. P. Ethanolysis of refined soybean oil assisted by sodium and potassium hydroxides. *J. Am. Oil Chem. Soc*. **2007**, *84*, 385 – 392.

[14] Naomi, S. K.; Hiroki, H.; Homare, K.; Takuji, T.; Takuya, F.; Toshikuni, Y. Biodiesel production using anionic ion-exchange resin as heterogeneous catalyst. *Bioresour. Technol*. **2007**, *98*, 416-421.

[15] Oing, S.; Bolun, Y.; Hong, Y.; Song, O.; Gangli, Z. Synthesis of biodiesel from soybean oil and methanol catalyzed by zeolite beta modified. *Catal. Commun*. **2007**, *8*, 2159-2165.

[16] Park, J. Y.; Kim, D.K.; Wang, Z. M.; Lee, J. P.; Park, S. C.; Lee, J. S. Production of biodiesel from soap stock using an ion-exchange resin catalyst. *Energy. Environ. Eng*. **2008**, *25*, 1350-1354.

[17] Dubé, M. A.; Tremblay, A. Y.; Liu, J. Biodiesel production using a membrane reactor. *Bioresour. Technol.* **2007**, *93*, 639–47.

[18] Cao, P.; Tremblay, A. Y.; Dubé, M. A.; Morse, K. Effect of membrane pore size on the performance of a membrane reactor for biodiesel production. *Ind. Eng. Chem. Res*. **2007**, *46*, 52–58.

[19] Cao, P.; Dubé, M. A.; Tremblay, A. Y. High-purity fatty acid methyl ester production from canola, soybean, palm, and yellow grease lipids by means of a membrane reactor. *Biomass Bioenerg*. **2008a**, *32*, 1028-1036.

[20] Cao, P.; Dubé, M. A.; Tremblay, A. Y. Methanol recycling in the production of biodiesel in a membrane reactor. *Fuel*. **2008b**, *87*, 825-833.

[21] Cao, P.; Tremblay, A. Y.; Dubé, M. A. Kinetics of canola oil transesterification in a membrane reactor. *Ind. Eng. Chem. Res*. **2009**, *48*, 2533-2541.

[22] Othman, R.; Mohammad, A. W.; Ismail, M.; Salimon, J. Application of polymeric solvent resistant nanofiltration membranes for biodiesel production. *J. Membr. Sci*. **2010**, *348*, 287–297.

[23] Wang, Y. L.; Ou, S.; Tan, Y.; Tang, S. Refining of biodiesel by ceramic membrane separation. *Fuel. Process. Technol*. **2009**, *90*, 422–427.

[24] Gomes, M. C. S.; Pereira, N. C.; Davantel de Barros, S. T. Separation of biodiesel and glycerol using ceramic membranes. *J. Membr. Sci.* **2010**, *352*, 271-276.

[25] Peng, H.; Tremblay, A. Y,; Veinot, D. E. The use of backflushed coalescing microfiltration as a pretreatment for the ultrafiltration of bilge water. *Desalination*. **2005**, *181*, 109-120.

[26] Saleh, J.; Tremblay, A. Y.; Dubé, M. A. Glycerol removal from biodiesel using membrane separation technology. *Fuel.* **2010**, *89*, 2260–2266.

[27] Porter, M. C. *Handbook of industrial membrane technology*, Noyes publications, NJ. **1990**.

[28] Van Gerpen, J.; Hammond, E. G.; Johnson, L.A.; Marley, S. J.; Yu, L.; Lee, I.; Monyem, A. Determining the influence of contaminants on biodiesel properties, Final report prepared for: The Iowa Soybean Promotion Board **1996**; July 31.

[29] Dhar, B. R.; Kirtania, K. Excess methanol recovery in biodiesel production process using a distillation column: a simulation study. *Chem. Eng. Research. Bulletin*. **2009**, *13*, 55-60.

[30] Strayer, R. C.; Blake, J. A.; Craig, W. K. Canola and high erucic rapeseed oil as substitues for diesel fuel: preliminary tests. *JAOCS.* **1983**, *60*, 1587-1592.

[31] Xiang, H. W.; Laesecke, A.; Huber, M. L. A new reference correlation for the viscosity of methanol. *J. Phys. Chem. Ref Data*. **2006**, *4*, 1598-1620.

[32] Leighton, D.; Acrivos, A. Measurement of shear-induced self-diffusion in concentrated suspensions of spheres. *J. Fluid. Mech*. **1987a**, *77*, 109-131.

[33] Leighton, D.; Acrivos, A. The shear-induced migration of particles in concentrated suspensions. *J. Fluid. Mech*. **1987b**, *181*, 415-430.

Chapter 5

Separation of glycerol from FAME using a ceramic membrane

Chapter 5 - Separation of glycerol from FAME using a ceramic membrane

Abstract.

International standards (e.g., ASTM D6751 and EN14214) limit the presence of free glycerol in biodiesel. The traditional water wash method for removing the glycerol from crude fatty acid methyl esters (FAME) obtained in the production of biodiesel results in waste waters that cannot be readily discharged. To circumvent the water wash purification method, a membrane separation system using ceramic membranes was designed, constructed and tested for the removal of glycerol from crude FAME from a biodiesel production process. Ceramic membranes in the ultrafiltration (0.05 μm) and microfiltration (0.2 μm) ranges were tested at three different operating temperatures: 0, 5 and 25°C. All runs separated glycerol from the crude FAME. International standards for glycerol content in biodiesel were met after 3 h when utilizing the ultrafiltration membrane setup at 25°C with a concentration factor greater than 1.6.

Keywords: membrane, biodiesel, glycerol, separation, fatty acid methyl ester (FAME), methanol

5.1 Introduction

Biodiesel is a renewable, biodegradable and environmentally safer fuel for use in diesel engines that can be produced from lipids such as vegetable oils, animal fats and used cooking oils via transesterification. It is comprised of fatty acid alkyl esters (FAAE) and can be used in its neat form or as a blend with conventional diesel fuel. The transesterification reaction occurs between the lipid and an alcohol to form esters and a glycerol by-product. Commercial biodiesel production occurs most frequently via alkali-catalyzed (e.g., sodium methoxide ($NaOCH_3$)) transesterification with an excess of methanol; the biodiesel product in this case is a fatty acid methyl ester (FAME). The transesterification consists of a number of consecutive, reversible reactions as shown in Figure 5.1. The triglyceride (TG) is first converted to diglyceride (DG), then to monoglyceride (MG) and finally, glycerol.

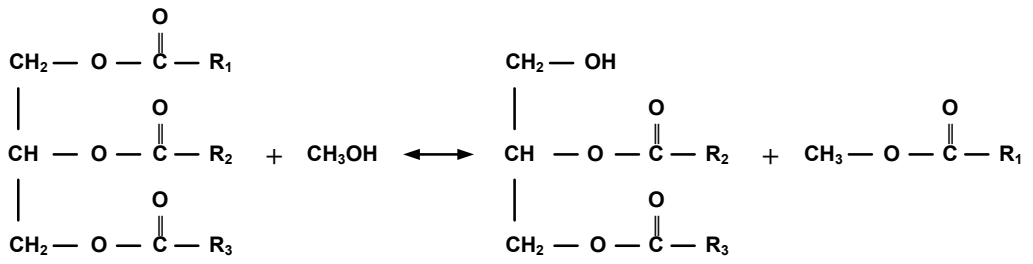

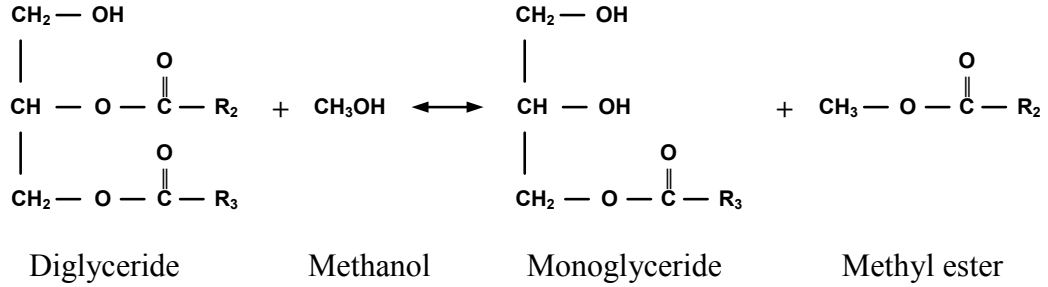

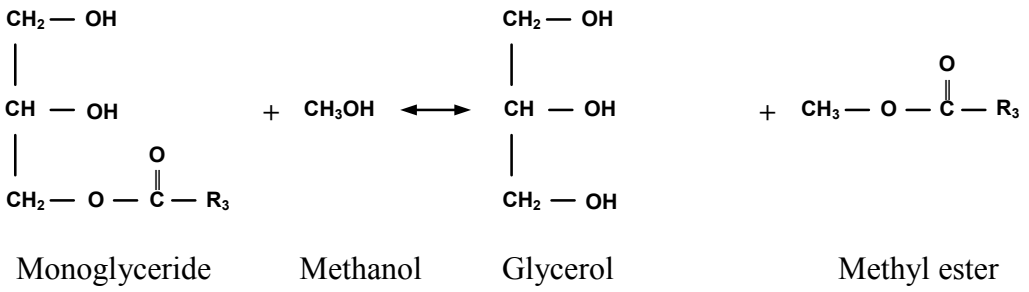

Figure 5.1: General reaction scheme for transesterification of triglycerides

The biodiesel production process includes transesterification followed by separation of the crude, non-polar FAME phase from a polar glycerol-rich layer, purification of the FAME, and possibly, recovery of the glycerol as a high-grade by-product. Due to the low solubility of the by-product glycerol in the FAME phase, the heavier glycerol phase tends to easily separate and settle from the FAME phase. However, traces of glycerol can remain suspended in the FAME phase along with small amounts of unreacted TG, DG and MG, while the residual catalyst and unreacted alcohol are distributed between the two layers. Thus, after the lower glycerol layer is removed, the FAME phase is typically washed with water to remove the residual glycerol, base catalyst and any soaps formed during the reaction. Finally, methanol and water present in the FAME phase are removed by distillation or evaporation [1, 2].

5.2 Biodiesel Purification Steps

The purity of biodiesel is an important issue for its safe and long-term use in engines. Biodiesel quality is regulated by standards such as ASTM D6751 and EN 14214 [3]. Achieving these standards plays a large role in the cost and widespread acceptance of biodiesel as a fuel. In order to produce high quality biodiesel, a series of purification processes are usually needed. These can include: gravitational settling, centrifugation, water washing, adsorption and distillation [4].

The most common method for purification of the FAME phase is water-washing. FAME and unreacted TG are essentially insoluble in water, while soap, methanol and glycerol are readily soluble in water. Therefore, adding water to the non-polar phase is

usually the first step in purifying it of these impurities. This water-washing step allows the soap, the alkaline catalyst residue and small amounts of glycerol, MG and DG in the product mixture to be removed. Unfortunately, the separation of the non-polar FAME phase from the water layer is usually difficult and this tends to increase the size and cost of the separation equipment. After the washing step, the waste wash water is contaminated by the extracted methanol, glycerol, soap and the residual catalyst. If the waste water is disposed without further treatment, loss of these materials and, potential environmental harm will result. Furthermore, significant quantities of this waste water are produced [5]. Results from the characterization of a typical waste water stream after biodiesel purification are shown in Table 5.1 along with the required levels for waste water disposal [6, 7, 8]. It is clear from these data that the waste water from the biodiesel process is highly contaminated and should be treated prior to disposal.

Table 5.1: Typical effluent characteristics from water washing purification [6, 7, 8].

Parameter	**Typical values for wastewater from a biodiesel process [6]**	**Required values for wastewater disposal [7, 8]**
Total chemical oxygen demand (mg/L)	18,362	100 – 200
pH	6.7	6 – 9
Conductivity (μS/cm)	1119	317 – 325
Total suspended solids (mg/L)	8850	30 – 90
Volatile suspended solids (mg/L)	8750	N/A
Mineral suspended solids (mg/L)	100	N/A

5.3 Objectives and approaches

Membrane separation technology has been used for many applications such as the purification of food and pharmaceutical products [9], water purification from surface waters, well water, brackish water and seawater, and also in industrial wastewater treatment [10]. The most widely used are microfiltration (MF) and ultrafiltration (UF) membranes.

Membrane separation technologies are relatively new to biodiesel purification processes. Recent work has shown the efficacy of using membrane technology in the production of biodiesel [11] as well as in its purification [12]. The compatibility of membrane materials, the effects of operating parameters and the possibility of using membrane separation processes in biodiesel purification have not been studied to a great extent.

He et al. [13] used a hollow-fibre membrane extraction process to avoid emulsification during the refining steps in a biodiesel process. Membrane extraction effectively avoided emulsification during refining and decreased the refining loss compared with the three traditional refining methods. The method used employed significant amounts of distilled water and the achievement of glycerol content standards was not reported.

In our previous work, we studied the use of polymeric membranes to separate free glycerol from FAME; the effect of water, methanol and soap on the separation was reported [12]. Results showed low concentrations of water had a considerable effect in removing glycerol from the FAME even at ~0.08 mass%. This is four orders of magnitude less than the amount of water required in conventional biodiesel purification processes using water washing. It was suggested that the mechanism of separation of free glycerol from FAME was due to the removal of an ultrafine dispersed glycerol-rich phase present in the untreated FAME. In this study, we turn our focus to the use of ceramic membranes to remove free glycerol from a post-transesterification FAME stream, without using a water wash step or other techniques. The effect of different membrane pore sizes, as well as the effect of temperature on the glycerol content from the membrane purification effluent was tested at certain fixed pressures.

5.4 Experimental section

5.4.1 Materials

Canola oil (refined/bleached/deodorized) was purchased from a local food store (Loblaws, ON, Canada). Methanol (99.85% purity, Commercial Alcohols Inc.; Brampton, ON, Canada), sodium hydroxide (NaOH, reagent grade, ACP Chemicals Inc.; Montreal, QC, Canada), other chemicals and standards for the gas chromatography

analysis (GC) such as glycerine, monoolein (for MG), diolein (for DG), triolein (for TG), N-methyl-N-(trimethylsilyl) trifluoroacetamide (MSTFA), butanetriol and tricaprin (Sigma Aldrich, Canada) were used as supplied.

5.4.2 Production of biodiesel

The FAME needed for purification experiments was produced using a batch process. A reactor with a capacity of 6 L was used. A molar ratio of methanol to oil of 6:1 with 1 mass % NaOH based on oil was employed for a one hour reaction time at 60°C. Thereafter, the reaction mixture was allowed to settle for 8 to 12 h. After settling, the lower, polar glycerol-rich layer was removed and the upper non-polar layer (FAME phase) was neutralized with sulphuric acid to a pH of 7. Many runs were performed to generate sufficient quantities of FAME for the purification experiments and the FAME was stored in suitable containers. The resulting, continuous FAME phase contained a dispersed polar phase that was composed of small amounts of methanol, water, and glycerol. These polar components formed stable emulsions that did not separate over time and formed fine droplets dispersed in the continuous FAME phase.

5.4.3 Membrane retention of glycerol from the FAME phase

A membrane separator system (see Figure 5.2) was used as a feed and bleed system [14] equipped with a feed pump and circulating pump. We employed two different ceramic membrane pore sizes: 0.2 μm in the microfiltration (MF) range and 0.05 μm in the ultrafiltration (UF) range. Table 5.2 shows the operating conditions for the ceramic membrane used. The ceramic membranes (Tami Industries, France) had an internal diameter of 5 mm and a length of 590 mm, which gave a total filtration surface area of 0.00927 m^2. The advantages of ceramic membranes are their enhanced mechanical strength and structural stiffness, corrosion and thermal resistance, stability of operating characteristics and the possibility of multiple regenerations, and resistance to bacterial attack [15]. This makes it possible to use ceramic membranes for the separation of solutions over a wide pH range (from 0 to 14), at high temperatures and pressures (1 – 10 MPa), and in corrosive media.

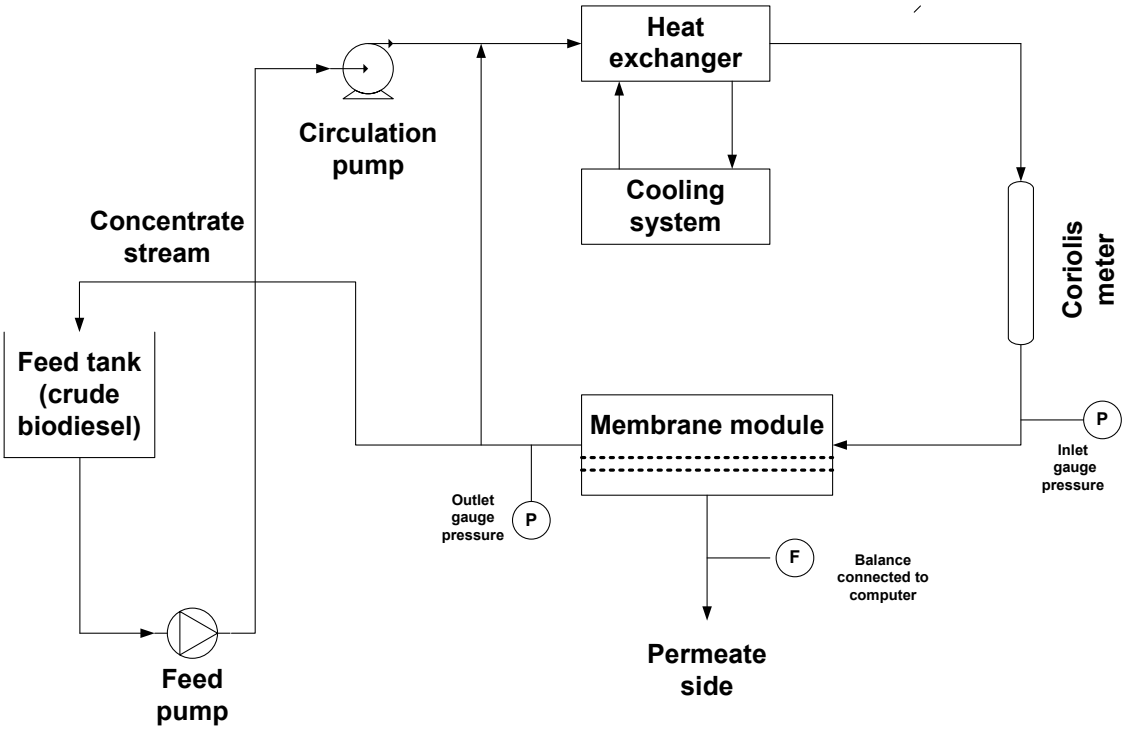

Figure 5.2: Schematic of membrane separation system.

Table 5.2: Operating conditions.

Membrane type	Temperature (°C)	Pressure (kPa)
Ultrafiltration (0.05 μm)	0, 5, 25	552
Microfiltration (0.2 μm)	0, 5, 25	207

Five litres of the FAME phase produced in the batch reactor were put in the feed tank and circulated/cross-filtered at a velocity of 2 m/s in the membrane separation system. The circulating pump was used to circulate the feed past the membranes at the operating conditions shown in Table 5.2. The inlet and outlet pressures of the membrane filtration system were achieved by adjusting the related valves. The temperature of the

system was controlled using a cooling system. The mass permeate collected was automatically recorded every minute on a computer by way of a balance.

All runs were stopped after three hours. Samples of the permeate (P) and retentate (R) were taken at 15 min, 30 min, 1 h, 2 h and 3 h; samples of the initial mixture were denoted as "original sample". All samples were analyzed for glycerol content using gas chromatography (GC) by way of ASTM method D6584. Prior to analysis, all samples were heated in a rotary evaporator for 30 min at 90^{o}C and 0.94 bar to remove any methanol and water. All runs were duplicated and all samples from all runs were analyzed twice. The %error from the calculated standard deviations for all runs was from 3 to 5%. Additional details on the membrane separation process can be found in a previous publication [12].

5.4.4 GC analysis

A GC, a Varian CP-3800, was used to determine the free and total glycerol in the FAME samples according to the ASTM D6584-00 method. A 15 m x 0.32 mm x 0.1 μm column from Restek (MXT – Biodiesel TG) was used with a guard column of 2 m x 0.53 mm. Calibration curves for the GC were generated using two internal standards (butanetriol and tricaprin) and four reference materials: glycerine, monoolein, diolein, and triolein. Three replicate injections at 5 separate concentrations were performed, yielding, a glycerol calibration curve, $R^2 = 0.9994$, that meets the ASTM requirement.

Each sample was prepared for analysis by weighing 100 mg of FAME in a 10 mL septa vial. 100 μL of butanetriol, tricaprin and MSTFA were then added to the vial and shaken. The vial was left to stand for 15 min at room temperature. Approximately 8 mL of n-heptane was then added to the vial. 1 μL of the prepared sample mixture was then injected into the cool on-column injection port. The operating conditions for the column oven were 50°C for 1 min, 15°C/min to 180°C, 7°C/min to 230°C, 30°C/min to 380°C, hold 10 min. The carrier gas was helium at a constant flow of 3.0 mL/min, the detector was a flame ionization detector (FID) held at 380°C, H_2 flow was at 35 mL/min, air was at 350 mL/min, and He (make-up) was at 30 mL/min.

5.5 Results and discussion

The free glycerol content in the original sample, in the permeate (P) and retentate (R) at three different temperatures as a function of concentration factor (CF) for all runs in the UF range are shown in Figure 5.3, where

$$CF = \frac{\text{Initial feed volume}}{\text{Retentate volume at time (t)}} \tag{5.1}$$

It should be noted that at each temperature condition each run was replicated, i.e., Run 2 is a replicate of Run 1, etc. Furthermore, the results are reported vs. CF in order to normalize membrane performance in light of the fact that, as will be discussed later, the membranes exhibited different fluxes. Results for the retention of glycerol at different temperatures and times are shown in Figure 5.4, where the glycerol retention was determined as:

$$\text{Glycerol retention (\%)} = \frac{\text{(Glycerol mass\% in retentate- Glycerol mass\% in permeate)}}{\text{Glycerol mass\% in retentate}} \times 100 \tag{5.2}$$

The retention of glycerol by the UF membrane was successful. The results in Figure 5.3 shows a reduction in glycerol content in the permeate with increasing CF for all temperatures. When these data are considered with respect to time, the most significant decline was noted to occur at 25°C; that is, after 3 h, glycerol content reductions of 74, 81 and 86% were measured for the runs at 0, 5 and 25°C, respectively as shown in Appendix B Table B6.

At 25°C, the ASTM standard was met (glycerol content = 0.018 mass%). From Figure 5.4, an increase in retention with CF was observed for all temperatures with the best retention at 25°C. These results are consistent with previous research [10] in the UF range using a modified polyacrylonitrile (PAN) membrane, with 100 kD molecular weight cut off at 25°C and 552 kPa operating pressure.

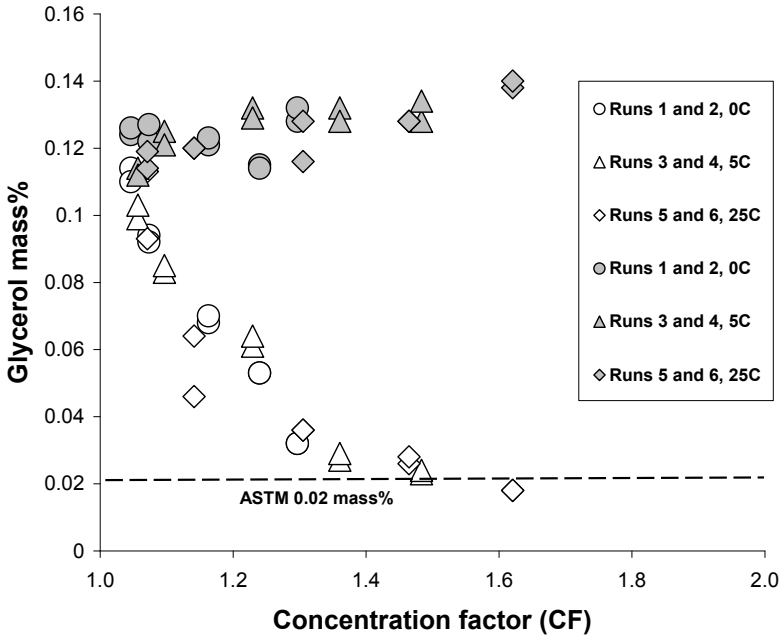

Figure 5.3: Glycerol content in permeate and retentate vs. concentration factor at different temperatures for ultrafiltration (0.05 μm) runs. (open symbols = permeate; closed symbols = retentate)

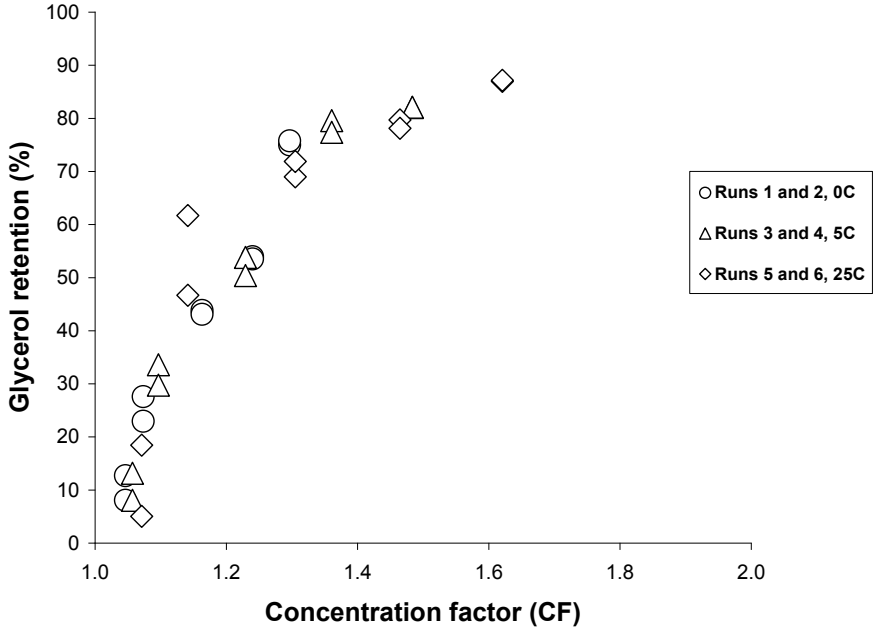

Figure 5.4: Glycerol retention vs. concentration factor for ultrafiltration (0.05 μm) runs at different temperatures.

The operating temperature is important especially when untreated FAME (i.e., FAME containing residual methanol, soap and water) is introduced to the membrane module. The miscibility of methanol and FAME tends to solubilize the dispersed glycerol droplets in the FAME phase and this will make the separation difficult if not impossible in the presence of methanol alone (i.e., without soap or water) in the FAME mixture, while the presence of soap alone (i.e., without methanol or water) in the FAME mixture will reduce the size of the glycerol droplets and separation will fail. These results and the effect of different parameters (i.e., water, methanol and soap) on the glycerol droplet size formed in FAME were addressed in recent work [16]. Our previous results with polymeric membranes [12] showed that UF failed to remove glycerol from FAME mixtures containing only methanol or only soap at 25°C. Wang et al. [17] were able to reduce the amount of glycerol in FAME using a ceramic membrane separation at a higher temperature (i.e., 60°C), but only after removing the methanol from the raw FAME. The actual glycerol concentration was not determined using a GC method as specified in both ASTM and EN standards. Gomes et al. [18], using ceramic membranes at 60°C in the presence of ethanol as opposed to methanol did not reach ASTM specifications.

Using temperatures above 25°C will increase the solubility of water in the FAME mixture. The solubility of water in biodiesel depends on the feed stock used to produce the ester, i.e., the degree of saturation of the esters, and has been reported to range from 1500 to 1785 ppm at 25°C [19, 20]**.** Temperature has been found to strongly increase the solubility of water in various commercial biodiesels [19]. Thus, using higher temperatures will increase the solubility of glycerol-rich droplets in FAME and make the separation more challenging.

A comparison of the results using the UF membrane to that employing a MF membrane on the separation of glycerol from FAME was made. The free glycerol content in the original sample, in the permeate (P) and retentate (R) at the three different temperatures studied as a function of CF for all runs in the MF range, are shown in Figure 5.5. The retention vs. CF for the MF membrane is plotted in Figure 5.6. The complete results for glycerol content in the original sample, permeate and retentate samples are shown in Appendix B Table B7.

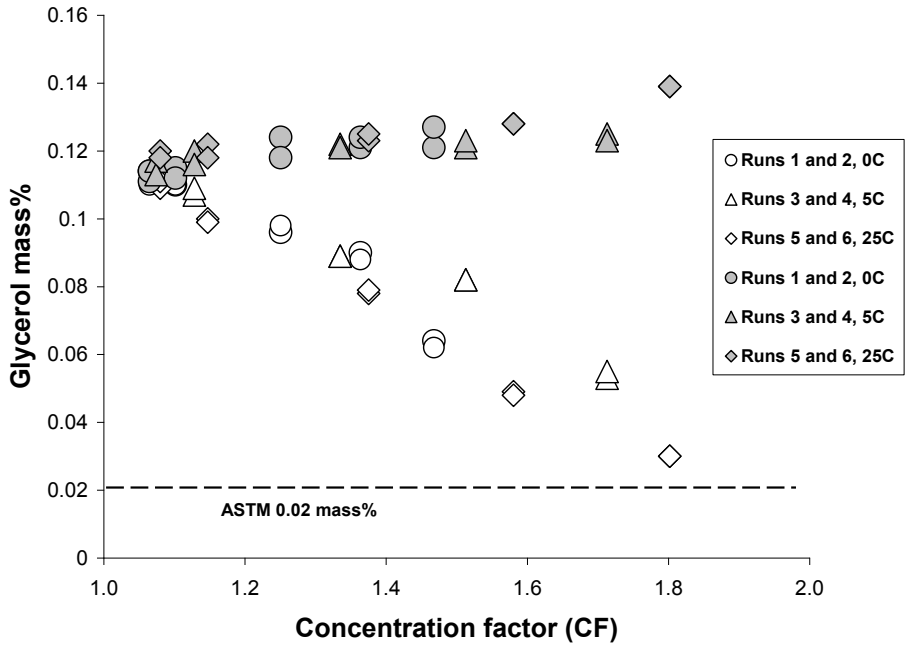

Figure 5.5: Glycerol content in permeate and retentate vs. concentration factor at different temperatures for microfiltration (0.2 µm) runs. (open symbols = permeate; closed symbols = retentate)

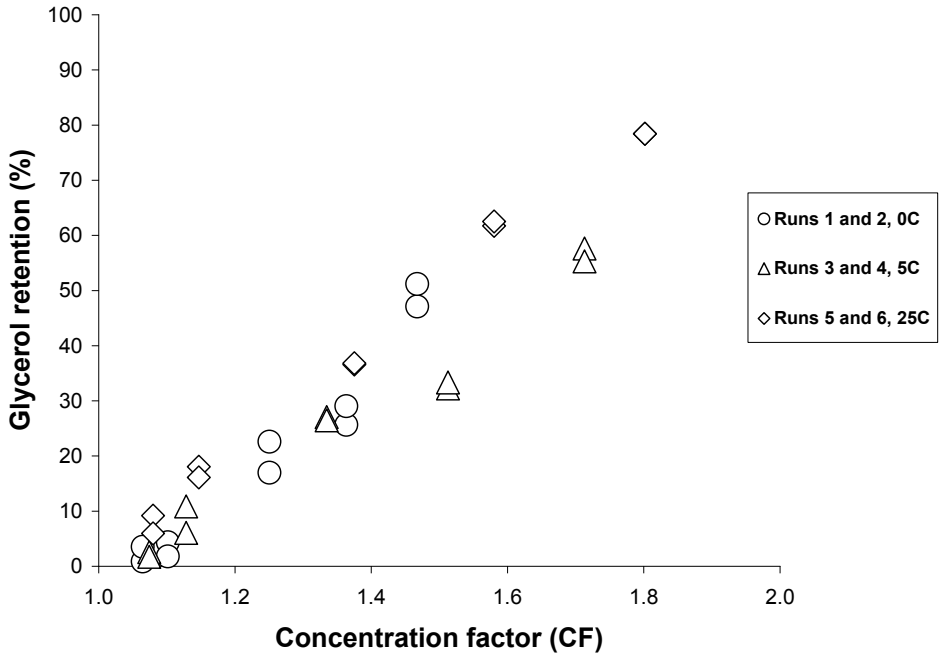

Figure 5.6: Glycerol retention vs. concentration factor for microfiltration (0.2 µm) runs at different temperatures.

As shown in Figure 5.5, while the MF ceramic membrane runs failed to reach the ASTM standard for all temperatures used, a significant retention was achieved for all the MF runs. It should be clear that continued operation of the process would have eventually resulted in the ASTM standard being achieved. Wang et al. [17] used a ceramic membrane in the MF range (pore sizes of 0.1, 0.2 and 0.6 μm) at 60°C and achieved their best results at the 0.1 μm pore size. Gomes et al. [18] investigated pore sizes of 0.2, 0.4 and 0.8 μm ceramic membranes at 60°C with ethanol as opposed to methanol and achieved their best results, 0.04 mass% glycerol content in the permeate, using a 0.2 μm pore size.

A glycerol material balance for this continuous process was performed for each run by determining the total amount of glycerol initially in the feed solution minus the total amount of glycerol leaving in the permeate. The glycerol concentration in the permeate declined with increasing CF for each membrane at each temperature studied. However, the concentration of glycerol in the retentate was relatively constant throughout the runs as shown in Figures 5.3 and 5.5. Thus, the amount of glycerol accumulated in the loop (either on the membrane surface or in the retentate) as a percentage of the initial feed was 27, 40 and 55 for the UF runs, and 20, 25 and 32 for the MF runs at 0, 5, and 25°C, respectively. These mass balances for both the UF and MF runs, show an increase in glycerol accumulation with temperature. This suggests that the dispersed droplets either aggregated over time into larger droplets, accumulated on the membrane surface, or de-phased in the feed tank. Only a very thin film of glycerol (i.e., a gel layer) was observed at the bottom of the feed tank for the 25°C UF runs indicating that some de-phasing did occur. This de-phasing was not observed for any of the other runs. Thus, the aggregation of glycerol-rich droplets or the accumulation of a glycerol layer on the membrane surface was most likely.

Using lower temperatures was initially hypothesized to positively influence the separation by increasing the viscosity and lowering the solubility of the glycerol phase in the FAME phase and causing the dispersed particles to aggregate for easier removal. When plotted against CF, the glycerol content in the permeate (see Figs. 5.3 and 5.5) as well as the retention (see Figs. 5.4 and 5.6) for each run overlapped. As mentioned above, it would appear that longer run times would inevitably result in the ASTM standard being

met at all temperatures. Of course, it is convenient that the ASTM standard was achieved at room temperature and thus, the lower temperature experiments were not extended to times greater than 3 h in order to reach the appropriate CF value.

The permeate flux as a function of time for the UF and MF membrane runs at different temperatures is shown in Figures 5.7 and 5.8, respectively. Comparing the two figures, one can see that, as expected, the larger pore size of the MF membrane provided a slightly larger flux at the expense of the retention of the glycerol droplets.

Under cross-flow operation, when the gel layer reaches a certain thickness, the polar compounds accumulated on the membrane surface will form larger droplets that can be removed from the layer. The layer eventually approached a steady state thickness as illustrated in Figure 7 and 8. It shows a remarkable reduction in the flux in the first 30 min after which the flux approaches a steady state value. From Figures 5.4 and 5.6, one observes that in the first 60 min, the value of retention was small before approaching a steady-state thickness, and thereafter the removal of glycerol increased. This is also consistent with results shown in Figures 5.3 and 5.5 for glycerol mass% in the permeate.

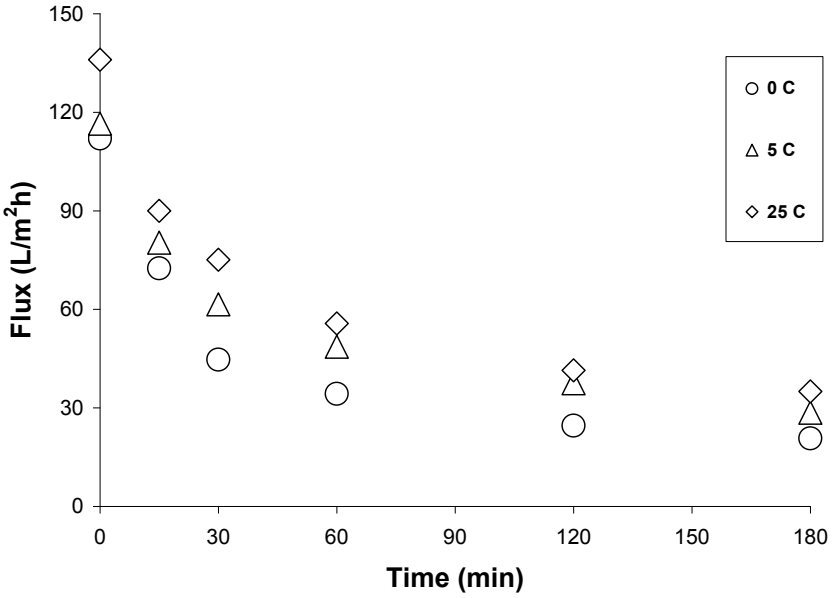

Figure 5.7: Flux vs. time for ultrafiltration runs at 0, 5 and 25°C.

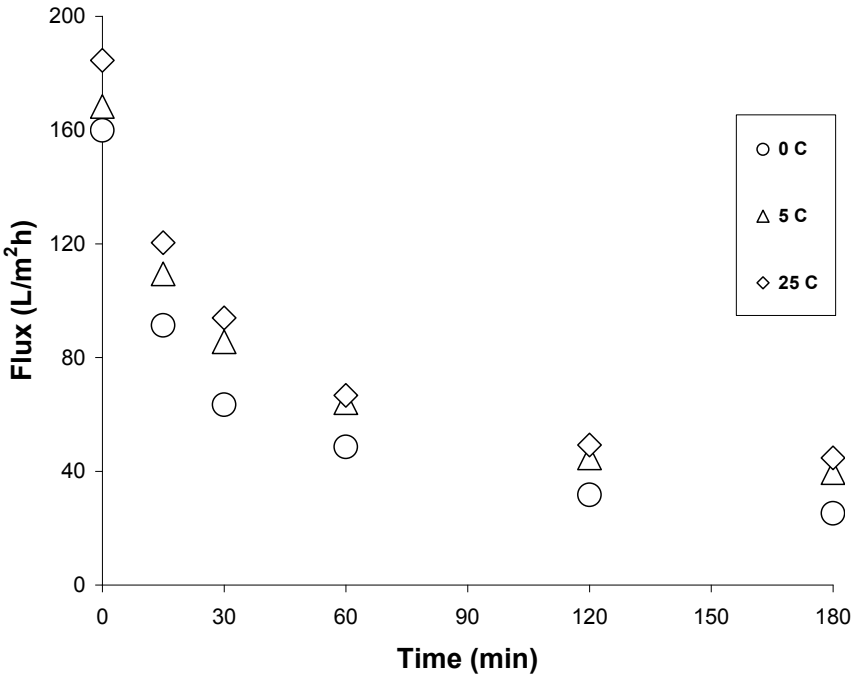

Figure 5.8: Flux vs. time for microfiltration runs at 0, 5 and 25°C.

5.6 Conclusion

A membrane process for the separation of free glycerol dispersed in a FAME phase after transesterification was developed. Ceramic membranes in the MF and UF ranges were used at different temperatures. The ASTM standard for glycerol content in biodiesel and CF greater than 1.6 was met using the UF ceramic membrane setup at 25^{o}C after 3 h. Additional time, i.e., increase in the CF, would be required to achieve the ASTM standard for lower temperature ranges and/or the use of the MF membrane.

The effect of temperature on glycerol removal was evident from its relation with the CF. Higher temperatures appeared to promote reaching the appropriate CF value sooner for faster separation of glycerol from the FAME-rich phase. In addition, the smaller pore size of the UF membrane facilitated glycerol removal compared to the MF membrane.

Membrane technology circumvents the need for traditional biodiesel purification methods such as water washing, which produce significant amounts of wastewater

containing impurities. This results in an economic gain and the avoidance of a serious environmental disposal problem.

5.7 Acknowledgements

The authors acknowledge the financial support from the Natural Sciences and Engineering Research Council of Canada (NSERC).

5.8 References

[1] J. Van Gerpen, Biodiesel processing and production, Fuel. Process. Technol. 86 (2005) 1097– 1107.

[2] M.J. Hass, A.J. Macaloon, W.C. Yee, T.A. Foglia, A process model to estimate biodiesel production costs, Bioresour. Technol. 97 (2006) 671–678.

[3] L.C. Meher, D.V. Sagar, S.N. Naik, Technical aspects of biodiesel production by transesterification — a review, Renew. Sust. Energ. Rev. 10 (2006) 248–268.

[4] F. Karaosmanoglu, K.B. Cigizoglu, M. Tuter, S. Ertekin, Investigation of the refining step of biodiesel production, Energy Fuels. 10 (1996) 890-895.

[5] D. Clements, G. Knothe, Biodiesel production technology August 2002–January 2004,
Iowa State University, NREL/SR-510-36244.

[6] M. Berrios, R.L. Skelton, Comparison of purification methods for biodiesel, J. Chem. Eng. 144 (2008) 459–465.

[7] M.V. Sperling, C.A.L. Chernicharo, Urban wastewater treatment technologies and the implementation of discharge standards in developing countries, Urban Water. 4 (2002) 105-114.

[8] J.C. Akan, F.I. Abdulrahman, E. Yusuf, Physical and chemical parameters in abattoir wastewater sample, PJST. 11 (2010) 640-648.

[9] H. Strathmann, Membrane separation processes: current relevance and future opportunities, J. AIChE. 47 (2001) 1077-1087.

[10] B. Nicolaisen, Developments in membrane technology for water treatment, Desalination. 153 (2002) 355–360.

[11] P. Cao, A.Y. Tremblay, M.A. Dubé, K. Morse, Effect of membrane pore size on the performance of a membrane reactor for biodiesel production, Ind. Eng. Chem. Res. 46 (2007) 52–58.

[12] J. Saleh, A.Y. Tremblay, M.A. Dubé, Glycerol removal from biodiesel using membrane separation technology, Fuel. 89 (2010) 2260–2266.

[13] H.Y. He, X. Guo, S.L. Zhu, Comparison of membrane extraction with traditional extraction methods for biodiesel production, J. Am. Oil. Chem. Soc. 83 (2006) 457-460.

[14] Y.I. Komolikov, L.A. Blaginina, Technology of ceramic micro and UF membranes (review), Refract. Ind. Ceram. 43 (2002) 5-6.

[15] M.C. Porter, Handbook of industrial membrane technology. Noyes publications, NJ, 1990.

[16] J. Saleh, M.A. Dubé, A.Y. Tremblay, Effect of soap, methanol and water on glycerol particle size in biodiesel purification, Energy & Fuels. (2010) In press.

[17] Y. Wang, X. Wang, Y. Liu, S. Ou, Y. Tan, S. Tang, Refining of biodiesel by ceramic membrane separation, Fuel. Process. Technol. 90 (2009) 422-427.

[18] M.C.S. Gomes, N.C. Pereira, S.T. Davantel de Barros, Separation of biodiesel and glycerol using ceramic membranes, J. Membr. Sci. 352 (2010) 271-276.

[19] P. Shah, C. Wee, J.M. White, S. Sanford, G. Meier, Experimental determination and thermodynamic modeling of water content in biodiesel-diesel blends, Renewable Energy Group, Inc., www.regfuel.com. (2010).

[20] J. Van Gerpen, E.G. Hammond, L.A. Johnson, S.J. Marley, L. Yu, l. Lee, A. Monyem, Determining the Influence of Contaminants on Biodiesel Properties, Final report prepared for: The Iowa Soybean Promotion Board, Iowa State University, July 31, 1996.

Chapter 6

Effect of soap, methanol and water on glycerol droplet size in biodiesel purification

Energy & Fuels, 2010, 24: 6179-6186

Chapter 6 - Effect of soap, methanol and water on glycerol droplet size in biodiesel purification

Abstract

For use as a transportation fuel, biodiesel must meet certain quality standards (e.g., ASTM D6751 and EN 14214). Free dispersed droplets of glycerol are among the important impurities in biodiesel that should be removed. The use of membrane separation technology to remove glycerol droplets from fatty acid methyl ester (FAME) has been demonstrated to be an effective biodiesel purification method. The presence of large glycerol droplets promotes its separation from FAME. The effect of water, methanol, soap and glycerol on the size of suspended droplets in FAME was studied using a 3-level Box-Behnken experimental design technique. The statistical analysis revealed the significant effect of water and glycerol on increasing droplet size while methanol and soap served to reduce the droplet size. Experimental verification using a polyacrylonitrile (PAN) membrane at a temperature of 25°C was completed. The addition of small amounts of water was found to improve the removal of glycerol from FAME and a glycerol content as low as 0.013 mass%, well below the standard of 0.020 mass%, was achieved.

Keywords: biodiesel, glycerol, separation, fatty acid methyl ester (FAME), DLS, membranes.

6.1 Introduction

Biodiesel is a renewable, biodegradable and environmentally safer fuel for use in diesel engines that can be produced from vegetable oils, animal fats and/or used cooking oils. It is comprised of fatty acid alkyl esters (FAAE) and can be used in its neat form or as a blend with conventional diesel fuel. The microstructural similarities between biodiesel and diesel fuel make biodiesel an interesting alternative for combustion in diesel engines. Compared to petroleum diesel, combustion emissions for biodiesel, such as carbon monoxide, particulates, unburned hydrocarbons and SOx emissions are much lower [1, 2].

Biodiesel is more commonly produced via the transesterification of an animal fat or vegetable oil with an alcohol to form esters and glycerol [3]. The process includes a reaction between a vegetable oil (triglyceride) such as soybean oil, rapeseed or canola oil, and an alcohol such as methanol, in the presence of catalyst such as sodium methoxide or sodium hydroxide. The reaction is usually carried out in an excess of the stoichiometric quantity of alcohol [4]. The products of the transesterification of triglyceride with methanol produce fatty acid methyl ester (FAME) and glycerol. Transesterification consists of a number of consecutive, reversible reactions in which a mole of FAME is liberated at each step while triglyceride is converted in turn to diglyceride, monoglyceride and finally, glycerol [5].

In the typical biodiesel production process, as a result of the transesterification, two layers are formed: one, the upper layer, is a FAME-rich phase while the other, lower layer, is richer in the glycerol by-product. The FAME phase often contains impurities such as free dispersed glycerol droplets, water, soap, unreacted methanol, and trace amounts of residual catalyst and mono-, di-, and triglycerides [6]. It is necessary to remove these impurities from the ester phase because they will strongly affect the properties of the biodiesel fuel produced. For instance, the presence of catalyst in biodiesel fuel may damage the injector pump and pose corrosion problems in the engine. The presence of high levels of methanol can accelerate the deterioration of natural rubber seals and gaskets. Monoglycerides can cause turbidity (i.e., from crystals) in the mixture of esters. This problem is particularly pernicious for the transesterification of animal fats such as beef tallow [7]. The presence of soap in large quantities can cause difficulties in

separation of the FAME phase from the glycerol-rich phase. Free glycerol can result in its eventual separation from the biodiesel during storage (e.g., in the fuel tank), forming gum-like deposits around injector tips and valve heads. Therefore, to reduce hazards, mechanical failure and promote engine life, standard specifications have been created that define the quality of biodiesel (e.g., ASTM D6751 and EN14214) [8].

The conventional purification of the FAME phase from these impurities begins with water washing to remove the residual glycerol, base catalyst and any soap formed during the reaction [9]. Methanol and water present in the FAME phase are eliminated by distillation or evaporation under vacuum or atmospheric pressure. The water washing treatment produces a large amount of highly polluting waste water [10, 11]. This increases the size and cost of the separation equipment, results in the loss of yield and causes an environmental disposal problem. Ion exchange resins and magnesium silicate solid adsorbents have been used as an alternative to water washing to remove hydrophilic materials such as glycerol and mono- and diglycerides [12]. However, the adsorbent cannot be recycled and alternatives for its final disposal are still unclear, particularly at the larger scale [13].

The use of membrane technology in biodiesel purification to avoid water washing can provide solutions for many environmental problems by recovering valuable products as well as treating effluents and minimizing their harm to the atmosphere. Membrane separation technology has been used for many applications in fields outside of biodiesel production and purification, such as desalination of sea and brackish water, for treating industrial effluents, and for purification of food and pharmaceutical products [14]. A membrane presents a physical barrier that restricts the transport of various chemical species. It can be homogeneous or heterogeneous, symmetric or asymmetric in its structure, and it may be either neutral, or may carry positive or negative charges, or both. Its thickness may vary between less than 100 nm to more than a centimetre [15]. The membrane can be either polymeric or ceramic, where common membrane processes include microfiltration, ultrafiltration, reverse osmosis, electro-dialysis, gas separation, nano-filtration, and pervaporation [16]. These are largely differentiated by the size of the molecules being separated and/or the pore size of the membrane.

We have recently introduced the use of membrane technology to remove dispersed glycerol droplets from FAME [17]. A key parameter in the use of this technology is the size of the glycerol droplets and the influence of other components such as water, methanol and soaps on that droplet size. The current research is focussed on elucidating the magnitude of the effect of different variables on the size of the glycerol droplets using dynamic light scattering (DLS).

The ASTM D6751 and EN14214 standards limit the free glycerol content in biodiesel to ≤0.02 mass% [18]. Following the transesterification reaction, the FAME phase contains dispersed glycerol droplets (free glycerol), unreacted methanol, water and soap. It is important to understand the nature of the materials present in the FAME phase and the relation of these materials with FAME and between each other. Knowing these relations enables the creation of a medium with large droplets that can be easily removed by membranes and avoids the water washing step.

The nature of the materials in the FAME phase is as follows: A) FAME and methanol are totally miscible; B) methanol, glycerol and water are totally miscible; C) glycerol and water have limited solubility in FAME; D) soap (surfactant) is a dispersing material and its hydrophobic part will be miscible in the FAME phase and its hydrophilic part will be miscible in water. Since the free glycerol droplets are present in the FAME phase either as dispersed droplets or as dissolved molecules, this implies that creating large droplets of glycerol will enhance their separation from the FAME phase using membrane technology. The question we raise here is: What materials present in the FAME phase may assist in or work against the creation of large droplets and facilitate the separation of glycerol from the FAME?

This paper focuses on studying the effect of different levels of the components of the FAME phase (i.e., water, methanol, soap and glycerol) on droplet size. To effectively and efficiently determine these effects, a regression model was constructed using a 3-level Box-Behnken experimental design technique [19]. Following this, verification of these effects using a membrane separation setup was pursued.

6.2 Experimental section

6.2.1 Production of biodiesel

A conventional alkaline transesterification reaction was used to prepare the FAME needed for the experiments using canola oil (food grade, refined/bleached/deodorized, purchased from Loblaws, ON, Canada), methanol (99.85% purity, Commercial Alcohols Inc.; Brampton, ON, Canada) and caustic soda (NaOH) (reagent grade, ACP Chemicals Inc.; Montreal, QC, Canada) in a 6 L batch reactor. A 6:1 molar ratio of methanol to oil and 1 mass% NaOH based on oil was used. The operating temperature was 60°C and the reaction time was 1 h. The reactor contents were mixed using a circulation pump in a pump-around loop. After separation, the FAME phase was neutralized with sulphuric acid to a pH of 7. Several runs were performed to produce ~30 L of FAME. All products for all runs from different batches were stored in separate containers. 5 L of the produced FAME was used for the DLS measurements. The remaining FAME (~25 L) was used to prepare mixtures for the membrane separation system. All of the FAME was evaporated under reduced pressure in a rotary evaporator (vacuum-treated FAME) at 90°C under vacuum (0.94 bar vacuum) for 30 min to ensure that neither methanol nor water was present. Furthermore, levels of mono-, di-, and triglycerides, as well as the acid number, were all within the ASTM D-6751 standard.

During the vacuum-treatment step, aggregates began to form and precipitate; these aggregates were removed from the FAME by settling. The nature of this precipitate was determined by analyzing two vacuum-treated FAME samples for soap content using the modified version of AOCS method Cc 17–79 [20]. One sample contained only the vacuum-treated FAME while to the other was added 1 mass% of the precipitate and 1 mass% distilled water. The vacuum-treated FAME sample gave a soap content reading of ~400 ppm, while the sample with added precipitate and water gave a soap content reading of ~3000 ppm. Thus, the aggregates were heretofore considered to be soap and were used in the preparation of samples for the DLS measurements.

The amount of water in the vacuum-treated FAME was determined by Karl Fisher coulometric analysis using a Titroline KF trace analyzer (Schott Instruments, Germany) and found to be 250 ppm. The vacuum-treated FAME was referred to as “raw FAME”,

and was later used for testing the membrane separation process. 5 L of this "raw FAME" was further treated for use in the DLS measurements, as outlined below.

6.2.2 Sample Preparation for DLS measurements

Materials used in preparing samples for the DLS measurements were: distilled and de-ionized water, methanol (99.9%, Fisher Scientific), glycerol (99.7%, VWR International), and soap (the aggregate material recovered from the FAME during the vacuum treatment step). The 5 L of the "raw FAME" was washed five times using distilled water to remove soap and glycerol then evaporated in a rotary evaporator at 90°C under vacuum (0.94 bar vacuum) for 30 min. Analysis of this washed and evaporated FAME (purified FAME), resulted in a soap content of 0 ppm and a glycerol content of 0.003 mass%, the latter measured using gas chromatography (GC) according to ASTM D6584-00. This purified FAME was used in all samples for DLS measurement.

The variables examined (water, methanol, soap and glycerol) and their concentration levels (coded as -1, 0 and +1) are shown in Table 6.1. According to the ASTM D-6751 standard, a maximum value of 0.2 mass% methanol is permitted in biodiesel. The methanol levels selected for the experiments were chosen to straddle the ASTM limit. For glycerol, the upper level corresponds to the maximum solubility of glycerol in FAME and the lower level slightly exceeds the maximum allowable amount as our goal was to reduce the level of glycerol below the standard. The equations used to convert the actual concentrations (x_i) to the coded levels (X_i) are also shown in Table 6.1. Two sets of DLS measurements were conducted using three-level Box-Behnken factorial designs [19]. This useful class of designs is used to estimate the coefficients of a second-order polynomial model of the form:

$$Y = \beta_0 + \beta_1 X_1 + \beta_2 X_2 + ... + \beta_K X_K + \beta_{11} X_1^2 + \beta_{22} X_2^2 + ... + \beta_{KK} X_K^2 + \beta_{12} X_1 X_2 + \beta_{13} X_1 X_3 + ... + \beta_{K-1,K} X_{K-1} X_K \quad (6.1)$$

where β_K are the parameters and X_K are the operating variables.

Table 6.1: Variables examined and their concentration levels

Operating variables	Concentration (mass%)			
	Low (-1)	Medium (0)	High (+1)	Equation
Water (X_1)	0.05	0.075	0.1	X1 = (x1-0.075)/0.025
Methanol (X_2)	0.1	0.6	1.1	X2 = (x2-0.6)/0.5
Soap (X_3)	0.1	0.2	0.3	X3 = (x3-0.2)/0.1
Glycerol (X_4)	0.05	0.1	0.15	X4 = (x4-0.1)/0.05

A total of 42 different sample compositions was prepared in 40 mL vials; 27 of these included methanol (see Table 6.2), and 15 did not (see Table 6.3). In addition, each sample composition was replicated twice for a total of 126 samples. The droplet diameter measurements were obtained by DLS. All samples used the same mass of purified FAME (~35 g) and the desired concentrations of glycerol, methanol and water were added using an Eppendorf pipette with adjustable volume settings. The soap was added by weighing the desired amount using a precision scale.

Glycerol was added first to the FAME and mixed vigorously using a stirrer for 20 min. Then, the desired amount of soap (aggregated material) was added and mixed for another 20 min, after which a mixture of the desired amounts of methanol and water was added and the entire mixture was mixed for 20 min. Prepared samples were left to settle at room temperature for 3 to 4 h before measurement by DLS. The DLS was a zetasizer nano series, model ZEN1600 from Malvern Instruments. Optical glass cuvettes with a 100 mm light path were used and ~2 mL of sample was added to each cuvette. The reported diameter was an intensity weighed droplet size, made of 6 measurements that were analyzed in 10 runs of 20 s each. The values used for the refractive index for dispersant material/biodiesel was (1.452) [21], and for the glycerol material the refractive index was (1.473) [22].

The experimental error was calculated by pooling the pure error variances for all replicate runs. This was used to verify the adequacy of the second-order models according to standard statistical methods [23].

Table 6.2: Coded variables with methanol and the observed droplet diameters for all runs.

Water	**Methanol**	**Soap**	**Glycerol**	**Average droplet size observed (nm)**		
X_1	**X_2**	**X_3**	**X_4**	**Run (1)**	**Run (2)**	**Run (3)**
-1	-1	0	0	741	667	702
-1	1	0	0	596	562	602
1	-1	0	0	993	991	931
1	1	0	0	845	965	819
0	0	-1	-1	1157	993	960
0	0	-1	1	1025	965	1085
0	0	1	-1	160	340	200
0	0	1	1	619	662	711
-1	0	0	-1	765	692	622
-1	0	0	1	715	641	874
1	0	0	-1	951	911	1083
1	0	0	1	1261	1227	1165
0	-1	-1	0	915	1087	1180
0	-1	1	0	348	351	414
0	1	-1	0	733	790	836
0	1	1	0	555	360	590
0	-1	0	-1	792	706	873
0	-1	0	1	802	895	799
0	1	0	-1	460	479	465
0	1	0	1	867	768	740
-1	0	-1	0	802	736	769
-1	0	1	0	516	519	466
1	0	-1	0	1400	1350	1315
1	0	1	0	616	686	755
0	0	0	0	940	988	1096
0	0	0	0	954	989	898
0	0	0	0	1059	967	933

Table 6.3: Coded variables without methanol and the observed droplet diameters for all runs.

Water	**Soap**	**Glycerol**	**Average droplet size observed (nm)**		
X_1	**X_3**	**X_4**	**Run (1)**	**Run (2)**	**Run (3)**
-1	0	-1	264	294	400
1	0	-1	632	800	784
-1	0	1	561	605	594
1	0	1	1424	1450	1470
-1	-1	0	657	574	482
1	-1	0	1322	1200	1194
-1	1	0	340	370	360
1	1	0	829	957	800
0	-1	-1	890	925	850
0	-1	1	1240	1240	1171
0	1	-1	500	269	610
0	1	1	805	888	846
0	0	0	792	807	826
0	0	0	807	793	859
0	0	0	866	995	900

6.2.3 Membrane separation procedure

Approximately 25 L of the “raw FAME” produced and treated according to the methods shown above was used in preparing six mixtures for testing in a membrane separation system. The composition of the mixtures is shown in Table 6.4. The desired amounts of water, methanol and soap were added to the “raw FAME” and mixed using a magnetic stirrer for one hour prior to each run.

Table 6.4: Composition of prepared mixtures for the membrane treatment.

Mixtures #	Type of mixtures (Water, methanol and soap in mass%)
(1)	Raw FAME only
(2)	Raw FAME + 1% methanol
(3)	Raw FAME + 1% soap
(4)	Raw FAME + 1% methanol + 1% soap + 0.06% water
(5)	Raw FAME + 0.1% water
(6)	Raw FAME + 0.2% water

A modified hydrophilic polyacrylonitrile (PAN) membrane (Ultrafilic™, Sterlitech Corporation, USA) with a molecular weight cut-off of (100 kD) was tested at a temperature of 25°C, and a pressure of 552 kPa. The membrane separation setup was used as a "feed and bleed" [24] system equipped with a feed pump and circulating pump. A total filtration surface area of 0.0276 m^2 (2 x [14.5 cm x 9.5 cm]) over two identical Sepa™ (GE Osmonics) cells containing polymeric membranes was used as shown in Figure 6.1. Further details on the membrane separation setup and operation can be found elsewhere [17].

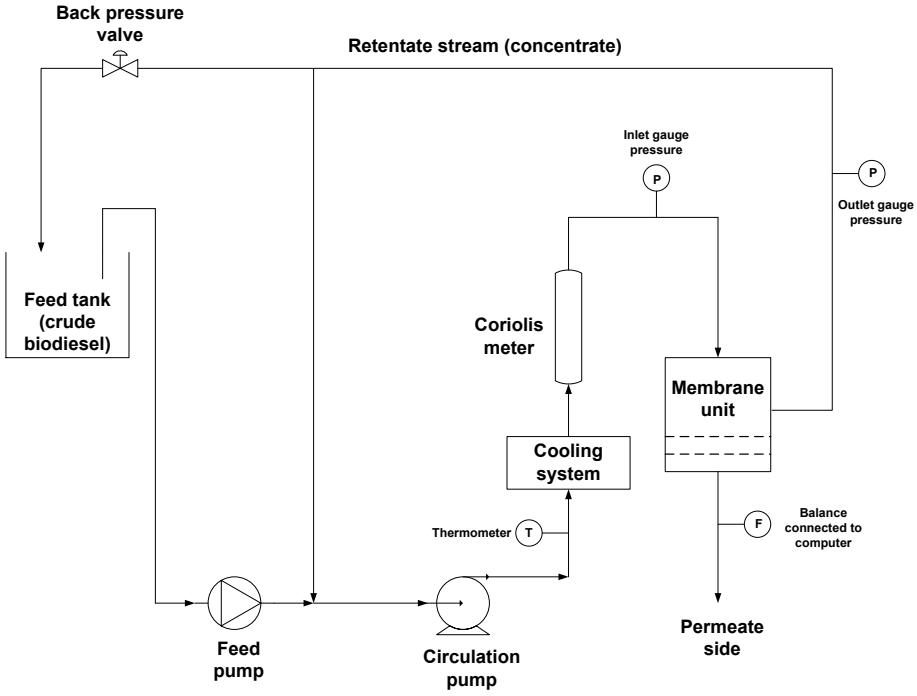

Figure 6.1: Schematic of membrane separation system.

Five litres of the FAME mixture was put in the feed tank and pumped to the membrane module. The flow rate of the FAME mixture over the two membrane modules was measured using a coriolis meter to give a constant cross-flow velocity of ~0.6 m/s. During the run, a circulating pump was used to circulate the feed through the membrane module. A cooling system was used to control the temperature to 25°C. The mass flow rate of the permeate side (g/min) was automatically recorded every minute on a computer.

Each experiment was run for three hours and samples from the permeate and retentate were taken at 0, 15, 30, 60, 120 and 180 min for glycerol concentration analysis by GC. A 3800 GC (Varian) with a column from Restek Chromatographic Specialties was used. The method used for the GC analysis is based on the test method for determination of free glycerine in biodiesel (ASTM D6584). Further details on the GC analysis can be found elsewhere [17]. Each sample was analyzed three times and the averages were reported. The calculated deviations from this average value were +/- 0.0045% for all samples.

6.3 Results and Discussion

6.3.1 Effect of methanol on glycerol droplet size

Droplet size measurements for the experiments using methanol in the Box-Behnken 3^4 design are shown in Table 6.2. The data were analyzed using standard statistical techniques (with SYSTAT 12™ software) and the following regression model was obtained (only statistically significant terms are shown):

$$Y = 975 + 174X_1 - 60X_2 - 256X_3 + 89X_4 - 172X_2^2 - 141X_3^2 - 80X_4^2 - 100X_1X_3 + 46X_1X_4 + 101X_2X_3 + 71X_2X_4 + 111X_3X_4 \quad (6.2)$$

where X_1 denotes water, X_2, methanol, X_3, soap and X_4, glycerol, as shown in Table 6.2. The regression model (Eq. 6.2) was found to describe a significant amount of variability in the data with $F = 5.3 \times 10^{-35}$ and $R^2 = 0.933$. The pure error variance was calculated to be 5.19×10^{-3} and no lack of fit was detected from the test statistic, $R = 1.39$, compared to *F-statistic* = 1.92.

The regression model shown in (Eq. 6.2) indicates that the droplet size was positively influenced by both the presence of water (X_1) and glycerol (X_4) and negatively influenced by the presence of methanol (X_2) and soap (X_3). The model reflects how droplet size increased with the addition of water, (water main effect parameter = +174) and glycerol, (glycerol main effect parameter = +89), while the decrease in droplet size was due to the addition of methanol (methanol main effect parameter = -60) and soap (soap main effect parameter = -256). The dominant effects, considering the magnitude of the parameter values of the main effects, interaction effects and quadratic terms were that of water, methanol, soap and glycerol. These effects are consistent with the notion that adding water and/or glycerol serves to decompatibilize the glycerol from the FAME and thus cause the droplet sizes to increase. At the same time, the addition of methanol tends to act in the opposite manner by enhancing the solubility of glycerol in FAME and reducing the droplet size. The addition of soap causes a reduction in droplet size by stabilizing more droplets, and thus, all else being equal, would result in smaller droplets.

Because the effect of the two-factor interaction parameters (X_iX_j) were, for the most part, statistically significant, the use of contour plots is helpful to illustrate their effect on droplet size. These contour plots are shown in Figures 6.2 through 6.7 and were generated using different concentration levels for the two parameters shown in each figure while keeping the values of the other two parameters constant at a coded level of zero. The units of the droplet size shown in these figures are in nanometre (nm).

The combined effect of methanol and water on droplet size is shown in Figure 6.2. Consistent with the regression analysis resulting in (Eq. 6.2), the methanol-water interaction effect (X_1X_2) was not significant, but the quadratic term for methanol (X_2^2) was significant. It is evident from Figure 6.2 that the droplet size effects are depicted as a rising ridge dictated by the individual concentrations of water and methanol; droplet size increases significantly with water concentration.

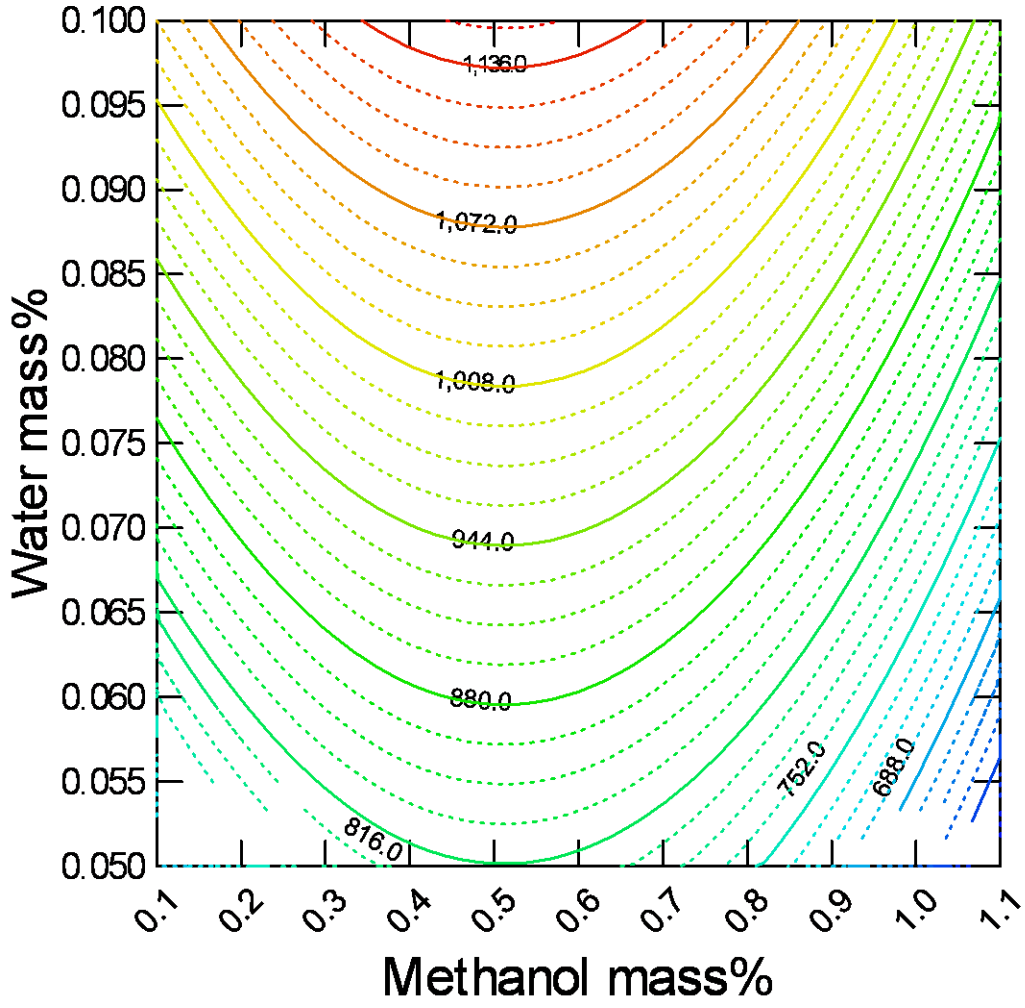

Figure 6.2: Effect of water and methanol on droplet size.

Figure 6.3 illustrates the joint effect of water and soap on droplet size as a sloping ridge on the contour plot. As the water-soap interaction effect (X_1X_3) was strongly significant, one sees that at lower soap concentrations, the increasing amount of water will promote the generation of larger glycerol-rich droplets. On the other hand, increasing the level of soap in the mixture serves to reduce the interfacial tension between water and FAME and stabilize the emulsion formed. This will enhance the dispersion of the droplets in the FAME phase and make increasing droplet size difficult. These results are

consistent with difficulties in phase separation of the FAME-rich and glycerol-rich layers in the presence of high amounts of soap.

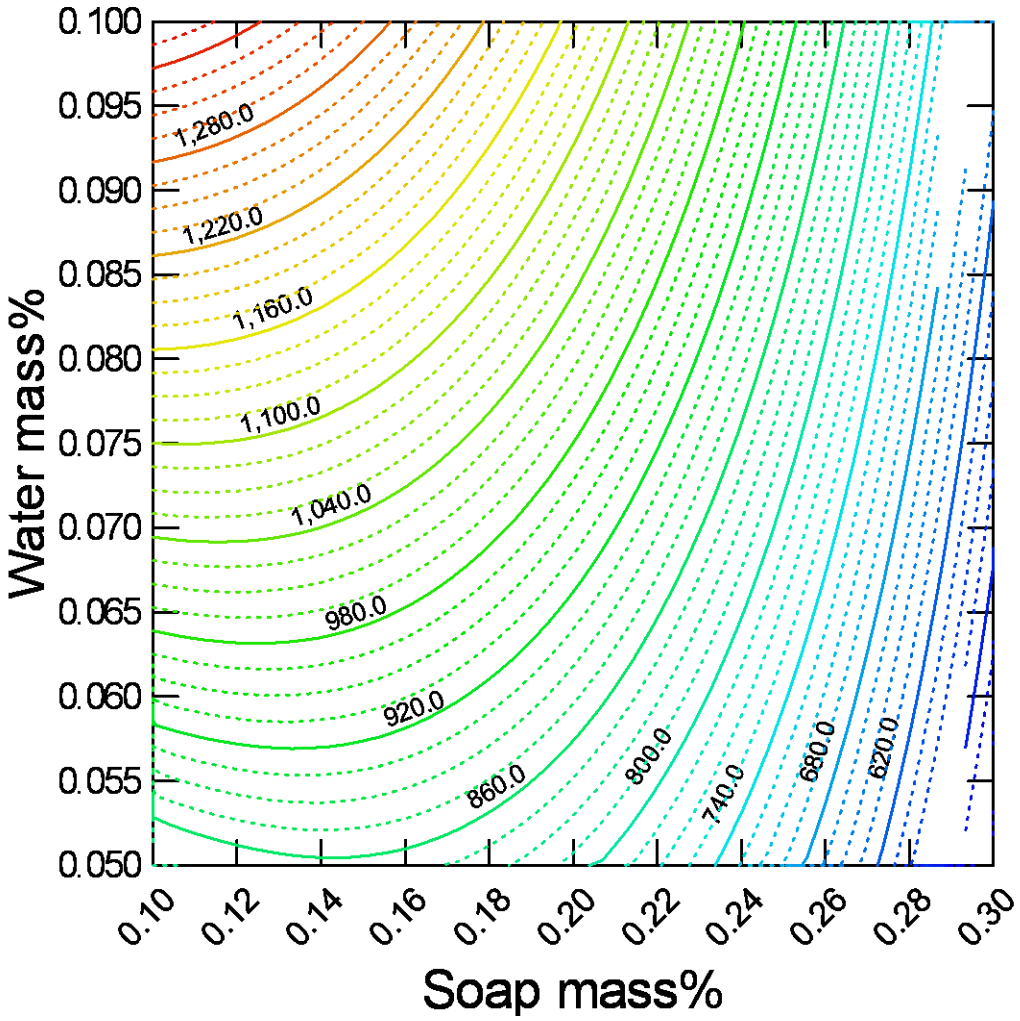

Figure 6.3: Effect of water and soap on droplet size.

The simultaneous manipulation of water and glycerol content is shown in Figure 6.4 as a rising ridge contour plot. The important effect of water at all glycerol levels, suggested by (Eq. 6.2), is evident in Figure 6.4. As water is added, even in small amounts, droplet size is increased and the separation of glycerol from FAME will be enhanced.

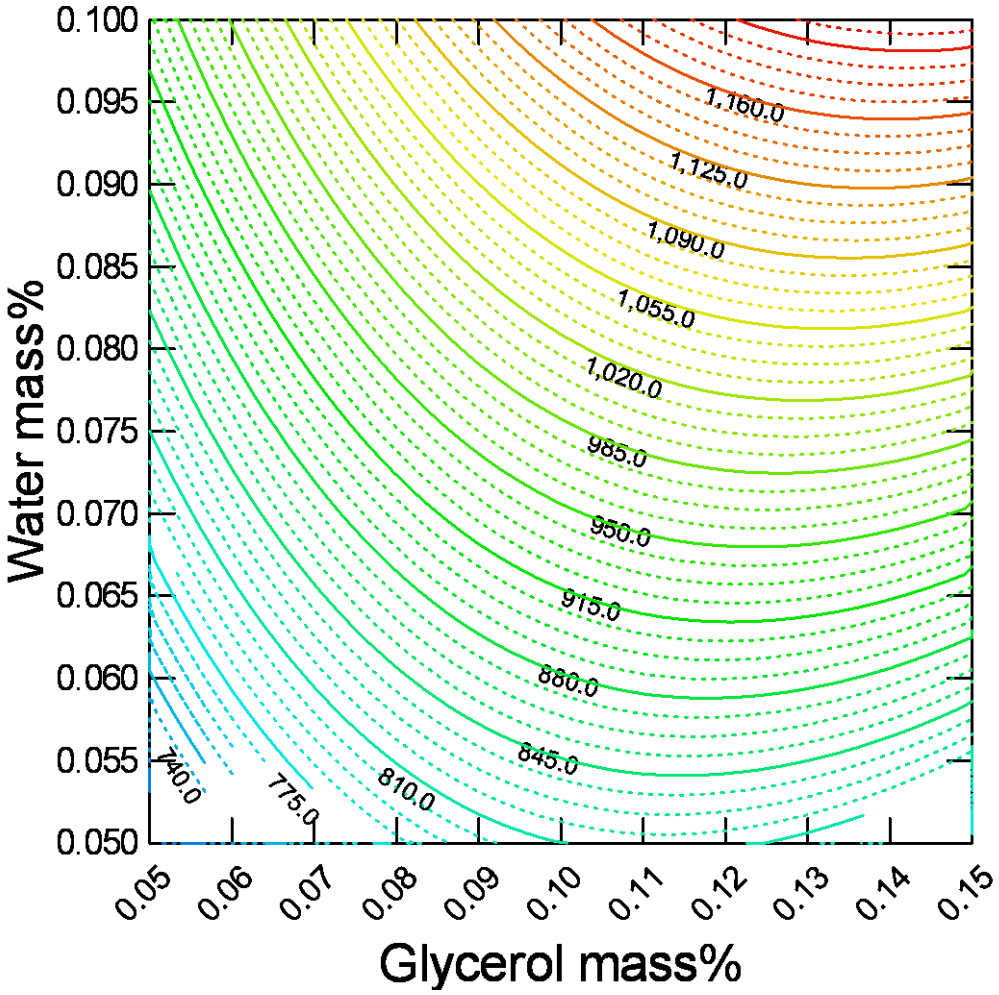

Figure 6.4: Effect of water and glycerol on droplet size.

In Figure 6.5, the effect of methanol and soap on the droplet size is consistent with the discussion above. The results in the figure clearly show a trend of reducing methanol and soap concentration to achieve larger droplets and thus, improved separation. Figure 6.6 provides evidence of a maximum droplet size at particular methanol and glycerol concentrations. The shape of the contour plot is a direct result of the miscibility of methanol and glycerol. A reduction in the amount of soap will yield large droplets according to Figure 6.7 which shows the joint effect of soap and glycerol on droplet size.

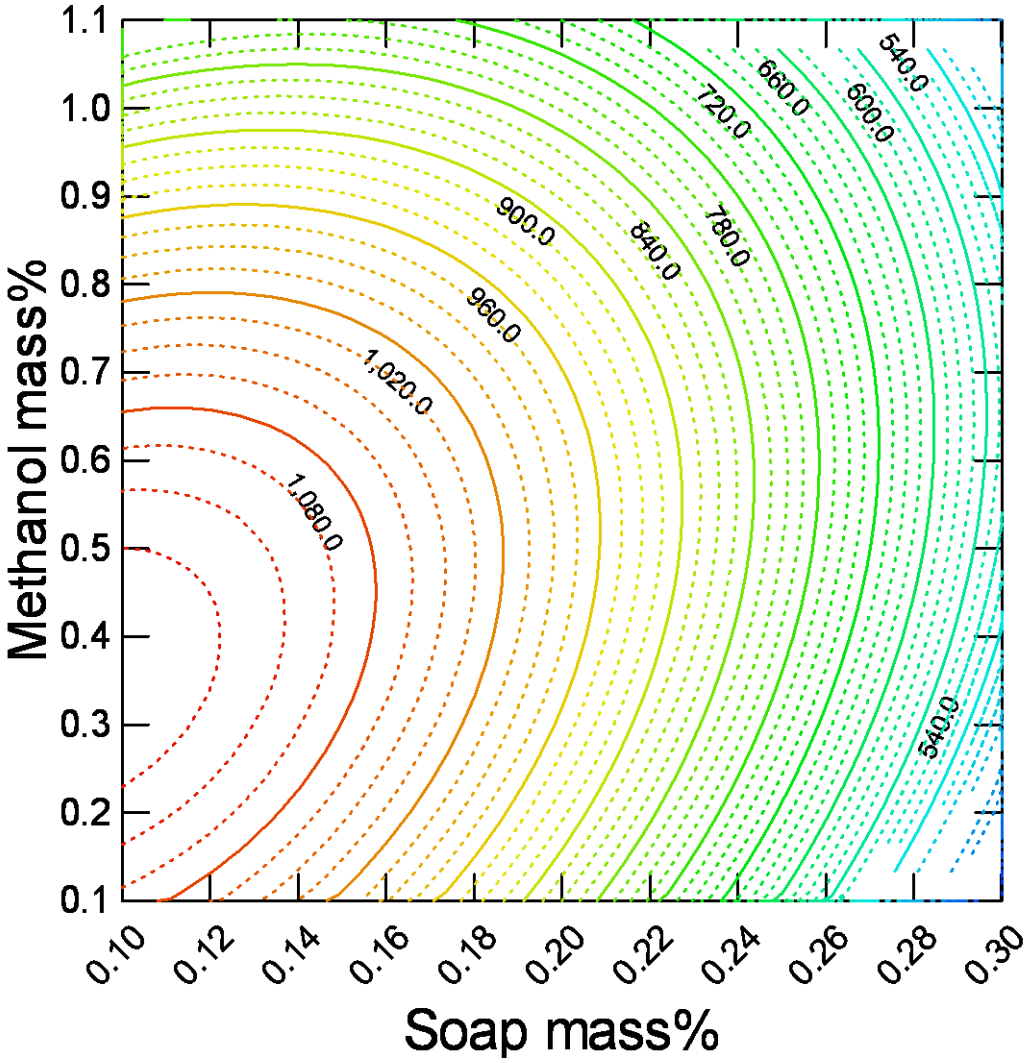

Figure 6.5: Effect of methanol and soap on droplet size.

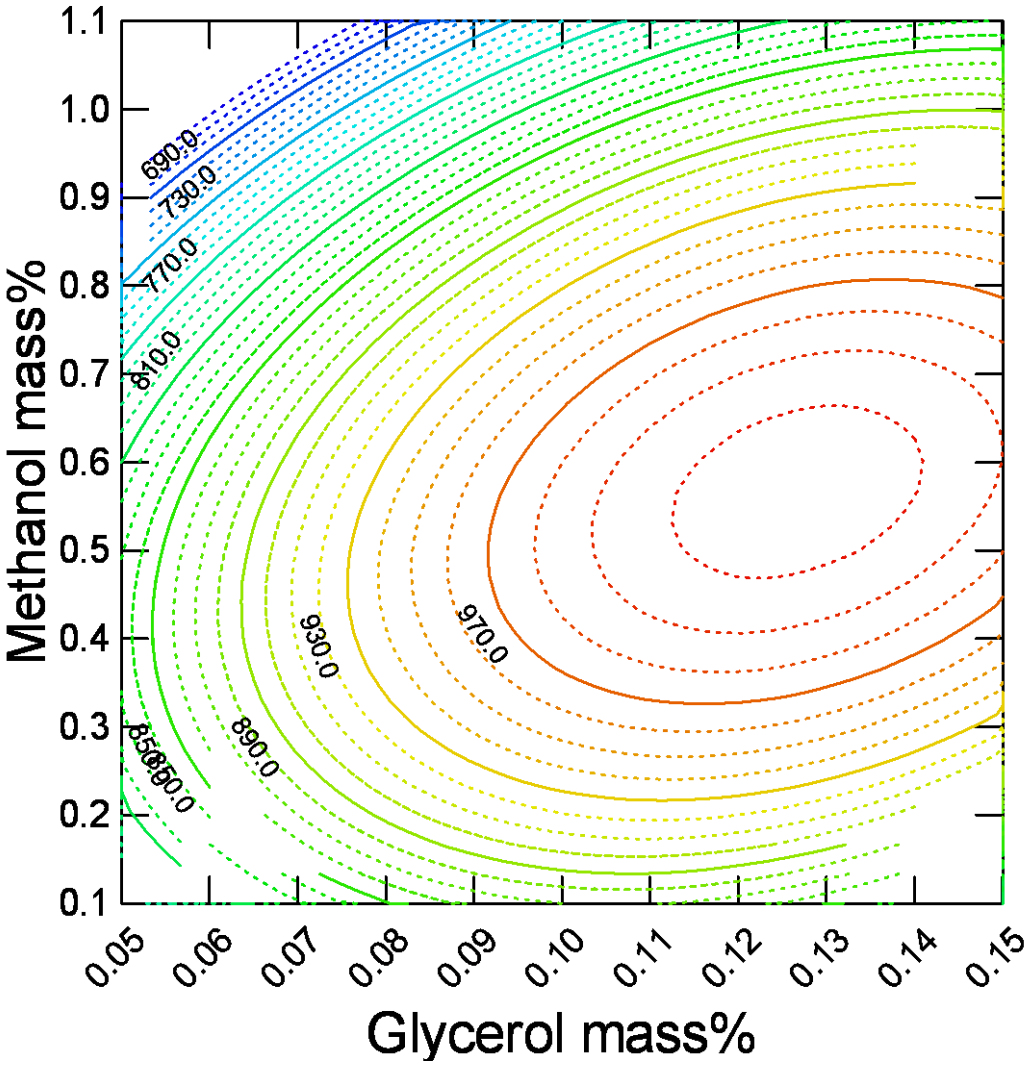

Figure 6.6: Effect of methanol and glycerol on droplet size.

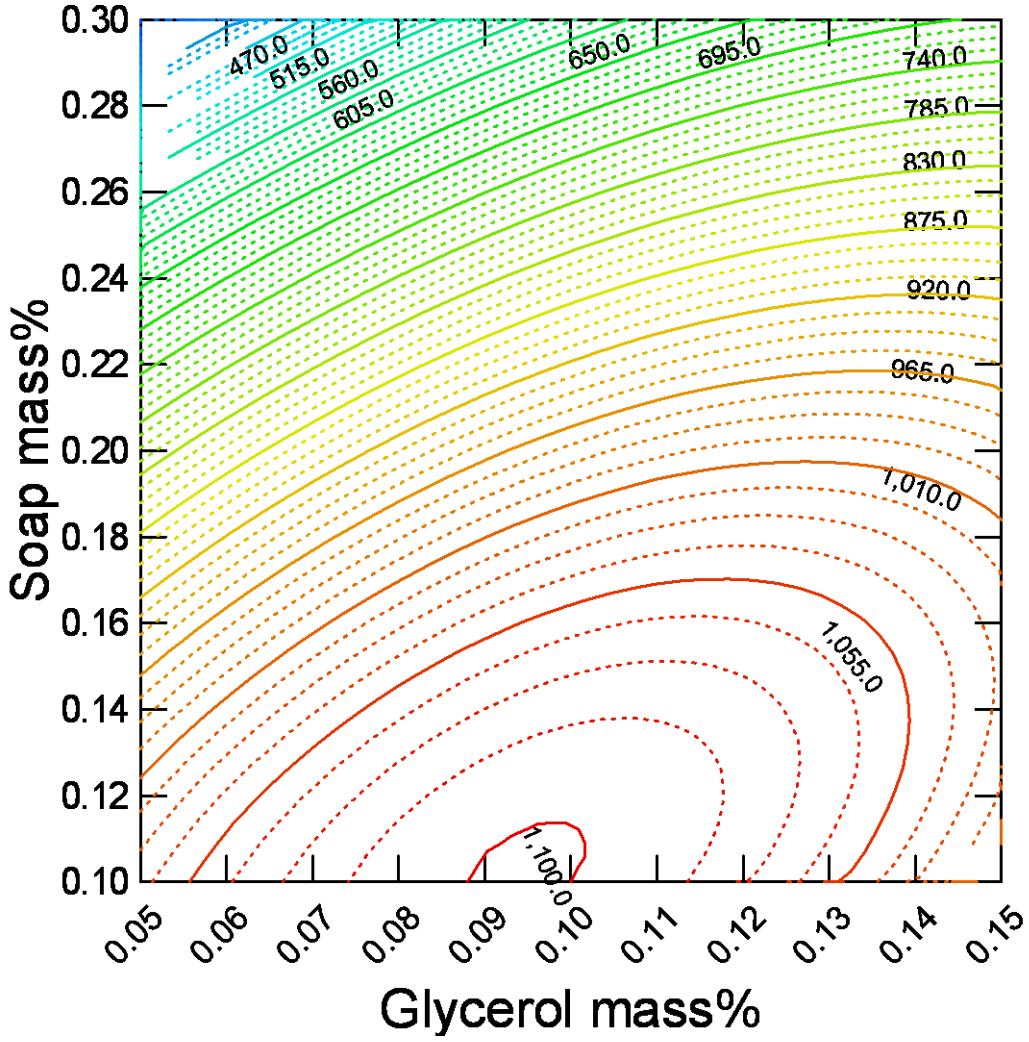

Figure 6.7: Effect of soap and glycerol on droplet size.

The second set of experiments, a 3^3 Box-Behnken design (see Table 6.3), consisted of repeating the same concentration levels of water, soap and glycerol as in the first set, but in the absence of methanol. The data were analyzed using standard statistical techniques and the following regression model was obtained (only statistically significant terms are shown):

$$Y = 851 + 307X_1 - 174X_3 + 212X_4 - 86X_1^2 + 111X_1X_4 \qquad (6.3)$$

where X_1 denotes water, X_3, soap and X_4, glycerol, as shown in Table 6.3 and Y is droplet size (nm). The regression model (Eq. 6.3) was found to describe a significant amount of

variability in the data with ($F = 1.3 \times 10^{-23}$) and ($R^2 = 0.946$). The pure error variance was calculated to be 5.19×10^{-3} and no lack of fit was detected from the test statistic, $R = 2.15$, compared to *F-statistic* = 2.42.

The regression model in (Eq. 6.3) shows the same trends as found in (Eq. 6.2). That is, the droplet size was strongly and positively influenced by both the presence of water (1) and glycerol (4), and negatively influenced by the presence of soap (3). In this case, the effect of water was clearly the dominant factor in the experiments.

It is clear from both sets of experiments, that water and methanol play important roles in the droplet size and would be expected, therefore, to strongly influence the operation of the membrane separation setup. As such, a series of separation experiments were conducted using the membrane separation setup to validate these findings.

6.3.2 Testing using membrane separation

Six different mixture compositions (see Table 6.4) were tested in the membrane separation apparatus in order to validate the above conclusions regarding the impact of water, methanol and soap on droplet size. The glycerol concentration profile for each run is shown in Table 6.5. The mass% glycerol in the permeate for each of the five experiments is shown in Figure 6.8; the dashed line indicates the ASTM D6751 standard for the level of free glycerol in biodiesel (0.02 mass%).

Table 6.5: Glycerol mass% in permeate and retentate streams after membrane separation.

	Time (min)	Free glycerol mass%					
		Raw FAME only (1)	Raw FAME + 1% methanol (2)	Raw FAME + 1% soap (3)	Raw FAME + 1% methanol + 1% soap + 0.06% water (4)	Raw FAME + 0.1% water (5)	Raw FAME + 0.2% water (6)
	Original sample	0.037	0.039	0.029	0.047	0.036	0.040
Permeate (P)	**15**	0.027	0.031	0.025	0.041	0.020	0.013
	30	0.027	0.035	0.029	0.038	0.018	0.012
	60	0.032	0.033	0.028	0.038	0.017	0.013
	120	0.032	0.031	0.029	0.041	0.017	0.014
	180	0.033	0.031	0.030	0.040	0.017	0.013
Retentate (R)	**15**	0.037	0.037	0.029	0.043	0.033	0.045
	30	0.037	0.037	0.032	0.042	0.034	0.037
	60	0.036	0.036	0.032	0.040	0.034	0.036
	120	0.034	0.034	0.029	0.043	0.032	0.034
	180	0.034	0.034	0.032	0.041	0.035	0.035

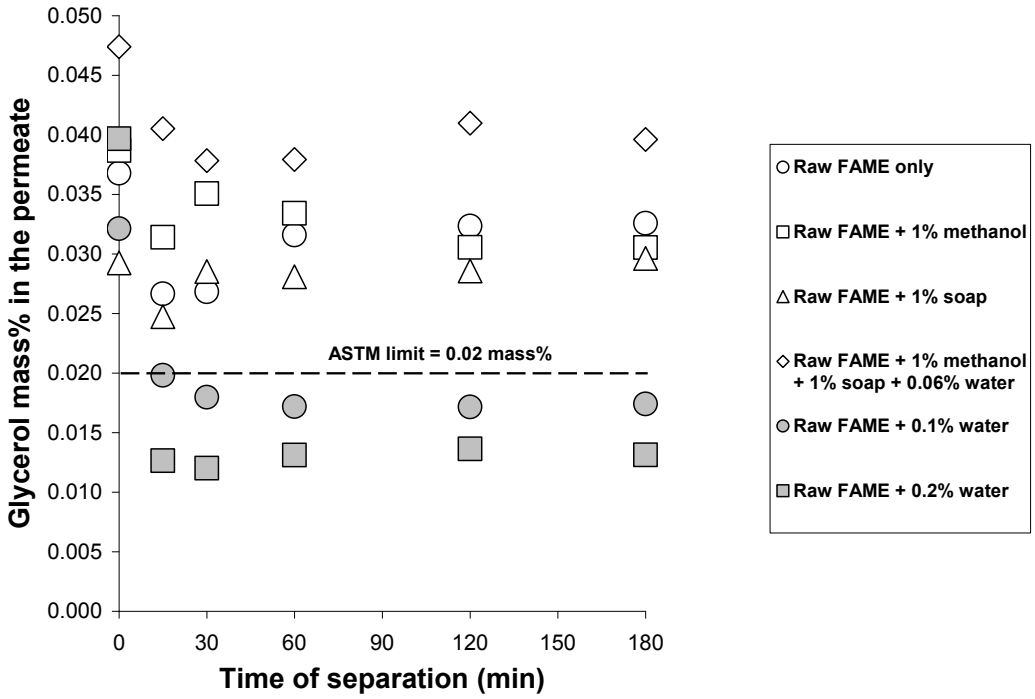

Figure 6.8: Glycerol content in permeate vs. time for (FAME + 1% methanol, FAME + 1% soap, FAME + 1% methanol + 1% soap + 0.06%, FAME + 0.1% water, and FAME + 0.2% water).

For the raw FAME (case 1), essentially no glycerol was removed by the membrane separation setup. The addition of 1% methanol to the raw FAME (case 2), had almost no effect on the removal of the glycerol and the ASTM standard was not met (see Figure 6.8). Due to the mutual solubility between glycerol and methanol and that between FAME and methanol, the resulting effect from the addition of methanol to the mixture was the dissolution of glycerol in the FAME phase. The amount of glycerol that was solubilized depended on the initial methanol content in the mixture. This was consistent with the findings in (Eq. 6.2).

The addition of 1% soap to the raw FAME (case 3), yielded an almost constant glycerol concentration in the permeate (see Table 6.5 and Figure 6.8). According to (Eq. 6.3), the addition of soap in the absence of water did not form micelles with glycerol.

Therefore membrane separation failed in removing the glycerol from the FAME in this case.

The mixture consisting of FAME + 1% soap + 1% methanol + 0.06% water (case 4) represents typical levels in the FAME phase for a conventional transesterification reaction. This mixture did not result in the ASTM standard being met despite the addition of water (see Figure 6.8). According to (Eq. 6.2), the concentrations of methanol and soap offset the additional water present in the mixture.

The addition of 0.1% water to the raw FAME (case 5) yielded highly positive results; the removal of glycerol began after a very short time (~15 min, see Figure 6.8), and within 30 min, the ASTM standard was exceeded. The complete miscibility of glycerol and water caused the formation of two immiscible phases: the FAME phase and a dispersed phase containing water and dissolved glycerol, which were unable to pass through the membrane pores. This supports the conclusions drawn from the regression models in (Eqs. 6.2 and 6.3) The use of additional water (0.2%) to the raw FAME (case 6) showed dramatic improvement to the glycerol removal (see Table 6.5 and Figure 6.8); the ASTM standard was achieved. The strong effect on separation from the addition of such small quantities of water was further confirmed by Hájek et al. [25].

Using Eq. 6.2 (when methanol was present in the mixture) or Eq. 6.3 (when no methanol was present in the mixture), we predicted the initial size of the dispersed droplets in the FAME mixture, i.e., prior to its introduction to the membrane module. This was plotted against the final glycerol content in the permeate, in Figure 6.9. It should be noted that the droplet size prediction for the raw FAME only mixture (case 1), would have been an extrapolation of the regression model to a range outside of the DLS measurement conditions and was therefore not included in the figure. Furthermore, none of the other mixture compositions (cases 2-6) were, strictly speaking, measured using DLS. Thus, the results from (Eqs. 6.2 and 6.3) indicate a droplet size trend where, in some cases, droplets would likely not exist (e.g., case 2). Nonetheless, plotting the predicted droplet size from these equations provided interesting and informative results that related to the performance in the membrane separation unit. Figure 6.9 displays a trend of larger predicted initial droplet sizes yielding lower final free glycerol contents in the permeate. This suggests that as the droplets increase in size, they tend to dephase

from the FAME and form a hydrophilic layer on the membrane surface. This permits increasing separation of glycerol from the FAME over time.

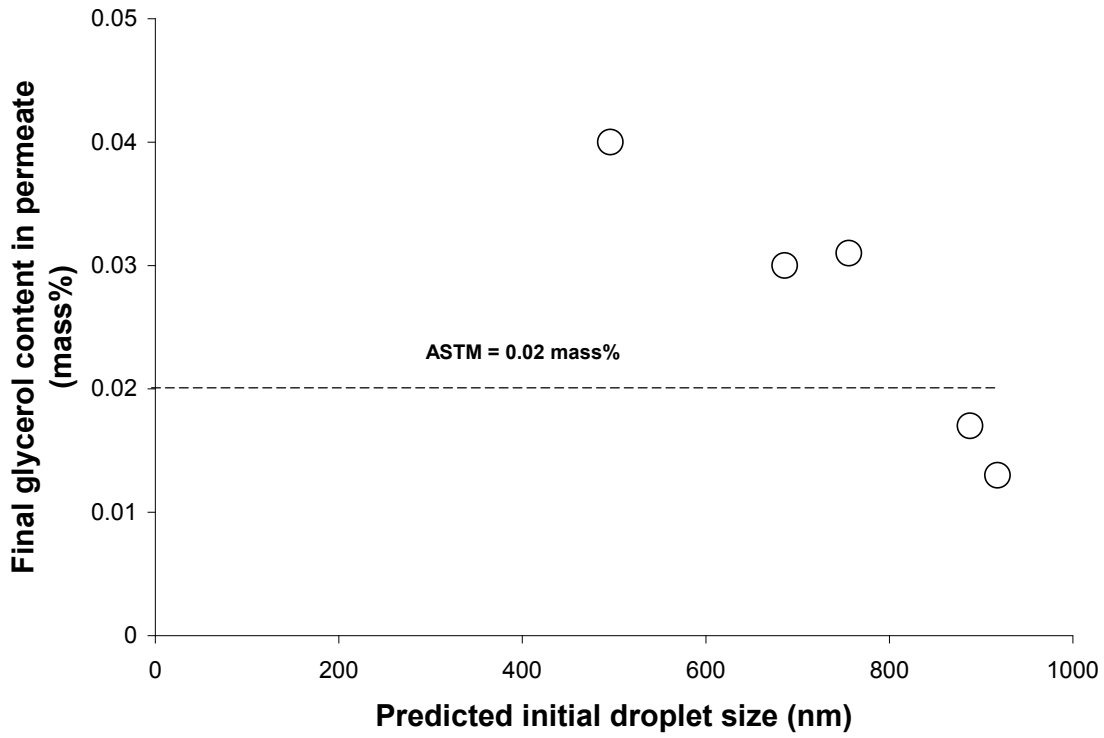

Figure 6.9: Predicted initial droplet size vs. final glycerol content in permeate.

6.4 Conclusion

Dynamic light scattering (DLS) was used to study the effect of water, methanol, soap and glycerol on droplet size for these materials dispersed in FAME. Clear indication of the dominant effect of water on improving the separation of glycerol from FAME was shown. The negative impact of methanol, and to a lesser extent, of soap, was also shown. In order to achieve ASTM standards for biodiesel, it is therefore recommended to minimize the amount of methanol and soap prior to any attempts to remove glycerol from raw FAME. Testing using a membrane separation setup confirmed the results of the DLS

measurements by showing the major effect of water on glycerol separation from FAME. In any case, a small amount of water (~0.1 wt%) is all that is necessary to permit the fuel quality standard to be achieved using membrane separation technology. This leads directly to reductions in both capital and operating costs as well as a reduction in the environmental impact of the biodiesel production process by avoiding the water washing step.

6.5 Acknowledgements

The authors acknowledge the financial support from the Natural Sciences and Engineering Research Council of Canada (NSERC).

6.6 References

[1] Demirbas, A.; Karslioglu, S. *Energ Sources* **2007**, 29, 133–141.

[2] Sharma, Y. C.; Singh, B.; Upadhyay, S. N. *Fuel* **2008**, 87, 2355–2373.

[3] Ma, F.; Milford, A. H. *Bioresour. Technol*. **1999**, 70, 1-15.

[4] Freedman, B.; Pryde, E. H.; Mounts, T. L. *J. Am. Oil Chem. Soc*. **1984**, 61, 1638-1643.

[5] Cao, P.; Dubé, M. A.; Tremblay, A. Y. *Fuel*. **2008**, 87, 825–833.

[6] Van Gerpen, J.; Hammond, E. G.; Johnson, L, A.; Marley, S. J.; Yu, L.; Lee, I.; Monyem, A. Final report prepared for: The Iowa Soybean Promotion Board, Iowa State University, July 31, 1996.

[7] Ma, F.; Clements, L. D.; Hanna, M. A. *Trans. ASAE* **1998**, 41, 1261–1264.

[8] Mao, V.; Konar, S. K.; Boocock, D. G. B. *J. Am. Oil Chem. Soc*. **2004**, 81, 803-808.

[9] Michal, C.; Skopal, F.; Hájek, M. C. *Eur. J. Lipid Sci. Technol*. **2009**,111, 663–668.

[10] Karaosmanoglu, F.; Cigizoglu, K. B.; Tuter, M.; Ertekin, S. *Energy Fuels* **1996**, 10, 890-895.

[11] Berrios, M.; Skelton, R. L. *J. Chem. Eng.* **2008**, 144, 459–465.

[12] Moser, B. R. *In Vitro Cell. Dev. Biol.: Plant* **2009**, 45, 229–266.

[13] Karla, T. K.; Maria, A. F.; Cesar, O.; Helena, M.; Wilhelm and Luiz, P. R. *J. Am. Oil Chem. Soc.* **2007**, 84, 385 – 392.

[14] Strathmann, H. *AIChE Journal*. **2001**, 47, 1077-1087.

[15] Strathmann, H. *Journal of Mernbrane Science*. **1981**, 9, 121-189.

[16] Yong, W.; Xingguo, W.; Yuanfa, L.; Shiyi, O.; Yanlai, T.; Shuze, T. *Fuel Process. Technol*. **2009**, 90, 422–427.

[17] Saleh. J.; Tremblay, A. Y.; Dubé, M. A. *Fuel*. **2010**, 89, 2260-2266.

[18] Meher, L. C.; Sagar, D. V.; Naik, S. K. *Renew. Sust. Energy Rev*. **2006**, 10, 248–268.

[19] Box, G. E. P.; Behnken, D. W. *Technometrics.* **1960**, 2, 455-475.

[20] Van Gerpen, J.; Shanks, B.; Pruszko, R. Biodiesel Analytical Methods, August 2002–January 2004, July 2004 • NREL/SR-510-36240.

[21] Sorichetti, P. A.; Romano, S. D. *Phys. Chem. Liq*. **2005**, 43, 37–48.

[22] Scholte, G. *J. Polym. Sci*. **1972**, 10, 519-526**.**

[23] Montgomery, D. C.; Design and analysis of experiments, fifth edition; 2001.

[24] Porter, M. C. Handbook of industrial membrane technology. NJ: Noyes 483 Publications; 1990.

[25] Hájek, M.; Skopal, F.; Machek, J. *Eur. J. Lipid Sci. Technol.* **2008**, 110, 347–350.

Chapter 7

Effect of different levels of water concentration, pressures and temperatures on the free glycerol removal from biodiesel using membrane separation

Chapter 7 - Effect of different levels of water concentration, pressures and temperatures on the free glycerol removal from biodiesel using membrane separation

Abstract

To meet the ASTM D6751 and EN 14110 standards for dispersed droplets of free glycerol in biodiesel, a membrane separation technology was used to avoid the need to use a water wash step typical of conventional purification techniques. The effect of trans-membrane pressure (TMP) when different concentrations of water are added to the fatty acid methyl ester (FAME) phase on glycerol removal using ultrafiltration (UF 0.03 μm, polyethersulfone (PES)) and microfiltration (MF 0.1 and 0.22 μm, PES) at 25, 40 and 60°C was studied. Samples collected after one hour for all operating conditions were analyzed for glycerol mass percentage in the permeate using gas chromatography (GC). The water content for these samples was determined using Karl Fisher titration. Results showed that running at 25°C for the two ranges of membranes produced the best results for glycerol removal and exceeded the ASTM and EN standards. An enhancement of glycerol removal was found by adding small amounts of water up to the maximum solubility limit in biodiesel. An increase in temperature resulted in an increase in the solubility of water in the FAME and less effective glycerol removal. Application of cake filtration theory and a gel layer model showed that the gel layer on the membrane surface is not compressible and the specific cake resistance and gel layer concentration decrease with increasing temperature. An approximate value for the limiting (steady-state) flux was reported and it was found that the highest fluxes were obtained at the lowest initial water concentrations at fixed temperatures.

Keywords: Fatty acid methyl ester (FAME), free glycerol, separation, water solubility, critical and limiting flux, ultra filtration, microfiltration.

7.1 Introduction

Due to increasing oil prices and concern due to the levels of environmental pollution resulting from petro-diesel production, researchers have started to look for a renewable and successful alternative source of energy [1, 2, 3]. Biodiesel is a renewable, biodegradable and environmentally safe fuel for use in diesel engines to replace petro-diesel and has the potential to lower the level of pollutants and carcinogens emitted to our environment [4, 5]. Biodiesel has been defined by the American Society for Testing and Materials (ASTM) as mono alkyl esters of long chain fatty acids derived from renewable lipid feedstocks, such as vegetable oils or animal fats, for use in compression ignition (diesel) engines [6]. Biodiesel is miscible with petro-diesel in any ratio and it can be used in its neat form or as a blend.

Transesterification is the most common method used to produce biodiesel, where it is commercially produced most frequently via alkali-catalyzed, e.g., sodium hydroxide (NaOH), reaction between animal fat or vegetable oil with excess alcohol (e.g., methanol) to form esters and a glycerol by-product [7]. The transesterification consists of three consecutive, reversible reactions in which a mole of ester is liberated at each step, where the transesterification of triglycerides (TG) with methanol produces fatty acid methyl esters (FAME) and glycerol. Diglycerides (DG) and monoglycerides (MG) are the intermediates in this process [8, 9, 10].

Upon the completion of the transesterification reaction, two separate layers form: the lower layer (glycerol layer) and the upper layer (FAME layer) which contains some impurities such as glycerol (referred to as “free” glycerol), unreacted methanol, residual catalyst, bound glycerol (i.e., unreacted TG, DG and MG), and perhaps small amounts of soap and water. Purifying the final FAME product is important by limiting the presence of these impurities and it was clearly specified in standards such as ASTM D6751 in North America and EN14214 in Europe [11, 12]. The conventional purification processes include: gravitational settling and centrifugation, water washing, adsorption and distillation. Water washing is one of the most important purification techniques in removing impurities from the FAME phase. This process usually needs to be repeated several times which produces a large amount of waste water containing hazardous materials, this adds to the capital and operating costs that reduce the environmental

benefits of using biodiesel [13, 14].

The use of membrane technology in biodiesel purification to avoid water washing can provide solutions for many environmental problems by recovering valuable products as well as treating effluents and minimizing their harm to the atmosphere. Recent work has shown the efficiency of using membrane technology in the production of biodiesel [15, 16]. Membrane separation technology has been used for many applications in fields outside of biodiesel production and purification such as: producing different qualities of water from surface water, well water, brackish water and seawater and, its use in industrial processes and wastewater treatment [17]. Recently, it has been applied in the areas of secondary and tertiary municipal wastewater treatment and oil field produced water treatment [17]. Reducing sludge, getting high quality permeate, possibility of total recycle water systems, small space requirements, moderate capital cost and ease of operation make it a very competitive alternative to conventional technologies [18]. The most widely used are membrane microfiltration (MF) and ultrafiltration (UF) which are typically made from polymeric or inorganic materials such as ceramics and metal oxides. Pressure-driven membrane processes are capable of separating large organic molecules, colloidal droplets and microorganisms. MF membranes act as a porous barrier to remove colloidal suspensions and reduce turbidity. UF offers higher colloidal removal than MF, but operates at higher pressures and can reject bacteria and macromolecules such as proteins and large droplets and microorganisms [19].

One of the most significant issues in pressure-driven membrane processes is the reduction of the flux below the measured level using pure water. The flux initially decreases followed by a long and gradual decline. Fouling is one of the main phenomena responsible for this [20]. Generally, the interactions between the membrane surface and the components in the mixture as well as the accumulation of solute or droplets need to be separated over time as the membrane surface causes a rapid and often irreversible loss of flux during the filtration process. A steady-state is generally reached and a limiting permeation flux appears for the given operating conditions [21, 22]. In cross-flow filtration the retentate side flows parallel to the membrane surface rather than normal to and toward it and limits the cake deposit (fouling), while in dead ended filtration, the hydrodynamic forces always drag droplets toward the membrane surface and cake builds

up [23].

Other different concepts which are used in cross flow filtration and are important for the membrane process are the limiting and critical fluxes. Limiting flux represents the maximum stationary permeation flux, which can be reached when increasing trans-membrane pressure (TMP) or a flux for which the fouling saturates the filtration capacity of the membrane. The critical flux is a concept that describes the flux at which irreversible fouling appears on a membrane or a flux for which fouling first occurs (it is then the maximum flux for which no fouling occurs) [24, 25]. The critical flux has mainly been obtained from flux-TMP measurements. Flux-pressure experiments can be made either by imposing a flux and measuring a pressure or by imposing a pressure and measuring a flux [25].

Our recent research in purifying biodiesel using membrane separations showed encouraging results in removing free glycerol by avoiding a water washing step. In the first study, it was found that adding a small amount of water up to 0.08 mass% improved the separation dramatically and removed the glycerol using a 100 kD Ultrafilic UF membrane at room temperature [26].

In the second study, we used three different molecular weight cut-offs of UF type at three different temperatures. The results indicated that glycerol could be separated from untreated FAME at methanol feed concentrations of up to 3 mass%. Formation of a hydrophilic glycerol--rich layer on the surface of the membrane was noticed for the best separation at room temperature with a time requirement of up to 3 h to achieve the ASTM level [27].

In the third study, we used ceramic membranes to remove free glycerol from a post-transesterification FAME stream, without using a water wash step or other techniques and by using membranes in the UF and MF ranges. The effect of temperature on the glycerol content from the membrane purification effluent was tested at certain fixed pressures. The ASTM standard for glycerol content in biodiesel was met using the UF ceramic membrane setup at 25^{o}C after 3 h. Membrane pore size was also found to affect separation performance. The smaller pore size of the UF membrane facilitated glycerol removal compared to the MF membrane [28].

The objectives of the present study were a) to study the effects of TMP,

temperature and water concentration in the FAME on the final glycerol removal for both UF and MF membrane types, b) to determine the best flux for different operating conditions under which the glycerol removal standard was and c) to determine the critical and limiting fluxes at various operating conditions.

To address these objectives, we employed three different pore sizes of PES membrane, one of them in the UF range (0.03 μm, polyethersulfone (PES)), and two in the MF range (0.1 and 0.22 μm, PES). The experiments were done by preparing a range of FAME-water mixtures at a fixed glycerol concentration (0.1 mass%) and different TMP values at 25, 40 and 60°C.

7.2 Experimental section

7.2.1 Materials

Canola oil, purchased from a local food store (Loblaws, ON, Canada), methanol (99.85% purity, Commercial Alcohols Inc.; Brampton, ON, Canada), sodium hydroxide (NaOH, reagent grade, ACP Chemicals Inc.; Montreal, QC, Canada), and glycerol (99.7% purity, VWR International; CITY) were used as received. Other chemical standards for the gas chromatography (GC) analysis such as N-methyl-N-(trimethylsilyl) trifluoroacetamide (MSTFA), butanetriol and tricaprin were purchased from (Sigma Aldrich, Canada).

7.2.2 Biodiesel production

A batch process was used to produce the FAME. The required amounts of materials were added to a 6 L jacketed reactor. The mixture was based on a 6:1 molar ratio of methanol to oil and 1 mass% NaOH based on oil. A heat exchanger was used to heat the mixture to 60°C and the reaction time was 1 h. A circulation pump was used to improve the mixing of the two-phase mixture. The finished product from the transesterification reaction was allowed to settle for 8 to 12 h in a separatory flask from which the bottom glycerol-rich layer was removed. The non-polar, FAME-rich phase was then neutralized with sulphuric acid to pH 7. Many runs were needed to produce a sufficient quantity of FAME for the purification experiments. The FAME produced in all runs was washed with distilled and de-ionized water 6 to 7 times to remove all the

impurities such as soap, glycerol, methanol, and catalyst. The washed FAME phase was then vacuum-treated (0.94 bar vacuum) in a rotary evaporator at 90°C for 30 min to ensure that no methanol and water were present in the FAME phase. After this step, different samples of treated FAME were taken for soap, water and glycerol analysis. The soap content was found to be 0 ppm using the modified version of AOCS method Cc 17-79 [29]. The amount of water in the treated FAME was determined by Karl Fisher coulometric analysis using a Titroline KF trace analyzer (Schott Instruments, Germany) and found to be 230 to 250 ppm. Therefore, this amount was considered when reporting the water concentration in the prepared FAME mixtures. The mass% glycerol of the treated FAME was found to range from 0.003 to 0.004% by GC. The total quantities of treated FAME were then stored for future.

In this study, five different initial water concentrations in the FAME mixture were used: 0.1, 0.125, 0.225, 0.425 and 0.825 mass% water. These concentrations include the water added to the FAME and the initial amount present in the vacuum-treated FAME. Each FAME-water mixture was treated by membrane separation at 25, 40 and 60°C and different TMP. The TMP range for the UF membrane was 0.12, 0.26, 0.4 and 0.53 MPa, while that for the MF membranes was 0.007, 0.012, 0.024, 0.052 and 0.085 MPa

7.2.3 Membrane conditioning

Three different pore sizes of polymeric membranes were used in these experiments, one of them in the UF range and two in the MF range. These membranes were PES (0.03, 0.1 and 0.22 μm), and were purchased from Sepa™ (GE Osmonics) A new membrane was used for each permeation run. Prior to use in the experiments, the membranes were exchanged with FAME by placing the membrane in de-ionized water for 48 h then, placing the membrane in iso-propanol for 24 h next, placing the membrane in a 50:50 mixtures of iso-propanol and FAME for 24 h, and finally, placing the membrane in pure FAME for 24 h. The membranes were then ready for use.

7.2.4 Membrane separation system

The separation of glycerol from FAME mixtures was performed using a membrane separation system in a “feed and bleed” [30] loop equipped with a feed pump

and circulating pump. The active surface area of the membrane was 0.0138 m^2 (14.5 cm x 9.5 cm). The mixtures of FAME, glycerol and water were prepared as follows: 3.5 L of treated FAME were put in a 4 L Erlenmeyer flask acting as a feed tank. The required amount of glycerol, 0.1 mass% for all mixtures, was first added into a 40 mL glass vial, then 35 g of treated FAME were added and mixed vigorously using a vortex stirrer for 10 min. This FAME-glycerol mixture was then added to the treated FAME in the feed tank. A magnetic stirrer was used to agitate the mixture for 20 min. The required amount of water used in the experiments was slowly added to the feed tank. The FAME solution was then mixed for an additional 30 min.

Figure 7.1 shows a schematic of the membrane separation setup. With the permeate valve on the permeate side of the membrane closed, the feed pump (see Fig. 7.1) was used to fill the system. The circulation pump (see Fig. 7.1) was turned on to circulate the feed. An additional volume of 1.5 L of treated FAME was added to the feed tank to bring the starting mixture volume up to a total of 5L. The mixture was circulated for 30 min to ensure homogeneity prior to the start of the run.

Permeate flowrate was monitored over a period of one hour and found to reach steady-state during this time. Samples of the permeate side (permeate) and rejection side (retentate) were taken at the end of one hour. The pressure of the system was then increased to the next TMP level for a period of one hour. Samples were again taken of the permeate and retentate after this one hour period. This procedure was repeated 4 to 5 times with sampling after each hour.

A coriolis meter was placed in the loop to measure the mass flow rate of the FAME mixture circulating in the membrane module. The cross-flow velocity across the membrane ranged from 0.6 m/s at (25^{o}C) to 0.75 m/s at 60^{o}C. The temperature of the system was controlled to its set-point using a heat exchanger. The mass flow rate of the permeate was automatically recorded every minute on a computer by way of a balance. The initial mixture, permeate and retentate samples were first analyzed for water concentration using the KF titrator and then analyzed using for glycerol concentration using the GC according to the ASTM D6584-00 method. Prior to GC analysis, all samples were heated to vaporize water using a rotary evaporator. Each sample was analyzed two times and the averages were reported. Each sample was analyzed two times

and the averages were reported. The calculated deviations from this average value were +/- 48 ppm for all samples.

.

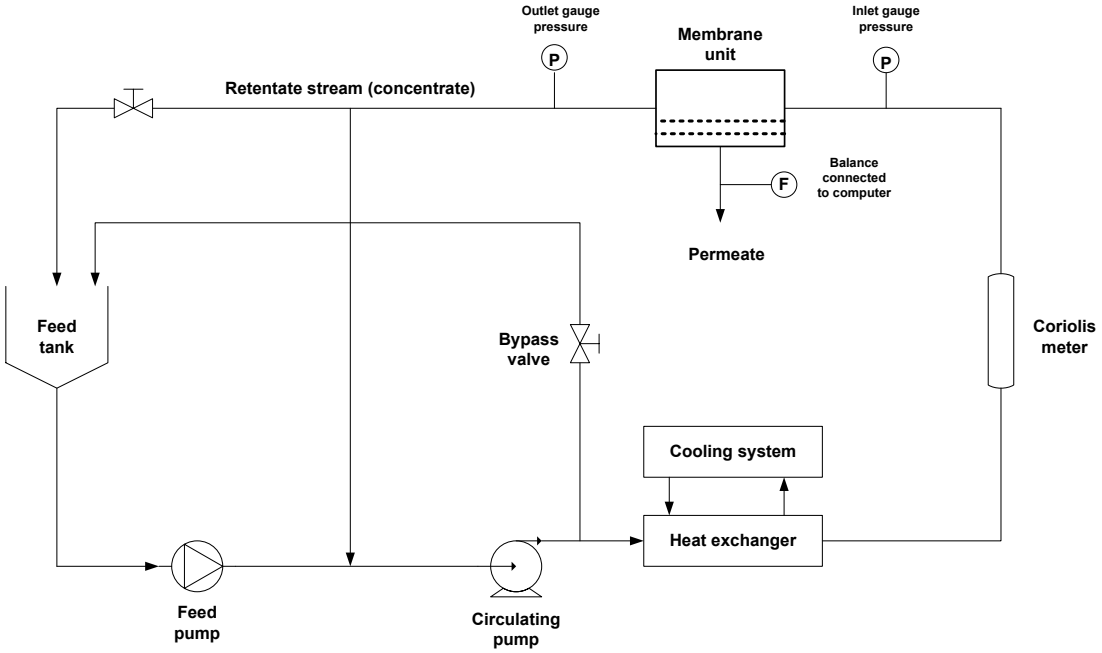

Figure 7.1: Schematic of membrane separation system

In a previous study, we reported on the effect of water concentration on glycerol droplet formation [26]. That study was limited to water concentrations of 0.2 mass%. For this study, several samples were analyzed for droplet size using dynamic light scattering (DLS) to extend the range of water concentrations to the conditions investigated herein. Nine samples were prepared using FAME which was water-washed 6 times with distilled water and treated in a rotary evaporator at 90°C under vacuum (0.94 bar vacuum) for 30 min. One sample was used as our base sample (no addition of glycerol or water) and the remaining eight samples had 1,000 ppm glycerol added to them. All samples were then mixed vigorously for 20 min. Different amounts of water were then added to each of the eight samples as follows: 0.02, 0.04, 0.06, 0.08, 0.1, 0.2, 0.4 and 0.8 mass%, and mixed

for another 40 min. These samples were left standing at room temperature for 2 to 3 h before analyzing them with the DLS system (zetasizer nano series from Malvern Instruments).

7.3 Results and discussion

Figure 7.2 shows the effect of TMP and initial water concentration on the final glycerol concentration in the permeate for the UF membrane (0.03 μm, PES) at 25°C. Operating the membrane separation unit at 25°C, the FAME met the ASTM and EN standards for free glycerol. The best performance (~126 ppm) was for the run with 0.225 mass% water.

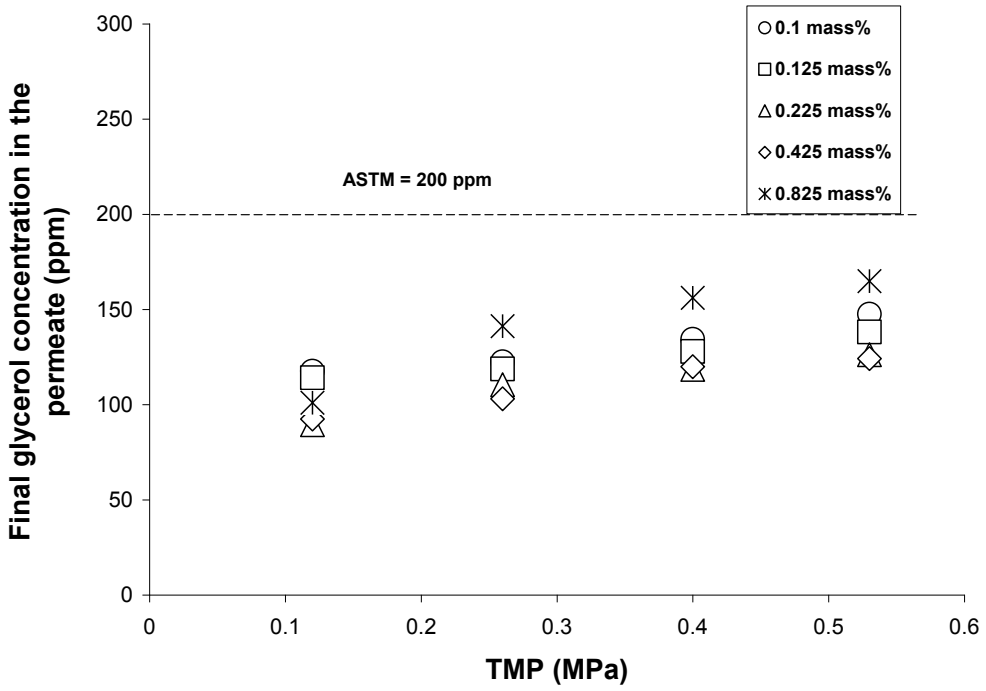

Figure 7.2: Effects of initial water concentration and trans-membrane pressure (TMP) on final glycerol concentration in the permeate for (0.03 μm, PES) at 25°C. The concentration of glycerol in the feed was 1000 ppm

Operation at 40°C was also successful in achieving and exceeding the standards as shown in Figure 7.3. At this temperature, the increase in TMP had a more significant effect on the final glycerol concentration in the permeate. The increasing TMP reduced the achievable glycerol concentration. Nonetheless, the standard for all cases and as for the 25^{o}C runs, the best separation performance was obtained for 0.225 mass% water at the lowest TMP.

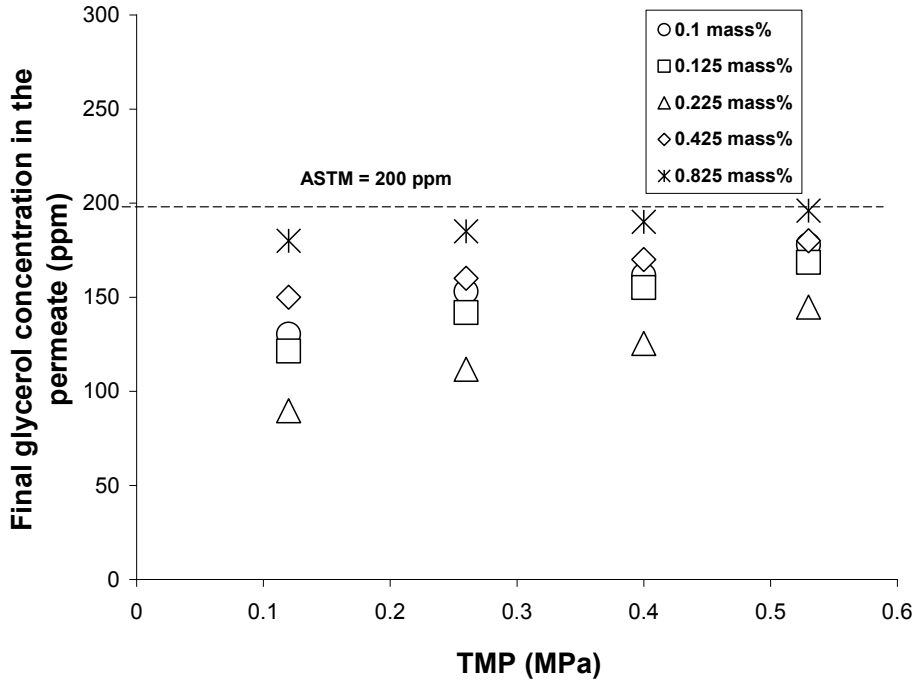

Figure 7.3: Effects of initial water concentration and trans-membrane pressure (TMP) on final glycerol concentration in the permeate for (0.03 μm, PES) at 40°C. The concentration of glycerol in the feed was 1000 ppm

Results at 60°C are shown in Figure 7.4 where we observe that under certain cases, the standard was not met. It appears that at a TMP of 0.26 and greater, the standard was not met, especially for the addition of 0.425 mass% water and larger.

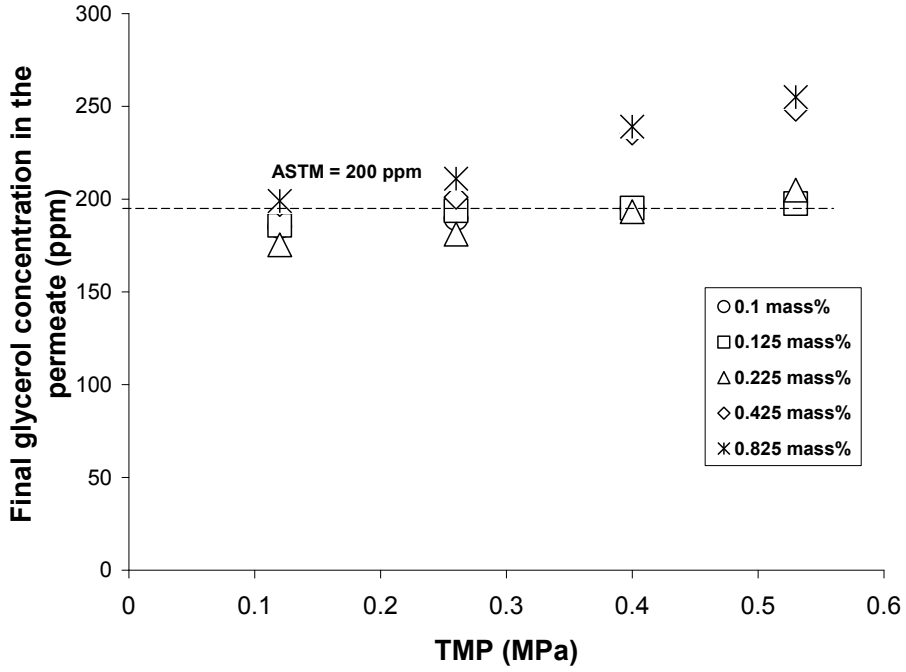

Figure 7.4: Effects of initial water concentration and trans-membrane pressure (TMP) on final glycerol concentraton in the permeate for (0.03 μm, PES) at 60°C. The concentration of glycerol in the feed was 1000 ppm

For the MF PES membranes, similar trends in the effect of temperature on glycerol separation are found (see Figures 7.5 through 7.10). At temperatures of 40 and 60°C, the effects of TMP and initial water concentration on membrane performance are also similar in trend with that of the UF membrane setup. At 25°C, we observe a plateau in the data. Figures 7.5 through 7.7 are for runs using PES membranes with a pore size of 0.1 μm while Figures 7.8 through 7.10 show the data for the 0.22 μm pore size PES membranes. In general, an increase in pore size resulted in degraded membrane performance.

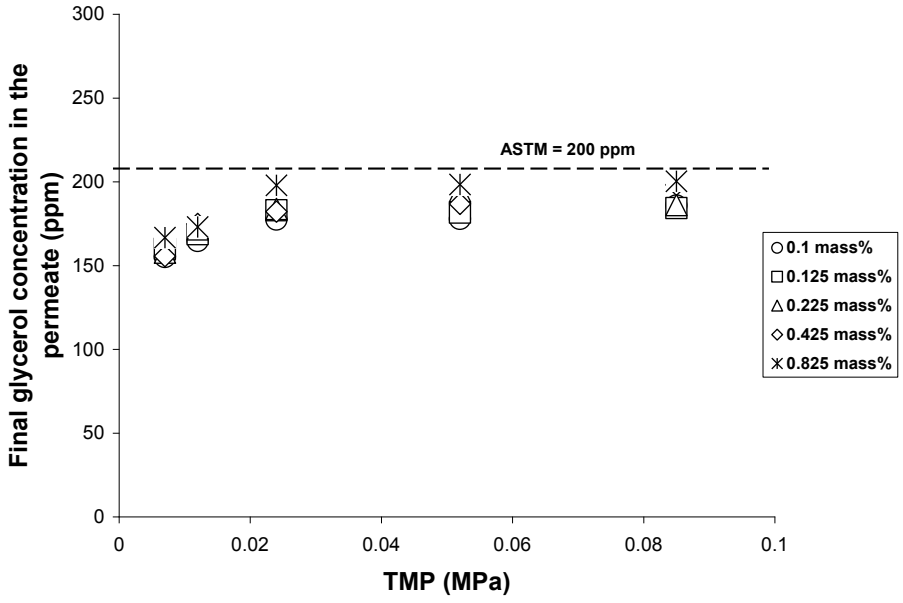

Figure 7.5: Effects of initial water concentration and trans-membrane pressure (TMP) on final glycerol concentration in the permeate for (0.1 μm, PES) at 25°C. The concentration of glycerol in the feed was 1000 ppm

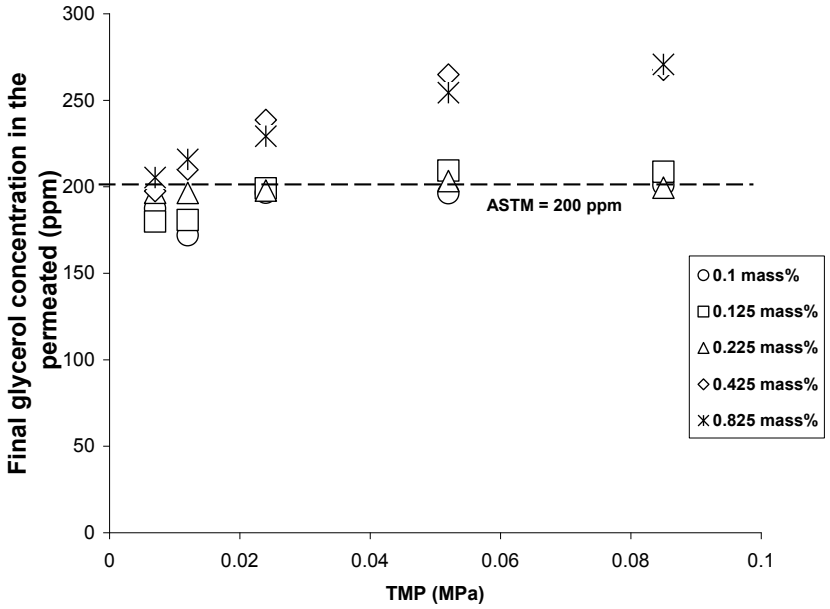

Figure 7.6: Effects of initial water concentration and trans-membrane pressure (TMP) on final glycerol concentration in the permeate for (0.1 μm, PES) at 40°C. The concentration of glycerol in the feed was 1000 ppm

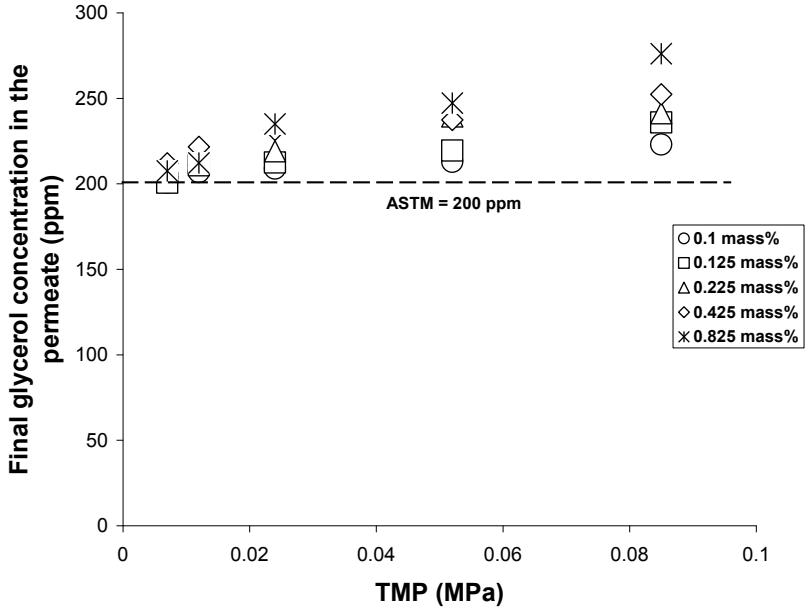

Figure 7.7: Effects of initial water concentration and trans-membrane pressure (TMP) on final glycerol concentration in the permeate for (0.1 µm, PES) at 60°C. The concentration of glycerol in the feed was 1000 ppm

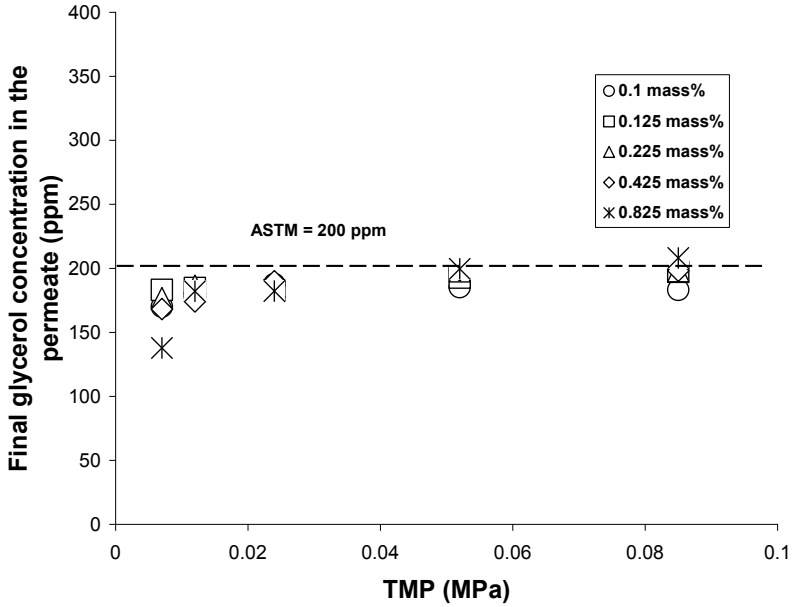

Figure 7.8: Effects of initial water concentration and trans-membrane pressure (TMP) on final glycerol concentration in the permeate for (0.22 µm, PES) at 25°C. The concentration of glycerol in the feed was 1000 ppm

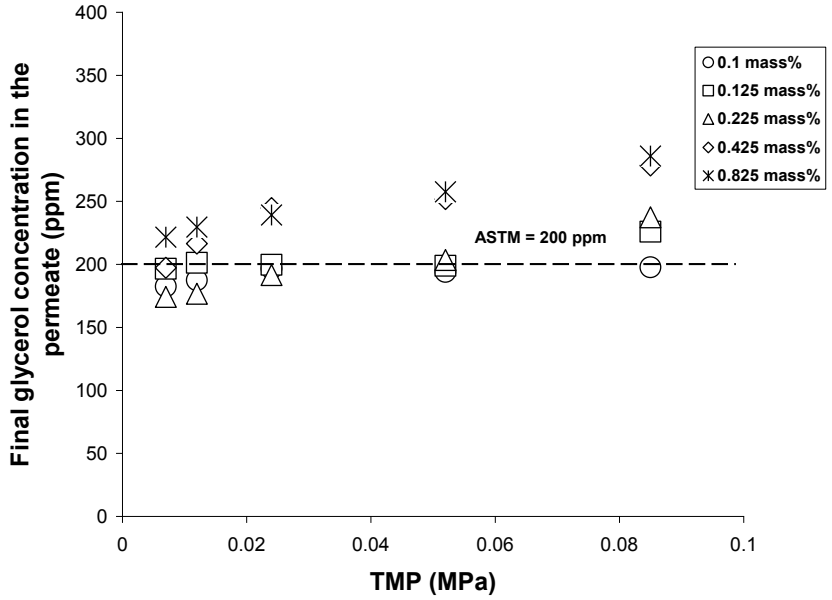

Figure 7.9: Effects of initial water concentration and trans-membrane pressure (TMP) on final glycerol concentration in the permeate for (0.22 µm, PES) at 40°C. The concentration of glycerol in the feed was 1000 ppm

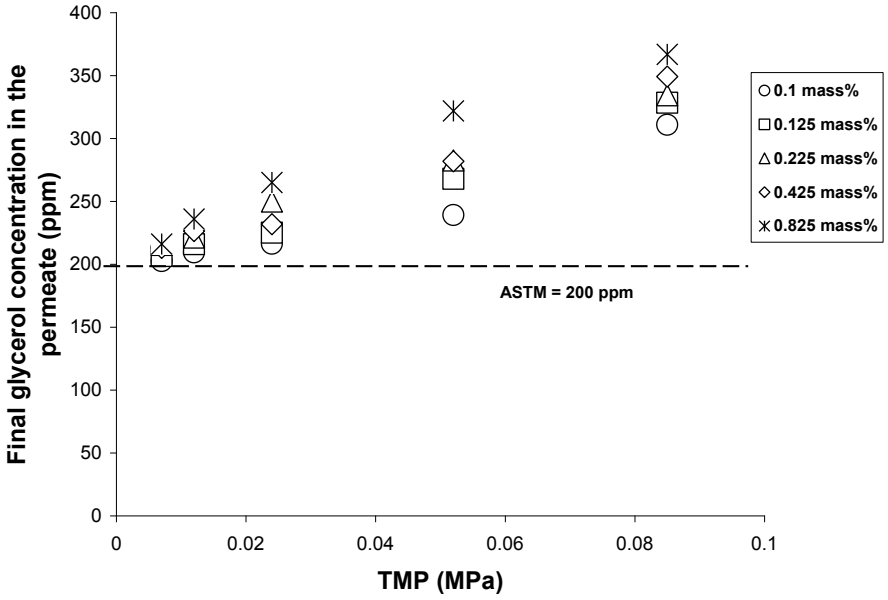

Figure 7.10: Effects of initial water concentration and trans-membrane pressure (TMP) on final glycerol concentration in the permeate for (0.22 µm, PES) at 60°C. The concentration of glycerol in the feed was 1000 ppm

The mechanism of removing a dispersed phase (i.e., suspended glycerol droplets) from a continuous phase using membrane technology is primarily based on the sizes of the dispersed droplets relative to the pore size of the membrane and the miscibility of the dispersed phase and the continuous phase. The miscibility of the two phases is affected by temperature. As the dispersed droplets increase in size, the separation performance of the membrane unit should increase.

We have previously identified the effect of water on glycerol droplet size up to a concentration of 0.2 mass% [26]. In this paper, we extended the range of water concentrations in addition to investigating the effect of TMP and temperature. All permeate samples were analyzed by Karl Fisher titration to determine the amount of water in the permeate. It was found that for all cases, water concentration in the permeate increased slightly with TMP and significantly with temperature. These results are shown in Tables 7.1, 7.2 and 7.3.

Table 7.1: Amount of water in the permeate (ppm) for UF membrane (0.03 μm, PES) at different temperatures and trans-membrane pressure (TMP)

Mass% water	TMP (MPa)	25°C	40°C	60°C
0.1	**0.12**	651	783	825
	0.26	696	789	925
	0.4	728	826	940
	0.53	748	967	967
0.125	**0.12**	809	910	1011
	0.26	855	919	1150
	0.4	921	934	1180
	0.53	935	1100	1210
0.225	**0.12**	1346	1369	1483
	0.26	1350	1479	1568
	0.4	1360	1545	1575
	0.53	1375	1585	1585
0.425	**0.12**	1339	1534	1600
	0.26	1451	1561	1622
	0.4	1465	1592	1625
	0.53	1475	1632	1792
0.825	**0.12**	1345	1616	1785
	0.26	1368	1625	1825
	0.4	1415	1645	1836
	0.53	1420	1656	1847

Table 7.2: Amount of water in the permeate (ppm) for MF membrane (0.1 μm, PES) at different temperatures and trans-membrane pressure (TMP)

Mass% water	TMP (MPa)	25°C	40°C	60°C
0.1	**0.007**	655	750	951
	0.012	668	900	961
	0.024	698	910	979
	0.052	800	940	979
	0.085	900	952	989
0.125	**0.007**	766	890	1125
	0.012	800	1120	1160
	0.024	860	1130	1190
	0.052	960	1180	1215
	0.085	1100	1190	1233
0.225	**0.007**	1000	1230	1250
	0.012	1100	1350	1390
	0.024	1120	1400	1450
	0.052	1200	1500	1580
	0.085	1270	1600	1700
0.425	**0.007**	1205	1642	1898
	0.012	1234	1657	1910
	0.024	1261	1671	1955
	0.052	1275	1727	2006
	0.085	1300	1760	2098
0.825	**0.007**	1864	2203	2627
	0.012	2002	2217	2865
	0.024	2016	2351	2924
	0.052	2089	2410	2957
	0.085	2095	2480	2967

Table 7.3: Amount of water in the permeate (ppm) for MF membrane (0.22 μm, PES) at different temperatures and trans-membrane pressure (TMP)

Mass% water	TMP (MPa)	25°C	40°C	60°C
0.1	**0.007**	685	778	1000
	0.012	734	925	983
	0.024	744	930	983
	0.052	810	944	989
	0.085	912	960	993
0.125	**0.007**	790	920	1130
	0.012	1089	1138	1173
	0.024	1099	1145	1189
	0.052	1110	1200	1230
	0.085	1130	1215	1245
0.225	**0.007**	1085	1240	1255
	0.012	1134	1370	1397
	0.024	1140	1444	1460
	0.052	1240	1530	1600
	0.085	1310	1610	1750
0.425	**0.007**	1230	1697	1980
	0.012	1287	1700	2031
	0.024	1298	1689	2124
	0.052	1330	1786	2020
	0.085	1390	1780	2150
0.825	**0.007**	1250	2257	2668
	0.012	2130	2244	2906
	0.024	2140	2391	2964
	0.052	2155	2450	2998
	0.085	2170	2520	3008

The maximum solubility of glycerol in FAME is listed in the literature as 1490 ppm [31]. In our experiments, we used a fixed initial glycerol concentration in FAME for all tests (1000 ppm) which still exceeds the ASTM standard (200 ppm). The water solubility in biodiesel is dependent on the type of feedstock used to make the ester and its degree of saturation and is reported at 25°C to be between 1675 – 1785 ppm [32]**.** Van Gerpen indicated a maximum of 1500 ppm at 25°C [31]. Shah et al. measured the solubility of water in commercial biodiesel at different temperatures up to 40°C and it was found that temperature had a remarkable effect on increasing the solubility of water in methyl esters [32]. Given the conditions in this study, one expects to generate a dispersed water-glycerol phase in the continuous FAME phase. This is partly due to the great affinity between water and glycerol. At the constant initial glycerol concentration used, increasing the water concentration will result in an increase in the size of the dispersed droplets. If the water concentration is increased up to its solubility limit in FAME, one would expect that the water will extract most if not all of the glycerol present in the FAME. Based on our results, it appears that 0.225 mass% water is the maximum value that can be used to effectively separate the glycerol from FAME. Adding water beyond 0.225 mass% (i.e., beyond its solubility in FAME) will cause the droplets to precipitate out of the FAME mixture.

The results for the glycerol concentration in the permeate for the UF membrane at 25°C (see Figure 7.2) shows that the ASTM standard (200 ppm) was met. As noted above, the TMP had only a small effect on water concentration in the permeate. As a result, the effect of TMP on glycerol separation was also small. On the other hand, increasing temperature significantly increased the water concentration in the permeate and this, in turn, had a strong effect on the separation of glycerol from the FAME phase. Thus, at lower temperatures (25°C), the ASTM standards were achieved at all of the conditions studied which coincided with water concentrations in the permeate within the range of the maximum solubility of water reported in the literature (see Table 7.1 and discussion above). It should be noted that the feed tank mixture was continuously agitated using a magnetic stirrer. This likely kept the droplets dispersed in the FAME phase rather than allowing them to precipitate in the feed tank.

The membrane feed and bleed system was operated using a cross-flow membrane

contacting technique. This approach serves to minimize fouling on the membrane surface. The continuous mixing and circulation experienced by the droplets will enhance coalescence and encourage the formation of large droplets, thus, making separation easier.

7.4 Effect of water concentration on droplet size

Using DLS, the effect of different initial water concentration on glycerol droplet size was estimated. As noted in the Methods section, a pure FAME sample along with eight FAME samples including 1,000 ppm glycerol over a range of different water concentrations (0.02 – 0.8 mass%). The average droplet diameters obtained by DLS are shown in Figure 7.11. The addition of water up to almost 0.2 mass% resulted in a remarkable increase in droplet size, while beyond that concentration, the droplet size increase was far less pronounced. The concentration of 0.2 mass% water is close to the maximum solubility limit of water in biodiesel. As shown earlier, this concentration level coincides with the best separation performance observed for the membrane system.

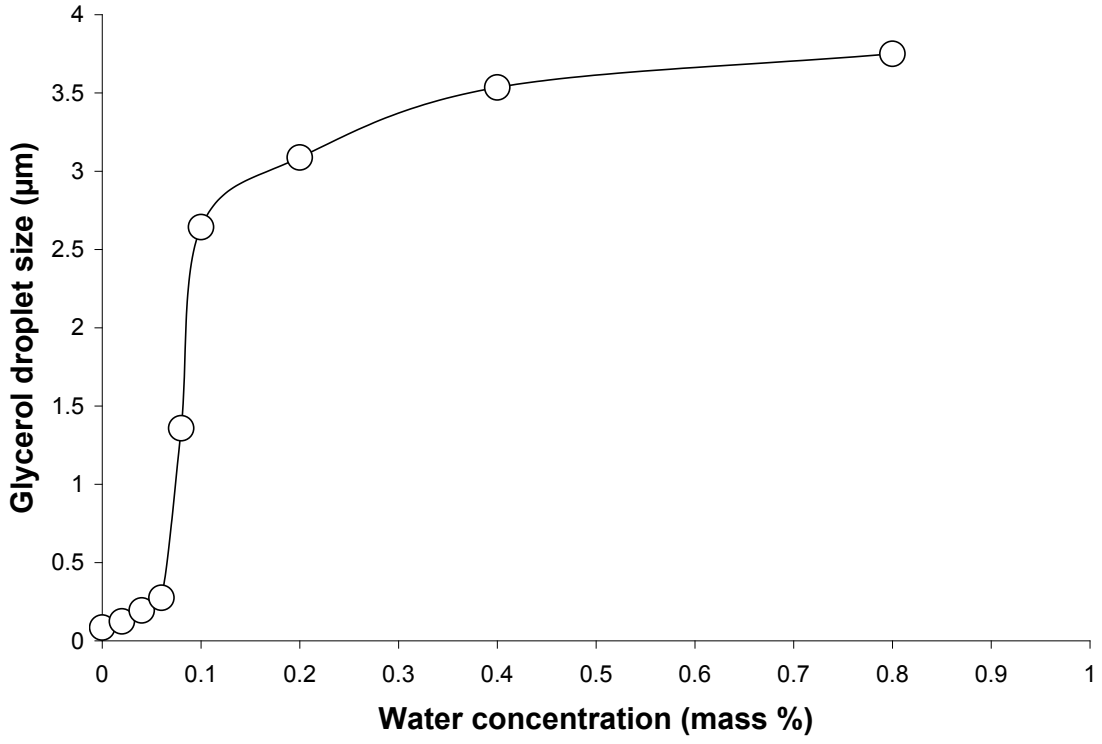

Figure 7.11: Effects of water concentration on glycerol droplet size at 25°C

7.5 Cake filtration theory and gel layer model

The experimental results showed that the solubility of dispersed water-glycerol phase in FAME was affected by temperature and water concentration in the FAME. This will affect membrane performance for glycerol removal from FAME. In previous work [27], formation of a hydrophilic glycerol-rich (gel) layer on the surface of the membrane was observed. This suggests a build-up of a selective layer on the surface of the membrane and that selective layer was capturing the dispersed glycerol as it attempted to permeate through the layer. This gel layer enhanced the separation capability of the membrane. In the early stages of filtration, the polar dispersed droplets gradually accumulate at the surface of the membrane in the form of a cake layer. As the filtration proceeds, a balance sets in and at steady-state, the deposition of droplets on the surface of the membrane is balanced by those leaving the layer due to the cross-flow of fluid above the membrane. Once the layer is formed, the droplets containing glycerol in the feed solution can be captured by the layer.

Cake filtration is a commonly applied operation for separating solid materials from suspensions [33]. In cake filtration, the solid/fluid suspension is pressurized, which allows the fluid to pass through the medium and the solid droplets are retained on the surface of the medium forming a cake layer [34]. During filtration, the cake thickness increases with time. In most cases, this cake layer becomes compacted and the fluid resistance to flow increases.

Applying cake filtration theory in our case was useful in evaluating the compressibility of the formed layer at the membrane surface and the effect of temperature on the specific resistance of the cake. The gel layer model is applied here to predict the concentration of the gel layer at the membrane surface and to know the effect of temperature on that concentration. The cake filtration equation is [35]:

$$\frac{t}{V} = \frac{\mu \alpha C}{2\Delta P A^2} V + \frac{\mu R_m}{\Delta P A} \qquad (7.1)$$

where t is time (s), V is the cumulative filtrate volume (m^3), μ is the dynamic viscosity (Pa.s), α is the specific resistance of the cake (m/kg), C is concentration of solute (kg/m^3),

ΔP is the applied TMP (Pa), A is the filtrate medium area (m^2), and R_m is the membrane resistance (m^{-1}). Equation (7.1) yields a straight line on a plot of t/V vs. V. From the slope, the value of the specific resistance of the cake (α) can be calculated and from the intercept, the value of the membrane resistance (R_m) can be found. Equation (7.1) can be rearranged in the form of resistances:

$$\frac{\Delta P A t}{\mu V} = \frac{\alpha C V}{2A} + R_m \qquad (7.2)$$

From Equation (7.2), resistance of the cake (R_s) is defined as:

$$R_s = \frac{\alpha C V}{2A} \qquad (7.3)$$

The conventional cake filtration equation model determines the flux (m/s) as:

$$J = \frac{\Delta P}{\mu (R_s + R_m)} \qquad (7.4)$$

The cake filtration model was applied to all of the data in this study. The estimated model parameters are shown in Appendix B (Tables B.9 to B.23). The results show that the specific cake resistance decreased with increasing temperature. In Figure 7.12 is an example of the cake filtration equation (Eqn. 7.1) plotted against the experimental data for different TMP at 0.1 mass% water and 25°C. Figure 7.13, shows the specific cake resistance (α) plotted against TMP for the UF membrane (0.03 μm, PES) at different temperatures and 0.1 mass% water. Similar trends were found for the other pore sizes and operating conditions. A slight decrease in specific cake resistance with TMP was observed at a fixed temperature. This explains the relatively slight increase in glycerol concentration with TMP (see Figures 7.2 to 7.4).

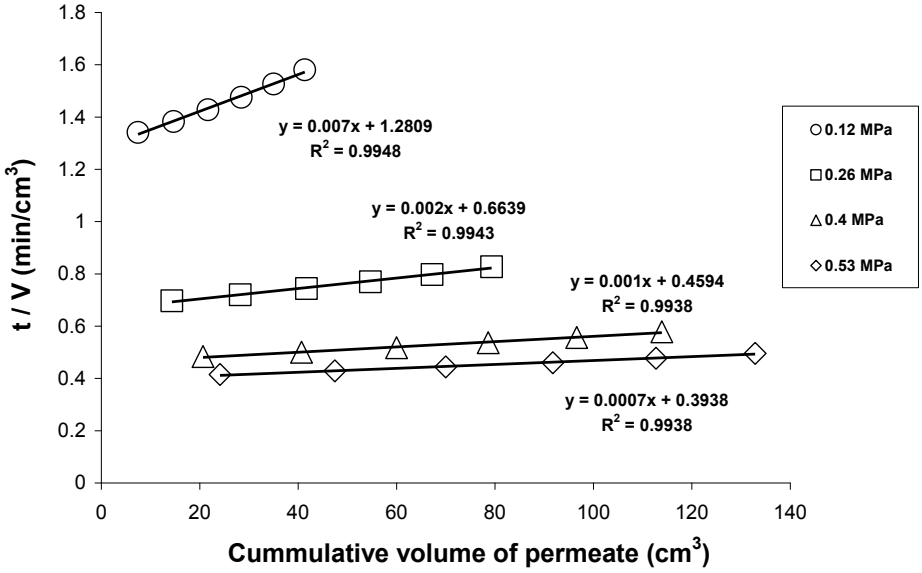

Figure 7.12: (t/V) vs cumulative volume of permeate for (0.03 μm, PES) at 25°C and different TMP for 0.1 mass% water

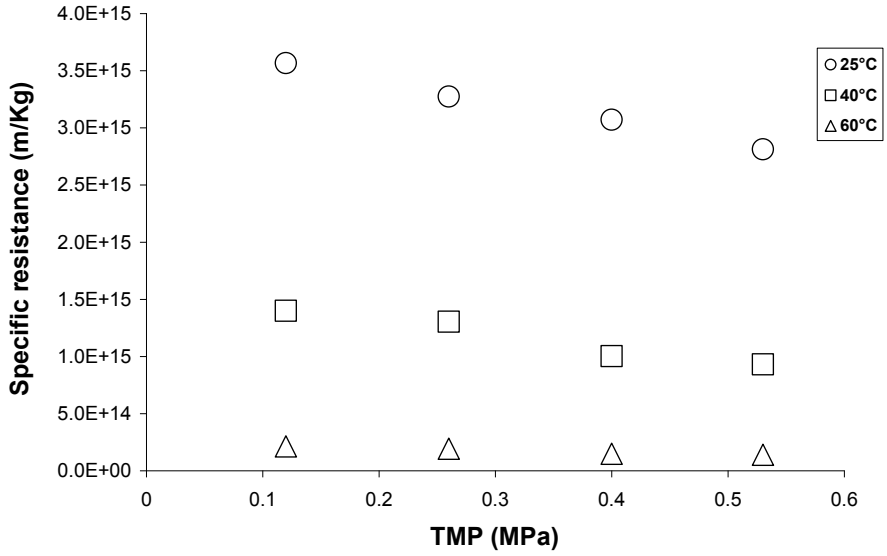

Figure 7.13: Specific resistance vs TMP for (0.03 μm, PES) for 0.1 mass% water at different temperature

The compressibility of the cake layer is based on the proportionality between the specific cake resistance and the applied pressure [36]. For example, data for the UF membrane at 0.1 mass% water indicates that the specific cake resistance at 25°C decreases with applied pressure while for the other temperatures it remains unchanged with TMP indicating that the cake layer is incompressible (see Figure 7.13). The results for all other runs are reported in the Appendix B, (see Tables B.9 to B.23). They indicate that the specific cake layer resistance was relatively constant with TMP indicating an incompressible cake layer.

Based on our results, it was of interest to predict the concentration of the gel layer formed at the membrane surface and the effect of that concentration with temperature. During membrane separation, concentration polarization occurs at the surface of the membrane. Concentration polarization leads to the accumulation of solute particulates at the surface of the membrane. This results in the build up of a cake, or gel layer on the membrane. In cross-flow filtration this cake layer continues to grow, causing a reduction in permeate flux, until steady-state conditions prevail. The thickness of the cake layer reaches a steady-state value when the flow of solute towards the cake layer equals the diffusion of solute from the cake layer and the flow of solute across the membrane by the cross-flow velocity. Directly above the cake layer is a boundary layer, where the concentration is in transition from the bulk to the greater cake layer concentration. Recent work [27] suggests that a build-up of a selective layer on the surface of the membrane was occurring.

The gel model was used to correlate UF experimental data. In such a system, droplets brought by the permeation flow to the membrane surface are balanced by back-diffused droplets from the membrane surface. This model has a well known relation as follows [37]:

$$J = \frac{D_m}{\delta} \ln\left(\frac{C_{gel} - C_p}{C_f - C_p}\right) \qquad (7.5)$$

where (J) is the permeation flux (m/s), C_f is the feed concentration (kg/m^3), (δ) denotes the thickness of the boundary layer, $(\frac{D_m}{\delta})$ represents the mass transfer coefficient, k (m/s), C_p is the concentration in the permeate (kg/m^3), and C_{gel} is the

concentration near the membrane surface (kg/m^3). The permeation flux is thus a linear function of $\ln(C_f - C_p)$ with a slope equal to –k and an intercept of $k \ln(C_{gel} - C_p)$. In this study, four different TMPs for the UF membrane and five different TMPs for the MF membranes were used. An iterative method was used to predict the concentration of the gel layer using Equation (7.5) above in a spreadsheet program. The complete results are shown in Tables 7.4 to 7.6. The root mean square error (RMSE) was calculated for individual TMPs as well as the overall (RMSE) to show how well the predicted values for fluxes fit the experimental ones. The following formula was used to calculate the (RMSE):

$$RMSE = \sqrt{\frac{\Sigma(f(x_i) - y_i)^2}{n}} \qquad (7.6)$$

Table 7.4: Results for the gel layer model for MF (0.03 µm, PES) at different temperatures. Mass transfer coefficients and Gel layer concentration are fitted parameters obtained at a given temperature

Temperature (°C)	**TMP (MPa)**	**Mass transfer coefficient (K) m/s * 10 ^{6}**	**Gel layer concentration (C_{gel}) mass%**	**RMSE for experimental fluxes (L/m^2h)**	**Overall RMSE (L/m^2h)**
25	**0.12**	0.07	31.4	0.22	0.29
	0.26	0.16		0.32	
	0.4	0.24		0.37	
	0.53	0.29		0.25	
40	**0.12**	0.12	24.7	0.27	0.47
	0.26	0.24		0.35	
	0.4	0.33		0.5	
	0.53	0.33		0.65	
60	**0.12**	0.37	3.74	0.32	0.53
	0.26	0.58		0.49	
	0.4	0.68		0.56	
	0.53	0.69		0.68	

Table 7.5: Results for the gel layer model for MF (0.1 μm, PES) at different temperatures. Mass transfer coefficients and Gel layer concentration are fitted parameters obtained at a given temperature

Temperature (°C)	**TMP (MPa)**	**Mass transfer coefficient (K) m/s * 10 ^{6}**	**Gel layer concentration (C_{gel}) mass%**	**RMSE for experimental fluxes (L/m^{2}h)**	**Overall RMSE (L/m^{2}h)**
25	**0.007**	0.34	1.49	0.83	1.88
	0.012	0.71		1.75	
	0.024	1.51		1.72	
	0.052	2.76		3.24	
	0.085	3.15		0.76	
40	**0.007**	0.30	1.34	0.29	1.33
	0.012	0.60		0.72	
	0.024	1.56		2	
	0.052	2.84		1.38	
	0.085	3.73		1.51	
60	**0.007**	0.26	1.28	1.18	4.52
	0.012	0.81		2.08	
	0.024	2.23		2.6	
	0.052	2.77		7.86	
	0.085	3.05		5.3	

Table 7.6: Results for the gel layer model for MF (0.22 μm, PES) at different temperatures. Mass transfer coefficients and Gel layer concentration are fitted parameters obtained at a given temperature

Temperature (°C)	**TMP (MPa)**	**Mass transfer coefficient (K) m/s * 10 ^{6}**	**Gel layer concentration (C_{gel}) mass%**	**RMSE for experimental fluxes (L/m^{2}h)**	**Overall RMSE (L/m^{2}h)**
25	**0.007**	0.35	1.46	0.93	2.16
	0.012	0.75		2.04	
	0.024	1.66		1.71	
	0.052	2.83		3.41	
	0.085	3.31		1.91	
40	**0.007**	0.28	1.41	0.47	1.44
	0.012	0.67		0.62	
	0.024	1.76		2.24	
	0.052	2.23		1.55	
	0.085	4.10		1.51	
60	**0.007**	0.32	1.14	1.31	5.76
	0.012	0.94		2.52	
	0.024	2.32		3.73	
	0.052	4.11		6.67	
	0.085	4.62		9.96	

Figures 7.14 to 7.22 show the flux versus (C_f – C_p) for all membranes and different conditions. The figures show that the concentration of the gel layer decreased as temperature increased and the mass transfer coefficient increased with TMP. This means that the higher temperature will affect the final glycerol concentration in the permeate by increasing the solubility of the water-glycerol allowing them to pass through the membrane pores. The droplets were retained to less of an extent on the surface of the membrane thus, reducing glycerol separation.

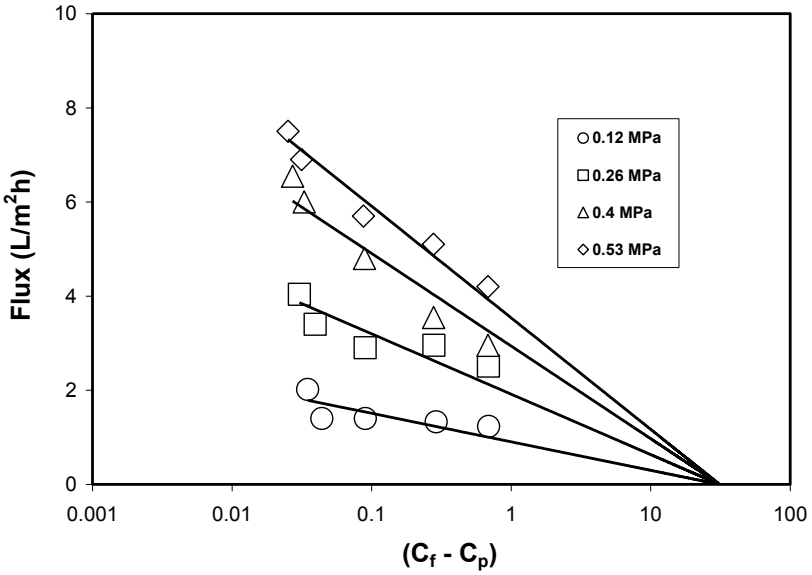

Figure 7.14: Flux vs ($C_f - C_p$) for UF (0.03 μm, PES) at 25°C

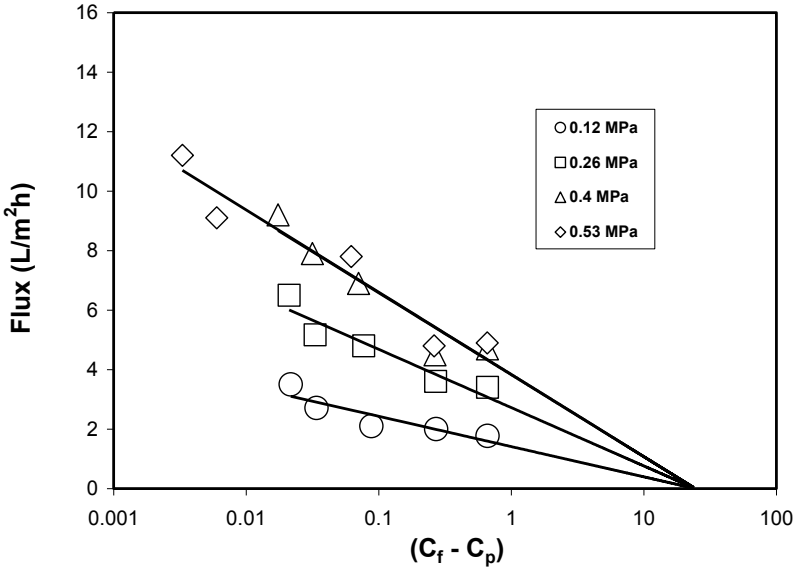

Figure 7.15: Flux vs ($C_f - C_p$) for UF (0.03 μm, PES) at 40°C

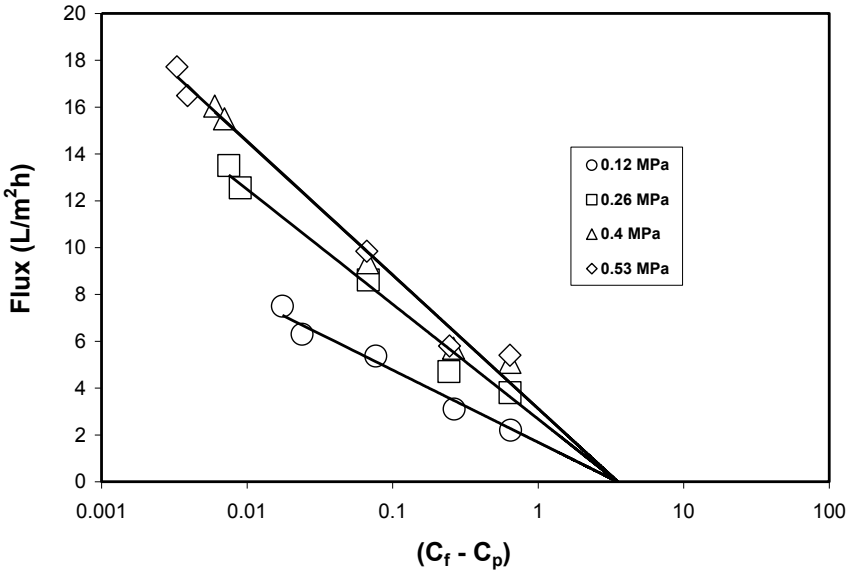

Figure 7.16: Flux vs ($C_f - C_p$) for UF (0.03 μm, PES) at 60°C

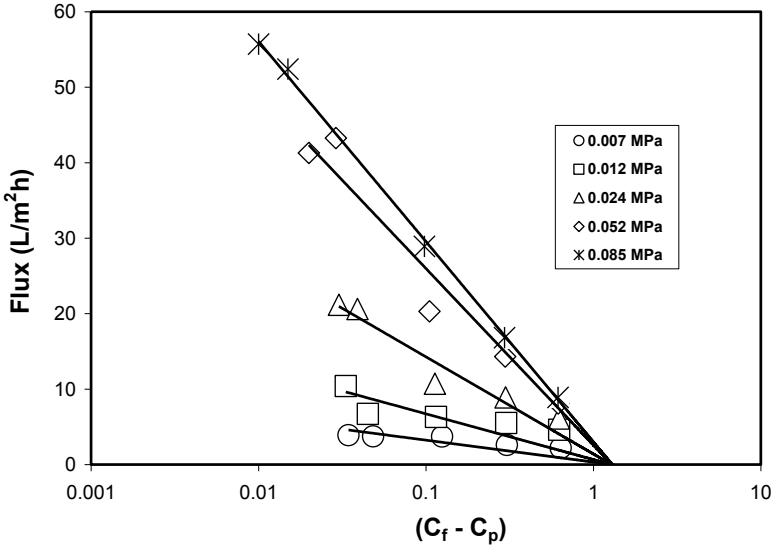

Figure 7.17: Flux vs ($C_f - C_p$) for MF (0.1 μm, PES) at 25°C

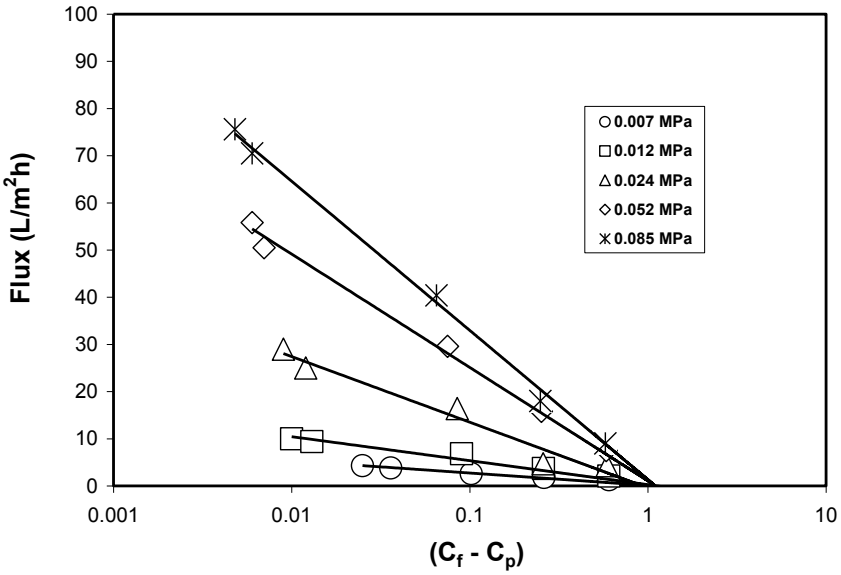

Figure 7.18: Flux vs ($C_f - C_p$) for MF (0.1 μm, PES) at 40°C

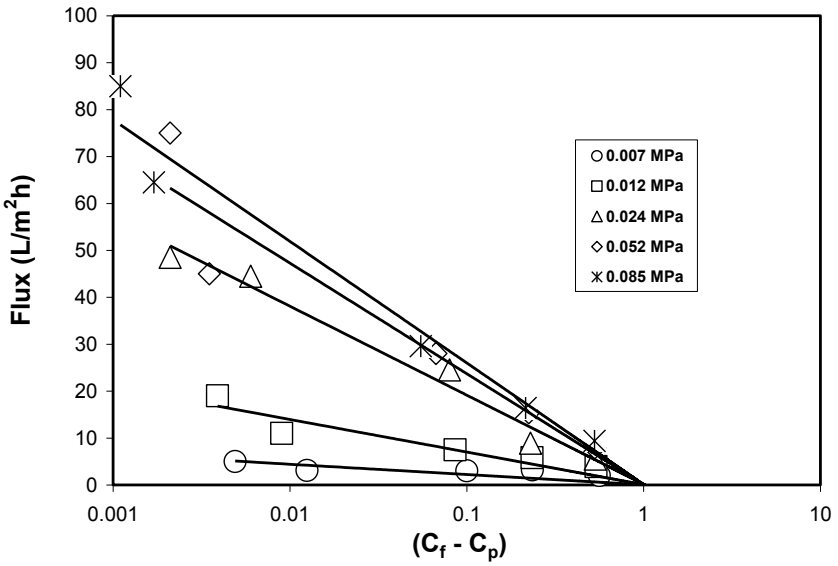

Figure 7.19: Flux vs ($C_f - C_p$) for MF (0.1 μm, PES) at 60°C

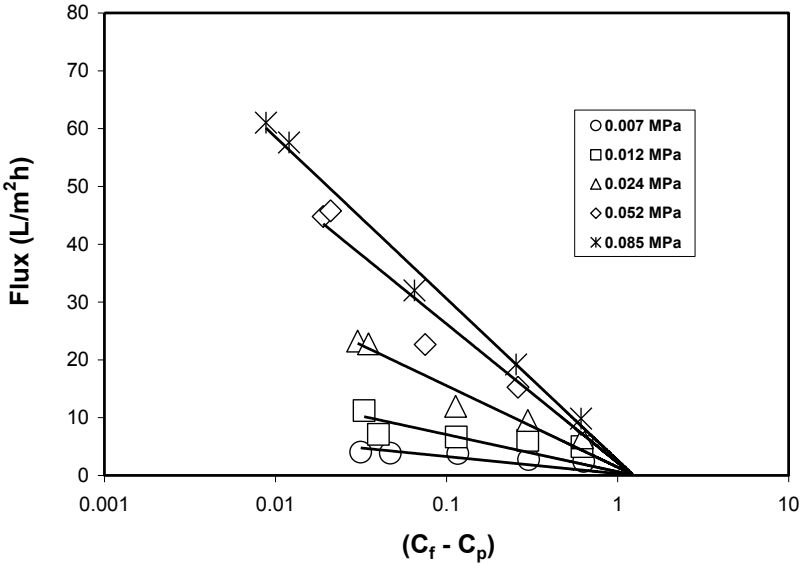

Figure 7.20: Flux vs ($C_f - C_p$) for MF (0.22 µm, PES) at 25°C

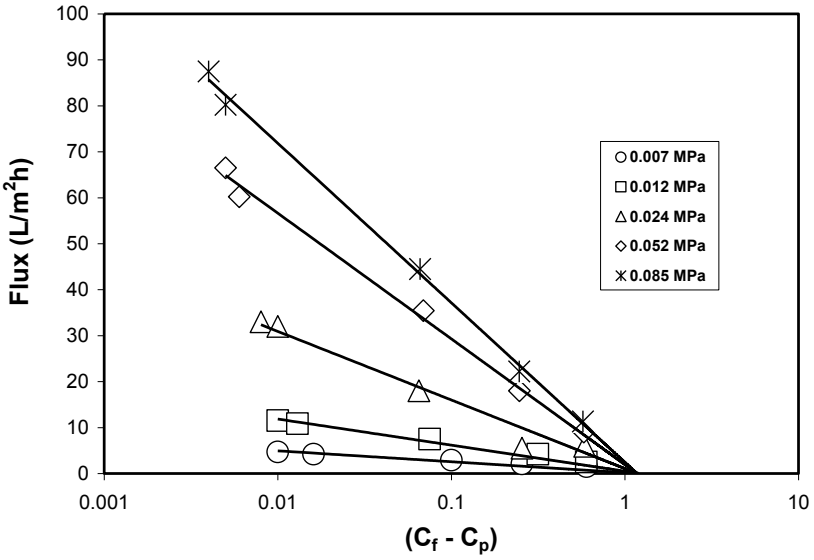

Figure 7.21: Flux vs ($C_f - C_p$) for MF (0.22 µm, PES) at 40°C

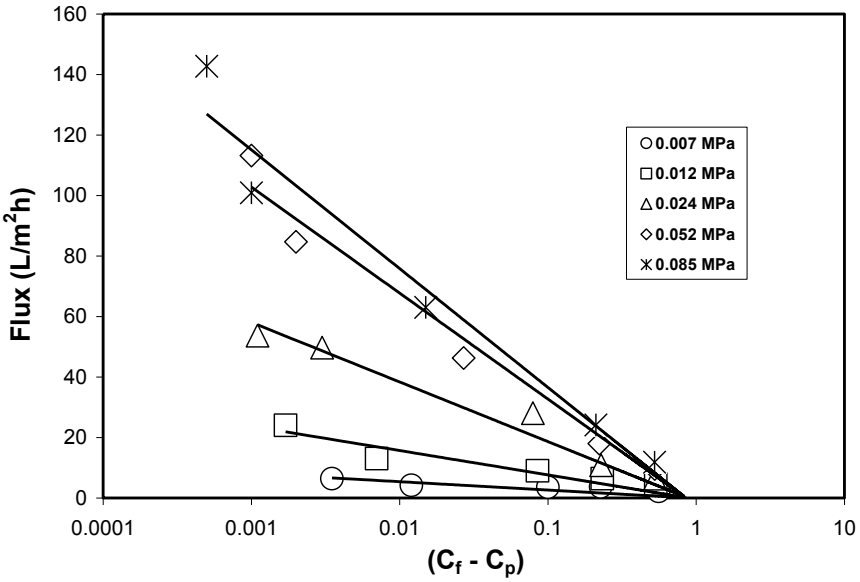

Figure 7.22: Flux vs ($C_f - C_p$) for MF (0.22 µm, PES) at 60°C

As previously mentioned, the mass transfer coefficient is inversely proportional to the thickness of the selective layer at the surface of the membrane. The increase in the values of the mass transfer coefficient with temperature and TMP indicated that the thickness of the gel layer decreased with the TMP and temperature. Figures 7.23 to 7.25, show the effect of temperature on the values of the mass transfer coefficient with TMP for the three pore sizes. For the MF membranes, the mass transfer coefficient is relatively unaffected by temperature. In the case of the UF membrane, it is lower than MF by a factor of 10. As seen in Figures 7.2 and 7.3 (UF membrane at 25 and 40°C) the glycerol retention is much higher for all TMPs than for all the remaining experiments Figures 7.4 to 7.10. These results coincide with the gel layer concentration at the surface of the membrane which is much higher in the case of the UF membrane at 25 and 40°C as shown in Table 7.4. They confirm the need for the existence of a substantial gel layer at the surface of the membrane to obtain good glycerol retention. The absence of this gel layer implies that glycerol will be poorly retained by the membrane. This indicates that the gel layer plays an important role in retaining the glycerol droplets by the membrane.

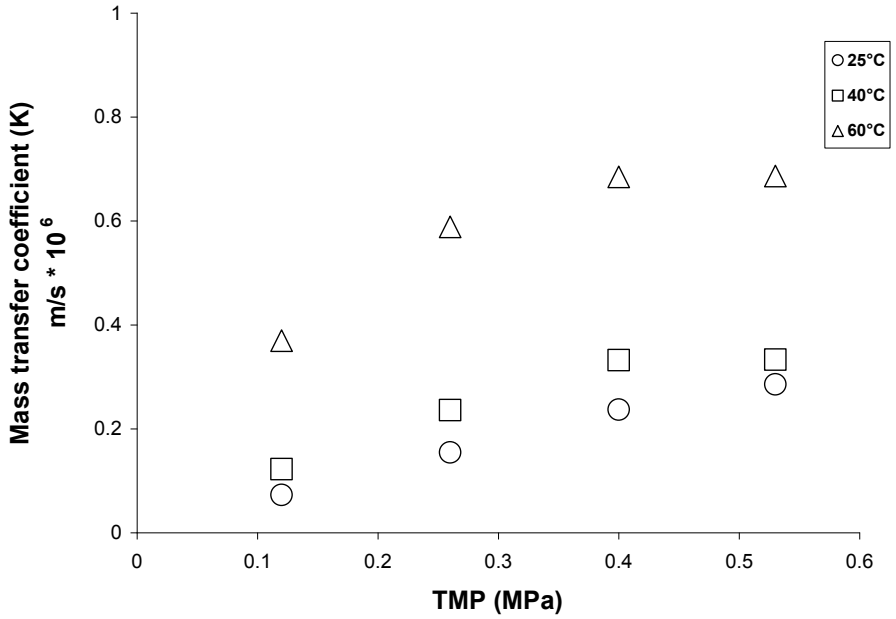

Figure 7.23: Effect of TMP on mass transfer coefficient for UF (0.03 μm, PES) at different temperatures

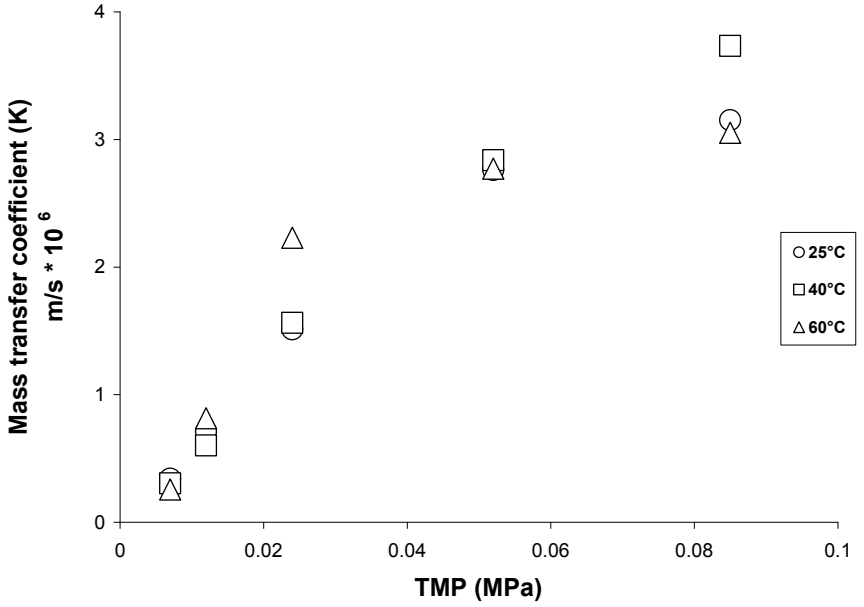

Figure 7.24: Effect of TMP on mass transfer coefficient for UF (0.1 μm, PES) at different temperatures

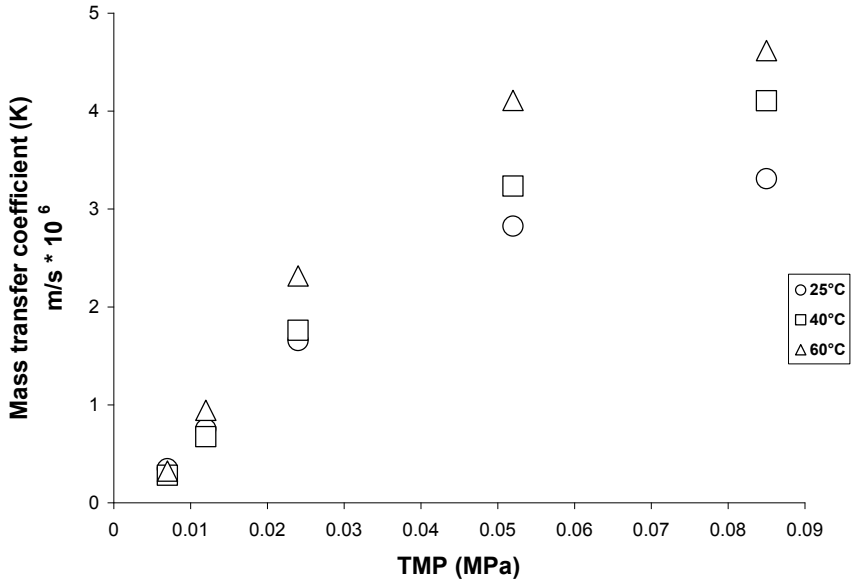

Figure 7.25: Effect of TMP on mass transfer coefficient for UF (0.22 μm, PES) at different temperatures

7.6 Critical and limiting fluxes

In this part of the work, we tried to determine the critical and limiting fluxes for the three different pore sizes at the different operating conditions used. To fulfill this objective a filtered batch of FAME was prepared to be used as our baseline and compare the fluxes obtained with other FAME mixtures prepared at different conditions.

This batch of filtered FAME was prepared as follows, a 20 L of un-treated FAME was taken and washed with distilled water 6 to 7 times, then treated in a rotary evaporator at 90°C under vacuum (0.94 bar vacuum) for 30 min. This washed and evaporated FAME was ultrafiltered a 0.03 μm, PES membrane at a TMP of 0.26 MPa and 25°C. This filtered FAME was kept for use to determine the pure FAME permeability for all membranes.

The steps used to determine the critical and limiting fluxes were based on changing the trans-membrane pressure (TMP) and measuring the mass flow rate of the permeate which then converted to get the flux values. For every temperature used in this experiment, a certain range of TMP was used as mentioned in section (7.2.2) on biodiesel

production. The TMP was changed after one hour of running. The values for the mass flow rates were recorded every 10 minutes. After that, an increase of the TMP was made for another hour of running. These steps were repeated for the all pore sizes at different conditions.

The results for the UF membrane of (0.03 μm, PES) for the pure FAME and different levels of initial water concentrations were shown in Figures 7.26 to 7.28 for 25, 40 and 60°C respectively. These figures show the experimental and the model results. The model results (lines) were calculated based on equation (4) shown above. The values of membrane and the cake resistances were calculated from the cake filtration equation (1) shown above. Comparing the other fluxes to the pure FAME flux, a remarkable decrease can be noticed and this decrease is proportional to the increase in water concentration level.

The results for the micro filtration membrane of (0.1 μm, PES) are shown in Figures 7.29 to 7.31 and for (0.22 μm, PES) are in Figures 7.32 to 7.34, for the pure FAME alone and different levels of water concentrations, for 25, 40 and 60°C, respectively.

From Figures it is found that determining the critical fluxes was difficult and approximation of this value was obtained by using the limiting flux. This is the flux that is pressure independent flux and it is the flux at the highest TMP. These limiting fluxes are reported in Table 7.7.

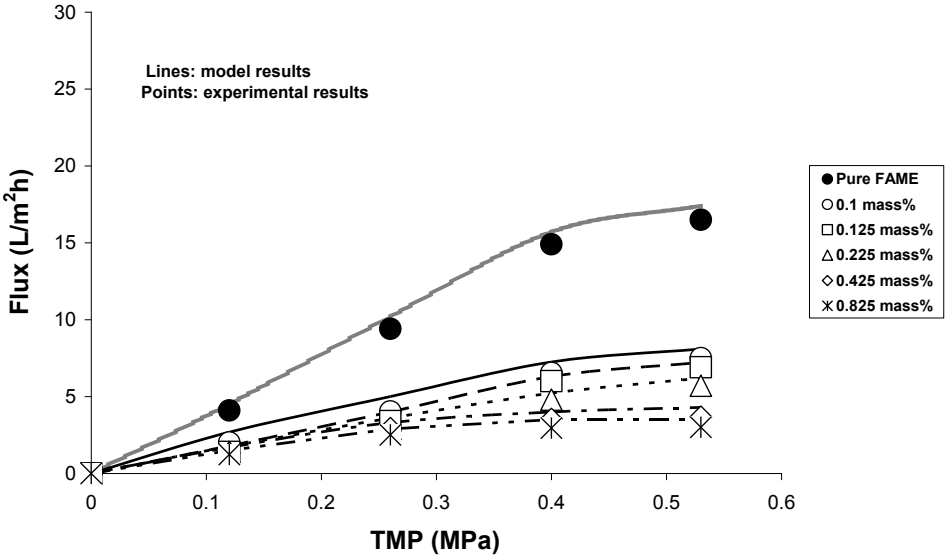

Figure 7.26: Fluxes for (0.03 μm, PES) at 25°C at different initial water concentrations vs. trans-membrane pressure (TMP)

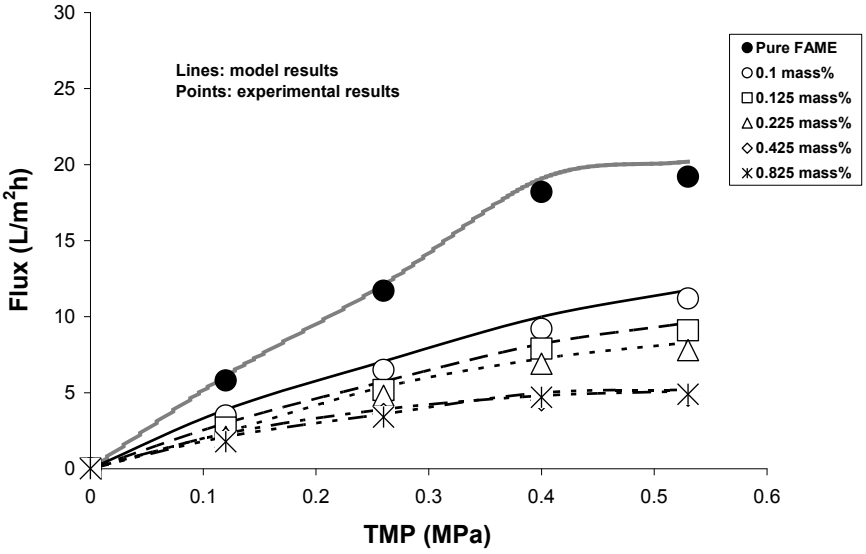

Figure 7.27: Fluxes for (0.03 μm, PES) at 40°C at different initial water concentrations vs. trans-membrane pressure (TMP)

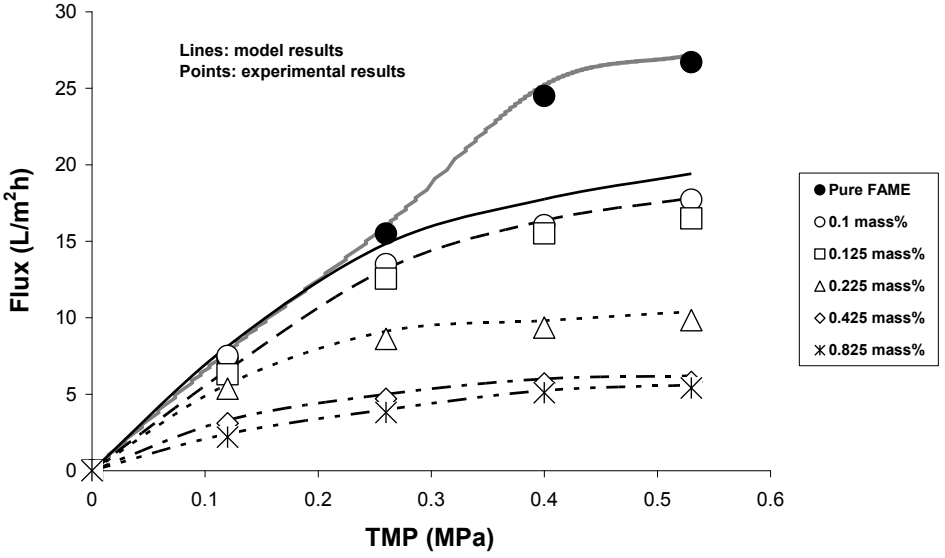

Figure 7.28: Fluxes for (0.03 μm, PES) at 60°C at different initial water concentrations vs. trans-membrane pressure (TMP)

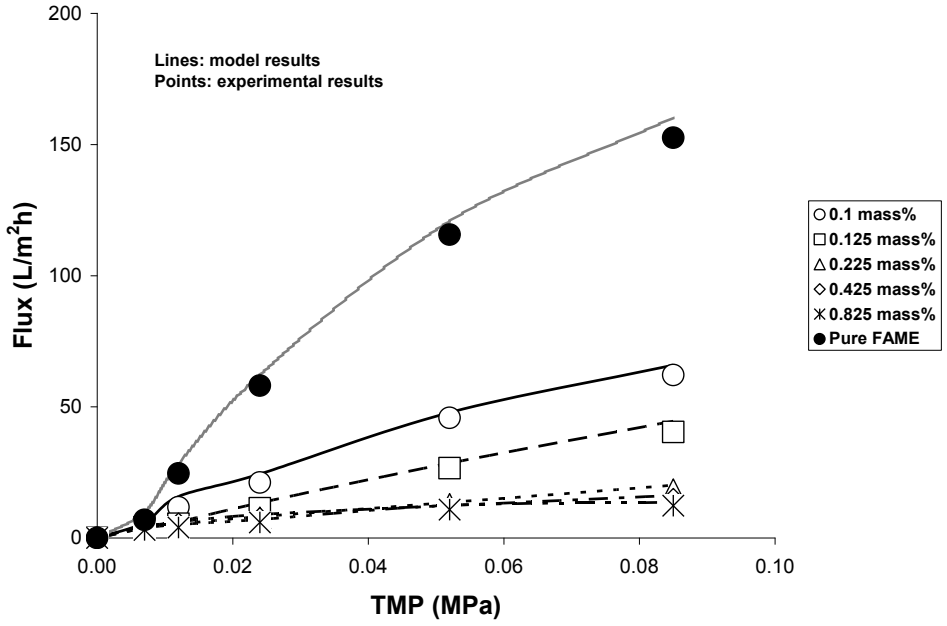

Figure 7.29: Fluxes for (0.1 μm, PES) at 25°C at different initial water concentrations vs. trans-membrane pressure (TMP)

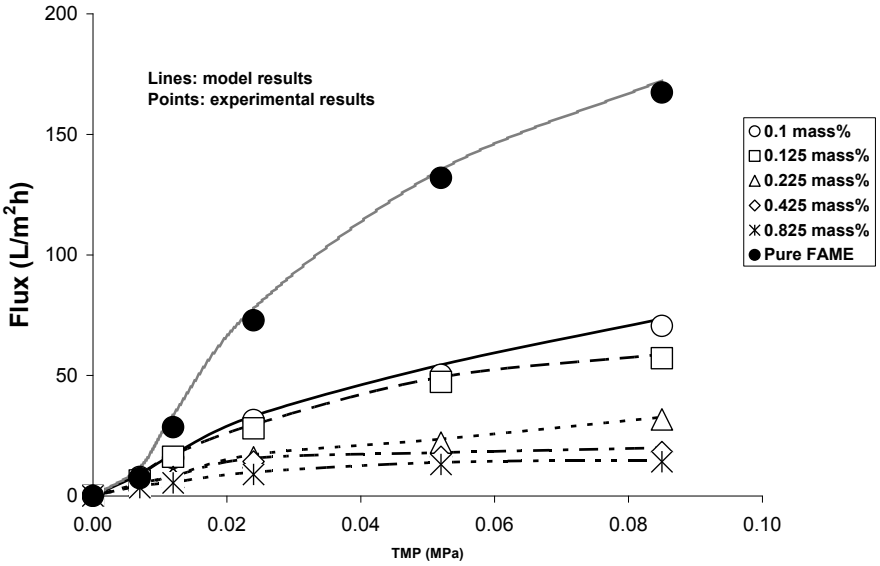

Figure 7.30: Fluxes for (0.1 μm, PES) at 40°C at different initial water concentrations vs. trans-membrane pressure (TMP)

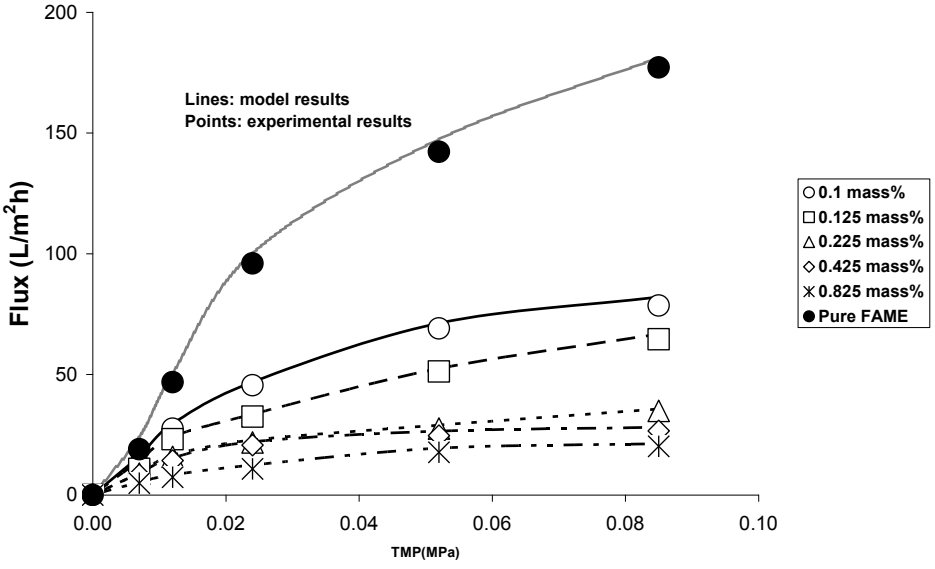

Figure 7.31: Fluxes for (0.1 μm, PES) at 60°C at different initial water concentrations vs. trans-membrane pressure (TMP)

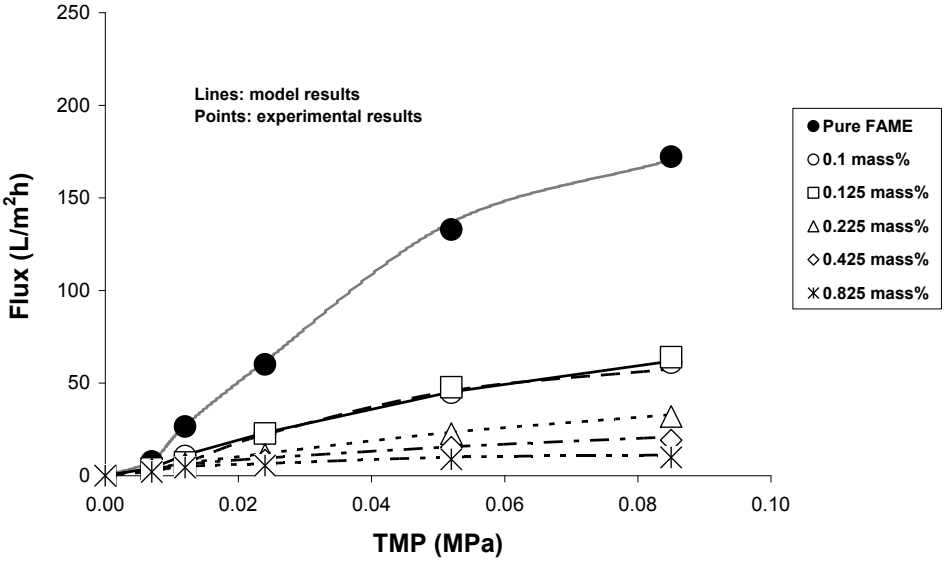

Figure 32: Fluxes for (0.22 μm, PES) at 25°C at different initial water concentrations vs. trans-membrane pressure (TMP)

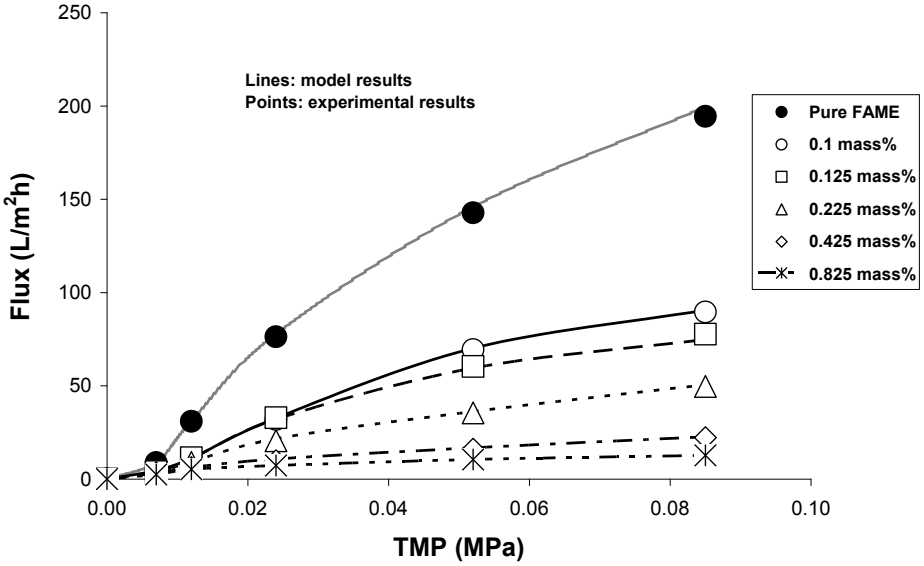

Figure 7.33: Fluxes for (0.22 μm, PES) at 40°C at different initial water concentrations vs. trans-membrane pressure (TMP)

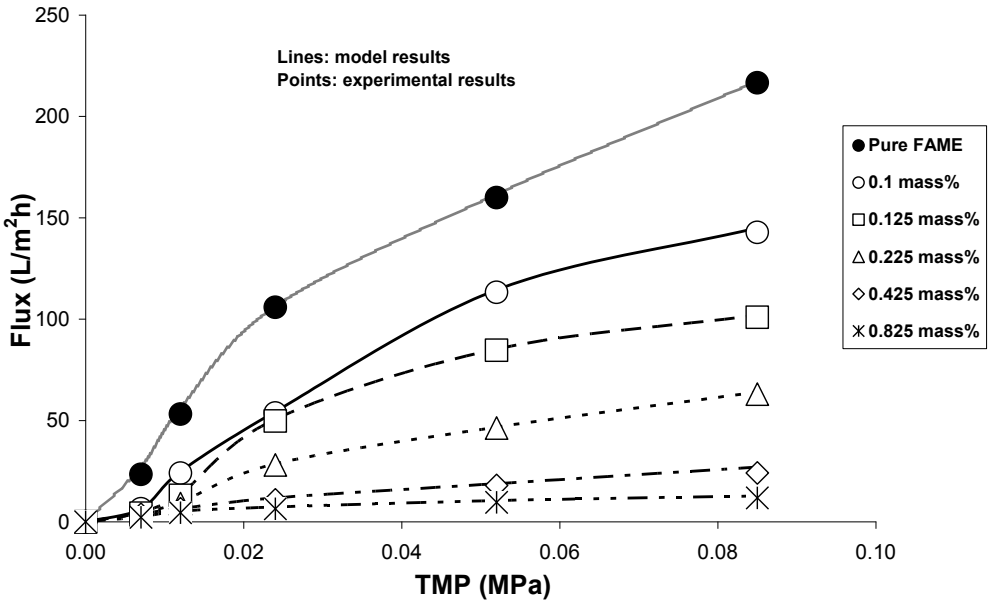

Figure 7.34: Fluxes for (0.22 μm, PES) at 60°C at different initial water concentrations vs trans-membrane pressure (TMP)

Table 7.7: Approximate values of limiting fluxes for the UF and MF membranes at different temperatures

PES µm	Water concentration (mass%)	25 °C	40 °C	60 °C
		Limiting flux (L/m^2h)	Limiting flux (L/m^2h)	Limiting flux (L/m^2h)
0.03	0.1	7.5	11.2	17.7
	0.125	6.9	9.1	16.5
	0.225	5.7	7.8	9.8
	0.425	3.7	4.8	5.8
	0.825	3.1	4.9	5.4
0.1	0.1	62.1	70.5	78.5
	0.125	40.4	57.1	64.5
	0.225	18.4	31.7	34.9
	0.425	14.8	18.2	23.6
	0.825	12.3	14.2	20.2
0.22	0.1	62.7	89.6	142.7
	0.125	57.6	74.8	100.9
	0.225	32.2	49.7	63.2
	0.425	19.2	22.2	24.1
	0.825	10.8	15.3	19.8

In order to meet ASTM standards, the best flux is the maximum flux where glycerol concentration is below 200 ppm (ASTM standard). The results showed that for the (0.03 µm, PES) at 25 and 40°C, and in order to get the best steady-state flux was at 0.1 mass% water at 0.53 MPa and the value for the fluxes were 7.5 and 11.2 L/m^2h with a glycerol concentration of 147.5 and 177.7 ppm respectively. At 60°C, also 0.1 mass% gave the highest flux of 17.7 L/m^2h, with a glycerol concentration to be 197.5 ppm. These values of the glycerol concentrations were not the lowest but still under the limits of the standard. The complete results for all cases showing the fluxes and the

corresponding concentrations obtained for glycerol concentration in the permeate are attached in Appendix B.

The results for the (0.1 and 0.22 μm) at 25°C, showed that 0.1 mass% water at the value of 0.085 MPa, gave the best flux (62.1 and 62.7 L/m^2h) with a glycerol concentration of 185.8 and 183.2 ppm respectively. For the 40 and 60°C, it is hard to indicate the best fluxes due to the very close values or higher than the standards for the glycerol concentration in the permeate.

The best values of flux were obtained at 0.1 wt % water in the FAME. The results indicate that the MF membranes at 25°C had a flux that was 3.5 times that of the UF membrane at 60°C. However, for the operation of a membrane system with a comfort margin the UF membrane operating at 40°C is a better choice.

7.7 Conclusion

Removing dispersed free glycerol droplets from FAME using membrane separation allows one to avoid the typically used water wash procedure for biodiesel purification. Our study of UF and MF membranes was focused on determining the performance of glycerol removal under the effect of temperatures, TMP and different initial water concentrations as well as trying to specify the best steady state fluxes that would give us optimal results for glycerol concentration in the permeate while meeting ASTM standards.

The results of this study showed that the ultra filtration range gave good results for 25 and 40°C for all water levels and TMP ranges used. These best results were correlated to the concentration of water in the permeate. It was found that heading the maximum water solubility (≈ 0.2 % water) and less in the FAME phase, can make the performance of removal for glycerol easy and effective no matter what is the TMP was (range we used). Using high temperature (60°C), showed that as we increase the water solubility in the FAME with temperature the removal of glycerol was worse. The MF membranes succeeded in meeting the standard at 25°C. At 40°C and up to 0.225 mass% water the standards were met while for higher water concentrations the glycerol removal failed to meet the standard. The standards were not achieved for the MF membranes, at 60°C.

The cake filtration theory and gel layer model were in good agreement with the experimental results. They showed a strong relation between the performance of glycerol removal at different temperatures and the values of the specific cake resistance and the concentration of the gel layer. Results showed that filtration cake layer at the membrane surface was not compressible and the values of specific cake resistance decreased with increasing temperature. The results also indicate that the presence of a cake at the surface of the membrane is necessary for the retention of glycerol by the membrane. The overall best result was obtained for the MF membranes at 25°C with the addition of 0.1 wt % water. The MF membranes at 25 C had a flux that was 3.5 times that of the UF membrane at 60°C. However, for a stable operation at 178 ppm glycerol, a UF membrane operating at 40°C is a better choice.

The results of the DLS measurements showed that adding more water beyond the solubility limit will not affect the size of droplets that will form. This further supports the separation mechanism proposed in this work, where free glycerol is best separated from FAME by the addition of a small amount of water to induce the formation of a dispersed water phase in the FAME. The presence of a filter cake at the surface of the membrane is necessary for separation. There should however be a sufficient amount of water to remove the free glycerol dissolved in the FAME phase and this amount should not greatly exceed the water solubility limit in the biodiesel. The glycerol water phase partitions as droplets dispersed in the FAME and can be removed easily using UF membranes.

7.8 Acknowledgements

The authors acknowledge the financial support from the Natural Sciences and Engineering Research Council of Canada (NSERC) for financial support.

7.9 References

[1] B. Nas, A. Berktay, Energy potential of biodiesel generated from waste cooking oil: an environmental approach, Energy Sources. Part B, 2 (2007) 63–71.

[2] J.M. Marchetti, V.U. Miguel, A.F. Errazu, Possible methods for biodiesel production, Renewable and Sustainable Energy Reviews.11 (2007) 1300–1311.

[3] P.A. Sorichetti, S.D. Romano, Physico-chemical and electrical properties for the

production and characterization of Biodiesel, Physics and Chemistry of Liquids. 43 (2005), 37–48.

[4] F. Ma, M. A. Hanna, Biodiesel production: a review, Bioresource Technology. 70 (1999) 1–15.

[5] H. Fukuda, A. Kondo, H. Noda, Review: Biodiesel Fuel Production by Transesterification of Oils, Journal of Bioscience and Bioengineering. 92 (2001) 405-416.

[6] P. Cao, M.A. Dube, A.Y. Tremblay, Methanol recycling in the production of biodiesel in a membrane reactor, Fuel.87 (2008) 825–833.

[7] A. Demirbas, Biodiesel fuels from vegetable oils via catalytic and non-catalytic supercritical alcohol transesterifications and other methods: a survey, Energy Conversion and Management. 44 (2003) 2093-2109.

[8] B. Freedman, R.O. Butterfield, E.H. Pryde, Transesterification kinetics of soybean oil, J. Am. Oil Chem. Soc. 63, (1986) 1375 – 1380.

[9] A.W. Schwab, M. O. Bagby, B. Freedman, Preparation and properties of diesel fuels from vegetable oils, Fuel. 66 (1987) 1372-1378.

[10] A. Demirbas, S. Karslioglu, Biodiesel Production Facilities from Vegetable Oils and Animal fats, Energy Sources. 29 (2007) 133–141.

[11] V. Mao, S.K. Konar, D.G.B. Boocock, The pseudo-single-phase, base-catalyzed transmethylation of soybean oil, J. Am. Oil Chem. Soc. 81 (2004) 803-808.

[12] S.O.V. Ghadge, H. Raheman, Biodiesel production from mahua (Madhuca indica) oil having high free fatty acids, Biomass Bioenergy. 28 (2005) 601–605.

[13] F. Karaosmanoglu, K. B. Cigizoglu, M. Tuter, S. Ertekin, Investigation of the refining step of biodiesel production, Energy & Fuels 10 (1996) 890-895.

[14] A. Demirbaş, Biodiesel fuels from vegetable oils via catalytic and non-catalytic supercritical alcohol transesterifications and other methods: a survey, Energy Conversion and Management 44 (2003) 2093–2109.

[15] M.A. Dubé, A.Y. Tremblay, J. Liu, Biodiesel production using a membrane reactor, Biores. Tech. 93 (2007) 639–47.

[16] P. Cao, A.Y. Tremblay, M.A. Dubé, K. Morse, Effect of membrane pore size on the performance of a membrane reactor for biodiesel production, Ind. Eng. Chem. Res. 46

(2007) 52–58.

[17] B. Nicolaisen, Developments in membrane technology for water treatment, Desalination. 153 (2002) 355–360.

[18] M. Jeffrey, C. Yanwei, H.D. Robert, Cross-flow microfiltration of oily water, J Membr Sci. 129 (1997) 221-235.

[19] K.S. Ashaghi, M. Ebrahimi, P. Czermak, Ceramic ultra- and nanofiltration membranes for oil field produced water treatment: a mini review, The Open Environmental Journal. 1 (2007) 1-8.

[20] R.W. Field, D. Wu, J.A. Howell, B.B. Gupta, Critical flux concept for microfiltration fouling, Journal of Membrane Science. 100 (1995) 259-272.

[21] O.M. Thomas, P. Jaouen, L. Patrick, Modeling of fouling in three ultrafiltration cell configurations: swirl, plane and axial annular, Chem. Eng. Technol. 24 (2001) 11.

[22] J.H. Kerry, M.C. Mark, Fouling of microfiltration and ultrafiltration membranes by natural waters, Environ. Sci. Technol. 36 (2002) 3571-3576.

[23] H.L. Chen, Y.S. Chen, R.S. Juang, Flux decline and membrane cleaning in cross-flow ultrafiltration of treated fermentation broths for surfactin recovery, Separation and Purification Technology. 62 (2008) 47–55.

[24] P. Bacchin, A possible link between critical and limiting flux for colloidal systems: consideration of critical deposit formation along a membrane, Journal of Membrane Science. 228 (2004) 237–241.

[25] P. Bacchin, P. Aimar, R.W. Field, Review, Critical and sustainable fluxes: Theory, experiments and applications, Journal of Membrane Science. 281 (2006) 42–69.

[26] J. Saleh, A.Y. Tremblay, M.A. Dubé, Glycerol removal from biodiesel using membrane separation technology, Fuel. 89 (2010) 2260–2266.

[27] A.Y. Tremblay, J. Saleh, M.A. Dubé, The removal of glycerol and methanol from crude FAME using ultrafiltration, to be submitted to Industrial and Engineering Chemistry Research (IECR).

[28] J. Saleh, M.A. Dubé, A.Y. Tremblay, Separation of glycerol from FAME using a ceramic membrane; submitted to Fuel Processing Technology.

[29] J. Van Gerpen, B. Shanks, R. Pruszko, Biodiesel Analytical Methods, August 2002–January 2004, July 2004 NREL/SR-510-36240.

[30] M. C. Porter, Handbook of Industrial Membrane Technology, Noyes publications, NJ, 1990.

[31] P. Shah, C. Wee, J.M. White, S. Sanford, G. Meier, Experimental determination and thermodynamic modeling of water content in biodiesel-diesel blends" Renewable Energy Group, Inc., www.regfuel.com. (2010).

[32] J. Van Gerpen, E.G. Hammond, L.A. Johnson, S.J. Marley, L. Yu, l. Lee, A. Monyem, Determining the Influence of Contaminants on Biodiesel Properties, Final report prepared for: The Iowa Soybean Promotion Board, Iowa State University, July 31, 1996.

[33] B.V. Ramarao, C. Tien, Approximate analysis of fine-particle retention in the cake filtration of suspensions, Ind. Eng. Chem. Res. 44, (2005) 1424-1432.

[34] C. Tien, R. Bai, An assessment of the conventional cake filtration theory, Chemical Engineering Science. 58 (2003) 1323 – 1336.

[35] Y.G. Park, H.S. Byun, Application of the cake-filtration theory to analyze the permeate performance in poly(vinylbenzyl chloride)-filled microfiltration membrane, J. Ind. Eng. Chem. 8, (2002), 537-545.

[36] B.L. Sorensen, P.B. Sorensen, Applying cake filtration theory on membrane filtration data, Wat. Res. 31, (1997), 665-670.

[37] O.M. Thomas, P. Jaouen, P. Legentilhomme, Modeling of fouling in three ultrafiltration cell configurations: swirl, plane and axial annular, Chem. Eng. Technol. 24 (2001) 11.

Chapter 8 General Discussion, Conclusions and Recommendation

Due to the recent rise in fossil-based petroleum prices, concerns about the depletion and availability of these resources as well as the environmental problems related to global warming researchers have focussed on alternative, renewable energy sources (Sheehan et al., 1998). Biodiesel is such an alternative. It is produced widely via the alkaline-catalyzed transesterification of vegetable oils or animal fats with an alcohol such as methanol in the presence of a catalyst such as sodium methoxide. This conversion method is fast, gives good yield and uses moderate reaction conditions. Biodiesel is non–toxic, biodegradable and renewable with lower emissions of carbon monoxide, unburned hydrocarbons, and particulate matter, and can safely be used in diesel engines without modification to the engine.

The transesterification reaction product is composed of two layers. At typical reaction conditions, the lower layer is a glycerol-methanol rich phase while the upper layer contains the fatty acid methyl ester (FAME or biodiesel) (Haas et al., 2006). The FAME-rich layer may also contain impurities such as glycerol (referred to as "free" glycerol), un-reacted methanol, residual catalyst, bound glycerol (i.e., un-reacted triglyceride (TG), diglyceride (DG) and monoglyceride (MG), and small amounts of soap and water. It is necessary to remove these impurities because they will strongly affect engine performance.

The purity of biodiesel is an important issue for its safe, long-term use in engines. Biodiesel quality is regulated by standards such as ASTM D6751 and EN 14214. Achieving these standards plays a large role in the cost and widespread acceptance of biodiesel as a fuel. In order to produce high quality biodiesel, a series of purification processes are usually needed. These can include: gravitational settling, centrifugation, water washing, adsorption and distillation (Karaosmanoglu et al., 1996).

As a downstream purification step, adding water to the FAME phase allows the soap, the alkaline catalyst residue and small amounts of glycerol, DG and MG in the product mixture to be removed. Unfortunately, the separation of the ester phase from the water phase is usually difficult, and this step results in a large amount of waste water containing methanol. After the washing step, the wash water containing the extracted methanol and the residual catalyst is treated to recover the methanol. If this wastewater is discharged without further treatment, a significant amount of product and reactants may

be lost and serious environmental damage may ensue. This waste water treatment is usually done at great capital and operating costs that also impact the environmental benefits of using biodiesel.

The presence of high amounts of free glycerol were of concern in this thesis. This free glycerol can separate during storage and form gum-like deposits around injector tips and valve heads, therefore causing problems in the fuel system. These challenges call for new purification technology to achieve the ASTM and EN standards where the limit of free glycerol is a maximum of 0.02 mass%. There is great potential that membrane technology can provide this purification solution by recovering the valuable by product glycerol as well as reducing the amount of water usage and thus reducing the environmental impact of the purification process.

8.1 General Discussion

The main objective of this project was to use the membrane process technology for the separation of free glycerol dispersed in the FAME phase (untreated biodiesel) after completion of the transesterification reaction to avoid the conventional water wash step. It was important to know the physical relationship between the normally present impurities and the FAME phase. The effect of different impurities on the free glycerol content will play a significant role in using membranes to remove the free glycerol from the FAME phase.

The principle of membrane separation of glycerol from FAME is based on introducing the continuous phase which is non-polar (hydrophobic, in this case, and FAME-rich) and the dispersed phase is polar (hydrophilic, in this case, and methanol/glycerol-rich) to a membrane separation module using a feed and bleed setup with continuous circulation. Methanol and glycerol have great affinity to each other and, at the same time, methanol is miscible with FAME. As a result, if glycerol is present above its solubility limit, it will dephase and form droplets in the continuous FAME phase. In addition to the presence of methanol and glycerol, there are often traces of soap, DG and MG in the FAME phase. These materials can act as surfactants (one polar end and one non-polar end), where the polar ends will prefer to associate with the polar

glycerol/MeOH dispersed phase and the non-polar ends will stay in the non-polar FAME phase.

In Chapter 3 we studied the effect of membrane separation technology to remove free glycerol from biodiesel in order to meet the ASTM D6751 and EN 14214 standards. FAME produced from canola oil and methanol was purified using ultrafiltration. The effect of different materials present in the transesterification reaction, such as water, soap, and methanol, on the final free glycerol separation was studied. Eight sample mixtures of varying composition were prepared using the "raw" FAME (untreated FAME), and varying amounts of methanol, water and soap. Table 8.1 shows the composition of the prepared FAME mixtures from different batches of FAME used.

Table 8.1: Mixtures prepared for testing in the membrane system.

Mixtures #	**Type of mixtures (Water, methanol and soap in mass%)**
1	FAME only
2	FAME + 0.06% water
3	FAME + 0.1% water
4	FAME + 0.2% water
5	FAME + 1% soap
6	FAME + 1% methanol
7	FAME + 1% methanol + 1% soap + 0.06% water
8	FAME + 1% soap + 0.06% water

A modified polyacrylonitrile (PAN) membrane, with 100 kD molecular weight cut off was used in all runs. Results showed low concentrations of water had a considerable effect in removing glycerol from the FAME even at ~0.08 mass%. It was suggested that the mechanism of separation of free glycerol from FAME was due to the removal of an ultrafine dispersed glycerol-rich phase present in the untreated FAME. In order to verify if the formation of a dispersed phase was responsible for this separation, the droplet size in FAME was determined at various water additions by dynamic light scattering (DLS). The size of the droplets and the free glycerol separation both increased

with increasing water content of the FAME. The trends of separation and droplet size vs. water content in the FAME phase were very similar and exhibited a sudden increase at 0.08 mass% water in the untreated FAME as shown in Figure 8.1, indicating that droplet size enlargement played a considerable role in the separation mechanism.

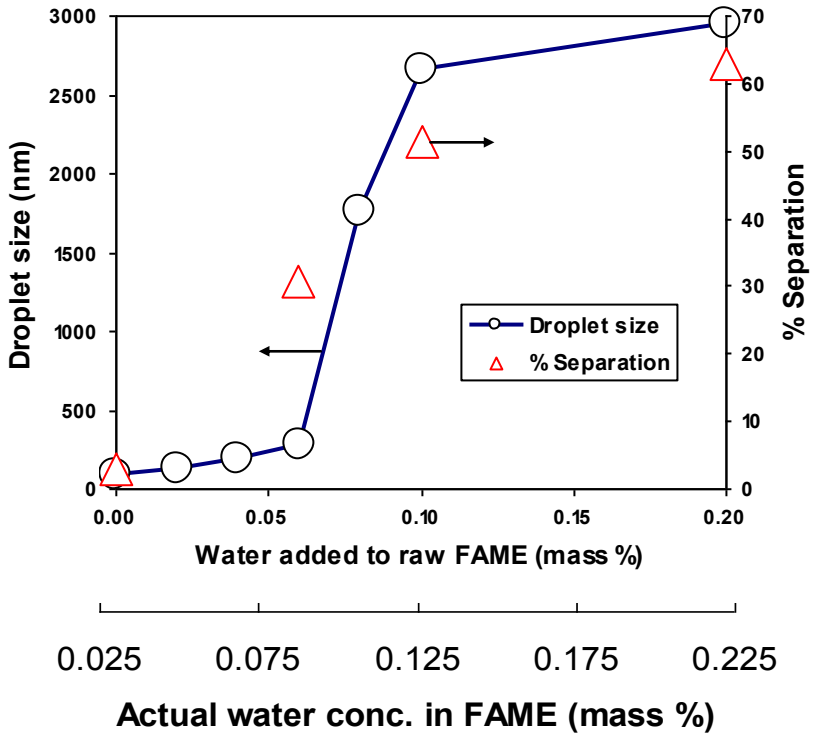

Figure 8.1: Plot of the droplet size and separation versus water added and water content of FAME.

The presence of methanol alone before introducing the crude FAME to the membrane separation system did not lead to the formation of a separate glycerol-methanol phase and glycerol separation by the membrane.

In the next step of this project, as described in Chapter 4, we proceeded in testing three types of polymeric membranes in the ultrafiltration range (5 kD (PES), 30 kD (PVDF), 100 kD Ultrafilic™ membrane) at three operating temperatures (0, 5 and 25°C) to remove glycerol from crude FAME originating from a transesterification reaction

without water washing or other post-treatments. We evaluated ultrafiltration as a means of removing free glycerol from the FAME phase and studied the effect of temperature and methanol concentration on membrane separation performance. The process relied on the formation of a dynamic polar layer on the surface of the membrane. The concentration of free glycerol in this layer was determined to be ~5.6 mass%. We hypothesized that this layer captured the small, polar, glycerol-rich droplets in the feed. Once the layer was formed, the concentration of free glycerol in the permeate reached ASTM and EN standards. The standards were met at a concentration factor (CF) of 1.4 for 5 kD PES and 30 kD PVDF and 2.25 for the 100 kD Ultrafilic membrane. Complete phase reversal in the cake present at the membrane surface did not occur. This was due to the aggregation of polar droplets and the substantial increase in shear diffusion of these larger droplets moving them away form the cake. This removed the possibility of phase inversion where only the polar phase would permeate through the membrane.

The advantage of ultrafiltration is that methanol was also retained by the membrane along with glycerol. The separation of methanol ranged from 79 to 85%. Using the smallest pore size (5 kD PES) membrane, the concentration of methanol in the permeate was reduced to ~0.5 mass% down from an initial feed containing 2.4 mass% methanol. This was close to the value of 0.2 mass% methanol specified in ASTM D6751-09 (EN 14110).

The three polymeric membranes showed a high degree of retention for free glycerol from the crude FAME at the end of the runs (3 h) at 25°C where the composition of glycerol in the permeate showed a decline in concentration with increasing CF as shown in Figure 8.2. The separation of free glycerol increased with CF as shown in Figure 8.3, which implies that the membrane was more selective as the batch of FAME was concentrated.

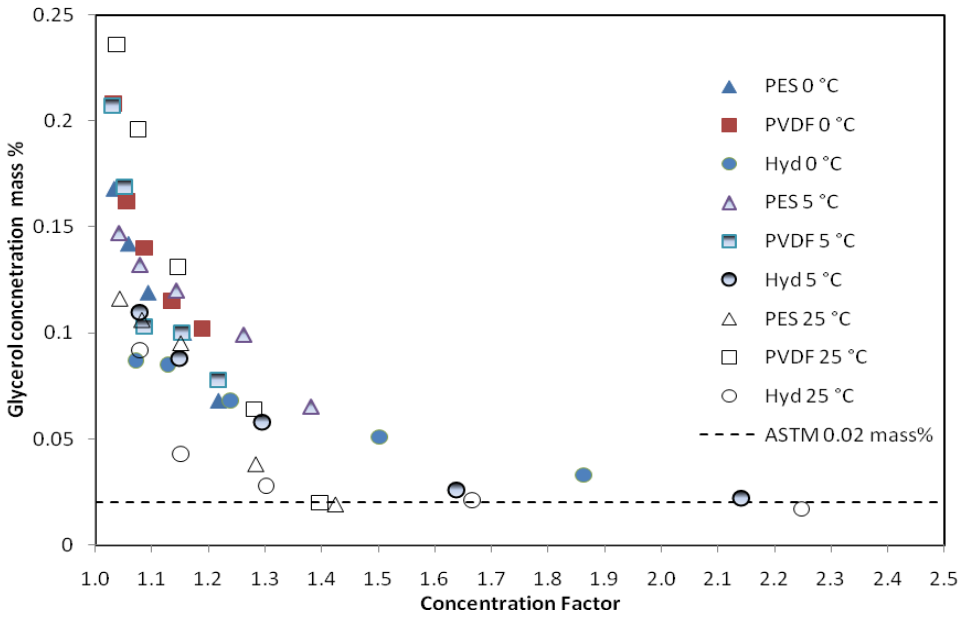

Figure 8.2: Free glycerol concentration vs. concentration factor (CF) for all membrane runs.

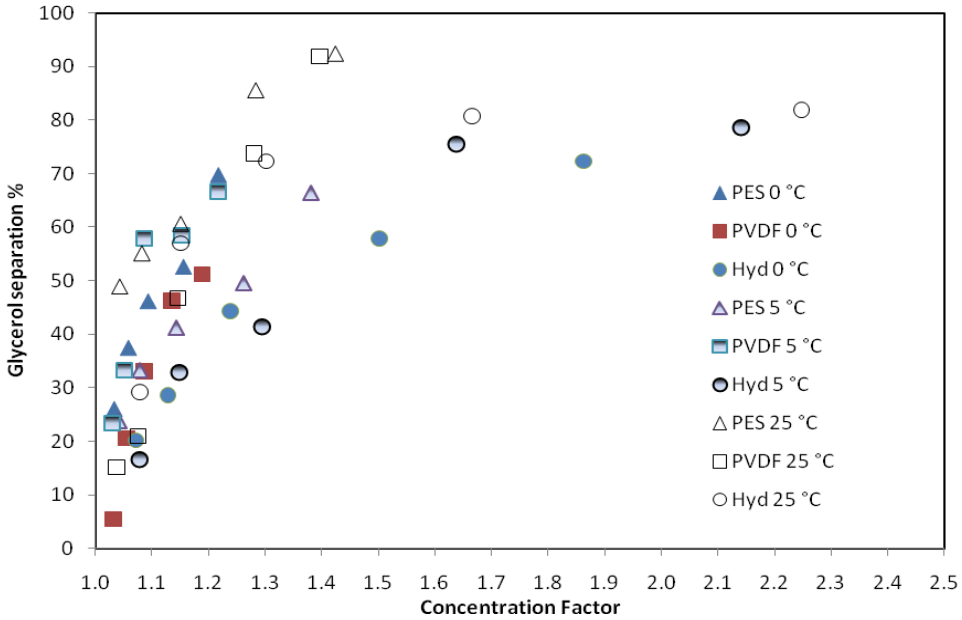

Figure 8.3: Free glycerol separation vs. concentration factor (CF) for all membrane runs.

In Chapter 5, our focus was on the use of ceramic membranes to remove free glycerol from a post-transesterification FAME stream. The effect of different membrane pore size, as well as the effect of temperature on the glycerol content from the membrane

purification effluent was tested at certain fixed pressures. The results of using ceramic membranes in the ultrafiltration (0.05 μm) and microfiltration (0.2 μm) ranges were reported at three different operating temperatures: 0, 5 and 25°C. All runs separated glycerol from the crude FAME and the international standards for glycerol content in biodiesel were met when utilizing the ultrafiltration membrane setup at 25°C after a concentration factor greater than 1.6. The effect of temperature on glycerol removal was evident from its relation with CF. Higher temperatures appeared to promote reaching the appropriate CF value sooner for faster separation of glycerol from the FAME-rich phase. Membrane pore size was also found to affect separation performance. The smaller pore size of the UF membrane facilitated glycerol removal compared to the MF membrane as shown in Figure 8.4.

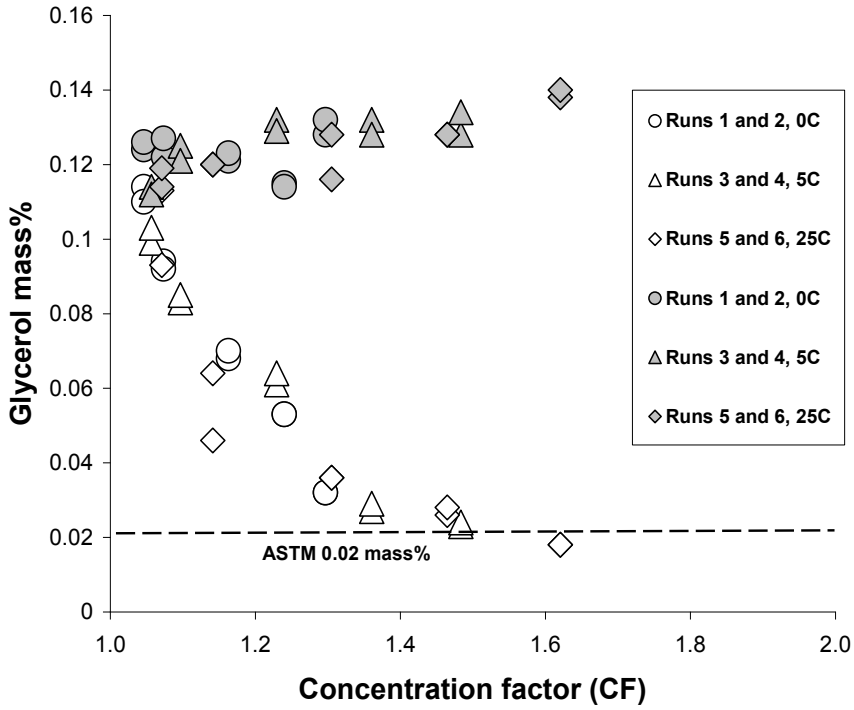

Figure 8.4: Glycerol content in permeate and retentate vs. concentration factor at different temperatures for the ultrafiltration (0.05 μm) runs. (open symbols = permeate; closed symbols = retentate)

In the subsequent study reported in Chapter 6, DLS was used to study the effect of water, methanol, soap and glycerol on droplet size for these materials dispersed in FAME. A total of 42 different sample compositions were prepared; 27 of these included methanol, and 15 did not. A regression model was constructed using a 3-level Box-Behnken experimental design technique. The addition of water and/or glycerol served to decompatibilize the glycerol from the FAME and thus caused the droplet sizes to increase. At the same time, the addition of methanol tended to act in the opposite manner by enhancing the solubility of glycerol in FAME and reducing the droplet size. The addition of soap caused a reduction in droplet size by stabilizing more droplets.

Six different mixture compositions (see Table 8.2) were tested in the membrane separation apparatus in order to validate the DLS results regarding the impact of water, methanol and soap on droplet size. A clear indication of the dominant effect of water on improving the separation of glycerol from FAME was shown. The negative impact of methanol, and to a lesser extent, of soap, was also shown. In order to achieve ASTM standards for biodiesel, it is therefore recommended to minimize the amount of methanol and soap prior to any attempts to remove glycerol from raw FAME. In any case, a small amount of water (~0.1 wt %) will permit the fuel quality standard to be achieved using membrane separation technology. The mass% glycerol in the permeate for each of the five experiments is shown in Figure 8.5.

Table 8.2: Composition of prepared mixtures for the membrane treatment.

Mixtures #	**Type of mixtures (Water, methanol and soap in mass%)**
(1)	Raw FAME only
(2)	Raw FAME + 1% methanol
(3)	Raw FAME + 1% soap
(4)	Raw FAME + 1% methanol + 1% soap + 0.06% water
(5)	Raw FAME + 0.1% water
(6)	Raw FAME + 0.2% water

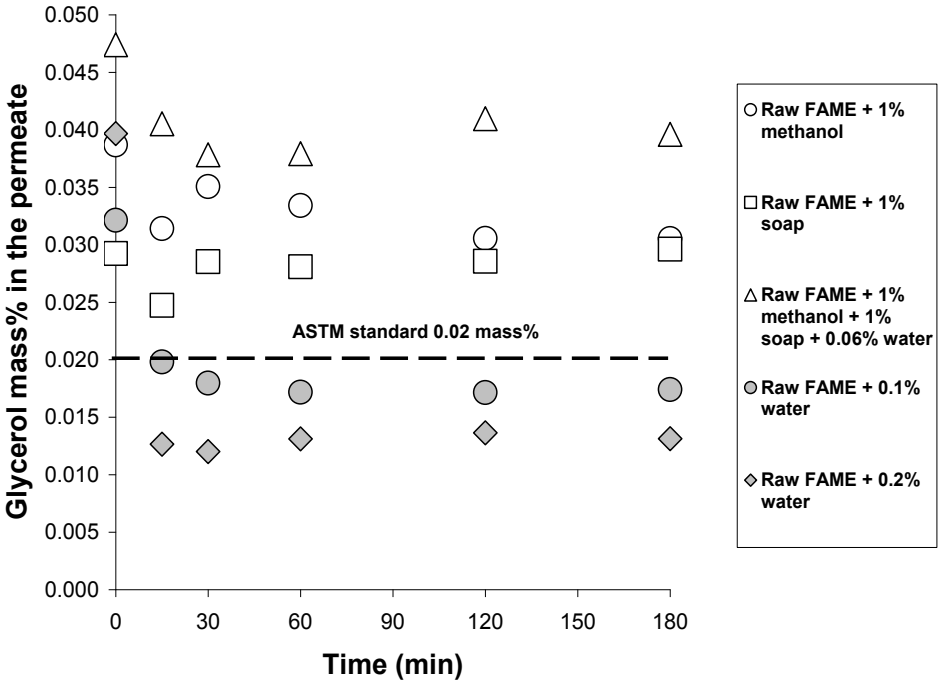

Figure 8.5: Glycerol mass% in permeate vs. time for (FAME + 1% methanol, FAME + 1% soap, FAME + 1% methanol + 1% soap + 0.06%, FAME + 0.1% water, and FAME + 0.2% water).

In Chapter 7, the effect of trans-membrane pressure (TMP) when different concentrations of water are added to the FAME phase on glycerol removal using ultrafiltration (UF 0.03 μm, polyethersulfone (PES)) and microfiltration (MF 0.1 and 0.22 μm, PES) at 25, 40 and 60°C was studied. Results showed that running at 25°C for the two ranges of membranes produced the best results for glycerol removal and exceeded the ASTM and EN standards as shown in Figures 8.6 to 8.8. An increase in temperature resulted in an increase in the solubility of water in the FAME and less effective glycerol removal.

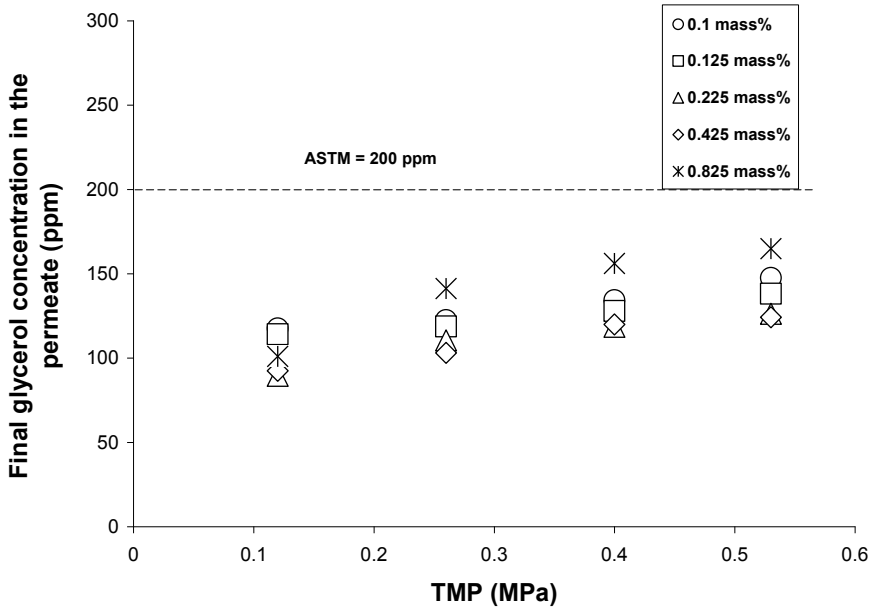

Figure 8.6: Effects of initial water concentration and trans-membrane pressure (TMP) on final glycerol concentration in the permeate for (0.03 µm, PES) at 25°C. The concentration of glycerol in the feed was 1000 ppm

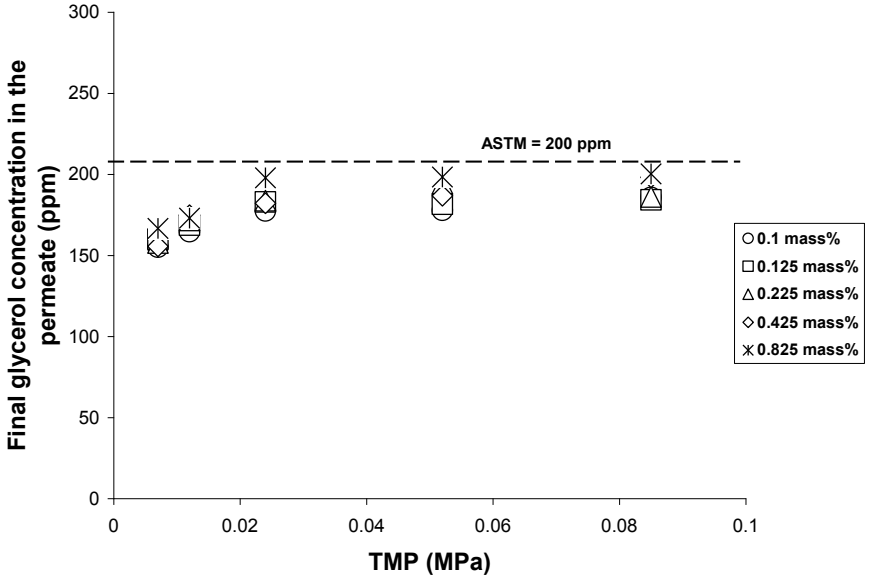

Figure 8.7: Effects of initial water concentration and trans-membrane pressure (TMP) on final glycerol concentration in the permeate for (0.1 µm, PES) at 25°C. The concentration of glycerol in the feed was 1000 ppm

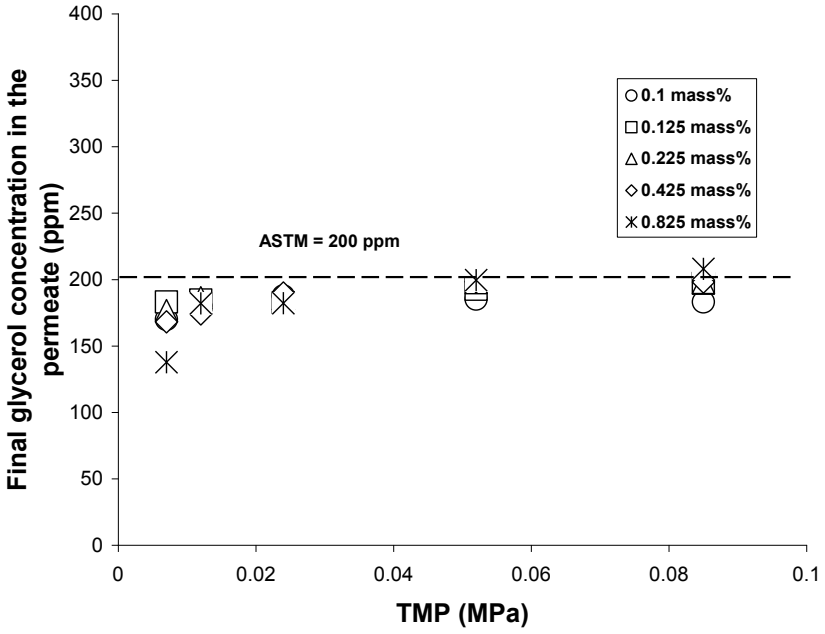

Figure 8.8: Effects of initial water concentration and trans-membrane pressure (TMP) on final glycerol concentration in the permeate for (0.22 μm, PES) at 25°C. The concentration of glycerol in the feed was 1000 ppm

The cake filtration theory and gel layer model were in good agreement with the experimental results. They showed a strong relation between the performance of glycerol removal at different temperatures and the values of the specific cake resistance and the concentration of the gel layer. Results showed that filtration cake layer at the membrane surface was not compressible and the values of specific cake resistance decreased with increasing temperature as shown in Figure 8.9. The results also indicate that the presence of a cake at the surface of the membrane is necessary for the retention of glycerol by the membrane. For a stable operation at 178 ppm glycerol, a UF membrane operating at 40^{o}C is found to be a better choice.

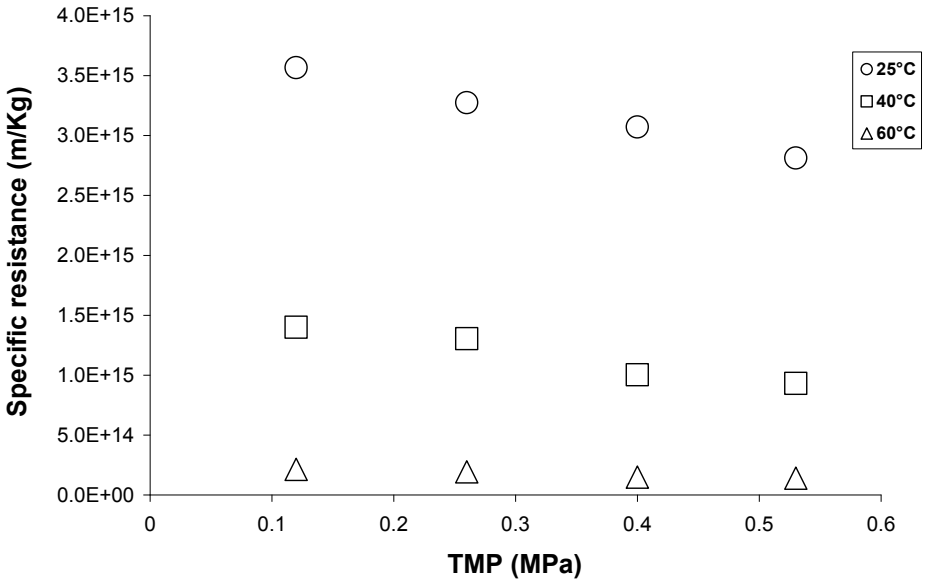

Figure 8.9: Specific resistance vs TMP for (0.03 μm, PES) for 0.1 mass% water at different temperature

8.2 Conclusion

The main objective of this thesis was to find a new purification method for the removal of dispersed glycerol from FAME while avoiding conventional purification methods such as water washing, ion exchange, and the use of sorbents. To achieve this target a membrane process was developed for the separation of free glycerol dispersed in FAME after completion of the transesterification reaction using vegetable oil (refined canola oil). In this work we investigated the effect of different factors on glycerol removal. These factors included membrane pore size, pressure, temperature, and methanol, soap and water content. The dispersed glycerol can be successfully removed from raw FAME (untreated FAME) using a membrane separation system to meet the ASTM biodiesel fuel standards.

Many experiments and statistical models were applied and performed to achieve the thesis goal. Different operating conditions and membrane pore sizes (MF vs. UF) ranges were used. Results showed that the size of the droplets of the free glycerol is

important in its removal. Factors present in the untreated FAME such as water, methanol and soap content, were found to have an impact on the performance of glycerol removal either by increasing or decreasing the size of the glycerol droplets. All runs performed resulted in the removal of the glycerol but not all of the runs resulted in the the standard being met. Adding small amounts of water up to its solubility limit in FAME improved the separation dramatically while methanol served to reduce the glycerol droplet size due to the solubility between glycerol and methanol and between methanol and FAME. However, experiments showed that ASTM standards can be met after three hours of running with the presence of small amounts of methanol when using UF membranes. Results also showed that separation becomes more effective when a gel layer exists on the membrane surface.

The range of temperatures used in this work showed that 25^{o}C gave the best results. Running higher than 25^{o}C will increase the solubility of water in FAME and glycerol removal becomes less effective, while running at temperatures lower than 25^{o}C will increase the time needed for glycerol removal to meet the standard.

The following is a summary of conclusions for this work:

1) International standards (European and North American) were met for free glycerol content using no water wash, sorbents or ion exchange resins.
2) Ultrafiltration was successful for glycerol removal in the presence of MeOH. However, it is better to reduce the amount of MeOH prior to glycerol removal.
3) The best glycerol-FAME separation was obtained at 25^{o}C with a very small amount of water added up to the solubility limit of water in FAME.
4) We demonstrated that a hydrophilic layer (gel layer) on the membrane surface played an important role in the separation. Best results are obtained when a gel layer is present.
5) Concentration of glycerol in the gel layer decreases as temperature increases. This is consistent with the concept that increasing temperature increases water solubility in FAME and compatibilizes glycerol in the FAME leading to a reduction in glycerol separation.

Table 8.3 shows the better results obtained for glycerol removal from FAME using different pore sizes at different concentrations of water, methanol and soap. These results were all obtained at 25 °C. The best results were for the microfiltration membranes and the PAN 100 kD UF membrane.

Tab le 8.3 Summary of the better results obtained during the study. All experiments were performed at 25 °C.

Membrane type	**TMP (MPa)**	**Water mass% (beginning of run)**	**Methanol mass% (beginning of run)**	**Soap mass% (beginning of run)**	**Glycerol mass% (end of run)**	**Best flux obtained (L/m2h)**
PES (5 kD)	0.53	Not measured	2.4	Not measured	0.018	13.3
PVDF (30 kD)	0.32	Not measured	4.1	Not measured	0.019	8.7
PAN (100 kD)	0.15	Not measured	5.2	Not measured	0.018	27.9
PAN (100 kD)	0.53	0.225	0.0	0.04	0.013	12.6
PES (0.03 μm)	0.53	0.125	0.0	0.0	0.0138	6.9
PES (0.03 μm)	0.53	0.225	0.0	0.0	0.0126	5.7
PES (0.1 μm)	0.085	0.1	0.0	0.0	0.0185	62.1
PES (0.1 μm)	0.085	0.225	0.0	0.0	0.0194	18.4
PES (0.22 μm)	0.085	0.1	0.0	0.0	0.0183	62.7
PES (0.22 μm)	0.085	0.225	0.0	0.0	0.0197	32.2

8.3 Economic feasibility of using membrane technology in biodiesel purification

In this thesis, the technical feasibility of using membrane separation technology to remove dispersed glycerol from FAME to meet ASTM and EN standards has been shown. A direct consequence of using membrane technology is that one can avoid the

use of large amounts of water for biodiesel purification thereby eliminating either the discharge or treatment of harmful wastes to the environment.

Of major concern to the biodiesel industry is the production cost. The primary component of biodiesel cost is the feedstock cost (Zhang et al. 2003). Many researchers have developed biodiesel process models to evaluate the economic feasibility of biodiesel production and estimating its cost (Bender, 1999; Tapasvi et al., 2004; Haas et al., 2006). While an in-depth economic study was not performed in this thesis, the estimated economic impact of replacing conventional water-based purification with membrane technology can be discussed.

From a capital cost perspective, the cost of implementation of membrane technology in lieu of water washing and subsequent waste water treatment is likely to be significantly higher. However, on the basis of operating costs, the membrane treatment is likely to be far less expensive (Singh and Cheryan, 1998). Thus, overall, the membrane separation process can be cost effective. This cost estimate also would be influenced by the optimization of the membrane process (Owen et al., 1995).

Aside from the process economics, the environmental cost must be factored into the discussion. All too frequently, the environmental cost of water usage and potential discharge of harmful waste waters is not considered in economic analyses. Such an analysis is beyond the scope of this thesis but the benefits of the membrane separation technology are very clear in this case.

8.4 Recommendations

Based on the results of this thesis, the following recommendations for ongoing research are proposed:

As briefly discussed above, the implementation of this technology in industry would require a detailed economic assessment. While a certain degree of optimization has been completed here, further optimization would be necessary incorporating economic factors. In addition, attempts to evaluate and predict the life time of the membranes should be undertaken. The impact of process conditions (e.g., temperature) on the membrane life time should also be considered.

As mentioned in Chapter 2 (Theoretical Background), due to the high cost of biodiesel feedstock, the use of low-grade feedstocks high in FFA is often done. This entails the use of higher catalyst levels and results in the production of significant amounts of soap. The use of different feedstocks with different FFA and/or alkali catalyst levels should be performed to evaluate the ability of the membranes in the face of these low-grade feedstocks and their resultant significant soap concentrations.

One concern in membrane separation is fouling of the membrane surface. Using different cross flow velocities in the feed and bleed setup should be studied in order to estimate the best conditions to meet the ASTM and EN standards to achieve high flux with minimum fouling and extend the life time for the membranes.

In this thesis, a limited number of membrane types were evaluated for the biodiesel purification process. The investigation of other membranes is recommended. This would include other membrane materials and possibly other membrane formats (e.g., hollow-fibre). A major consideration in this type of study aside from flux and fouling would be the resistance of the membrane to the organic materials it would be exposed to (i.e., methanol and FAME).

Our preliminary results showed that the type of mixtures used and the operating conditions applied to the purification method had a negligible effect on the removal of other important impurities such as MG, DG and TG. These results were not included in this thesis due to our focus on dispersed glycerol. A study on the removal of those other materials may be of interest.

8.5 References

[1] Bender, M., Economic feasibility review for community-scale farmer cooperatives for biodiesel, *Biores. Tech*., 70: 81-87, **1999**.

[2] Haas, M.J., McAloon, A.J., Yee, W.C., Foglia, T.A., A process model to estimate biodiesel production costs, *Biores. Tech*., 97: 671–678, **2006.**

[3] Karaosmanoglu, F., Cigizoglu, K.B., Tuter, M., Ertekin, S., Investigation of the refining step of biodiesel production, Energy Fuels., 10: 890-895, **1996.**

[4] Owen, G., Bandi, M., Howell, J.A., Churchouse, S.J., Economic assessment of membrane Processes for water and waste water treatment, J. Membrane. Sci., 102: 77-91,

1995

[5] Sheehan, J., Camobreco, V., Duffield, J., Graboski, M., Shapouri, H., Life cycle inventory of biodiesel and petroleum diesel for use in an urban bus: Final Report NREL/SR-580- 24089 UC Category, May **1998**.

[6] Singh, N., Cheryan, M., Process design and economic analysis of a ceramic membrane system for microfiltration of corn starch hydrolysate, *J. Food. Eng*., 38: 57-67, **1998.**

[7] Tapasvi, D., Wiesenborn, D., Gustafson, C., Process modeling approach for evaluating the economic feasibility of biodiesel production, written for presentation at the 2004 North Central ASAE/CSAE Conference Sponsored by the Manitoba Section of CSAE Winnipeg, Manitoba, Canada September 24-25, **2004**

[8] Zhang, Y., Dubé, M.A., McLean, D.D., Kates, M. Biodiesel production from waste cooking oil: 2. Economic assessment, *Bioresour. Technol.,* 90: 229-240, **2003**.

Appendix

Appendix A: Gas chromatography (GC) operation guide (ASTM D6584 – Cold on column injector)

Sample Preparation

(*all steps written below are done under nitrogen in the glove compartment)*

1. Weigh 100 mg of sample into a 10 ml septa vial.
2. Add 100 µl of each Butanetriol (internal standard 1), Tricaprin (internal standard 2), and MSTFA into the sample vial. Both internal standards are located in the refrigerator in room D403 - *Make sure you put the standard solutions back in the refrigerator after you're done*.
3. Shake the vial and let it set for 20 minutes at room temperature.
4. Add 8 ml of high grade n-heptane into the vial and shake for a few seconds.
5. Remove approximately 1 ml of the sample mixture into GC auto sampler vials.
6. Label the 10 ml vial and the auto sampler vial accordingly.

Getting Ready

1. Check that gas filters are still functional. All carrier and detector filters should be changed when indicator shows filter is spent. Oxygen contamination in carrier gas can produce excessive column bleed and hydrocarbons cause ghost peaks or increase detector noise.
2. Open the valves on the helium, air, and hydrogen tanks. Verify that they are set to the appropriate pressures; if not, adjust the set-screw accordingly.
    - Helium, carrier gas, set point is ~80 psi
    - Compressed air, set point is ~60 psi
    - Hydrogen, set point is ~40 psi
3. Always leave at least 400 psi residual gas in a depleted cylinder. As the cylinder pressure drops, the concentration of the impurities such as moisture and hydrocarbons increase which will lead to column damage. In addition, if the cylinder pressure drops below the supply pressure required by the GC, retention times and detector sensitivities can slowly change and affect the validity of data gathered.

Biodiesel6584 Data Handling Method

1. 8410 Autosampler

Syringe size: 10 µl
Injection mode: User defined
Solvent penetration depth: 90%
Sample penetration depth: 90%

Default clean vial: I
Default clean volume: 5 µl
Default clean strokes: 1
Default clean drawup speed: 5 µl/sec

Clean mode pre-inj solvent flushes: 2
Clean mode post-inj solvent flushes: 2
Clean mode pre-inj sample flushes: 2
Clean Mode solvent source: I & III

Use internal standard: no
Internal standard vial: II
Internal standard volume: 1 µl
Internal standard drawup speed: 5 µl/sec
Internal standard pause time: 0 sec
Internal standard air gap: no

Solvent plug vial: III
Solvent plug volume: 0 µl
Solvent plug drawup speed: 5 µl/sec
Solvent plug pause time: 0 sec
Solvent plug air gap: no

Viscosity delay: 6 sec

Plunger fill speed: 2 µl/sec

Plunger inject speed: 5 µl/sec

Pre-injection delay: 0 sec

Post-injection delay: 6 sec

Fill volume: 5 µl

Fill strokes: 0

Sample air gap: yes

Air plug after sample: 1 µl

Use prepahead: no

Delay time: 0 min

2. Injector

- Front injector type 1079

  Oven power: on

  Coolant: on

  Enable coolant at: 300 ^{o}C

  Coolant timeout: 20 min

Temp (C)	Rate (C/min)	Hold (min)	Total (min)
50	0	0.10	0.10
370	150	32.50	34.73

Time (min)	Split state	Split ratio
initial	off	off

- Middle injector type 1177 (not in use)

  Oven power: on

  Temperature: 100 ^{o}C

- Rear injector type 1041 (not in use)

  Oven power: on

  Temperature: 100 ^{o}C

3. Flow/Pressure
   - Front injector EFC type 1

     Constant column flow: 3 ml/min

     Pressure pulse: none
   - Middle EFC type 1 (not in use)
   - Rear EFC type 3 (not in use)

4. Column oven

   Coolant: off

   Enable coolant at: 50 ^{o}C

   Coolant timeout: 20 min

   Stabilization time: 0 min

Temp (C)	Rate (C/min)	Hold (min)	Total (min)
50	0	1	1
180	15	0	9.67
230	7	0	16.81
370	10	4.19	35

5. Detector
   - Front FID Detector

     Oven power: on

     Temperature: 380 ^{o}C

     Electronics: On

     Time constant: fast

Time (min)	Range	Autozero
initial	12	yes

Front type 11 Detector EFC

Make up flow: 28 ml/min

H_2 flow: 30 ml/min

Air flow: 300 ml/min

6. Output

   Time: initial

   Port A signal source: front

   Attenuation: 1

7. Data acquisition

   Detector bunch rate: 4 points

   Noise monitor length: 64

   FID/TCD detector full scale for front, middle, and rear: 1 V

GC Instructions

1. Turn on GC (external switch).
2. As the GC begin its initializing step, click the *ComputerLike* button located on the top left hand corner on Varian workstation toolbar to achieve a communication between the software and the GC instrument.
3. "System Control - Configuration" window appears. Working from the Workstation Star software to change method and parameters is preferable than from CP-3800 GC keyboard.
4. Select File → Activate Method. The "Activate a System Control Method File" window opens and select Biodiesel-ASTM6584 folder → Biodiesel6584, press Open. The method name that is activated will now shown in the System Control window's toolbar.

5. Always check the column, injector and detector status; and confirm that the GC is in the Ready state for sample injection. The amber "Ready" light should be illuminated and green circles should be shown for all the parameters set in the system control window. The red "Not Ready" light will be illuminated and red circles will appear if one or more of the set conditions are not reached.
6. You can inject a single sample or multiple samples from System Control.
    a) Select Inject → Inject Single Sample or by clicking on the *Inject Single Sample* button in the toolbar.
    b) Select File → New SampleList or by clicking on the *New or Open Automation File* button on the tool bar.
7. Both functions on step 6 will open up a sample dialog box.
    - Sample name
    - Sample type → set as Analysis
    - Number of Injection needed
    - Injection notes
    - Auto Link → leave as none
    - Vial position number
    - Injection Volume → set as 0.5 µl
    - Injectors Used → set as position 1
    - Click the scroll bar to scroll past the list of values for the Amount Standard, Unid Peak Factor, Multiplier, and Divisor. Leave them set to their default values.
8. After filling all the parameters mentioned in step 7, below the row of the last sample Select Sample Type → Activate Method and click on *None* button under Auto Link column. The "Activate Method" window opens and select Biodiesel-ASTM6584 folder → Stdby, press Open.
9. Click the *Inject* button to start the run.

Remarks

- All samples' chromatogram are saved in the "Data" folder automatically and it's preferred that the chromatograms are copied into a disk to be analyzed.
- GC can be left in Stdby mode for 2 weeks in between sample analysis. If it is predicted that it will not be used for long time i.e. a month or longer then it can be turn off to preserve the gas carrier. The shut down procedure is turning off GC, closing the air and hydrogen tank valves, and finally the carrier gas, both the regulator valve and the top tank valve.

Operating conditions for GC (from ASTM D6584-00)

Injector		
Cool on column injection		
Sample size	1 μL	
Column Temperature Program		
Initial temperature	50 °C	hold 1 min
Rate 1	15 C/min to 180 °C	
Rate 2	7 C/min to 230 °C	
Rate 3	30 C/min to 380 °C	hold 10 min
Detector		
Type	Flame ionization	
Temperature	380 °C	
Carrier Gas		
Type	Hydrogen or Helium	Measured at 50°C
Flow rate	3 mL/min	

The retention times of standards for GC

Standard	Retention time (min)	Relative Retention Times (RRT)
Glycerol	5.70	0.91
Internal STD 1	6.20	1
Monoolein (MG)	16.22	0.76
Internal STD 2	21.08	1
Diolein (DG)	24.89	1.18
Triolein (TG)	30.42	1.44

Standard Solution prepared for GC Calibration

Compound	Satndard Solutin Number				
	(1)	(2)	(3)	(4)	(5)
µL of glycerol	10	30	50	70	100
µL of monoolein	20	50	100	150	200
µL of diolein	10	20	40	70	100
µL of triolein	10	20	40	70	100
µL of STD 1	100	100	100	100	100
µL of STD 2	100	100	100	100	100

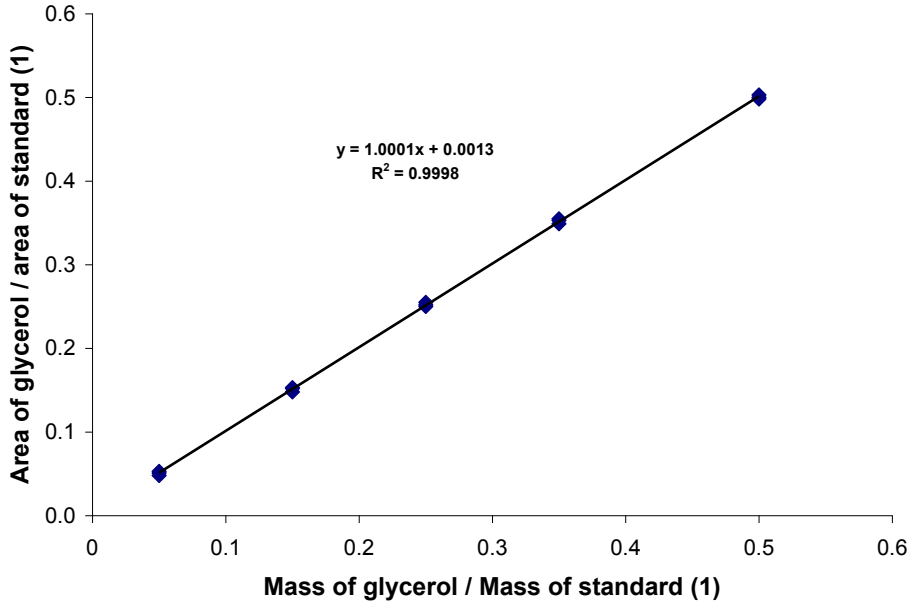

Glycerol calibration based on the area under the curve

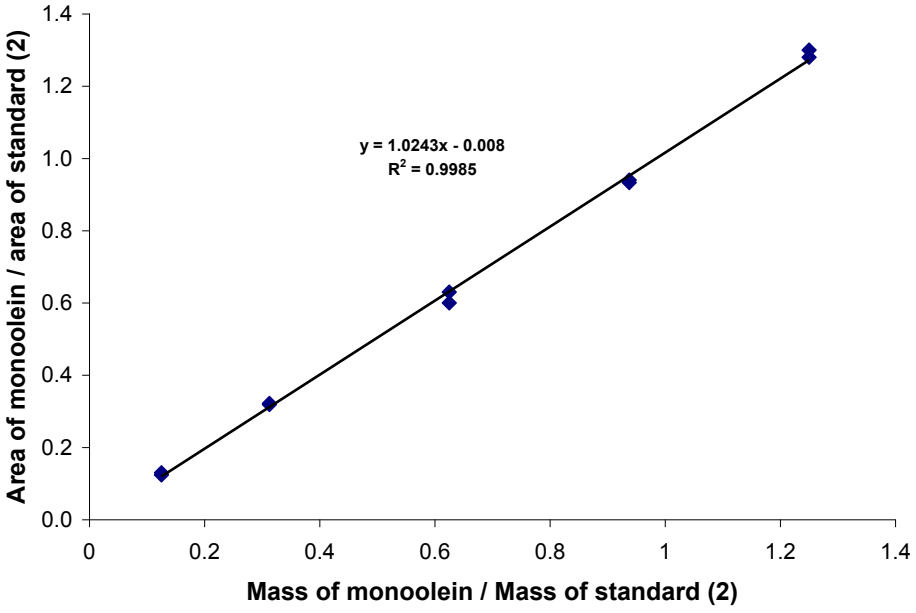

Monoolein calibration based on the area under the curve.

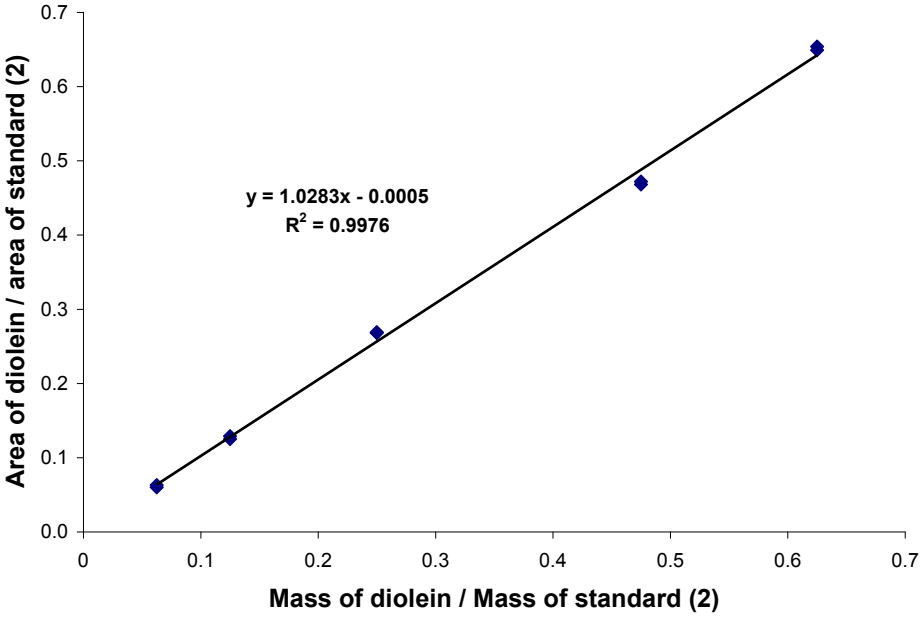

Diolein calibration based on the area under the curve.

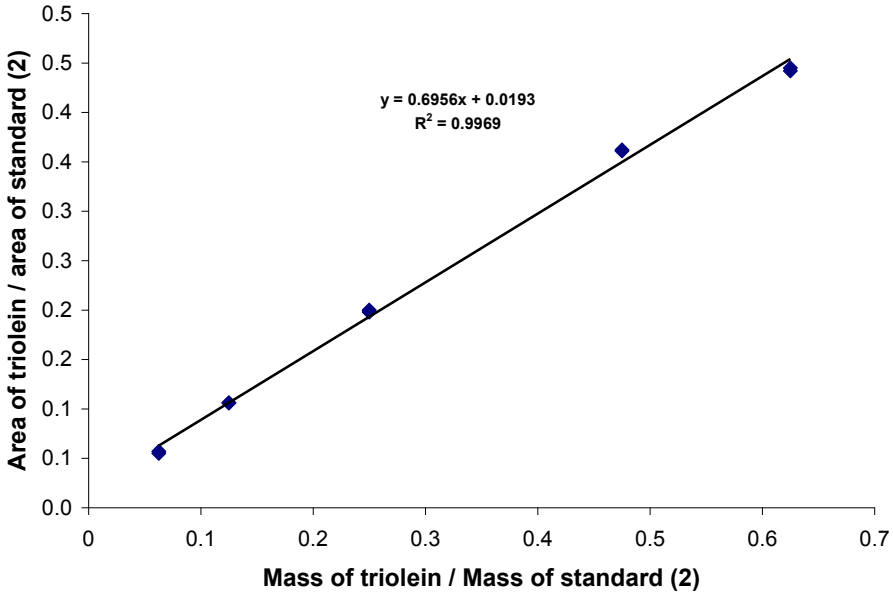

Triolein calibration based on the area under the curve

Appendix B: Additional Tables and Figures for chapter 3 to 7.

Tables and figures for chapter 3

Table B.1: Fluxes of different FAME compositions (chapter 3)

Time (min)	**Flux of permeate (L/h.m^2) at 551.6 kPa**							
	FAME only	**FAME + 0.06% water**	**FAME + 0.1% water**	**FAME + 0.2% water**	**FAME + 1% soap**	**FAME + 1% methanol**	**FAME + 1% Soap + 1% methanol + 0.06% water**	**FAME + 1% Soap + 0.06% water**
0	21.1	19.9	12.4	12.6	20.4	23.6	17.2	13.2
15	19.2	14.6	12.4	10.5	13.7	13.5	15.3	12.4
30	18.3	14.3	12.1	10.3	13.1	12.4	14.4	12.1
60	18.1	14.1	11.8	10.1	12.4	12.1	11.5	11.3
120	16.2	12.9	11.2	9.8	12.3	5.9	9.8	10.6
180	12.9	12.4	10.8	8.7	12.2	4.7	9.3	9.9

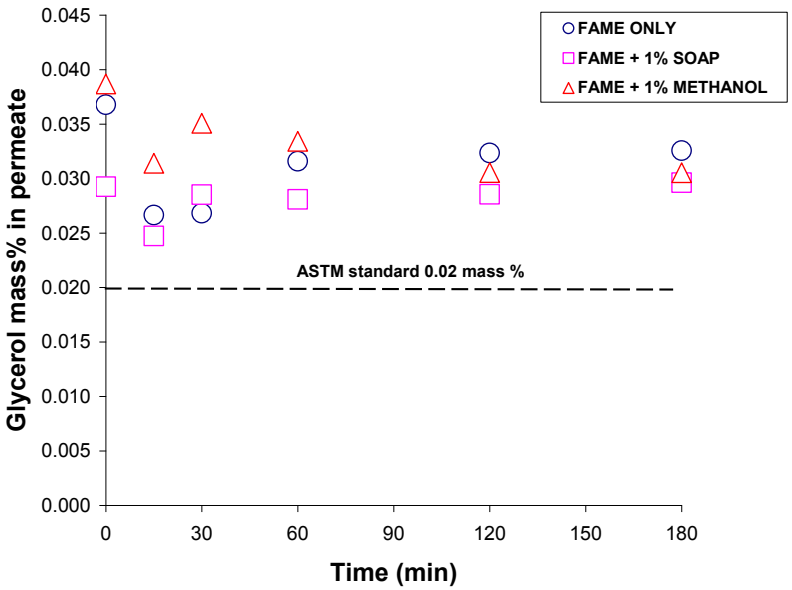

Figure B.1: Glycerol mass% in permeate vs time for (FAME only, FAME + 1% soap, FAME + 1% methanol) at 25°C (chapter 3)

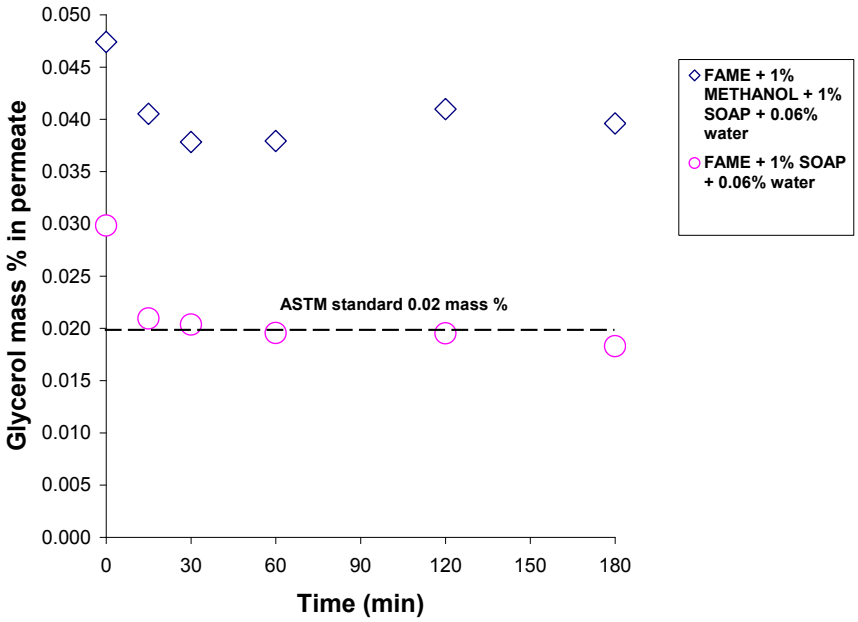

Figure B.2: Glycerol mass% in permeate vs time for (FAME + 1% methanol + 1% soap + 0.06% water, and, FAME + 1% soap + 0.06% water) at 25°C (chapter 3)

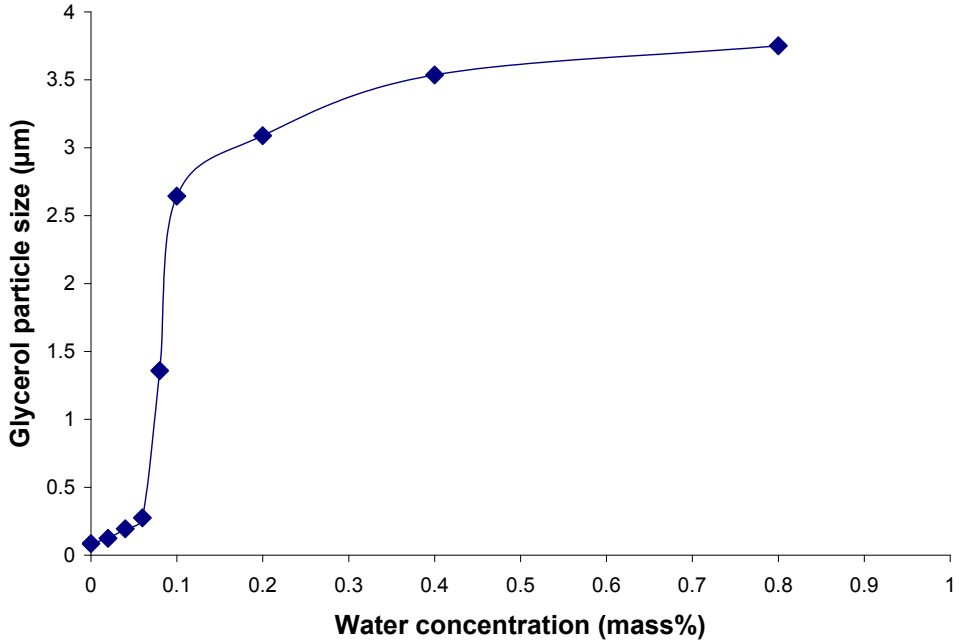

Figure B.3: Effect of water concentration on glycerol droplet size (chapter 3)

Tables for chapter 4

Table B.2: The separation (%) for different polymeric membranes at different temperatures (chapter 4)

Time (min)	% Separation at 0°C			% Separation at 5°C			% Separation at 25°C		
	PES (5 kD)	PVDF (30 kD	Ultrafilic (100 kD)	PES (5 kD)	PVDF (30 kD	Ultrafilic (100 kD)	PES (5 kD)	PVDF (30 kD	Ultrafilic (100 kD)
15	13.9	5.3	8.9	19.1	17.5	12.3	39.7	23.7	14.9
30	33.9	22.4	31.3	31.0	32.1	23.4	53.9	42.3	52.7
60	46.5	33.4	34.5	50.2	53.2	44.8	62.8	52.1	70.2
120	51.6	50.6	50.1	54.7	64.5	78.1	82.6	67.0	76.1
180	65.4	66.1	77.2	68.1	77.1	83.6	93.2	93.9	88.2

Table B.3: Flux for (PES, 5 kD) at different temperatures (chapter 4)

Time (min)	Flux at 0°C L/(m^{2}h)	Flux at 5°C L/(m^{2}h)	Flux at 25°C L/(m^{2}h)
0	26.1	30.1	33.1
15	20.9	26.6	28.1
30	12.4	21.6	22.0
60	9.4	17.2	17.9
120	8.5	12.6	14.6
180	7.4	12.0	13.3

Table B.4: Flux for (PVDF, 30 kD) at different temperatures (chapter 4)

Time (min)	Flux at 0°C L/(m^{2}h)	Flux at 5°C L/(m^{2}h)	Flux at 25°C L/(m^{2}h)
0	24.8	25.9	28.7
15	19.4	16.1	24.6
30	12.2	12.2	23.7
60	7.4	10.2	18.1
120	7.2	9.1	15.0
180	7.0	7.4	8.7

Table B.5: Flux for (Ultrafilic, 100 kD) at different temperatures (chapter 4)

Time (min)	Flux at 0°C L/(m^{2}h)	Flux at 5°C L/(m^{2}h)	Flux at 25°C L/(m^{2}h)
0	57.1	60.1	62.1
15	39.6	44.6	43.6
30	29.2	39.0	40.7
60	27.9	32.0	32.5
120	23.5	26.8	28.5
180	23.3	25.3	27.9

Tables for chapter 5

Table B.6: Free glycerol mass% for permeate and retentate of the UF for different runs at different temperatures (chapter 5)

Time (min)	**Free glycerol mass% for ultrafiltration (0.05 µm)**					
	0°C		**5°C**		**25°C**	
	Run (1)	Run (2)	Run (1)	Run (2)	Run (1)	Run (2)
Original Sample	0.121	0.125	0.117	0.121	0.125	0.129
15 (P)	0.114	0.110	0.099	0.103	0.093	0.113
30 (P)	0.094	0.092	0.083	0.085	0.046	0.064
60 (P)	0.068	0.070	0.061	0.064	0.036	0.036
120 (P)	0.053	0.053	0.027	0.029	0.026	0.028
180 (P)	0.032	0.032	0.023	0.024	0.018	0.018
15 (R)	0.124	0.126	0.114	0.112	0.114	0.119
30 (R)	0.122	0.127	0.125	0.121	0.120	0.120
60 (R)	0.121	0.123	0.132	0.129	0.116	0.128
120 (R)	0.115	0.114	0.132	0.128	0.128	0.128
180 (R)	0.128	0.132	0.128	0.134	0.138	0.140

Table B.7: Free glycerol mass% for permeate and retentate of the MF for different runs at different temperatures (chapter 5)

Time (min)	**Free glycerol mass% for the microfiltration (0.2 µm)**					
	0°C		**5°C**		**25°C**	
	Run (1)	Run (2)	Run (1)	Run (2)	Run (1)	Run (2)
Original Sample	0.123	0.121	0.122	0.120	0.127	0.128
15 (P)	0.114	0.110	0.114	0.114	0.109	0.111
30 (P)	0.110	0.110	0.107	0.109	0.100	0.099
60 (P)	0.096	0.098	0.089	0.089	0.078	0.079
120 (P)	0.090	0.088	0.082	0.082	0.049	0.048
180 (P)	0.064	0.062	0.053	0.055	0.030	0.030
15 (R)	0.111	0.114	0.117	0.113	0.120	0.118
30 (R)	0.115	0.112	0.120	0.116	0.122	0.118
60 (R)	0.124	0.118	0.122	0.121	0.123	0.125
120 (R)	0.121	0.124	0.121	0.123	0.128	0.128
180 (R)	0.121	0.127	0.125	0.123	0.139	0.139

Table B.8: The % separation for the UF and MF with time at operatingdifferent temperatures (chapter 5)

Time (min)	%separation for ultrafiltration (100 kD)			%separation for microfiltration (0.2 µm)		
	0°C	**5°C**	**25°C**	**0°C**	**5°C**	**25°C**
15	8.9	10.6	11.2	0.9	0.9	7.6
30	25.6	31.7	54.2	2.7	8.5	17.5
60	43.4	51.5	70.5	19.8	26.4	37.1
120	53.5	78.5	78.9	27	32.8	61.7
180	75.4	82.4	87.1	49.2	56.8	78.4

Tables related to paper 7

Table B.9: Results of UF (0.03 µm, PES) for 0.1 mass% water using the cake filtration theory (chapter 7)

TMP (MPa)	**0.1 mass% water**								
	25°C			**40°C**			**60°C**		
	α (m/Kg)	**R_m (m^{-1})**	**R^2**	**α (m/Kg)**	**R_m (m^{-1})**	**R^2**	**α (m/Kg)**	**R_m (m^{-1})**	**R^2**
0.12	2.0E+15	1.9E+13	0.995	1.0E+15	1.8E+13	0.981	3.2E+14	1.4E+13	0.989
0.26	1.8E+15	3.0E+13	0.994	9.5E+14	2.5E+13	0.994	3.3E+14	1.8E+13	0.995
0.4	1.1E+15	3.2E+13	0.994	9.0E+14	2.7E+13	0.997	3.1E+13	2.4E+13	0.996
0.53	1.0E+15	3.9E+13	0.994	8.8E+14	3.0E+13	0.992	2.2E+14	2.9E+13	0.997

Table B.10: Results of UF (0.03 µm, PES) for 0.125 mass% water using the cake filtration theory (chapter 7)

TMP (MPa)	**0.125 mass% water**								
	25°C			**40°C**			**60°C**		
	α (m/Kg)	**R_m (m^{-1})**	**R^2**	**α (m/Kg)**	**R_m (m^{-1})**	**R^2**	**α (m/Kg)**	**R_m (m^{-1})**	**R^2**
0.12	3.6E+15	4.2E+13	0.996	1.4E+15	2.8E+13	0.995	2.1E+14	2.0E+13	0.999
0.26	3.3E+15	4.3E+13	0.991	1.3E+15	3.1E+13	0.994	1.9E+14	2.1E+13	0.998
0.4	3.1E+15	4.1E+13	0.990	1.0E+15	3.3E+13	0.994	1.5E+14	2.7E+13	0.998
0.53	2.8E+15	3.6E+13	0.978	9.3E+14	3.8E+13	0.994	1.4E+14	3.2E+13	0.998

Table B.11:Results of UF (0.03 μm, PES) for 0.225 mass% water using the cake filtration theory (chapter 7)

TMP (MPa)	0.225 mass% water								
	25°C			40°C			60°C		
	α (m/Kg)	R_m (m^{-1})	R^2	α (m/Kg)	R_m (m^{-1})	R^2	α (m/Kg)	R_m (m^{-1})	R^2
0.12	2.5E+15	3.6E+13	0.985	1.4E+15	3.5E+13	0.991	3.1E+14	2.3E+13	0.999
0.26	2.7E+15	4.0E+13	0.984	1.4E+15	3.2E+13	0.990	3.3E+14	2.7E+13	0.997
0.4	1.9E+15	4.2E+13	0.989	1.0E+15	3.7E+13	0.992	4.1E+14	4.9E+13	0.999
0.53	1.8E+15	4.7E+13	0.989	1.3E+15	3.7E+13	0.985	3.7E+14	5.1E+13	0.990

Table B.12: Results of UF (0.03 μm, PES) for 0.425 mass% water using the cake filtration theory (chapter 7)

TMP (MPa)	0.425 mass% water								
	25°C			40°C			60°C		
	α (m/Kg)	R_m (m^{-1})	R^2	α (m/Kg)	R_m (m^{-1})	R^2	α (m/Kg)	R_m (m^{-1})	R^2
0.12	4.0E+15	2.0E+13	0.960	4.3E+15	1.4E+13	0.974	3.4E+15	1.8E+13	0.973
0.26	3.7E+15	2.3E+13	0.995	3.1E+15	2.4E+13	0.965	3.0E+15	3.7E+13	0.961
0.4	3.8E+15	3.3E+13	0.977	3.5E+15	2.7E+13	0.950	2.9E+15	4.1E+13	0.951
0.53	3.7E+15	4.3E+13	0.999	3.7E+15	4.8E+13	0.981	3.0E+15	2.7E+13	0.956

Table B.13: Results of UF (0.03 μm, PES) for 0.825 mass% water using the cake filtration theory (chapter 7)

TMP (MPa)	0.825 mass% water								
	25°C			40°C			60°C		
	α (m/Kg)	R_m (m^{-1})	R^2	α (m/Kg)	R_m (m^{-1})	R^2	α (m/Kg)	R_m (m^{-1})	R^2
0.12	3.9E+15	1.8E+13	0.979	2.8E+15	9.1E+12	0.956	2.0E+15	1.0E+13	0.954
0.26	3.5E+15	2.9E+13	0.956	2.4E+15	1.6E+13	0.948	2.2E+15	3.8E+13	0.958
0.4	3.5E+15	3.4E+13	0.951	2.5E+15	2.1E+13	0.953	1.9E+15	3.7E+13	0.951
0.53	3.9E+15	4.2E+13	0.957	2.8E+15	2.3E+13	0.931	2.1E+15	4.6E+13	0.946

Table B.14: Results of MF (0.1 µm, PES) for 0.1 mass% water using the cake filtration theory (chapter 7)

TMP (MPa)	**0.1 mass% water**								
	25°C			**40°C**			**60°C**		
	α (m/Kg)	**R_m (m^{-1})**	**R^2**	**α (m/Kg)**	**R_m (m^{-1})**	**R^2**	**α (m/Kg)**	**R_m (m^{-1})**	**R^2**
0.007	8.5E+12	7.3E+11	0.997	7.1E+12	5.1E+11	0.991	2.7E+12	5.1E+11	0.999
0.012	5.2E+12	4.8E+11	0.999	5.8E+12	4.9E+11	0.996	1.0E+12	3.6E+11	0.999
0.024	4.6E+12	7.0E+11	0.999	4.1E+12	5.4E+11	0.999	2.3E+12	5.0E+11	0.999
0.052	4.8E+12	7.2E+11	0.999	5.9E+12	6.8E+11	0.997	2.2E+12	8.3E+11	0.999
0.085	5.7E+12	8.4E+11	0.999	4.8E+12	7.6E+11	0.996	2.1E+12	2.2E+11	0.999

Table B.15: Results of MF (0.1 µm, PES) for 0.125 mass% water using the cake filtration theory (chapter 7)

TMP (MPa)	**0.125 mass% water**								
	25°C			**40°C**			**60°C**		
	α (m/Kg)	**R_m (m^{-1})**	**R^2**	**α (m/Kg)**	**R_m (m^{-1})**	**R^2**	**α (m/Kg)**	**R_m (m^{-1})**	**R^2**
0.007	2.4E+13	9.1E+11	0.995	4.3E+13	7.1E+11	0.996	2.3E+12	6.0E+11	0.995
0.012	2.9E+13	1.1E+12	0.989	6.8E+12	5.3E+11	0.999	5.0E+12	5.5E+11	0.999
0.024	3.4E+13	1.2E+12	0.997	5.4E+12	6.0E+11	0.999	4.0E+12	8.0E+11	0.999
0.052	9.9E+12	1.2E+12	0.999	2.9E+12	7.4E+11	0.999	2.6E+12	1.1E+12	0.999
0.085	4.1E+12	1.1E+12	0.999	2.4E+12	1.1E+12	0.999	2.8E+12	1.4E+12	0.999

Table B.16: Results of MF (0.1 µm, PES) for 0.225 mass% water using the cake filtration theory (chapter 7)

TMP (MPa)	**0.225 mass% water**								
	25°C			**40°C**			**60°C**		
	α (m/Kg)	**R_m (m^{-1})**	**R^2**	**α (m/Kg)**	**R_m (m^{-1})**	**R^2**	**α (m/Kg)**	**R_m (m^{-1})**	**R^2**
0.007	3.7E+13	1.0E+12	0.999	2.6E+13	1.2E+12	0.999	1.2E+13	8.6E+11	0.999
0.012	4.9E+13	1.4E+12	0.998	3.4E+13	1.1E+12	0.999	1.0E+13	8.0E+11	0.999
0.024	5.7E+13	1.9E+12	0.998	1.4E+13	1.0E+12	0.998	1.2E+13	1.2E+12	0.999
0.052	5.3E+13	2.2E+12	0.996	2.1E+13	1.6E+12	0.998	1.3E+13	2.0E+12	0.999
0.085	4.5E+13	2.4E+12	0.998	2.4E+13	1.7E+12	0.996	1.3E+13	2.5E+12	0.973

Table B.17: Results of MF (0.1 µm, PES) for 0.425 mass% water using the cake filtration theory (chapter 7)

TMP (MPa)	**0.425 mass% water**								
	25°C			**40°C**			**60°C**		
	α (m/Kg)	**R_m (m^{-1})**	**R^2**	**α (m/Kg)**	**R_m (m^{-1})**	**R^2**	**α (m/Kg)**	**R_m (m^{-1})**	**R^2**
0.007	1.6E+14	1.0E+12	0.993	5.5E+13	9.8E+11	0.992	2.6E+13	8.1E+11	0.997
0.012	1.2E+14	1.1E+12	0.992	6.2E+13	1.1E+12	0.992	2.0E+13	8.2E+11	0.996
0.024	1.4E+14	1.4E+12	0.982	5.1E+13	1.1E+12	0.995	1.8E+13	1.2E+12	0.998
0.052	1.2E+14	2.3E+12	0.991	5.9E+13	2.0E+12	0.995	2.5E+13	2.1E+12	0.997
0.085	1.3E+14	3.1E+12	0.996	5.4E+13	3.0E+12	0.996	2.8E+13	3.3E+12	0.999

Table B.18: Results of MF (0.1 µm, PES) for 0.825 mass% water using the cake filtration theory (chapter 7)

TMP (MPa)	**0.825 mass% water**								
	25°C			**40°C**			**60°C**		
	α (m/Kg)	**R_m (m^{-1})**	**R^2**	**α (m/Kg)**	**R_m (m^{-1})**	**R^2**	**α (m/Kg)**	**R_m (m^{-1})**	**R^2**
0.007	3.0E+14	9.4E+11	0.979	1.6E+14	1.0E+12	0.983	9.3E+13	1.4E+12	0.996
0.012	3.4E+14	1.1E+12	0.971	1.2E+14	1.6E+12	0.999	9.1E+13	1.4E+12	0.992
0.024	2.5E+14	1.8E+12	0.989	1.4E+14	1.6E+12	0.997	8.7E+13	1.9E+12	0.992
0.052	1.2E+14	2.4E+12	0.992	1.3E+14	2.8E+12	0.997	8.7E+13	2.8E+12	0.996
0.085	1.2E+14	3.8E+12	0.996	1.4E+14	4.1E+12	0.997	8.4E+13	3.7E+12	0.996

Table B.19: Results of MF (0.22 µm, PES) for 0.1 mass% water using the cake filtration theory (chapter 7)

TMP (MPa)	**0.1 mass% water**								
	25°C			**40°C**			**60°C**		
	α (m/Kg)	**R_m (m^{-1})**	**R^2**	**α (m/Kg)**	**R_m (m^{-1})**	**R^2**	**α (m/Kg)**	**R_m (m^{-1})**	**R^2**
0.007	7.4E+13	1.1E+12	0.982	3.7E+12	1.1E+12	0.990	5.8E+11	1.2E+12	0.993
0.012	7.8E+13	1.2E+12	0.997	3.4E+12	8.2E+11	0.991	8.2E+11	5.4E+11	0.981
0.024	8.4E+13	1.6E+12	0.993	1.4E+12	5.6E+11	0.967	3.0E+11	5.1E+11	0.972
0.052	8.7E+13	2.7E+12	0.977	3.1E+12	5.8E+11	0.980	2.2E+11	5.2E+11	0.989
0.085	8.1E+13	3.8E+12	0.976	2.6E+12	7.4E+11	0.968	2.1E+11	6.7E+11	0.991

Table B.20: Results of MF (0.22 μm, PES) for 0.125 mass% water using the cake filtration theory (chapter 7)

TMP (MPa)	0.125 mass% water								
	25°C			40°C			60°C		
	α (m/Kg)	R_m (m^{-1})	R^2	α (m/Kg)	R_m (m^{-1})	R^2	α (m/Kg)	R_m (m^{-1})	R^2
0.007	6.5E+12	1.1E+12	0.998	5.2E+12	1.2E+12	0.987	5.7E+12	1.4E+12	0.997
0.012	5.1E+12	1.1E+12	0.967	3.9E+12	7.6E+11	0.972	5.8E+12	9.4E+11	0.963
0.024	1.5E+12	6.8E+11	0.979	1.8E+12	5.4E+11	0.974	2.7E+11	5.5E+11	0.973
0.052	3.6E+12	6.9E+11	0.993	3.3E+12	6.7E+11	0.989	1.4E+11	7.1E+11	0.983
0.085	3.6E+12	7.8E+11	0.986	4.3E+11	8.2E+11	0.994	2.5E+11	9.6E+11	0.968

Table B.21: Results of MF (0.22 μm, PES) for 0.225 mass% water using the cake filtration theory (chapter 7)

TMP (MPa)	0.225 mass% water								
	25°C			40°C			60°C		
	α (m/Kg)	R_m (m^{-1})	R^2	α (m/Kg)	R_m (m^{-1})	R^2	α (m/Kg)	R_m (m^{-1})	R^2
0.007	2.5E+13	1.1E+12	0.998	5.7E+13	1.2E+12	0.999	1.8E+13	1.9E+12	0.999
0.012	1.1E+13	1.1E+12	0.995	4.2E+12	9.9E+11	0.992	1.9E+13	1.3E+12	0.995
0.024	1.1E+13	1.2E+12	0.978	2.9E+12	8.3E+11	0.980	1.2E+12	9.5E+11	0.993
0.052	1.1E+13	1.4E+12	0.968	7.2E+11	1.1E+12	0.991	5.4E+11	1.3E+12	0.991
0.085	1.4E+13	1.6E+12	0.976	5.9E+11	1.3E+12	0.988	6.6E+11	1.5E+12	0.980

Table B.22: Results of MF (0.22 μm, PES) for 0.425 mass% water using the cake filtration theory (chapter 7)

TMP (MPa)	0.425 mass% water								
	25°C			40°C			60°C		
	α (m/Kg)	R_m (m^{-1})	R^2	α (m/Kg)	R_m (m^{-1})	R^2	α (m/Kg)	R_m (m^{-1})	R^2
0.007	5.8E+13	1.5E+12	0.994	2.9E+12	1.5E+12	0.989	8.5E+12	1.9E+12	0.991
0.012	2.1E+13	1.1E+12	0.993	5.2E+12	1.5E+12	0.984	5.7E+12	2.1E+12	0.998
0.024	2.0E+13	1.4E+12	0.992	5.9E+12	1.6E+12	0.991	7.5E+12	2.2E+12	0.994
0.052	2.4E+12	2.2E+12	0.992	5.6E+12	2.3E+12	0.989	6.6E+12	3.1E+12	0.970
0.085	7.7E+12	2.4E+12	0.996	2.7E+12	2.9E+12	0.980	5.4E+12	3.8E+12	0.982

Table B.23: Results of MF (0.22 μm, PES) for 0.825 mass% water using the cake filtration theory (chapter 7)

TMP (MPa)	**0.825 mass% water**								
	25°C			**40°C**			**60°C**		
	α (m/Kg)	**R_m (m^{-1})**	**R^2**	**α (m/Kg)**	**R_m (m^{-1})**	**R^2**	**α (m/Kg)**	**R_m (m^{-1})**	**R^2**
0.007	3.5E+13	1.5E+12	0.984	2.9E+13	1.7E+12	0.986	2.6E+13	2.6E+12	0.986
0.012	1.9E+13	1.4E+12	0.993	2.7E+13	1.4E+12	0.988	2.3E+13	2.1E+12	0.986
0.024	3.3E+13	1.9E+12	0.983	2.8E+13	1.9E+12	0.978	2.6E+13	2.7E+12	0.981
0.052	2.1E+13	3.0E+12	0.993	2.2E+13	3.4E+12	0.994	2.9E+13	4.7E+12	0.992
0.085	3.1E+13	4.2E+12	0.991	2.6E+13	4.5E+12	0.993	2.8E+13	6.6E+12	0.995

Table B.24: Limiting fluxes and glycerol concentration in the permeate for different initial water concentrations and TMP at 25°C for UF (0.03μm, PES) (chapter 7)

Mass% water	**TMP (MPa)**	**Limiting flux (L/m^2h)**	**Glycerol concentration in the permeate (ppm)**
0.1	**0.12**	2.0	117.6
	0.26	4.0	122.5
	0.4	6.5	134.4
	0.53	7.5	147.5
0.125	**0.12**	1.4	114.1
	0.26	3.4	118.7
	0.4	6.0	127.9
	0.53	6.9	138.2
0.225	**0.12**	1.4	89.5
	0.26	2.9	110.5
	0.4	4.8	118.5
	0.53	5.7	126.3
0.425	**0.12**	1.3	92.4
	0.26	3.0	103.1
	0.4	3.5	120.0
	0.53	3.7	124.1
0.825	**0.12**	1.2	101.0
	0.26	2.5	141.2
	0.4	3.0	156.2
	0.53	3.0	164.9

Table B.25: Limiting fluxes and glycerol concentration in the permeate for different initial water concentrations and TMP at 40°C for UF (0.03µm, PES) (chapter 7)

Mass% water	TMP (MPa)	Limiting flux (L/m^2h)	Glycerol concentration in the permeate (ppm)
0.1	**0.12**	3.5	130.3
	0.26	6.5	153.0
	0.4	9.2	161.7
	0.53	11.2	177.7
0.125	**0.12**	2.7	121.4
	0.26	5.2	141.7
	0.4	7.9	155.1
	0.53	9.1	168.4
0.225	**0.12**	2.1	89.7
	0.26	4.8	111.7
	0.4	6.9	125.4
	0.53	7.8	144.7
0.425	**0.12**	2.0	150.0
	0.26	3.6	160.0
	0.4	4.5	170.0
	0.53	4.8	180.0
0.825	**0.12**	1.8	180.0
	0.26	3.4	185.0
	0.4	4.7	190.0
	0.53	4.9	196.0

Table B.26: Limiting fluxes and glycerol concentration in the permeate for different initial water concentrations and TMP at 60°C for UF (0.03µm, PES) (chapter 7)

Mass% water	TMP (MPa)	Limiting flux (L/m^2h)	Glycerol concentration in the permeate (ppm)
0.1	**0.12**	7.5	185.1
	0.26	13.5	189.4
	0.4	16.0	194.9
	0.53	17.7	197.5
0.125	**0.12**	6.3	185.9
	0.26	12.6	193.7
	0.4	15.5	195.1
	0.53	16.5	197.6
0.225	**0.12**	5.4	175.3
	0.26	8.6	181.1
	0.4	9.4	193.2
	0.53	9.8	204.8
0.425	**0.12**	3.1	197.0
	0.26	4.7	201.0
	0.4	5.7	235.6
	0.53	5.8	248.4
0.825	**0.12**	2.2	199.0
	0.26	3.8	211.0
	0.4	5.1	239.0
	0.53	5.4	255.0

Table B.27: Limiting fluxes and glycerol concentration in the permeate for different initial water concentrations and TMP at 25°C for MF (0.1µm, PES) (chapter 7)

Mass% water	TMP (MPa)	Limiting flux (L/m^2h)	Glycerol concentration in the permeate (ppm)
0.1	**0.007**	5.4	155.1
	0.012	11.7	164.7
	0.024	21.2	177.5
	0.052	45.8	177.9
	0.085	62.1	185.8
0.125	**0.007**	4.1	160.0
	0.012	5.4	168.7
	0.024	11.3	183.0
	0.052	26.6	181.6
	0.085	40.4	184.3
0.225	**0.007**	4.3	157.7
	0.012	5.1	171.6
	0.024	7.7	183.8
	0.052	12.8	186.1
	0.085	18.4	194.2
0.425	**0.007**	3.4	155.6
	0.012	5.4	174.8
	0.024	7.4	182.2
	0.052	10.8	186.8
	0.085	14.8	197.2
0.825	**0.007**	3.1	166.7
	0.012	3.9	173.0
	0.024	5.9	197.9
	0.052	10.8	198.4
	0.085	12.3	199.1

Table B.28: Limiting fluxes and glycerol concentration in the permeate for different initial water concentrations and TMP at 40°C for MF (0.1µm, PES) (chapter 7)

Mass% water	TMP (MPa)	Limiting flux (L/m^2h)	Glycerol concentration in the permeate (ppm)
0.1	**0.007**	7.9	187.4
	0.012	15.7	171.9
	0.024	31.5	196.5
	0.052	50.2	196.3
	0.085	70.5	200.9
0.125	**0.007**	6.4	179.9
	0.012	16.2	180.7
	0.024	28.1	199.1
	0.052	47.3	209.3
	0.085	57.1	208.7
0.225	**0.007**	4.4	194.5
	0.012	7.9	195.4
	0.024	16.0	197.8
	0.052	22.1	199.7
	0.085	31.7	199.5
0.425	**0.007**	4.2	197.4
	0.012	6.9	210.1
	0.024	14.3	238.6
	0.052	16.2	264.9
	0.085	18.2	267.6
0.825	**0.007**	3.4	205.3
	0.012	5.4	215.8
	0.024	8.9	229.2
	0.052	13.1	254.4
	0.085	14.2	270.7

Table B.29: Limiting fluxes and glycerol concentration in the permeate for different initial water concentrations and TMP at 60°C for MF (0.1µm, PES) (chapter 7)

Mass% water	TMP (MPa)	Limiting flux (L/m^2h)	Glycerol concentration in the permeate (ppm)
0.1	**0.007**	12.4	200.7
	0.012	27.5	206.8
	0.024	45.5	208.9
	0.052	69.0	212.9
	0.085	78.5	223.0
0.125	**0.007**	10.8	200.6
	0.012	23.1	210.7
	0.024	32.5	212.5
	0.052	51.2	219.4
	0.085	64.5	235.8
0.225	**0.007**	8.9	210.1
	0.012	15.8	217.1
	0.024	21.8	219.0
	0.052	27.6	239.4
	0.085	34.9	241.3
0.425	**0.007**	8.4	212.0
	0.012	14.3	221.6
	0.024	20.7	231.5
	0.052	24.6	237.3
	0.085	23.6	252.3
0.825	**0.007**	4.9	207.5
	0.012	7.4	212.2
	0.024	10.8	235.0
	0.052	17.7	247.2
	0.085	20.2	276.1

Table B.30: Limiting fluxes and glycerol concentration in the permeate for different initial water concentrations and TMP at 25°C for MF (0.22µm, PES) (chapter 7)

Mass% water	TMP (MPa)	Limiting flux (L/m^2h)	Glycerol concentration in the permeate (ppm)
0.1	**0.007**	3.7	170.0
	0.012	10.6	180.1
	0.024	22.6	187.6
	0.052	44.8	185.2
	0.085	62.7	183.2
0.125	**0.007**	3.7	183.1
	0.012	7.0	184.6
	0.024	22.1	182.5
	0.052	45.8	192.7
	0.085	57.6	197.1
0.225	**0.007**	3.6	176.5
	0.012	6.5	186.2
	0.024	11.3	185.8
	0.052	22.6	197.7
	0.085	32.2	197.9
0.425	**0.007**	2.5	168.1
	0.012	5.4	174.0
	0.024	8.4	189.9
	0.052	15.3	198.3
	0.085	19.2	198.1
0.825	**0.007**	2.0	137.8
	0.012	4.4	182.0
	0.024	5.4	182.2
	0.052	8.9	199.5
	0.085	10.8	208.1

Table B.31: Limiting fluxes and glycerol concentration in the permeate for different initial water concentrations and TMP at 40°C for MF (0.22μm, PES) (chapter 7)

Mass% water	TMP (MPa)	Limiting flux (L/m^2h)	Glycerol concentration in the permeate (ppm)
0.1	**0.007**	4.4	182.3
	0.012	11.1	187.4
	0.024	32.0	196.5
	0.052	69.4	194.0
	0.085	89.6	197.6
0.125	**0.007**	3.7	196.4
	0.012	10.8	201.2
	0.024	32.0	199.6
	0.052	59.6	198.8
	0.085	74.8	225.9
0.225	**0.007**	3.5	174.1
	0.012	8.9	176.7
	0.024	20.6	191.5
	0.052	35.4	203.4
	0.085	49.7	237.3
0.425	**0.007**	3.2	197.2
	0.012	6.2	216.4
	0.024	9.8	244.7
	0.052	16.0	251.8
	0.085	22.2	278.4
0.825	**0.007**	2.1	221.6
	0.012	4.4	229.6
	0.024	5.9	239.2
	0.052	9.4	257.5
	0.085	15.3	285.9

Table B.32: Limiting fluxes and glycerol concentration in the permeate for different initial water concentrations and TMP at 60°C for MF (0.22µm, PES) (chapter 7)

Mass% water	TMP (MPa)	Limiting flux (L/m^2h)	Glycerol concentration in the permeate (ppm)
0.1	**0.007**	6.4	202.5
	0.012	24.0	209.4
	0.024	53.6	216.4
	0.052	113.2	239.1
	0.085	142.7	310.8
0.125	**0.007**	4.2	206.4
	0.012	13.0	216.0
	0.024	49.7	225.1
	0.052	84.7	267.9
	0.085	100.9	328.4
0.225	**0.007**	3.5	215.4
	0.012	9.0	221.2
	0.024	28.1	249.9
	0.052	46.3	282.5
	0.085	63.0	334.4
0.425	**0.007**	3.7	213.0
	0.012	6.4	226.5
	0.024	10.8	231.9
	0.052	18.0	281.8
	0.085	24.1	349.2
0.825	**0.007**	2.2	216.0
	0.012	4.5	236.0
	0.024	6.4	265.0
	0.052	9.6	321.9
	0.085	11.8	366.8